

UNIVERSIDAD COMPLUTENSE DE MADRID  
FACULTAD DE CIENCIAS MATEMÁTICAS

PHD THESIS

---

# Monodromies as tête-à-tête graphs

---

## Monodromías como grafos tête-à-tête

---

*Author:*  
Pablo PORTILLA CUADRADO

*Supervisors:*  
Javier FERNÁNDEZ DE BOBADILLA  
María PE PEREIRA

May, 2018





# Contents

	Page
Acknowledgements	<i>iii</i>
Abstract	<i>v</i>
Resumen	<i>vii</i>
Introduction	<i>ix</i>
<b>I Preliminary theory</b>	
<b>1 Ribbon graphs</b>	<b>3</b>
<b>2 Mapping class groups</b>	<b>7</b>
2.1 Periodic automorphisms in $MCG^+(\Sigma)$ . . . . .	9
2.2 Dehn twists . . . . .	11
2.3 Freely periodic automorphisms . . . . .	12
2.4 Pseudo-periodic automorphisms . . . . .	15
<b>3 Graph manifolds</b>	<b>19</b>
3.1 Seifert manifolds . . . . .	20
3.2 Graph manifolds . . . . .	22
<b>4 Graph manifolds fibered over the circle</b>	<b>29</b>
4.1 Horizontal surfaces in Seifert manifolds . . . . .	29
4.2 Horizontal open books in graph manifolds. . . . .	34
4.2.1 Waldhausen graphs and horizontal surfaces . . . . .	35
4.3 Description of the monodromy . . . . .	37

<b>5</b>	<b>Singularity theory</b>	<b>41</b>
<b>II Tête-à-tête graphs and twists</b>		
<b>6</b>	<b>Tête-à-tête graphs</b>	<b>47</b>
<b>7</b>	<b>Tête-à-tête twists</b>	<b>53</b>
7.1	Signed tête-à-tête graphs and freely periodic automorphisms . . . . .	53
7.2	Truly periodic automorphisms and tête-à-tête graphs . . . . .	62
7.3	General tête-à-tête structures . . . . .	63
<b>8</b>	<b>Mixed tête-à-tête graphs</b>	<b>69</b>
<b>9</b>	<b>Mixed tête-à-tête twists</b>	<b>73</b>
<b>10</b>	<b>Realization theorem</b>	<b>79</b>
<b>III Algorithms</b>		
<b>11</b>	<b>Tête-à-tête graphs and Seifert manifolds</b>	<b>89</b>
11.1	From general tête-à-tête graph to star-shaped plumbing graph . . . . .	89
11.2	From star-shaped plumbing graph to tête-à-tête graphs . . . . .	91
<b>12</b>	<b>Mixed tête-à-tête graphs and graph manifolds</b>	<b>93</b>
12.1	From open books to mixed tête-à-tête graphs . . . . .	93
12.2	From mixed tête-à-tête graphs to open books . . . . .	94
<b>Appendices</b>		<b>101</b>
<b>A</b>	<b>Mixed tête-à-tête structures on filtered metric ribbon graphs</b>	<b>103</b>
A.1	The $\tau$ number. . . . .	105
A.2	Mixed tête-à-tête structures on filtered metric ribbon graphs . . . . .	108
<b>B</b>	<b><math>\Lambda</math>-blow up</b>	<b>111</b>
B.1	Brieskorn-Pham singularities . . . . .	117
B.2	Mixed tête-à-tête graph for isolated plane curve singularities . . . . .	118
<b>C</b>	<b>Examples</b>	<b>123</b>
<b>Index</b>		<b>155</b>

# *Acknowledgments*

First of all and prior to the rest, I would like to thank my supervisors Javier Fernández de Bobadilla and María Pe Pereira. I am greatly indebted to them. They saved me four years ago from what could have been the premature end of my mathematical career. They have been very generous both with their ideas and their time and I owe them much of this work.

I want to thank the singularity theory group at Universidad de Zaragoza which I have visited several times. In special, I would like to thank Enrique Artal Bartolo for answering my many questions and enlightening the many details (that tend to be sloppy in the textbooks) of the theory of plumbing graphs. He has never doubted in dedicating me part of his time. Of this university I would also like to thank Miguel Ángel Marco Buzunámiz for sharing with me his expertise in the mathematical software Sage. Thanks to him I have been able to translate many of the constructions of this work into packages of the cited software.

I thank Universidad Complutense de Madrid, ICMAT and BCAM where most of this work was done. During these four years I have had the opportunity to meet mathematicians in many other workplaces. I thank Columbia University for providing me with an ideal environment during my stay in early 2015. I thank Northeastern University and specially David B. Massey for taking care of me during my stay there in Winter 2016. He listened carefully to my work and helped me improve the exposition in many ways.

I cannot stress enough how grateful I am to Baldur Sigurðsson who has collaborated with me in the most important parts of this work. He has been an excellent partner and a better mentor. Like a third supervisor to me.

Finally, I would like to thank Andrea for making my life easier. Without her, these would have been much much tougher years.

The author was partially supported by the ERCEA 615655 NMST Consolidator Grant, by SVP-2013-067644 Severo Ochoa FPI grant by the Spanish Ministry of Economy and by BCAM Severo Ochoa excellence accreditation SEV-2013-0323.



## Abstract

This is a brief abstract in the requirements of Universidad Complutense de Madrid. For a more comprehensive summary jump to Introduction.

In [A'C10] N. A'Campo introduced the notion of pure tête-à-tête graph in order to model monodromies of plane curves. These are metric ribbon graphs without univalent vertices that satisfy a special property. If one sees the ribbon graph  $\Gamma$  as a strong deformation retract of a surface  $\Sigma$  with boundary, the tête-à-tête property says that starting at any point  $p$  and walking a distance of  $\pi$  in any direction and always turning right at vertices, gets you to the same point. This property defines an element in the mapping class group  $\text{MCG}^+(\Sigma, \partial\Sigma)$  which is freely periodic, and is called the *tête-à-tête twist* associated with  $\Gamma$ .

This work starts with the preliminary theory necessary to understand the rest of the work. All the results that are gathered in this part are known. It consists of the first five chapters of the work.

After this, we introduce all the definitions that were originally given by A'Campo. We show that the tête-à-tête property induces a periodic automorphism on the ribbon graph  $\Gamma$  and a freely periodic automorphism on its thickening. We prove the first main theorem of the text which characterizes the mapping classes that contain a tête-à-tête twist and obtain some corollaries from it. This result is contained in the joint work [FPP17] co-authored with J. Fernández de Bobadilla and M. Pe Pereira. This first realization result (which previously appeared in [FPP17]) says

**Theorem A.** *The set of mapping classes in  $\text{MCG}^+(\Sigma, \partial\Sigma)$  that can be realized by a pure tête-à-tête graph (in the sense of A'Campo) is precisely the set of freely periodic mapping classes with strictly positive fractional Dehn twists.*

This improves the main result of [Gra15] who proves the same result but allowing univalent vertices whereas we restrict ourselves to the original set of tête-à-tête graphs defined by A'Campo.

After this we introduce general tête-à-tête graphs. These are metric ribbon graphs with some special subset of univalent vertices. We prove that these are enough to model all periodic mapping classes of a given oriented surface with boundary. This part is contained in [Por17].

Tête-à-tête graphs only model automorphisms whose mapping classes are periodic in  $\text{MCG}(\Sigma)$  and these do not model monodromies of plane branches with at least two Puiseux pairs. With this motivation, we introduce the notion of mixed tête-à-tête graph which appeared first in [FPP17]. These are metric ribbon graphs endowed with a decreasing filtration  $\Gamma^\bullet$  and a set of locally constant functions  $\delta_i : \Gamma^i \rightarrow \mathbb{R}_{\geq 0}$ . They satisfy a mixed tête-à-tête property which generalizes the tête-à-tête property. We associate a pseudo-periodic mapping class in  $\text{MCG}^+(\Sigma, \partial\Sigma)$  to a given mixed tête-à-tête graph: the mixed tête-à-tête twist.

Then we prove the main result of the work (Theorem 10.7) which originally appeared in a joint work with B. Sigurdson [PS17]. It characterizes the set of mapping classes that can be realized by

mixed tête-à-tête twists.

**Theorem B.** *Let  $\phi : \Sigma \rightarrow \Sigma$  be an automorphism with fixed boundary. Then there exists a mixed tête-à-tête graph in  $\Sigma$  inducing its mapping class in  $\text{MCG}^+(\Sigma, \partial\Sigma)$  if and only if some power of  $\phi$  is a composition of right handed Dehn twists around disjoint simple closed curves including all boundary components.*

As a corollary of this theorem and a result in [NP07] we get

**Theorem C.** *Mixed tête-à-tête twists are precisely the monodromies associated with reduced function germs defined on isolated surface singularities.*

This generalizes a previous result in [FPP17] in which we proved that mixed tête-à-tête twists model monodromies of plane branches.

The mapping torus of a pseudo-periodic surface automorphism is a graph manifold. Conversely, a horizontal surface of a fiber-oriented graph manifold has a pseudo-periodic monodromy induced on it. Hence, it is a natural problem to assign a graph manifold and a horizontal surface to each mixed tête-à-tête graph and, whenever possible, assign a mixed tête-à-tête graph to a given horizontal surface in a graph manifold. In this part we provide algorithms producing a graph manifold and a fibration over  $S^1$  from a mixed tête-à-tête graph and vice versa. In particular, this provides a direct and effective way to check if two mixed tête-à-tête graphs represent conjugate mapping classes in  $\text{MCG}^+(\Sigma, \partial\Sigma)$ .

The work ends with three appendices that are additional content and are not strictly necessary to understand the previous content.



## Resumen

Este es un breve resumen en cumplimiento de la normativa de la Universidad Complutense de Madrid. Para una introducción más exhaustiva saltar a Introduction.

En [A'C10] N. A'Campo presentó la noción de tête-à-tête puro con el objetivo de modelar las monodromías de curvas planas. Estos son grafos ribbon sin vértices univalentes que satisfacen una propiedad especial. Si piensas en el grafo ribbon  $\Gamma$  como en un retracto de la superficie con borde  $\Sigma$ , la propiedad tête-à-tête te dice que empezando en cualquier punto  $p$  y caminando una distancia de  $\pi$  en cualquier dirección y siempre girando a la derecha en cualquier vértice, llegas al mismo punto. Esta propiedad define un elemento del mapping class group  $\text{MCG}^+(\Sigma, \partial\Sigma)$  que es periódico a frontera libre. Este elemento es el *tête-à-tête twist* asociado con  $\Gamma$ .

El trabajo empieza con la teoría preliminar necesaria para entender el resto de contenidos. Todos los resultados de esta parte son conocidos. Consiste de los primeros cinco capítulos.

Después, presentamos las definiciones originales de grafos tête-à-tête de A'Campo. Mostramos que la propiedad tête-à-tête induce un automorfismo periódico del grafo ribbon  $\Gamma$  y un automorfismo periódico a frontera libre en el engordamiento del grafo  $\Sigma$ . Demostramos el primero de los resultados principales del trabajo el cual caracteriza las mapping classes que contienen algún representante tête-à-tête. Este resultado está contenido en [FPP17], trabajo conjunto con J. Fernández de Bobadilla and M. Pe Pereira. El enunciado es

**Theorem A.** *El conjunto de mapping classes en  $\text{MCG}^+(\Sigma, \partial\Sigma)$  que son inducidas por grafos tête-à-tête (en el sentido original de A'Campo) es precisamente el conjunto de mapping classes periódicas a frontera libre que tienen coeficientes fraccionales de Dehn twist estrictamente positivos.*

A continuación presentamos los grafos tête-à-tête generales. Estos son grafos ribbon métricos con un conjunto especial de vértices univalentes. Satisfacen una propiedad tête-à-tête y demostramos que son suficientes para modelar todas las mapping classes periódicas de una superficie orientada con borde. Esta parte está contenida en [Por17].

Con los grafos definidos hasta el momento tan solo podemos modelar automorfismos que son periódicos vistos como mapping classes en  $\text{MCG}(\Sigma)$ . [FPP17]. Esto no es suficiente para modelar monodromías de curva plana con más de un par de Puiseux. Con esta motivación definimos los grafos tête-à-tête mixtos. Son grafos ribbon con una métrica y una filtración decreciente  $\Gamma^\bullet$  junto con una colección de funciones  $\delta_i : \Gamma^i \rightarrow \mathbb{R}_{\geq 0}$  localmente constantes. Satisfacen una propiedad tête-à-tête mixta que generaliza la propiedad tête-à-tête y definen una mapping class pseudo-periódica.

Demostramos un teorema de realización sobre grafos mixtos caracterizando qué automorfismos pseudo-periódicos son capaces de modelar.

**Theorem B.** *Sea  $\phi : \Sigma \rightarrow \Sigma$  un automorfismo que fija el borde. Entonces existe*

*un grafo tête-à-tête mixto in  $\Sigma$  que induce su mapping class en  $\text{MCG}^+(\Sigma, \partial\Sigma)$  si y solo si alguna potencia suficientemente grande de  $\phi$  es una composición de twist de Dehn hacia la derecha a lo largo de curvas cerradas disjuntas que incluyen todos las componentes de borde.*

Aplicando el teorema previo junto con un resultado en [NP07], probamos el siguiente corolario:

**Theorem C.** *Los automorfismos tête-à-tête mixtos son precisamente las monodromías asociadas a gérmenes reducidos de función holomorfa definidos en singularidades de superficie aisladas.*

Este teorema mejora un teorema previo del trabajo conjunto [FPP17] donde demostramos que los automorfismos tête-à-tête mixtos modelan monodromías de singularidades irreducibles de curva plana.

Observamos que el mapping torus de un automorfismo pseudo-periódico es una variedad de grafo. Por otro lado, una superficie horizontal en una variedad de graph con fibras orientadas tiene una monodromía pseudo-periódica asociada. En los últimos dos capítulos de la tesis detallamos algoritmos que llevan de un mundo a otro partiendo de información combinatoria en ambos lados.

El trabajo termina con tres apéndices que son contenido adicional y no necesarios para entender lo anterior. Hay un tercer apéndice consistente de una lista exhaustiva de ejemplos ilustrando los principales resultados y algoritmos del trabajo.

# Introduction

In [A'C10] N. A'Campo introduced the notion of *tête-à-tête graph* in order to model monodromies of plane curves. These are metric ribbon graphs without univalent vertices that satisfy a special property. If one sees the ribbon graph  $\Gamma$  as a strong deformation retract of a surface  $\Sigma$  with boundary, the tête-à-tête property says that starting at any point  $p$  and walking a distance of  $\pi$  in any direction and always turning right at vertices, gets you to the same point. These particular paths are called *safe walks*, in A'Campo's words:

*“If we think of the graph as streets with intersections on the surface, we can image a safe walk as a walk staying always at the sidewalk of the street and making only right turns. So, in New York, a safe walk goes around the block by right turns only, and hence, in the same direction as the cars do. In Tokio, a safe walk is even safer, since it is opposite to the direction of the car traffic.”*

The property that the two safe walks starting at a given point have the same end, defines an element in the mapping class group  $\text{MCG}^+(\Sigma, \partial\Sigma)$  which is freely periodic, and is called the *tête-à-tête twist* associated with  $\Gamma$ . However, the monodromy of a irreducible plane branch with at least two Puiseux pairs is not freely periodic as A'Campo originally proved in [A'C73]. The goal of modeling monodromies of plane curves was not successfully achieved in that work.

In [Gra15], C. Graf dropped the singularity theory point of view and took the subject from a low-dimensional topology perspective. He proved that by allowing univalent vertices in tête-à-tête graphs, one is able to model all freely periodic mapping classes of  $\text{MCG}^+(\Sigma, \partial\Sigma)$  with positive fractional Dehn twist coefficients. He also left several questions opened as for example providing a definition to model periodic automorphisms that permute all boundary components of a surface.

This work is an organized and somehow, extended exposition of three preprints produced during the realization of the author's PhD. In order of appearance: [FPP17] (joint work with J. Fernández de Bobadilla and M. Pe Pereira), [Por17] and [PS17] (joint work with B. Sigurdsson).

We address the first issue (which we consider the most important one) of modeling monodromies of plane branches. We give a definition of mixed tête-à-tête graph (originally in [FPP17]) and prove that one can model monodromies of reduced holomorphic function germs on isolated complex singularities (originally in [PS17]). Which is the main result of the paper and is beyond the original scope of A'Campo. This result improves a previous result in [FPP17] which showed that mixed tête-à-tête graphs model monodromies of plane branches.

On the way to prove this main result, we address as well some of the questions left open by

C. Graf. First we prove a stronger version of his main result by using the original definition of tête-à-tête given by A'Campo and not allowing univalent vertices (this result originally appeared in [FPP17]). We introduce the notion of general tête-à-tête graph and prove that it is enough to model all orientation preserving periodic automorphisms of surfaces (originally in [Por17]).

We also relate the work with the existent literature on the topic of pseudo-periodic mapping classes as well as the closely related subject of graph manifolds.

This work is meant to be an introductory text to the theory of tête-à-tête graphs. It is (nearly) self-contained in the following sense: a reader which had a similar experience as the author had at the beginning of his PhD, should be able to easily follow the arguments by, only maybe, looking at references occasionally.

Below, we summarize the content of the text chapter by chapter. We highlight the main results and how they relate to the existent literature on the topic. We also specify in which of the three previous pre-prints each of these results appeared.

## Part I

Chapters 1 and 2 are the preliminaries for Part II and Chapters 3 and 4 for Part III. It also serves to fix a lot of notation and conventions. All the results that are gathered in this part are known. However, to make the text as self contained as possible we review this theory a detailed manner. Sometimes we prove some basic (but key) results for which we could not find a reference, and sometimes we re-write part of a known theory in a language that best fits our purposes. In any case, we take no priority at all in this part. It is divided in five chapters. The content of this part appeared, up to minor modifications and corrections, on preprints during the realization of this thesis as follows: Chapters 1 and 2 were contained in [FPP17] (co-authored with J. Fernández de Bobadilla and M. Pe Pereira); Chapter 3 appeared in [Por17]; the first part of Chapter 4 appeared in [Por17] and the second part in [PS17] (co-authored with B. Sigurðsson). Next, we summarize the contents of these chapters and the dependency of further chapters on these.

**Chapter 1.** It contains notions, definitions and conventions about ribbon graphs and their thickenings. This content is not used until Chapter 6 and from that chapter on, it is used in all chapters and appendices.

**Chapter 2.** Here we review the necessary theory about the mapping class group of a surface with non-empty boundary in four sections. First we focus on mapping classes in the mapping class group where isotopies are allowed to change the action on the boundary. After that, we introduce the basic blocks of which the mapping classes are built: Dehn twists. Then we treat the boundary-fixed mapping class group and study those mapping classes that are freely periodic. In this section, we introduce the important concept of *fractional Dehn twist coefficient*. In the last section we state the Nielsen-Thurston classification of automorphisms of surfaces and study those mapping classes that only have periodic pieces in their decomposition: pseudo-periodic mapping classes. For this, we state some more results on automorphisms of annuli. In particular, we introduce the *screw number* of an pseudo-periodic automorphism at an orbit of annuli. In the first three sections we mainly follow [FM12] and in the last section we mainly follow [MM11]. The theory of this chapter is necessary for Chapters 7 and 9.

**Chapter 3.** In this chapter we do a quick study of Seifert manifolds. We fix conventions and state the main properties that we use. In the end of the chapter we briefly introduce *graph manifolds*

and a combinatorial way of encoding their topology: *plumbing graphs*. The main result of this chapter is Lemma 3.13 that relates a bamboo of a plumbing graph with a gluing of two Seifert pieces of a graph manifold. This is a key tool for Part III. In this chapter we follow different references [Neu81, Ped09, JN83, NR78, Hat07] keeping our own language.

**Chapter 4.** Here we work a thorough study of horizontal open books of closed graph manifolds. The main result of this chapter is the classification given in Proposition 4.21 which depends on a previous result in the weaker context of Seifert manifolds with boundary (Lemma 4.7). We end this chapter with a section devoted to give recipes that extract the conjugacy and isotopy invariants of a pseudo-periodic automorphism from the combinatorial information that encodes a horizontal open book. This is the important content of the chapter that is used in Part III. The content of this chapter (with varying conventions) can be extracted from [Hat07, NP07, LP05, EN85].

**Chapter 5.** In this section we briefly review the concepts of singularity theory that appear somewhere in the text. We sketch some constructions and provide with references for the main results.

## Part II

The second part of the text is the main part of the document. We introduce all the definitions that were originally given by A'Campo. We introduce the notion of mixed tête-à-tête graph and we prove the main results of the work, which are *realization theorems* for each of the different types of tête-à-tête graphs. We also obtain some interesting corollaries. It is divided in five chapters.

**Chapter 6.** This is an introduction to tête-à-tête graphs. We present the original definitions and ideas by A'Campo [A'C10] of pure tête-à-tête graph and relative tête-à-tête graph. We show that the tête-à-tête property induces a periodic homeomorphism on the graph  $\Gamma$ . We also review the blow-up operation (also an idea of A'Campo) that produces relative tête-à-tête graphs from pure tête-à-tête graphs. The contents of this chapter appeared previously in [FPP17].

**Chapter 7.** We start the chapter by introducing the notion of signed tête-à-tête graph which was previously introduced by C. Graf in [Gra15], but we keep the restriction of not allowing univalent vertices. We show how a signed tête-à-tête graph defines a mapping class in  $\text{MCG}^+(\Sigma, \partial\Sigma)$  which is called tête-à-tête twist. We prove the first main theorem of the text which characterizes the mapping classes that contain a tête-à-tête twist and obtain some corollaries from it. The results of the first two sections of this chapter are contained in the joint work [FPP17] co-authored with J. Fernández de Bobadilla and M. Pe Pereira. The last section of the chapter about general tête-à-tête graphs is contained in [Por17]. The main result (which previously appeared in [FPP17]) says

**Theorem A.** *The set of mapping classes in  $\text{MCG}^+(\Sigma, \partial\Sigma)$  that can be realized by a signed tête-à-tête graph is precisely the set of freely periodic mapping classes.*

*The set of mapping classes in  $\text{MCG}^+(\Sigma, \partial\Sigma)$  that can be realized by a pure tête-à-tête graph (in the sense of A'Campo) is precisely the set of freely periodic mapping classes with strictly positive fractional Dehn twists.*

This improves the main result of [Gra15] by not allowing univalent vertices. Using relative tête-à-tête graphs we can change  $\partial\Sigma$  by a non-empty subset of it in the previous theorem. These results correspond with Theorem 7.18, Corollary 7.19 and Theorem 7.30 in the text.

We observe that one can define a truly periodic automorphism from a tête-à-tête graph as well. And obtain as a corollary of the theorem above that any truly periodic automorphism of a surface that leaves at least one boundary component invariant can be realized by a relative tête-à-tête graph. This is contained in Theorem 7.33.

To complete the theory, we introduce general tête-à-tête graphs which are ribbon graphs in which we allow some special set of univalent vertices endowed with a permutation. An analogous general tête-à-tête property is defined and a truly periodic automorphism is associated with each general tête-à-tête graph. We prove Theorem 7.40 (which previously appeared in [Por17]) and which says:

**Theorem B.** *The set of automorphisms that can be realized by a general tête-à-tête graph is the set of truly periodic automorphisms.*

**Chapter 8.** We introduce the notion of mixed tête-à-tête graph which appeared first in [FPP17]. These are metric ribbon graphs endowed with a decreasing filtration  $\Gamma^\bullet$  and a set of locally constant functions  $\delta_i : \Gamma^i \rightarrow \mathbb{R}_{\geq 0}$ . They satisfy a mixed tête-à-tête property which generalizes the tête-à-tête property.

**Chapter 9.** In this section we associate a pseudo-periodic mapping class in  $\text{MCG}^+(\Sigma, \partial\Sigma)$  to a given mixed tête-à-tête graph: the mixed tête-à-tête twist. We obtain the screw numbers from the combinatorial data of the mixed tête-à-tête graph. We prove that a mixed tête-à-tête twist has positive fractional Dehn twists and negative screw numbers, i.e., some power of a mixed tête-à-tête twist is a composition of (powers of) right-handed Dehn twists around disjoint simple closed curves.

**Chapter 10.** This chapter contains the main result of the work (Theorem 10.7) which originally appeared in a joint work with B. Sigurdson [PS17]. It characterizes the set of mapping classes that can be realized by mixed tête-à-tête twists.

**Theorem C.** *Let  $\phi : \Sigma \rightarrow \Sigma$  be an automorphism with fixes the boundary. Then there exists a mixed tête-à-tête graph in  $\Sigma$  inducing its mapping class in  $\text{MCG}^+(\Sigma, \partial\Sigma)$  if and only if some power of  $\phi$  is a composition of right handed Dehn twists around disjoint simple closed curves including all boundary components.*

A reduced holomorphic function germ on an isolated surface singularity has an associated Milnor fibration with a monodromy which fixes the boundary. It is known that this monodromy is pseudo-periodic and a power of it is a composition of right-handed Dehn twists around disjoint simple closed curves, which include all the boundary curves. It follows that the Milnor fiber associated with such a function germ contains a mixed tête-à-tête graph which defines the monodromy. Conversely, a result by Neumann and Pichon [NP07] says that any such a surface automorphism is realized as the monodromy associated with a function germ. Hence we get the corollary (which also appeared in [PS17])

**Theorem D.** *Mixed tête-à-tête twists are precisely the monodromies associated with reduced function germs defined on isolated surface singularities.*

It is worth noting that this result improves a previous result in the joint work [FPP17] where we proved that mixed tête-à-tête graphs model monodromies of plane branches (which was the expected scope of the definition). To be able to refine the proof in that work in order to prove Theorem C., one has to deal with certain non-trivial combinatorics problems. This process is carried out with detail in this chapter.

## Part III

The mapping torus of a pseudo-periodic surface automorphism is a graph manifold. Conversely, a horizontal surface of a fiber-oriented graph manifold has a pseudo-periodic monodromy induced on it. Hence, it is a natural problem to assign a graph manifold and a horizontal surface to each mixed tête-à-tête graph and, whenever possible, assign a mixed tête-à-tête graph to a given horizontal surface in a graph manifold. In this part we provide algorithms producing a graph manifold and a fibration over  $S^1$  from a mixed tête-à-tête graph and vice versa. In particular, this provides a direct and effective way to check if two mixed tête-à-tête graphs represent conjugate mapping classes in  $\text{MCG}^+(\Sigma, \partial\Sigma)$ .

It is divided in two chapters. Chapter 11 solves the problem for the weaker case of horizontal surfaces in Seifert manifolds with boundary and Chapter 12 analyzes the case of horizontal open books in closed graph manifolds. We use the theory developed in Chapters 3 and 4.

## Appendices

The work ends with three appendices that are additional content and are not strictly necessary to understand the previous content. Appendices A and B appeared in an early version of [FPP17] but were subsequently removed.

**Appendix A.** We take the notion of *regular* filtered metric ribbon graph which is a restricted type of graph which in particular includes the mixed tête-à-tête graphs of plane branches. In this appendix we study which  $\delta_\bullet$  functions can endow a given regular filtered metric ribbon graph with the structure of mixed tête-à-tête graph.

**Appendix B.** We follow the construction of the monodromy of an irreducible plane curve singularity given in [AC73] to, algorithmically, produce a mixed tête-à-tête graph that models that monodromy. More concretely, we give a recipe for the mixed tête-à-tête graph from the characteristic Puiseux pairs of the singularity.

**Appendix C.** We end the work with a collection of detailed examples that are cited throughout the text. They illustrate the main theorems and constructions as well as the algorithms of the last part.

Part I



Preliminary theory





## Chapter 1

---

# Ribbon graphs

This first chapter fixes some notation, conventions and basic constructions about ribbon graphs that are used throughout the text.

**Definition 1.1.** *A graph  $\Gamma$  is a 1-dimensional finite CW-complex.*

We denote by  $v(\Gamma)$  the 0-skeleton and refer to it as the *set of vertices*. We denote by  $e(\Gamma)$  the disjoint union of the 1-cells and refer to it as the *set of edges*. With this definition we allow *loops*, which correspond to 1-cells whose attaching map is constant, and we also allow several edges connecting two vertices. For a vertex  $v$  we denote by  $e(v)$  the set of edges adjacent to  $v$ , where an edge  $e$  appears twice in case it is a loop joining  $v$  with  $v$ . The *valency* of a vertex is the cardinality of  $e(v)$  (a loop counts twice). Unless we state the contrary we assume that there are no vertices of valency 1.

We consider graphs that appear as regular retracts of oriented surfaces  $\Sigma$  with non-empty boundary.

**Definition 1.2.** *A graph  $\Gamma$  embedded in a surface  $\Sigma$  is a regular retract or a spine if there exists a strong deformation retraction  $r : \Sigma \times [0, 1] \rightarrow \Sigma$  onto  $\Gamma$  such that  $r|_{\partial\Sigma \times [0, 1]}$  is a homeomorphism onto  $\Sigma \setminus \Gamma$  and  $r(\cdot, 1)|_{\partial\Sigma} : \Sigma \rightarrow \Gamma$  is locally injective. We say that  $r$  is a regular retraction and that  $\Sigma$  is a regular neighborhood or a regular thickening of  $\Gamma$ .*

A *regular thickening* of a graph  $\Gamma$  is codified by a cyclic order of  $e(v)$  for every  $v \in v(\Gamma)$  in the following way. Assume that for every  $v \in v(\Gamma)$  the set  $e(v)$  is cyclically ordered:

$$e(v) = \{e_1, \dots, e_k\}.$$

For each vertex  $v \in v(\Gamma)$  we draw in  $\mathbb{R}^2$  a star-shaped graph consisting of  $v$  and as many arms as elements in  $e(v) = \{e_1, \dots, e_k\}$  which are drawn counterclockwise. Now, we thicken it constructing a star-shaped planar piece as in Figure 1.4, which comes equipped with a unique orientation if the valency of the vertex is at least 3. In the case of valency-2-vertices choose one of the possible orientations.

**1.3.** Whenever there is an edge  $e$  joining vertices  $v_i$  and  $v_j$ , we glue the corresponding thickened arms of the star-shaped pieces in the way that produces an oriented surface, and identifying points of the corresponding edges. If there is at least a vertex in the graph with valency at least 3, this procedure gives a unique orientation in the surface. If there are only valency-2-vertices, then the surface is an oriented annulus, and the orientation depends on the choice of orientations of the 2-star shaped pieces. We choose one of the possible orientations.

In this way we obtain a connected oriented surface  $\Sigma$  with boundary and with the graph  $\Gamma$  embedded in it. We say  $\Sigma$  is the *thickening* of  $\Gamma$  and we write  $(\Sigma, \Gamma)$ .

Reciprocally, every connected oriented surface with finite topology and non-empty boundary has a *spine*  $\Gamma$  (i.e. an embedded graph in  $\Sigma \setminus \partial\Sigma$  that is a *regular retract* of  $\Sigma$ ) and certain cyclic orders in the subsets of edges adjacent to every vertex such that  $\Sigma$  is homeomorphic to the thickening of  $\Gamma$ .

In this way, we can model the topology of every connected oriented surface with non-empty boundary except the disk.

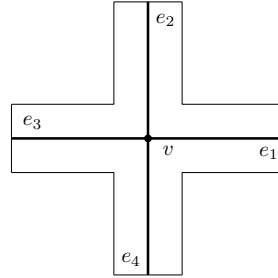


**Figure 1.4:** Star-shaped piece for some vertex  $v$  of valency 4.

**Definition 1.5.** A ribbon graph is a graph  $\Gamma$  equipped with a cyclic order of  $e(v)$  for each  $v \in v(\Gamma)$ . The surface  $\Sigma$  constructed above is the thickening of  $\Gamma$ . And  $\Gamma$  is a spine of  $\Sigma$ .

**Example 1.6.** Let  $K_{p,q}$  be the bipartite complete graph  $(p, q)$ . The set of vertices is the union of two sets  $A$  and  $B$  of  $p$  and  $q$  vertices respectively. The edges are exactly all the possible non-ordered pairs of points one in  $A$  and one in  $B$ .

Now we fix cyclic orders in  $A$  and  $B$ . These give cyclic orders in the sets of edges adjacent to vertices in  $B$  and  $A$  respectively. One can check that the thickening surface has as many boundary components as  $\gcd(p, q)$  and genus equal to  $\frac{1}{2}[(p-1)(q-1) - \gcd(p, q) + 1]$ .

In Figure 1.7 we can see the example of  $K_{2,3}$ .

Following A'Campo [A'C10], we introduce a generalization of the notion of spine of a surface with boundary  $\Sigma$ , which treats in a special way a certain union of boundary components. Let us start by the corresponding graph theoretic notion.

Let  $(\Gamma, A)$  be a pair formed by a graph  $\Gamma$  and an oriented subgraph  $A$ , such that each of its connected components  $A_i$  is homeomorphic to the oriented circle  $\mathbb{S}^1$ . Let  $v$  be any vertex of  $\Gamma$ . If  $v \in A$ , since the connected components of  $A$  are circles, there are at most two elements in  $e(v)$  that belong to  $A$ , and in this case they belong to the same component  $A_i$ . We say that a cyclic order of  $e(v)$  is *compatible* with the orientation of  $A$  if the elements of  $e(v)$  can be enumerated as  $e(v) = \{e_1, \dots, e_k\}$  in such a way that

1.  $e_i < e_{i+1}$  and  $e_k < e_1$ ,

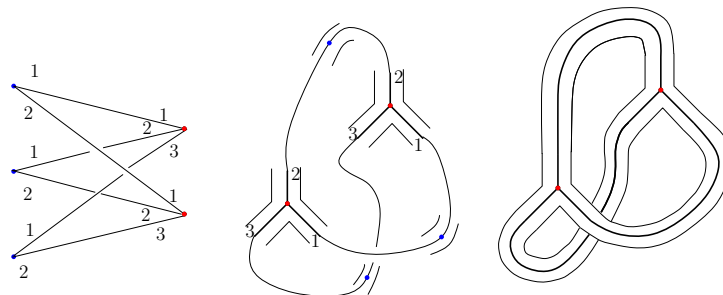


**Figure 1.7:** Thickening of the graph  $K_{2,3}$  in three steps. First we have a planar projection of  $K_{2,3}$  where the two subsets of vertices are vertically ordered in two parallel lines. Then we thicken a neighborhood of every vertex and finally we glue the pieces. The resulting surface is homeomorphic to the once-punctured torus.

2. the edges belonging to  $A_i$  are  $e_1$  and  $e_k$ ,
3. if we consider a small interval in  $A_i$  around  $v$  and we parametrize it in the direction induced by the orientation of  $A_i$ , then we pass first by  $e_1$  and after by  $e_k$ .

**Definition 1.8.** Let  $(\Gamma, A)$  be a pair formed by a graph  $\Gamma$  and a oriented subgraph  $A$  as above. The pair is a relative ribbon graph if for any vertex  $v$  the set of incident edges  $e(v)$  is endowed with a cyclic order compatible with the orientation of  $A$ .

We define the *thickening surface* of a relative ribbon graph  $(\Gamma, A)$  as follows.

**1.9.** We consider star shaped pieces as in Figure 1.4 for every vertex in  $\Gamma \setminus A$ . For every component  $A_i$  we consider a partial thickening of  $A_i$  with as many arms as edges with a vertex in  $A_i$  as in Figure 1.10. We glue arms of different pieces corresponding to the same edges as in 1.3, in such a way that the resulting surface admits an orientation that induces on  $A$  its opposite orientation. This is the orientation that we had previously fixed on  $\Sigma$ . The output of this procedure is a pair  $(\Sigma, A)$  given by an oriented surface and an union  $A$  of its boundary components.

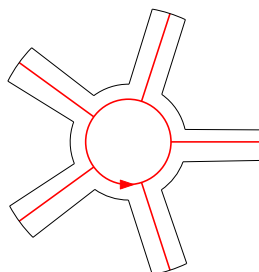


**Figure 1.10:** Partial thickening of  $A_i$  with 5 arms, this corresponds to a collar of a boundary component of a surface. The arrow indicates the orientation of  $A_i$  which is the opposite orientation that it inherits as boundary component of  $\Sigma$ .

It is clear that  $\Gamma$  is a regular retract of the thickening surface. Reciprocally: for any pair  $(\Sigma, A)$  given by an oriented surface and a union of some boundary components, if there is a graph  $\Gamma$  embedded in  $\Sigma$  and containing  $A$ , such that  $\Gamma$  is a regular retract of  $\Sigma$ , then we say that  $(\Sigma, A)$  is the thickening of  $(\Gamma, A)$ .

**Notation 1.11.** From now on the letter  $I$  denotes an interval. Unless it is otherwise specified, it denotes the unit interval  $I$ . Let  $(\Gamma, A)$  be a relative ribbon graph, whose thickening is  $(\Sigma, A)$ . There is a connected component of  $\Sigma \setminus \Gamma$  for each boundary component  $C_i$  of  $\Sigma$  not contained in  $A$ , this component is homeomorphic to  $C_i \times [0, 1)$  (this homeomorphism or *product structure* is given by the choice of regular retraction Definition 1.2).

We denote by  $\tilde{\Sigma}_i$  the compactification of  $C_i \times (0, 1]$  to  $C_i \times I$ . We denote by  $\Sigma_\Gamma$  the surface obtained by *cutting*  $\Sigma$  *along*  $\Gamma$ , that is the disjoint union of the  $\tilde{\Sigma}_i$ . An identification of  $\Sigma_\Gamma$  with  $\partial\Sigma \times I$  is also called a *product structure*. This identification is not unique.

Let

$$g_\Gamma : \Sigma_\Gamma \rightarrow \Sigma$$

be the gluing map. We denote by  $\tilde{\Gamma}_i$  the boundary component of the cylinder  $\tilde{\Sigma}_i$  that comes from the graph (that is  $g_\Gamma(\tilde{\Gamma}_i) \subset \Gamma$ ) and by  $C_i$  the one coming from a boundary component of  $\Sigma$  (that is  $g_\Gamma(C_i) \subset \partial\Sigma$ ). From now on, we take the convention that  $C_i$  is identified with  $C_i \times \{0\}$  and that  $\tilde{\Gamma}_i$  is identified with  $C_i \times \{1\}$ . We set  $\Sigma_i := g_\Gamma(\tilde{\Sigma}_i)$  and  $\Gamma_i := g_\Gamma(\tilde{\Gamma}_i)$ . Finally we denote  $g_\Gamma(C_i)$  also by  $C_i$  since  $g_\Gamma|_{C_i}$  is bijective. The orientation of  $\Sigma$  induces an orientation on every cylinder  $\tilde{\Sigma}_i$  and on its boundary components.

## Chapter 2

---

# Mapping class groups

In this chapter we review some aspects of the group of homeomorphisms of a surface up to isotopy: *the mapping class group*. We distinguish between isotopies that are allowed to change the action on the boundary and those which are not. This distinction leads to different notions of mapping class group .

All of this material is widely known. For example, two good references on the topic are [FM12] for the general theory of mapping class group of surfaces, and [CB88] for the more specific subject of the Nielsen-Thurston classification of automorphisms of surfaces. For the sake of completeness and to make this work as self contained as possible, we prove some of these basic results for which there was not a canonical reference.

We start with the first notion of mapping class group.

**Definition 2.1.** *We say that two homeomorphisms  $\phi$  and  $\psi$  of  $\Sigma$  are boundary free isotopic or freely isotopic if there exists a family of homeomorphisms of  $\Sigma$ , namely, a continuous map*

$$\theta : \Sigma \times I \rightarrow \Sigma$$

*such that  $\theta_s(x) := \theta(x, s)$  is a homeomorphism of  $\Sigma$  for each  $s \in I$ , and such that  $\theta_0 = \phi$  and  $\theta_1 = \psi$ . We write  $[\psi] = [\phi]$ . The mapping class group  $\text{MCG}(\Sigma)$  is the group of equivalence classes with the operation induced by composition of homeomorphisms.*

*We denote by  $\text{MCG}^+(\Sigma)$  the subgroup of orientation preserving homeomorphisms up to isotopy.*

*A homeomorphism of a surface is periodic in  $\text{MCG}(\Sigma)$  or periodic up to boundary free isotopy if there exists  $n \in \mathbb{N}$  such that  $[\phi^n] = [id]$ , i.e. if it is a finite order element of the mapping class group.*

We are also interested in isotopy classes of automorphisms where we ask the isotopy to preserve the action on the boundary. This leads to a different notion of mapping class group.

**Definition 2.2.** *Given two homeomorphisms  $\phi$  and  $\psi$  of  $\Sigma$  that both leave invariant some subset  $B \subset \partial\Sigma$  such that  $\phi|_B = \psi|_B$ , we say they are isotopic relative to the action  $\phi|_B$  if there exists a family of homeomorphisms of  $\Sigma$  that isotope them as before and such that any homeomorphism of*

the family has the same restriction to  $B$  as  $\phi$  and  $\psi$ . We write  $[\phi]_{B, \phi|_B} = [\psi]_{B, \phi|_B}$ . We denote by  $\text{MCG}(\Sigma, B, \phi|_B)$  the set of classes  $[\phi]_{B, \phi|_B}$  with respect to this equivalence relation. We denote by  $\text{MCG}^+(\Sigma, B, \phi|_B)$  if we restrict to homeomorphisms preserving orientation.

If the action is the identity on  $B$ , we omit the action in the notation and recover the classical notion of isotopy relative to  $B$ , that means that all the homeomorphisms in the isotopy fix  $B$  pointwise. We write these classes simply by  $[\phi]_B$  and we denote by  $\text{MCG}^+(\Sigma, B)$  the set of homeomorphisms up to isotopy relative to  $B$  that preserve orientation.

In the case  $B = \partial\Sigma$  we will simply write  $[\phi]_{\partial, \phi|_{\partial}}$  or  $[\phi]_{\partial}$ .

If  $B$  is the whole boundary  $\partial\Sigma$  we recover the classical notion of mapping classes fixing pointwise the boundary and the group  $\text{MCG}(\Sigma, \partial\Sigma)$ . If  $B$  is empty we are in the case of Definition 2.1 and we recover the mapping class group up to *boundary free isotopy*. These two extreme cases are the most important, but we will need the more general notion when we develop later relative tête-à-tête homeomorphisms fixing pointwise the union of some boundary components that we denote by  $\partial^1\Sigma$ .

Observe that  $\text{MCG}(\Sigma, \partial, \phi|_{\partial})$  is not a group. However, the group  $\text{MCG}(\Sigma, \partial\Sigma)$  acts transitive and freely on it, i.e., it is a  $\text{MCG}(\Sigma, \partial\Sigma)$ -torsor.

**Remark 2.3.** There exists analogous definitions changing *homeomorphism* by *diffeomorphism* in Definitions 2.1 and 2.2. Nevertheless, it is proved in [FM12, Section 1.4] that in each class of homeomorphisms there is a unique class of diffeomorphisms contained. So the two mapping class groups are canonically isomorphic. For this reason, when differentiability is not a central matter of the discussion we use either the term homeomorphism or the term *automorphism* of a surface.

In 1974, Thurston proved what is known as the *Nielsen-Thurston classification*. This classification says that, up to isotopy, you can break any diffeomorphism  $\phi : \Sigma \rightarrow \Sigma$  of a surface into *periodic* pieces and *pseudo-Anosov* pieces by cutting along an invariant system of simple closed curves.

A periodic piece is a subsurface  $\tilde{\Sigma} \subset \Sigma$  such that  $\phi|_{\tilde{\Sigma}}$  is a finite-order diffeomorphism.

A pseudo-Anosov piece is a subsurface  $\tilde{\Sigma} \subset \Sigma$  such that  $\phi|_{\tilde{\Sigma}}$  is pseudo-Anosov: there is a couple of singular transverse measured foliations  $(\mathcal{F}^u, \mu_u), (\mathcal{F}^s, \mu_s)$  that are preserved by  $\phi|_{\tilde{\Sigma}}$  and whose stretch factors are  $\lambda$  and  $\lambda^{-1}$ . Since the present work does not deal with pseudo-Anosov diffeomorphisms we omit definitions for these diffeomorphisms. A detailed exposition of the topic can be found in [FM12, Chapters 13 and 14].

A refined version of the Nielsen-Thurston classification is the following theorem.

**Theorem 2.4** (Equivalent to Corollary 13.3 in [FM12]). *Let  $\phi : \Sigma \rightarrow \Sigma$  be an orientation preserving diffeomorphism that fixes pointwise a subset of boundary components  $\partial^1\Sigma \subset \Sigma$  possibly empty. Then, there exist*

- A collection  $\mathcal{C}$  of disjoint simple closed curves that includes boundary-parallel curves for all boundaries in  $\partial^1\Sigma$ .
- A collection  $\mathcal{A}$  of pairwise disjoint tubular neighborhoods  $\mathcal{A}_i$  for each curve  $C_i$  in  $\mathcal{C}$ .
- A diffeomorphism in the same class, that is,  $\hat{\phi} \in [\phi]_{\partial^1}$ .

Such that:

- $\hat{\phi}(\mathcal{C}) = \mathcal{C}$  and  $\hat{\phi}(\mathcal{A}) = \mathcal{A}$ .
- $\hat{\phi}$  restricted to each connected component of  $\overline{\Sigma \setminus \mathcal{A}}$  (and its iterations by  $\hat{\phi}$ ) is either periodic or pseudo-Anosov.

In this work, we focus on the study of automorphisms that only contain periodic pieces in this classification: pseudo-periodic automorphisms. We start by talking about finite-order mapping classes in  $\text{MCG}(\Sigma)$  which is the most simple case. Then we do a brief introduction to Dehn twists and we pass on to the study of mapping classes in  $\text{MCG}^+(\Sigma, \partial\Sigma)$  which are of finite order when seen in  $\text{MCG}^+(\Sigma)$ . These sections prepare the reader with the necessary tools to understand Chapter 7.

We end the chapter with a review of the theory of mapping classes that only contain periodic pieces in their classification but that are not (in general) of finite order: pseudo-periodic mapping classes. This last section also contains results about automorphisms of collections of cylinders. It prepares the reader to understand the constructions in Chapter 9.

## 2.1 Periodic automorphisms in $\text{MCG}^+(\Sigma)$

In this section we focus on the case  $\partial^1\Sigma = \emptyset$ . Thus we assume all isotopies to be boundary free. A key result, only true in dimension 2 (see [RS77]), is the following classical theorem:

**Theorem 2.5** (Nielsen's Realization Theorem [Nie43], also see Theorem 7.1 in [FM12]). *If  $\phi^n$  is isotopic to the identity, then there exists  $\hat{\phi} \in [\phi]$  such that  $\hat{\phi}^n = \text{Id}$ . Moreover, there exists a metric on  $\Sigma$  such that  $\hat{\phi}$  is an isometry.*

Note that the theorem above is included in Theorem 2.4.

**Lemma 2.6.** *Let  $\phi : \Sigma \rightarrow \Sigma$  be an orientation-preserving isometry of  $\Sigma$ . Then either the fixed points are isolated or  $\phi$  is the identity. Moreover, if  $\phi$  is a periodic homeomorphism, then the ramification points are also isolated.*

*Proof.* Let  $x$  be an accumulation point of the set of fixed points, let  $B$  be a small geodesic ball around  $x$  and let  $y \in B$  be a different fixed point. Let  $z \in B$  be any other point. We are going to show that  $z$  is also a fixed point. Take the only geodesic path  $\gamma$  joining  $x$  and  $y$  and the only geodesic path  $\gamma'$  joining  $x$  and  $z$ . Since  $x$  and  $y$  are fixed points and the image of a geodesic by an isometry is a geodesic, then  $\gamma$  is fixed by  $\phi$ . We have that the image of  $\gamma'$  by  $\phi$  is also a geodesic and since the angle that  $\gamma$  and  $\gamma'$  form at  $x$  must be preserved, there are only two possibilities for the image of  $\gamma'$ . One of them inverts orientation and the other sends  $\gamma'$  to itself. So  $\gamma'$  is also formed by fixed points, and in particular  $z$  is a fixed point.

The second part of the statement follows by applying the same argument to a power of  $\phi$ .  $\square$

**Notation 2.7.** Let  $\phi$  be a periodic orientation preserving homeomorphism of  $\Sigma$  that is not the identity. Since  $\phi$  acts properly discontinuously on  $\Sigma$ , the orbit space  $\Sigma^\phi$  is a surface and the quotient map

$$p : \Sigma \rightarrow \Sigma^\phi$$

is a Galois branched covering map. The set of points in  $\Sigma$  whose orbit has cardinality strictly smaller than the order of  $\phi$  are called *ramification* points. Its images by  $p$  are called *branch* points.

**Remark 2.8.** Since the covering map  $p$  is Galois, any point at the preimage by  $p$  of a branch point is a ramification point.



**Definition 2.9.** Let  $\phi$  be a homeomorphism of  $\Sigma$  that leaves a boundary component  $C_i \subseteq \partial\Sigma$  invariant. We cap this boundary component  $C_i$  with a disk  $D^2$  obtaining a new surface  $\Sigma'$ . We extend  $\phi$  to a periodic orientation-preserving homeomorphism of  $\Sigma'$  as follows: if  $\theta$  is the angular and  $r$  the radial coordinates for  $D^2$  then we define  $\Phi : D^2 \rightarrow D^2, (\theta, r) \mapsto (r, \phi(\theta))$ . The homeomorphisms  $\Phi$  and  $\phi$  glue along  $C_i$ . This procedure is called the Alexander trick.

**Lemma 2.10.** Let  $\phi : \Sigma \rightarrow \Sigma$  be an orientation-preserving periodic homeomorphism of  $\Sigma$  that is not the identity. Then all the ramification points of  $p : \Sigma \rightarrow \Sigma^\phi$  are in the interior of  $\Sigma$ .

*Proof.* A ramification point is a point such that  $\phi^k(x) = x$  but  $\phi^k \neq \text{id}$ . Hence, replacing  $\phi$  by  $\phi^k$  it is enough to prove that there are no fixed points at the boundary. If there is a fixed point  $p$  at the boundary, since  $\phi$  leaves invariant the boundary and preserves orientation, it has to fix the boundary near  $x$ , but since ramification points are isolated, then  $\phi$  has to be the identity.  $\square$

**Corollary 2.11.** Given a periodic homeomorphism  $\phi$  of a surface that leaves all the boundary components invariant, the restriction to any boundary component has the same order than  $\phi$ .

**Remark 2.12.** Given  $\phi$  and  $\psi$  two homeomorphisms of  $\Sigma$  that both leave a spine  $\Gamma$  invariant, if  $\phi|_\Gamma$  and  $\psi|_\Gamma$  are isotopic, then  $\phi$  and  $\psi$  are isotopic. In other words, the isotopy type of the restriction of a homeomorphism to an invariant spine determines the isotopy type of the homeomorphism of  $\Sigma$ . This follows from the fact that  $\Sigma_\Gamma$  is a collection of cylinders  $\tilde{\Sigma}_i$  and the mapping class group  $\text{MCG}(\tilde{\Sigma}_i, \tilde{\Gamma}_i, \phi|_{\tilde{\Gamma}_i})$  is trivial. Recall Notation 1.11 and Definition 2.2.

**Lemma 2.13.** Let  $\Sigma$  be a surface with  $\partial\Sigma \neq \emptyset$  which is not a disk or a cylinder. Let  $\phi : \Sigma \rightarrow \Sigma$  be an orientation preserving homeomorphism. Then  $\phi$  is periodic up to isotopy if and only if there exists  $\hat{\phi} \in [\phi]$  such that there exists a spine  $\Gamma$  of  $\Sigma$  which is invariant by  $\hat{\phi}$ .

*Proof.* Assume  $\phi$  is periodic up to isotopy. By Nielsen's realization Theorem (Theorem 2.5) we can assume that  $\phi$  is periodic. Let  $\Sigma^\phi$  be the orbit space of  $\phi$ .

The quotient map  $p : \Sigma \rightarrow \Sigma^\phi$  is a branched covering map whose ramification points are isolated and are contained in the interior of  $\Sigma$  by Lemmas 2.6 and 2.10. Pick any spine  $\Gamma^\phi$  for  $\Sigma^\phi$  containing all the branch points. We claim that  $\Gamma := p^{-1}(\Gamma^\phi)$  is an invariant spine for  $\Sigma$ . Indeed, it is invariant by construction since the preimage of every point is precisely the orbit of that point. Since  $\Gamma^\phi$  is a spine of  $\Sigma^\phi$  then there exists a regular retraction  $\Sigma^\phi \times I \rightarrow \Gamma^\phi$ . Since  $\Gamma^\phi$  contains all ramification points, that retraction lifts to a retraction from  $\Sigma$  to  $\Gamma$ .

Conversely, assume that an invariant spine  $\Gamma$  exists for some  $\hat{\phi} \in [\phi]$ . Since  $\hat{\phi}$  leaves the spine invariant. We consider the spine with a graph structure only with vertices of valency greater than 2. Then  $\hat{\phi}$  acts as a permutation on edges and the vertices. Then, there is a power of  $\hat{\phi}$ , say  $\hat{\phi}^m$  that leaves all the edges and vertices invariant. Then, we just observe that given any two intervals  $I, I'$ , any two orientation preserving homeomorphisms  $h, g : I \rightarrow I'$  are isotopic relative to the boundary of  $I$ . Thus,  $\hat{\phi}^m|_\Gamma$  is isotopic to the identity. Since  $\Gamma$  is a spine, by Remark 2.12 we find that  $\hat{\phi}^m$  is isotopic to the identity.  $\square$

In the theorem above we excluded the cases when  $\Sigma$  is a cylinder or a disk for being trivial. In this case every homeomorphism is isotopic to a periodic one.

**Notation 2.14.** If a homeomorphism  $\phi$  of  $\Sigma$  leaves a spine  $\Gamma$  invariant, then the homeomorphism lifts to a homeomorphism of  $\Sigma_\Gamma$  that we denote by  $\tilde{\phi}$ .

For a periodic homeomorphism that leaves a boundary component invariant there is a notion of rotation number associated to that boundary component:

**Definition 2.15.** Let  $\phi : \mathbb{S}^1 \rightarrow \mathbb{S}^1$  be an orientation preserving periodic homeomorphism of the circle of order  $q$ . Let  $x \in \mathbb{S}^1$  and let  $x^\phi$  be the orbit of  $x$  by  $\phi$  and let  $p$  be the number of points in  $x^\phi$  that lie on the arc connecting  $x$  with  $\phi(x)$  in the positive direction. We define the rotation number of  $\phi$  as the quotient  $\frac{p}{q}$  and we denote it by  $\text{rot}(\phi)$ . The fraction  $\frac{p}{q}$  is always reduced and the number  $p/q$  is in the interval  $(0, 1]$ .

The above definition corresponds to Poincaré's classical notion of rotation number of a homeomorphism of a circle into itself. Poincaré's rotation number takes values in  $\mathbb{R}/\mathbb{Z}$ , and in  $\mathbb{Q}/\mathbb{Z}$  if the homeomorphism is periodic. We are taking the unique representative in the interval  $(0, 1]$ .

The following is well-known:

**Lemma 2.16.** Let  $\phi$  be an orientation preserving periodic homeomorphism of the circle such that  $\text{rot}(\phi) = p/q$ , then  $\phi$  is conjugate to the rotation of  $2\pi\frac{p}{q}$  radians.

**Corollary 2.17.** An orientation preserving periodic homeomorphism of the cylinder which leaves invariant each boundary component is conjugate to a rotation.

## 2.2 Dehn twists

Let  $\mathcal{A}$  be an annulus. The mapping class group  $\text{MCG}^+(\mathcal{A}, \partial\mathcal{A}) \simeq \mathbb{Z}$  and it is generated by a right-handed Dehn twist. All its elements are freely isotopic to the identity, i.e.  $\text{MCG}^+(\Sigma) \simeq \{1\}$ .

**Definition 2.18** (Dehn twist). Let  $\mathcal{D} : \mathbb{S}^1 \times I \rightarrow \mathbb{S}^1 \times I$  be the homeomorphism defined by  $\mathcal{D}(x, t) = (x + t, t)$  where  $\mathbb{S}^1 = \mathbb{R}/\mathbb{Z}$ . A homeomorphism  $\phi : A \rightarrow A$  of an annulus is said to be a right-handed Dehn twist if there exists a parametrization  $\eta : \mathbb{S}^1 \times I \rightarrow A$  such that  $\phi$  is isotopic to  $\eta \circ \mathcal{D} \circ \eta^{-1}$ .

Let  $\Sigma$  be a surface and let  $\alpha$  be a simple closed curve in  $\Sigma$  and  $N$  a tubular neighborhood of  $\alpha$ . A right-handed Dehn twist around  $\alpha$  is a homeomorphism of  $\Sigma$  that is a Dehn twist in  $N$  and the identity outside  $N$ . It is well defined up to isotopy.

The inverse of a right-handed Dehn twist is a left-handed Dehn twist.

**Remark 2.19.** In this work we take the convention that what we call *negative* Dehn twists are *right-handed* Dehn twists. See Figure 2.20.

Note that depending on the source, these are sometimes called *positive* Dehn twists. Our convention agrees, for example, with [MM11].

Let  $\Sigma$  be a surface with non empty boundary  $\partial\Sigma$ . Consider a non-empty union  $\partial^1\Sigma$  of boundary components. Let  $\phi$  be an orientation preserving homeomorphism of  $\Sigma$ , fixing pointwise  $\partial^1\Sigma$  and freely isotopic to a periodic one  $\hat{\phi}$ . Our next aim is to define a notion of *fractional Dehn twist coefficient* at each connected component of  $\partial^1\Sigma$ .

We start recalling some facts about Dehn twists. If we do not say the contrary, the letter  $\mathcal{D}$  with a subindex, denotes a negative (right-handed) Dehn twist around some curve that will be clear from the context.

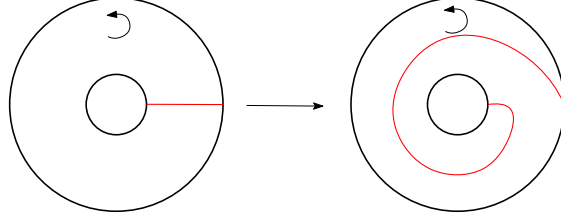


**Figure 2.20:** We see an oriented annulus on the left and the image of the red curve by a right-handed Dehn twist on the right. The little curve on the top of each picture represents the orientation on the annulus.

**Lemma 2.21.** *Let  $\alpha_1, \dots, \alpha_m$  be a set of non-trivial, pairwise disjoint, and pairwise non-homotopic closed curves. Then the group generated by Dehn twists along those curves  $\langle \mathcal{D}_{\alpha_1}, \dots, \mathcal{D}_{\alpha_m} \rangle$  is free abelian of rank  $m$ .*

*Proof.* See [FM12, Lemma 3.17]. □

**Corollary 2.22.** *Let  $\Sigma$  be a surface with  $r > 0$  boundary components that is not a disk or an annulus. Then the group generated by the Dehn twists  $\mathcal{D}_1, \dots, \mathcal{D}_r$  along curves parallel to each boundary component is free abelian of rank  $r$ .*

*Proof.* Except when  $\Sigma$  is a disk or an annulus, the set of boundary parallel curves is in the hypothesis of Lemma 2.21. □

## 2.3 Freely periodic automorphisms

Now we focus on the mapping class group where homeomorphisms and isotopies fix pointwise the union of some boundary components that we denote by  $\partial^1 \Sigma \subset \partial \Sigma$  (recall Definition 2.2).

Consider a non-empty union  $\partial^1 \Sigma$  of boundary components. In this section we study the elements of  $\text{MCG}^+(\Sigma, \partial^1 \Sigma)$  that are freely isotopic to a periodic one. If  $\phi : \Sigma \rightarrow \Sigma$  is a homeomorphism with  $\phi|_{\partial^1 \Sigma} = \text{id}$ , we denote by  $[\phi]_{\partial^1}$  its class in  $\text{MCG}^+(\Sigma, \partial^1 \Sigma)$ .

In the following lemma we see in that the isotopy class fixing  $\partial^1 \Sigma$  pointwise there is always a representative leaving a spine invariant.

**Lemma 2.23.** *Let  $\phi$  be an orientation preserving homeomorphism of a surface  $\Sigma$  which fixes pointwise a non-empty union  $\partial^1 \Sigma$  of boundary components, and which is freely isotopic to a periodic homeomorphism  $\hat{\phi}$ . Then there exists a collar  $U$  of  $\partial^1 \Sigma$ , a homeomorphism  $f : \Sigma \rightarrow \Sigma \setminus \overline{U}$ , and a homeomorphism  $\psi$  of  $\Sigma$  such that:  $\psi$  is isotopic relative to  $\partial^1 \Sigma$  to  $\phi$  and the restriction  $\psi|_{\Sigma \setminus \overline{U}}$  is periodic and equal to  $f \circ \hat{\phi} \circ f^{-1}$ .*

*In particular  $\psi$  leaves a spine  $\Gamma$  invariant and  $\psi|_{\Gamma}$  is periodic.*

*Proof.* Let  $V$  be a collar neighborhood of  $\partial^1 \Sigma$  parametrized as  $V \simeq \partial^1 \Sigma \times I$  where  $\partial^1 \Sigma \cap V$  corresponds to  $\partial^1 \Sigma \times \{1\}$ . Let  $U_t := \partial^1 \Sigma \times [1-t/2, 1]$  with  $t \in I$  be a family of collar neighborhoods contained in  $V$  and denote  $U := U_1$ .

Let  $f_t : \Sigma \rightarrow \Sigma \setminus \overline{U_t}$  with  $t \in I$ , be a family of maps defined by

$$f_t|_V(x, s) := (x, (1-t/2) \cdot s), \quad f_t|_{\Sigma \setminus \overline{V}} := \text{id}.$$

Observe that  $f_0 = \text{id}$  and that  $f := f_1$  sends  $\Sigma$  to  $\overline{\Sigma \setminus U}$  homeomorphically.

We define  $\psi$  as follows:

$$\psi|_{\overline{\Sigma \setminus U}} := f \circ \hat{\phi} \circ f^{-1}, \quad \psi|_U := \Phi|_{\partial^1 \Sigma \times I}.$$

And observe that it satisfies the condition of the statement.

And finally, we define the isotopy  $\Psi_t$  from  $\phi$  to  $\psi$  by:

$$\Psi_t(x) = \begin{cases} f_t \circ \Phi_t \circ f_t^{-1} & \text{if } x \in \overline{\Sigma \setminus U_t} \\ (\Phi_s(x'), s) & \text{if } x = (x', s) \in U_t \simeq \partial^1 \Sigma \times [1 - t/2, 1] \end{cases}$$

The last assertion of the theorem is Lemma 2.13 applied to  $\psi|_{\overline{\Sigma \setminus U}}$ .  $\square$

**Lemma 2.24.** *Let  $\Sigma$  be a surface that is neither a disk nor a cylinder. Let  $\partial^1 \Sigma$  be non-empty union of  $r$  boundary components of  $\Sigma$ . Let  $\phi$  be an orientation preserving homeomorphism of  $\Sigma$  fixing  $\partial^1 \Sigma$  pointwise. If  $\phi$  is freely isotopic to the identity then there exist unique integers  $n_1, \dots, n_r$  such that the following equality of mapping classes holds:*

$$[\phi]_{\partial^1} = [D_1^{n_1}]_{\partial^1} \cdot \dots \cdot [D_r^{n_r}]_{\partial^1}.$$

*Proof.* By Lemma 2.23 we can assume that  $\phi$  is the identity outside a collar neighborhood  $U = \bigsqcup U_i$  of  $\partial^1 \Sigma$  where  $U_i$  is a collar for the boundary component  $C_i$ . The restrictions  $[\phi|_{U_i}]_{\partial}$  are elements in  $\text{MCG}^+(U_i, \partial U_i)$ . Since the  $U_i$  are cylinders, the group  $\text{MCG}^+(U_i, \partial U_i)$  is generated by the boundary Dehn twist  $[D_i]_{\partial}$  and we can use Corollary 2.22 and get that  $[\phi]_{\partial^1} = [D_1^{n_1}]_{\partial^1} \cdot [D_2^{n_2}]_{\partial^1} \cdot \dots \cdot [D_r^{n_r}]_{\partial^1}$  and the numbers  $n_1, \dots, n_r$  are unique.  $\square$

In the next definition we introduce the concept of *fractional Dehn twist coefficient* which is a rational number that measures the amount of twisting at boundary components of an element in  $\text{MCG}^+(\Sigma, \partial^1 \Sigma)$  that is periodic in  $\text{MCG}^+(\Sigma)$ .

**Definition 2.25.** *Let  $\Sigma$  be a surface that is neither a disk nor a cylinder. Let  $\partial^1 \Sigma$  be a non-empty union of  $r$  boundary components of  $\Sigma$ . Let  $\phi : \Sigma \rightarrow \Sigma$  be a homeomorphism fixing pointwise  $\partial^1 \Sigma$  and freely isotopic to a periodic one. Let  $m \in \mathbb{N}$  such that  $[\phi^m] = [\text{id}]$ . Let  $t_1, \dots, t_r$  be integers such that  $[\phi^m]_{\partial^1} = [D_1^{t_1}]_{\partial^1} \cdot \dots \cdot [D_r^{t_r}]_{\partial^1}$ . We define the fractional Dehn twist coefficient at  $C_i$  by*

$$\text{rot}_{\partial^1}(\phi, C_i) := t_i/m.$$

Note that the fractional Dehn twist coefficients do not depend on the number  $m$  we choose to compute them or the representative  $\phi \in [\phi]_{\partial^1}$ .

Now we describe how to compute the fractional Dehn twist coefficient in terms of a invariant spine. Let  $\phi$  be an orientation preserving homeomorphism of  $\Sigma$  that fixes a non-empty union  $\partial^1 \Sigma$  of components of the boundary and which is freely isotopic to a periodic one. Let  $A$  be the union of the remaining components of the boundary. Suppose that there exists a relative spine  $(\Gamma, A)$  in  $(\Sigma, (\Gamma, A))$  which is invariant by  $\phi$  (recall 1.9).

We cut  $\Sigma$  along  $\Gamma$  into a disjoint union of cylinders, one for each component  $C_i$  of  $\partial^1 \Sigma$ . We use notations Notation 1.11 and Notation 2.14. We lift the regular retraction  $\Sigma \rightarrow \Gamma$  to a regular retraction  $\Sigma_\Gamma \rightarrow \tilde{\Gamma}$  and the homeomorphisms  $\phi$  to a homeomorphism  $\tilde{\phi}$  of  $\Sigma_\Gamma$ .

Let  $\frac{p_i}{n}$  be the rotation number of  $\tilde{\phi}|_{\tilde{\Gamma}_i}$  measure with the orientation of  $\tilde{\Gamma}_i$  as boundary of the cylinder. Choose in the cylinder  $\tilde{\Sigma}_i$  an oriented retraction line  $L_i$  from  $C_i$  to  $\tilde{\Gamma}_i$ . Consider the

orientation in  $\tilde{\Sigma}_i$  inherited from the orientation in  $\Sigma$ . We take the classes  $[L_i]$  and  $[\phi(L_i)]$  in  $H_1(\tilde{\Sigma}_i, \partial\tilde{\Sigma}_i)$ . The class

$$\tilde{\phi}|_{\tilde{\Gamma}_i}^n([L_i]) - [L_i]$$

belongs to  $H_1(\tilde{\Sigma}_i)$  since  $\tilde{\phi}|_{\tilde{\Gamma}_i}^n$  is the identity at the boundary. Let

$$k_i := (\tilde{\phi}|_{\tilde{\Gamma}_i}^n([L_i]) - [L_i]) \cdot [L_i],$$

that is the oriented intersection number of the two homology classes.

**Definition 2.26.** *According with the previous procedure we define*

$$\text{rot}(\phi, \Gamma, C_i) := k_i/n$$

In the next lemma we see that the two definitions of fractional Dehn twist coefficient coincide:

**Lemma 2.27.** *Let  $\Sigma$  be a oriented surface with non-empty boundary that is neither a disk nor a cylinder. Let  $\phi : \Sigma \rightarrow \Sigma$  be an orientation preserving homeomorphism that fixes a non-empty union  $\partial^1\Sigma$  of boundary components. Denote by  $A$  the union of the remaining boundary components. Assume that  $\phi$  fixes a relative spine  $(\Gamma, A)$  and that its restriction to it is periodic. Let  $C_i$  be a boundary component contained in  $\partial^1\Sigma$ . Then the equality  $\text{rot}_{\partial^1}(\phi, C_i) = \text{rot}(\phi, \Gamma, C_i)$  holds. In particular  $\text{rot}(\phi, \Gamma, C_i)$  does not depend on the chosen spine  $\Gamma$  or even on the representative of  $[\phi]_{\partial}$ .*

*Proof.* Let  $\text{rot}(\phi, \Gamma, C_i) = k_i/n$  be the fractional Dehn twist coefficients as in Definition 2.26. Note that  $\phi^n$  fixes  $\Gamma$  and that the lifting  $\tilde{\phi}^n|_{\tilde{\Sigma}_i}$  is isotopic relative to the boundary to the composition of  $k_i$  right boundary Dehn twist if  $k_i$  is positive (and  $-k_i$  left Dehn twists if  $k_i$  is negative) around the boundary component  $C_i$ . Then  $[\phi^n]_{\partial^1} = [D_1]^{k_1} \cdot \dots \cdot [D_r]^{k_r}$  and the result follows.  $\square$

**Corollary 2.28.** *Let  $g, h : \Sigma \rightarrow \Sigma$  be two homeomorphisms that fix pointwise a non empty union  $\partial^1\Sigma$  of components of the boundary  $\partial\Sigma$ . Let  $A$  be the union of the remaining boundary components. Assume that both preserve a common relative spine  $(\Gamma, A)$  and that they coincide at it. Then the equality  $\text{rot}_{\partial}(g, C_i) = \text{rot}_{\partial}(h, C_i)$  holds for every  $i$  if and only if  $h$  and  $g$  are isotopic relative to  $\partial^1\Sigma$ .*

*Proof.* The two properties we want to prove equivalent are straightforward equivalent to the equality  $\text{rot}_{\partial}(f, \Gamma, C_i) = \text{rot}_{\partial}(g, \Gamma, C_i)$  which is contained in Lemma 2.27.  $\square$

**Corollary 2.29.** *Let  $\phi : \Sigma \rightarrow \Sigma$  be a homeomorphism that fixes pointwise a non-empty union  $\partial^1\Sigma$  of components of the boundary, and that is isotopic to a periodic homeomorphism  $\hat{\phi}$ . Let  $C_i$  be a component in  $\partial^1\Sigma$ . Then the usual rotation number up to an integer  $\text{rot}(\hat{\phi}|_{C_i})$  equals  $|\text{rot}_{\partial}(\phi, C_i) - \lfloor \text{rot}_{\partial}(\phi, C_i) \rfloor|$  with  $\lfloor x \rfloor$  is the biggest integer less than  $x$ .*

**Remark 2.30.** We observe that by our convention on Remark 2.19, negative (or equivalently right-handed Dehn twists) produce positive fractional Dehn twist coefficients.

## 2.4 Pseudo-periodic automorphisms

In this section we focus on automorphisms of surfaces whose mapping classes only contain periodic pieces in their classification by Theorem 2.4: *pseudo-periodic automorphisms*. Since we have already studied freely-periodic automorphisms, the only part that is left to study of a pseudo-periodic automorphism are the separating annuli. Hence, most of this section is devoted to study and give names to phenomena related to automorphisms of collection of annuli.

Most of this section is contained in [MM11].

**Definition 2.31.** *An automorphism  $\phi : \Sigma \rightarrow \Sigma$  is pseudo-periodic if it is isotopic to an automorphism satisfying that there exists a finite collection of disjoint simple closed curves  $\mathcal{C}$  such that*

1.  $\phi(\mathcal{C}) = \mathcal{C}$
2.  $\phi|_{\Sigma \setminus \mathcal{C}}$  is freely isotopic to a periodic automorphism.

*Assuming that none of the connected components of  $\Sigma \setminus \mathcal{C}$  is either a disk or an annulus and that the set of curves is minimal, which is always possible, we name  $\mathcal{C}$  an admissible set of curves for  $\phi$ .*

The following theorem is a particularization on pseudo-periodic automorphisms of the more general result Theorem 2.4 that describes a *canonical form* for every automorphism of a surface.

**Theorem 2.32** (Almost-Canonical Form and Canonical Form). *Let  $\Sigma$  be a surface with  $\partial\Sigma \neq \emptyset$ . Any pseudo-periodic map of  $\Sigma$  is isotopic to an automorphism in almost-canonical form, that means a automorphism  $\phi$  which has an admissible set of curves  $\mathcal{C} = \{\mathcal{C}_i\}$  and tubular neighborhoods  $\mathcal{A} = \{\mathcal{A}_i\}$  with  $\mathcal{C}_i \subset \mathcal{A}_i$  such that:*

1.  $\phi(\mathcal{A}) = \mathcal{A}$  and  $\phi(\mathcal{C}) = (\mathcal{C})$ .
2. The map  $\phi|_{\overline{\Sigma \setminus \mathcal{A}}}$  is periodic.

*When the set  $\mathcal{C}$  is minimal we say that  $\phi$  is in canonical form.*

**Remark 2.33.** In the case that we are considering a pseudo-periodic automorphism of  $\Sigma$  that fixes pointwise some components  $\partial^1\Sigma$  of the boundary  $\partial\Sigma$  we can always find a canonical (or almost-canonical) form as follows. We can find an automorphism isotopic relative to  $\partial^1\Sigma$  that coincides with a canonical form as in the previous theorem outside a collar neighborhood  $U$  of  $\partial^1\Sigma$ . We may assume that there exists an isotopy connecting the automorphism and its canonical form relative to  $\partial^1\Sigma$ . That is, just use the stronger Theorem 2.4 in the case where there are not pseudo-Anosov pieces.

### Automorphisms of annuli that are periodic on the boundary

The rest of the chapter consists in results and definitions about automorphisms of the cylinder that are periodic on the boundary. These are of extreme importance for the understanding of pseudo-periodic automorphisms since the separating annuli in  $\mathcal{A}$  are cylinders with automorphisms of this type. Most of the following results and definitions are contained in [MM11].

**Notation 2.34.** Let  $s, c \in \mathbb{R}$ . We denote by  $\mathcal{D}_{s,c}$  and call *linear twist* the automorphism of  $\mathbb{S}^1 \times I$  given by  $(x, t) \mapsto (x + st + c, t)$  (we are taking  $\mathbb{S}^1 = \mathbb{R}/\mathbb{Z}$ ). Observe that

$$\mathcal{D}_{s,c} \circ \mathcal{D}_{s',c'} = \mathcal{D}_{s+s',c+c'},$$

$$\mathcal{D}_{s,c}^{-1} = \mathcal{D}_{-s,-c}.$$

In this work we always have  $s \in \mathbb{Q}$ .

**Remark 2.35.** We can isotope  $\mathcal{D}_{s,c}$  to a automorphism  $\mathcal{D}_{s,c}^p$  that is periodic on some tubular neighborhood of the core curve  $\mathbb{S}^1 \times \{1/2\}$  of the annulus while preserving the action on the boundary  $\partial(\mathbb{S}^1 \times I)$ :

$$\mathcal{D}_{s,c}^p(x, t) = \begin{cases} (x + 3s(t - \frac{1}{3}) + c, t) & 0 \leq t \leq \frac{1}{3} \\ (x + c, t) & \frac{1}{3} \leq t \leq \frac{2}{3} \\ (x + 3s(t - \frac{2}{3}) + c, t) & \frac{2}{3} \leq t \leq 1 \end{cases} \quad (2.36)$$

**Definition 2.37.** Let  $C \subset \Sigma$  be a simple closed curve embedded in an oriented surface  $\Sigma$ . And let  $\mathcal{A}$  be a tubular neighborhood of  $C$ . Let  $\mathcal{D} : \Sigma \rightarrow \Sigma$  be a automorphism of the surface with  $\mathcal{D}|_{\Sigma \setminus \mathcal{A}} = \text{id}$ . We say that  $\mathcal{D}$  is a *negative Dehn twist* around  $C$  or a *right-handed Dehn twist* if there exist a parametrization  $\eta : \mathbb{S}^1 \times I \rightarrow \mathcal{A}$  preserving orientation such that

$$\mathcal{D} = \eta \circ \mathcal{D}_{1,0} \circ \eta^{-1}.$$

A *positive Dehn twist* is defined similarly changing  $\mathcal{D}_{1,0}$  by  $\mathcal{D}_{-1,0}$  in the formula above. Compare this definition with Definition 2.18.

**Remark 2.38.** If  $\phi|_{\partial \mathcal{A}_i}$  is the identity then

$$\phi = \eta \circ \mathcal{D}_{s,0} \circ \eta^{-1}$$

for some  $s \in \mathbb{Z}$ , that is  $\phi = \mathcal{D}^s$  for some right-handed Dehn twist as in Definition 2.37.

**Lemma 2.39** (Linearization). *Let  $\mathcal{A}_i$  be an annulus and let  $\phi : \mathcal{A}_i \rightarrow \mathcal{A}_i$  be a automorphism that does not exchange boundary components. Suppose that  $\phi|_{\partial \mathcal{A}_i}$  is periodic. Then, after an isotopy of  $\phi$  preserving the action on the boundary, there exists a parametrization  $\eta : \mathbb{S}^1 \times I \rightarrow \mathcal{A}_i$  such that*

$$\phi = \eta \circ \mathcal{D}_{-s,-c} \circ \eta^{-1}$$

for some  $s \in \mathbb{Q}$ , some  $c \in \mathbb{R}$ .

Let  $\phi_j : \mathcal{A}_1 \rightarrow \mathcal{A}_1, j = 0, 1$  be automorphisms of the form  $\eta_j \circ \mathcal{D}_{-s,-c} \circ \eta_j$ . Then there exists  $h : \mathcal{A}_1 \rightarrow \mathcal{A}_1$  isotopic to the identity such that  $\phi_0 = h \circ \phi_1 \circ h^{-1}$ .

*Proof.* See [MM11, Theorem 2.3]. □

Now we treat automorphisms of the cylinder that exchange boundary components.

**Definition 2.40.** Let  $\phi$  be a pseudo-periodic automorphism in some almost-canonical form. Let  $C_1, \dots, C_k$  be a subset of curves in  $\mathcal{C}$  that are cyclically permuted by  $\phi$ , i.e.  $\phi(C_i) = C_{i+1}$  for  $i = 1, \dots, k-1$  and  $\phi(C_k) = C_1$ . Suppose that we give an orientation to  $C_1, \dots, C_k$  so that  $\phi|_{C_i}$  for  $i = 1, \dots, k-1$  is orientation preserving. We say that the curves are *amphidrome* if  $\phi|_{C_k} : C_k \rightarrow C_1$  is orientation reversing.

**Notation 2.41.** We denote by  $\tilde{\mathcal{D}}_s$  and call *special twist* the automorphism of  $\mathbb{S}^1 \times I$  given by

$$\tilde{\mathcal{D}}_s(x, t) = \begin{cases} (-x - 3s(t - \frac{1}{3}), 1 - t) & 0 \leq t \leq \frac{1}{3} \\ (-x, 1 - t) & \frac{1}{3} \leq t \leq \frac{2}{3} \\ (-x - 3s(t - \frac{2}{3}), 1 - t) & \frac{2}{3} \leq t \leq 1 \end{cases} \quad (2.42)$$

In this work case we always assume  $s \in \mathbb{Q}$ .

**Lemma 2.43** (Specialization). *Let  $\mathcal{A}_i$  be an annulus and let  $\phi : \mathcal{A}_i \rightarrow \mathcal{A}_i$  be an automorphism that exchanges boundary components. Suppose that  $\phi|_{\partial\mathcal{A}_i}$  is periodic. Then after an isotopy fixing the boundary, there exists a parametrization  $\eta : \mathbb{S}^1 \times I \rightarrow \mathcal{A}_i$  such that*

$$\phi = \eta \circ \tilde{\mathcal{D}}_{-s} \circ \eta^{-1}$$

for some  $s \in \mathbb{Q}$ .

*Proof.* See [MM11, Lemma 2.3]. □

**Definition 2.44** (Screw number). *Let  $\phi$  be a pseudo-periodic automorphism in almost-canonical form. Let  $n$  be the order of  $\phi|_{\Sigma \setminus \mathcal{A}}$ . Then  $\phi^n|_{\partial\mathcal{A}_i} = \text{id}$ , so  $\phi^n|_{\mathcal{A}_i}$  equals  $\mathcal{D}|_{\mathcal{A}_i}^{s_i}$  for a certain  $s_i \in \mathbb{Z}$ .*

*Let  $\alpha$  be the length of the orbit in which  $\mathcal{A}_i$  lies and let  $\tilde{\alpha} \in \{\alpha, 2\alpha\}$  be the smallest number such that  $\phi^{\tilde{\alpha}}$  does not exchange the boundary components of  $\mathcal{A}_1$ . We define*

$$s(\mathcal{A}_i) := \frac{-s_i}{n} \tilde{\alpha}.$$

We call  $s(\mathcal{A}_i)$  the screw number of  $\phi$  at  $\mathcal{A}_i$  or at  $\mathcal{C}_i$ .

**Lemma 2.45.** *Let  $\phi$  be an automorphism in almost-canonical form (recall Theorem 2.32) and let  $\{\mathcal{A}_i\} \subset \mathcal{A}$  be a set of  $k$  annuli cyclically permuted by  $\phi$ , i.e.  $\phi(\mathcal{A}_i) = \mathcal{A}_{i+1}$  such that  $\phi^k$  does not exchange boundary components. Then there exist coordinates*

$$\eta_i : \mathbb{S}^1 \times I \rightarrow \mathcal{A}_i$$

for the annuli in the orbit such that

$$\eta_{j+1}^{-1} \circ \phi \circ \eta_j = \mathcal{D}_{-s/k, -c/k}$$

where  $s$  and  $c$  are associated to  $\mathcal{A}_1$  as in Lemma 2.39.

*Proof.* Isotope  $\phi$  if necessary in order to take a parametrization of  $\mathcal{A}_1$ , associated to  $\phi^\alpha : \mathcal{A}_1 \rightarrow \mathcal{A}_1$  as in Lemma 2.39. Denote this parametrization by  $\eta_1 : \mathbb{S}^1 \times I \rightarrow \mathcal{A}_1$ .

Define recursively  $\eta_j := \phi \circ \eta_{j-1} \circ \mathcal{D}_{s/\alpha, c/\alpha}$  (see Notation 2.34).

Then,

$$\eta_{j+1}^{-1} \circ \phi \circ \eta_j = \mathcal{D}_{-s/\alpha, -c/\alpha}.$$

For every  $j$ , the equation

$$\eta_j = \phi^{j-1} \circ \eta_1 \circ \mathcal{D}_{s(j-1)/\alpha, c(j-1)/\alpha}$$

holds. So

$$\eta_1^{-1} \circ \phi \circ \eta_\alpha = \eta_1^{-1} \circ \phi \circ \phi^{\alpha-1} \circ \eta_1 \circ \mathcal{D}_{s(\alpha-1)/\alpha, c(\alpha-1)/\alpha} = \mathcal{D}_{-s/\alpha, -c/\alpha}.$$

□



**Remark 2.46.** By Remark 2.35 we can substitute  $\mathcal{D}_{-s/k, -c/k}$  by  $\mathcal{D}_{-s/k, -c/k}^p$  in the previous lemma.

**Remark 2.47.** After this proof we can check that  $\eta_k^{-1} \circ \phi^\alpha \circ \eta_k = \mathcal{D}_{-s, -c}$  to see that the screw number  $s = s(\mathcal{A}_i)$  and the parameter  $c$  modulo  $\mathbb{Z}$  of Lemma 2.45 only depend on the orbit of annuli in which  $\mathcal{A}_i$  lies.

We observe also that the numbers  $s$  and  $c$  of Lemma 2.45 satisfy

- The number  $s$  equals  $s(\mathcal{A}_i)$ .
- The number  $c$  is only determined modulo  $\mathbb{Z}$  and equals the usual rotation number (recall Definition 2.15)  $\text{rot}(\phi^{\alpha_i}|_{\eta(\mathbb{S}^1 \times \{0\})})$  but taking the representative in  $[0, 1)$  (instead of  $(0, 1]$ ).

We have similar results for orbits of annuli that are amphidrome.

**Lemma 2.48.** *Let  $\phi$  be a automorphism in almost canonical form and let  $\{\mathcal{A}_i\} \subset \mathcal{A}$  be a set of  $k$  annuli cyclically permuted by  $\phi$ , i.e.  $\phi(\mathcal{A}_i) = \mathcal{A}_{i+1}$  such that  $\phi^k$  exchanges boundary components. Then there exist coordinates*

$$\eta_i : \mathbb{S}^1 \times I \rightarrow \mathcal{A}_i$$

for the annuli in the orbit such that

$$\eta_{j+1}^{-1} \circ \phi \circ \eta_j = \tilde{\mathcal{D}}_{-s/\alpha}$$

where  $s$  is associated to  $\mathcal{A}_1$  as in Lemma 2.43.

*Proof.* The proof is completely analogous to that of Lemma 2.45. □

Similarly as in Remark 2.47 we may deduce that the screw number does not depend on the annulus, but rather on the orbit of annuli.

We end the section and the chapter with a definition that is important for the construction of the *mixed tête-à-tête twist* in Chapter 9. It also gives us alternative understanding of the main concept of Chapter 6.

**Definition 2.49.** *Let  $C$  be a component of  $\partial\Sigma$  and let  $\mathcal{A}$  be a compact collar neighborhood of  $C$  in  $\Sigma$ . Suppose that  $C$  has a metric and its total length is equal to  $\ell$ . Let  $\eta : \mathbb{S}^1 \times I \rightarrow \mathcal{A}$  be a parametrization of  $\mathcal{A}$ , such that  $\eta|_{\mathbb{S}^1 \times \{1\}} : \mathbb{S}^1 \times \{1\} \rightarrow C$  is an isometry.*

*Suppose that  $\mathbb{S}^1$  has the metric induced from taking  $\mathbb{S}^1 = \mathbb{R}/\ell\mathbb{Z}$  with  $\ell \in \mathbb{R}_{>0}$  and the standard metric on  $\mathbb{R}$ . A boundary Denh twist of length  $r \in \mathbb{R}_{>0}$  along  $C$  is a automorphism  $\mathcal{D}_r^\eta(C)$  of  $\Sigma$  such that:*

1. *It is the identity outside  $\mathcal{A}$*
2. *The restriction of  $\mathcal{D}_r^\eta(C)$  to  $\mathcal{A}$  in the coordinates given by  $\eta$  is given by  $(x, t) \mapsto (x + r \cdot t, t)$ .*

*The isotopy type of  $\mathcal{D}_r^\eta(C)$  by isotopies fixing the action on  $\partial\Sigma$  does not depend on the parametrization  $\eta$ . When we write just  $\mathcal{D}_r(C)$ , it means that we are considering a boundary Dehn twist with respect to some parametrization  $\eta$ .*

## Chapter 3

---

# Graph manifolds

In this chapter we recall some theory about graph manifolds and combinatorial ways of encoding their topology. We start by studying Seifert manifolds which are the building blocks for graph manifolds. We take the time to fix conventions and notation carefully since they are important for both chapters of Part III.

For more on this topic, see [Neu81], [NR78], [Neu97], [JN83], [HMK71], [Hat07] or [Ped09]. In many aspects we follow [Ped09].

### Fibered tori

Let  $p, q \in \mathbb{Z}$  with  $q > 0$  and  $\gcd(p, q) = 1$ . Let  $D^2 \times [0, 1]$  be a solid cylinder. We consider the natural orientation on  $D^2 \times [0, 1]$ .

Let  $(t, \theta)$  be polar coordinates for  $D^2$ . Let  $r_{p/q} : D^2 \rightarrow D^2$  be the rotation  $(t, \theta) \mapsto (t, \theta + 2\pi p/q)$ . Let  $T_{p,q}$  be the mapping torus of  $D^2$  induced by the rotation  $r_{p/q}$ , that is, the quotient space

$$\frac{D^2 \times [0, 1]}{(t, \theta, 1) \sim (t, r_{p/q}(\theta), 0)}.$$

If  $p, p' \in \mathbb{Z}$  with  $p \equiv p' \pmod{q}$ , then the rotations  $r_{p/q}$  and  $r_{p'/q}$  are exactly the same map so  $T_{p',q} = T_{p,q}$ . The resulting space is diffeomorphic to a solid torus naturally foliated by circles which we call *fibers*. We call this space a solid  $(p, q)$ -torus or a solid torus of type  $(p, q)$ . It has an orientation induced from the orientation of  $D^2 \times [0, 1] \subset \mathbb{R}^3$ . The torus  $\partial T_{p,q}$  is oriented as boundary of  $T_{p,q}$ .

We call the image of  $\{(0, 0)\} \times [0, 1] \subset D^2 \times [0, 1]$  in  $T_{p,q}$  the *central fiber*. We say that  $q$  is the *multiplicity* of the central fiber. If  $q = 1$  we call the central fiber a *typical fiber* and if  $q > 1$  we call the central fiber a *special fiber*. Also any other fiber than the central fiber is called a typical fiber.

If  $a$  and  $b$  are two oriented simple closed curves in  $\partial T_{p,q}$ , let  $[a] \cdot [b]$  denote the oriented intersection number of their classes in  $H_1(\partial T_{p,q}; \mathbb{Z})$ . We describe 4 classes of simple closed curves in the torus  $\partial T_{p,q}$ :

- (1) A *meridian*  $m := \partial D^2 \times \{y\} \subset T_{p,q}$ . We orient it as boundary of  $D^2 \times \{y\}$ .
- (2) A *fiber*  $f$  on the boundary  $\partial T_{p,q}$ . We orient it so that the radial projection to the central fiber is orientation preserving. It satisfies that  $[m] \cdot [f] = q$ .
- (3) A *longitude*  $l$  is a curve such that  $[l]$  is a generator of  $H_1(T_{p,q}; \mathbb{Z})$  and  $[m] \cdot [l] = 1$ .
- (4) A *section*  $s$ . That is a curve that intersects each fiber exactly once. It is well defined up integral multiples of  $f$ . It is oriented so that  $[s] \cdot [f] = -1$ .

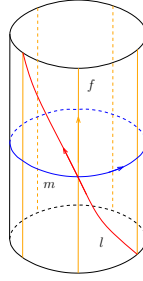


**Figure 3.1:** A torus  $T_{2,5}$  with some closed curves marked on its boundary. In orange a fiber  $f$ , in blue a meridian  $m$  and in red a longitude  $l$ . Their orientations are indicated.

We have defined two basis of the homology of  $\partial T_{p,q}$ , so there exist unique  $a, b \in \mathbb{Z}$  such that the equation

$$([s][f]) = ([m][l]) \begin{pmatrix} a & p \\ b & q \end{pmatrix} \quad (3.2)$$

holds in  $H_1(\partial T_{p,q}; \mathbb{Z})$ . The matrix is nothing but a change of basis. It has determinant equal to  $-1$  because  $[s], [f]$  is, by definition, a negative basis in the homology group  $H_1(\partial T_{p,q}; \mathbb{Z})$ . Therefore  $bp \equiv 1 \pmod{q}$ . Changing the class  $[s]$  by adding integer multiples of  $[f]$  to it, changes  $b$  by integer multiples of  $q$ .

### 3.1 Seifert manifolds

We now fix conventions on Seifert manifolds. Let  $B'$  be an oriented surface of genus  $g$  and  $r + k$  boundary components,  $Y' := B' \times \mathbb{S}^1$  and  $s' : Y' \times \mathbb{S}^1 \rightarrow B'$  the projection onto  $B'$ . Let

$$(\alpha_1, \beta_1), \dots, (\alpha_k, \beta_k)$$

be  $k$  pairs of integers with  $\alpha_i > 0$  and  $\gcd(\alpha_i, \beta_i) = 1$  for all  $i = 1, \dots, k$ . Let  $N_1, \dots, N_k$  be  $k$  boundary tori on  $Y'$ . On each of them consider the following two curves  $s_i := B' \times \{0\} \cap N_i$  and any fiber  $f_i \subset N_i$ . Orient them so that  $\{[s_i], [f_i]\}$  is a positive basis of  $N_i$  as boundary of  $Y'$ . For each  $i$ , consider a solid torus  $T_i = D^2 \times \mathbb{S}^1$  and the curves  $m = \partial D^2 \times \{0\}$  and  $l := \{pt\} \times \mathbb{S}^1$  oriented so that  $\{[m], [l]\}$  is a positive basis of  $\partial T_i$ . Attach  $T_i$  to  $N_i$  along its boundary by

$$\begin{pmatrix} -\alpha_i & c \\ -\beta_i & d \end{pmatrix} : \partial T_i \rightarrow N_i \quad (3.3)$$

with respect to the two given basis. The numbers  $c$  and  $d$  are integers such that the matrix has determinant  $-1$ . Note that, since the first column defines the attaching of the meridian, the gluing is well defined up to isotopy independently of  $c$  and  $d$ .

The foliation on  $N_i$  extends to all  $T_i$  and gives it a structure of a fibered solid torus. After gluing and extending the foliation to all  $k$  tori, we get a manifold  $Y$  and a collapsing map

$$s : Y \rightarrow B$$

where  $B$  is the surface of genus  $g$  and  $r$  boundary components.

**Definition 3.4.** *If a manifold  $Y$  can be constructed as above, we say that it is a Seifert manifold and the map  $s : Y \rightarrow B$  is a Seifert fibering for  $Y$ . We denote the resulting manifold by*

$$M(g, r, (\alpha_1, \beta_1), \dots, (\alpha_k, \beta_k)).$$

*Each pair  $(\alpha_i, \beta_i)$  is called Seifert pair and we say that it is normalized when  $0 \leq \beta_i < \alpha_i$ . The collection of numbers  $g, r, k, \alpha_1, \beta_1, \dots, \alpha_k, \beta_k$  are called Seifert invariants. The number  $\sum \beta_i/\alpha_i$  is called orbifold Euler number and is well defined when  $r \neq 0$ . When  $Y$  is a locally trivial circle bundle, its orbifold Euler number coincides with its classical Euler number.*

It is a theorem of Epstein [Eps72] that every 3-dimensional manifold foliated by circles is diffeomorphic as a circle bundle to a Seifert fibering.

**Example 3.5.** Let  $E \rightarrow B$  be the circle bundle over the closed surface of genus  $g$  with Euler class equal to  $e$ . Then  $E$  is diffeomorphic as a circle bundle to

$$M(g, 0, (1, e)).$$

**Remark 3.6.** We gather a few properties of Seifert manifolds and Seifert fiberings that are useful to have in mind:

- (1) Two Seifert fiberings  $M(g, r, (\alpha_1, \beta_1), \dots, (\alpha_k, \beta_k))$  and  $M(g', r', (\alpha'_1, \beta'_1), \dots, (\alpha'_k, \beta'_k))$  are diffeomorphic as circle bundles if and only if  $g = g'$ ,  $r = r'$  and after a permutation of the indices  $\beta_i/\alpha_i \equiv \beta'_i/\alpha'_i \pmod{1}$ . And if  $r = 0$  it is also necessary that  $\sum \beta_i/\alpha_i = \sum \beta'_i/\alpha'_i$ . See [Hat07, Proposition 2.1] (which has different conventions on the  $(\alpha, \beta)$  invariants).
- (2) A Seifert manifold  $Y$  admits a unique Seifert fibering  $Y \rightarrow B$  (up to diffeomorphism of circle bundles) except in certain, well-understood, cases where it admits infinitely many Seifert fiberings. For more on this see [Hat07, Theorem 2.3].

We find, by definition of fibered solid torus and the construction of a Seifert manifold from its invariants, the following lemma and corollary.

**Lemma 3.7.** *Let  $Y \rightarrow B$  be a Seifert fibering. If a fiber  $f$  has a neighborhood diffeomorphic to a  $(p, q)$ -solid torus, then there exists  $b \in \mathbb{Z}$  such that the (possibly unnormalized) Seifert invariant corresponding to  $f$  is  $(q, -b)$  with  $bp \equiv 1 \pmod{q}$ . Conversely, the special fiber  $f$  corresponding to a Seifert pair  $(\alpha, \beta)$  has a neighborhood diffeomorphic as a circle bundle to a  $(-c, \alpha_i)$ -solid torus with  $c\beta \equiv 1 \pmod{\alpha}$ .*

*Proof.* One only needs to compare eq. (3.2) and eq. (3.3) and observe that one matrix is the inverse of the other.  $\square$

**Corollary 3.8.** *Let  $\phi : \Sigma \rightarrow \Sigma$  be an orientation preserving periodic automorphism of a surface  $\Sigma$  of order  $n$  and let  $\Sigma_\phi$  be the corresponding mapping torus. Let  $x \in \Sigma$  be a point whose isotropy group in the group  $\langle \phi \rangle$  has order  $k$  with  $n = k \cdot s$ . Then  $\phi^s$  acts as a rotation in a disk around  $x$  with rotation number  $p/k$  for some  $p \in \mathbb{Z}$  and the (possibly unnormalized) Seifert pair of  $M_\phi$  (the mapping torus of  $\phi$ ) corresponding to the fiber passing through  $x$  is of the form  $(k, -b)$  with  $bp \equiv 1 \pmod k$ .*

*Proof.* That  $\phi^s$  acts as a rotation in a disk  $D \subset \Sigma$  around  $x$  with rotation number  $p/k$  for some  $p \in \mathbb{Z}_{>0}$  follows from the fact that  $x$  is a fixed point for  $\phi^{n/k}$ . By construction of the mapping torus of  $\Sigma$  we observe that the two mapping tori  $M_{\phi|_D} \simeq D_{\phi^{n/k}}$  are diffeomorphic where  $D$  is a small disk around  $x$ . By definition of fibered torus we observe that  $D_{\phi^{n/k}} \simeq T_{p,k}$ . The rest follows from Lemma 3.7.  $\square$

## 3.2 Graph manifolds

In this section we study graph manifolds and links in graph manifolds. Briefly, a graph manifold is a 3-dimensional manifold that can be cut along some tori in such a way that each remaining piece is a Seifert manifold. It happens that these manifolds are quite *combinatorial* in the sense that there exist graphs with decorations that encode their topology. We introduce graph manifolds after introduce the first of these graphs

### Plumbing graphs

**Definition 3.9.** *A plumbing graph is a decorated graph  $\Lambda$  that encodes the information to recover the topology of a certain 3-manifold.*

*It has vertex set  $\mathcal{V} \sqcup \mathcal{A}$  with  $\mathcal{A}$  possibly empty. The valency  $r_v$  of a vertex  $v$  is the number of edges stemming from  $v$  where loops are counted twice. Vertices in  $\mathcal{A}$  are represented by arrowheads and always have valency 1.*

*Now we describe the decoration of  $\Lambda$  and its meaning.*

- (1) *Each vertex  $v \in \mathcal{V}$  is decorated with 2 integers  $e_v$  (placed on top) and  $g_v$  placed on bottom. Let  $r_v$  be its valency. It represents the circle bundle  $Y_v$  over the surface of genus  $g_v$  and  $r_v$  boundary components such that (after picking a section on each boundary torus) its Euler number is well defined and equal to  $e_i$ . When  $g$  is omitted it is assumed to be 0. We consider the sections as part of the data that comes with a plumbing graph. One can always change the section at a given boundary torus provided that the section of another boundary torus in the same circle bundle is also changed accordingly to preserve the Euler number. A collection of sections defines an identification (up to isotopy) of each boundary torus with  $\mathbb{S}^1 \times \mathbb{S}^1$  that sends the section to the first factor and the fiber to the second. This identification is called frame .*
- (2) *Each edge is weighted by a sign  $+$  or  $-$  (when omitted,  $+$  is assumed). It tells us that the circle bundles corresponding to the ends of the edge are glued along a boundary torus by the gluing map  $J(x, y) = (y, x)$  if the sign is  $+$ , and  $-J$  if the sign is  $-$ . This map is defined with respect to the chosen frame on each boundary torus. The section has been fixed in (1) and the fiber does not change the diffeomorphism type of the resulting manifold after the gluing.*

(3) An arrowhead (or vertex in  $\mathcal{A}$ ) represents that an open fibered solid torus is removed from the corresponding circle bundle from where the edge comes out.

**Definition 3.10.** A manifold that is diffeomorphic to a manifold arising from a plumbing graph is called graph manifold.

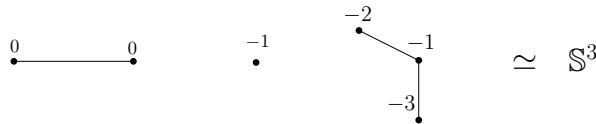
**3.11.** The construction of the 3-manifold  $Y$  associated to a plumbing graph is included in the description of its decoration above. However, we make the following observation: we can interpret a plumbing graph with arrows either as a graph manifold with non-empty boundary or as a closed manifold together with a link. If we consider the first interpretation, we observe that we can assume that all the arrows stem from of nodes since we can contract a bamboo (and not change the diffeomorphism type of  $Y$ ) if the arrow stems from of the end of the bamboo. In the second case, we consider the manifold  $Y$  resulting from removing all the arrowheads (and their edges) from  $\Lambda$ . Now, for each arrow we pick a Seifert fiber of the corresponding circle bundle from which the arrow stems. For example:



These two plumbing graphs produce diffeomorphic 3-dimensional manifolds with boundary. However, seen as closed manifolds with a link (in this case a knot) they are not diffeomorphic. The plumbing graph on the left can be proved to be  $\mathbb{S}^3$  together with a knot. In particular, it is a Seifert manifold with two special fibers and the knot is a generic Seifert fiber. The plumbing graph on the right represents a Seifert manifold with 3 special fibers and the knot consists of one of these special fibers, concretely the one with Seifert invariants  $(6, 1)$ . Observe that a (generic) Seifert fiber of the circle bundle with Euler weight  $-6$  corresponds to a special Seifert fiber of the total 3-dimensional manifold seen as a Seifert manifold.

In Lemma 3.13 we see that star-shaped plumbing graphs correspond with Seifert fiberings and how to obtain the Seifert invariants from the Euler weights.

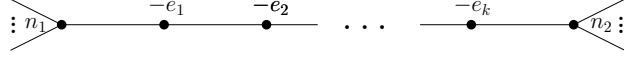
**Example 3.12.** The following are three examples of plumbing graphs that recover the 3-sphere. The first one corresponds to the gluing of two solid tori matching section with fiber. The second one corresponds with the Hopf fibration (which has Euler number  $\pm 1$  depending on the convention on the orientation of the fibers). The third one below corresponds with the resolution graph of the singularity  $x^2 + y^3$  where we have added the link (the concepts of singularity theory are to be defined in Chapter 5).



We point out a minor correction to an argument in [Neu81] and reprove a known lemma which is an essential ingredient in Part III. See also discussion after the lemma in Remark 3.16.

**Lemma 3.13.** Let  $\Lambda$  be a plumbing graph.

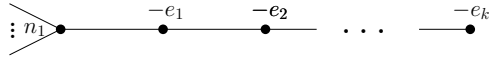
(1) If a portion of  $\Lambda$  has the following form:



Then the piece corresponding to the node  $n_1$  is glued to the piece corresponding to the node  $n_2$  along a torus by a matrix of the form  $G = \begin{pmatrix} a & b \\ c & d \end{pmatrix}$  with  $\det(G) = -1$  and where  $\frac{b}{-a} = [e_1, \dots, e_k]$  with the numbers in brackets being the continued fraction expansion

$$\frac{-b}{a} = e_1 - \frac{1}{e_2 - \frac{1}{e_3 - \frac{1}{\dots}}}$$

(2) If a portion of  $\Lambda$  has the following form:



Then the piece corresponding to the node  $n_i$  is glued along a torus to the boundary of a solid torus  $D^2 \times \mathbb{S}^1$  by a matrix of the form  $G = \begin{pmatrix} a & b \\ c & d \end{pmatrix}$  that also has determinant equal to  $-1$  and where  $-d/c = [e_1, e_2, \dots, e_k]$ .

Furthermore, if any of the two bamboos in the statement has a odd number of  $-$  signs on its edges, then change the gluing matrix for  $-G$  in each case.

*Proof.* Let  $T := D^2 \times \mathbb{S}^1$  be a solid torus naturally foliated by circles by its product structure. Let  $s$  be the closed curve  $\partial D^2 \times \{0\}$  and let  $f$  be any fiber on the boundary of the solid torus. Orient them so that  $\{[s], [f]\}$  is a positive basis of  $H_1(\partial T; \mathbb{Z})$ . Let  $T, T'$  be two copies of the solid torus. The node with Euler number  $-e_i$  corresponds to the circle bundle  $T \sqcup_{E_i} T'$  where the gluing map  $E_i : \partial T \rightarrow \partial T'$  is the matrix

$$\begin{pmatrix} -1 & 0 \\ e_i & 1 \end{pmatrix}.$$

In particular  $[f] = [f']$  in  $H_1(Y_i; \mathbb{Z})$ . The  $-1$  in the upper left part reflects the fact that  $s$  inherits different orientations from the two tori.

We treat the case (1) first. If  $Y_i$  is the piece corresponding to the node  $n_i$  with  $i = 1, 2$  we find that the gluing from  $Y_1$  to  $Y_2$  is

$$M_1 \sqcup_J (A \times \mathbb{S}^1 \sqcup_{E_1} A \times \mathbb{S}^1) \sqcup_J \dots \sqcup_J (A \times \mathbb{S}^1 \sqcup_{E_k} A \times \mathbb{S}^1) \sqcup_J Y_2$$

Where  $A \times \mathbb{S}^1$  is the trivial circle bundle over the annulus  $A := [1/2, 1] \times \mathbb{S}^1$ . Let  $(r, \theta)$  be polar coordinates for  $A$ . The two tori forming the boundary of  $A \times \mathbb{S}^1$  are oriented as boundaries of  $A \times \mathbb{S}^1$ . Observe that the map  $r((1/2, \theta), \eta) = ((1, \theta), \eta)$  is orientation reversing.

Let  $\mathbb{S}_t^1$  be the circle  $\{t\} \times \mathbb{S}^1 \subset A$ . We define  $s = \{S_{1/2}^1\} \times \{0\} \subset A \times \mathbb{S}^1$  and  $f = \{(1/2, 0)\} \times \mathbb{S}^1 \subset A \times \mathbb{S}^1$  and orient them so that the ordered basis  $\{[s], [f]\}$  is a positive basis for  $H_1(S_{1/2}^1 \times \mathbb{S}^1; \mathbb{Z})$  seen as boundary of  $A \times \mathbb{S}^1$ . We define similarly  $s' = \{S_1^1\} \times \{0\}$ ,  $f' = \{(1, 0)\} \times \mathbb{S}^1$  and orient them so that  $\{[s'], [f']\}$  is a positive basis for  $H_1(S_1^1 \times \mathbb{S}^1; \mathbb{Z})$ . Then the homology classes  $[r(s)]$  and  $[r(f)]$  form a negative basis. In fact  $[s'] = -[r(s)]$  and  $[f] = [r(f)]$  in  $H_1(A \times \mathbb{S}^1; \mathbb{Z})$ . This is the reason of the matrices  $\begin{pmatrix} -1 & 0 \\ 0 & 1 \end{pmatrix}$  in the eq. (3.14) below.

So the gluing matrix  $G$  from a torus in the boundary of  $Y_1$  to a torus in the boundary of  $Y_2$  is given by the following composition of matrices:

$$\begin{aligned} G &= \begin{pmatrix} 0 & 1 \\ 1 & 0 \end{pmatrix} \begin{pmatrix} -1 & 0 \\ 0 & 1 \end{pmatrix} \begin{pmatrix} -1 & 0 \\ e_k & 1 \end{pmatrix} \begin{pmatrix} -1 & 0 \\ 0 & 1 \end{pmatrix} \begin{pmatrix} 0 & 1 \\ 1 & 0 \end{pmatrix} \cdots \begin{pmatrix} 0 & 1 \\ 1 & 0 \end{pmatrix} \begin{pmatrix} -1 & 0 \\ 0 & 1 \end{pmatrix} \begin{pmatrix} -1 & 0 \\ e_1 & 1 \end{pmatrix} \begin{pmatrix} -1 & 0 \\ 0 & 1 \end{pmatrix} \begin{pmatrix} 0 & 1 \\ 1 & 0 \end{pmatrix} \\ &= \begin{pmatrix} 0 & 1 \\ 1 & 0 \end{pmatrix} \begin{pmatrix} -1 & 0 \\ -e_k & 1 \end{pmatrix} \begin{pmatrix} 0 & 1 \\ 1 & 0 \end{pmatrix} \cdots \begin{pmatrix} 0 & 1 \\ 1 & 0 \end{pmatrix} \begin{pmatrix} -1 & 0 \\ -e_1 & 1 \end{pmatrix} \begin{pmatrix} 0 & 1 \\ 1 & 0 \end{pmatrix} \\ &= \begin{pmatrix} 0 & 1 \\ 1 & 0 \end{pmatrix} \begin{pmatrix} 0 & -1 \\ 1 & -e_k \end{pmatrix} \cdots \begin{pmatrix} 0 & -1 \\ 1 & -e_1 \end{pmatrix} \end{aligned} \quad (3.14)$$

Observe that each matrix in the definition of  $G$  has determinant  $-1$  so  $\det(G) = -1$  because there is an odd number of matrices. Hence  $G$  inverts orientation on the boundary tori, preserving the orientation on the global 3 manifold. The result about the continued fraction follows easily by induction on  $k$ .

Now we treat similarly the case (2). The gluing from a boundary torus from  $Y_1$  to  $\partial D^2 \times \mathbb{S}^1$  is

$$Y_1 \sqcup_J (A \times \mathbb{S}^1 \sqcup_{E_1} A \times \mathbb{S}^1) \sqcup_J \cdots \sqcup_J (A \times \mathbb{S}^1 \sqcup_{E_k} D^2 \times \mathbb{S}^1).$$

Hence, by a similar argument to the previous case, the matrix that defines the gluing is

$$\begin{aligned} G &= \begin{pmatrix} -1 & 0 \\ e_k & 1 \end{pmatrix} \begin{pmatrix} -1 & 0 \\ 0 & 1 \end{pmatrix} \begin{pmatrix} 0 & 1 \\ 1 & 0 \end{pmatrix} \cdots \begin{pmatrix} 0 & 1 \\ 1 & 0 \end{pmatrix} \begin{pmatrix} -1 & 0 \\ 0 & 1 \end{pmatrix} \begin{pmatrix} -1 & 0 \\ e_1 & 1 \end{pmatrix} \begin{pmatrix} -1 & 0 \\ 0 & 1 \end{pmatrix} \begin{pmatrix} 0 & 1 \\ 1 & 0 \end{pmatrix} \\ &= \begin{pmatrix} -1 & 0 \\ e_k & 1 \end{pmatrix} \begin{pmatrix} -1 & 0 \\ 0 & 1 \end{pmatrix} \begin{pmatrix} 0 & 1 \\ 1 & 0 \end{pmatrix} \begin{pmatrix} 0 & -1 \\ 1 & -e_{k-1} \end{pmatrix} \cdots \begin{pmatrix} 0 & -1 \\ 1 & -e_1 \end{pmatrix} \\ &= \begin{pmatrix} 0 & 1 \\ 1 & -e_k \end{pmatrix} \begin{pmatrix} 0 & -1 \\ 1 & -e_{k-1} \end{pmatrix} \cdots \begin{pmatrix} 0 & -1 \\ 1 & -e_1 \end{pmatrix} \end{aligned} \quad (3.15)$$

By the expression in the last line we see that all matrices involved but the one on the left, have determinant 1 so we get  $\det(G) = -1$ . Again, by induction on  $k$ , the result on the continued fraction follows straight from the last line.

We treat now the last part of the statement about the case when there are a number of odd  $-$  sign edges. This follows because each of these  $-$  signs amounts to multiplying  $G$  by  $-1 \cdot \text{Id}$  (which is a matrix that commutes with any other matrix).  $\square$

**Remark 3.16.** Note the differences between the lemma above and [Neu81, Lemma 5.2] and the discussion before it in that same reference: there the author does not observe that in each piece  $A \times \mathbb{S}^1$ , the natural projection from one boundary torus to the other is orientation reversing. So the matrices  $\begin{pmatrix} -1 & 0 \\ 0 & 1 \end{pmatrix}$  are not taken into account there.

In a more extended manner. The problem is with the claim that the matrix  $C$  (in equation (\*) pg.319 of [Neu81]) is the gluing matrix. The equation above equation (\*) in that page, describes the gluing between the two boundary tori as a concatenated gluing of several pieces. In particular you glue a piece of the form  $A \times \mathbb{S}^1$  with another piece of the same form using the matrix  $H_k$  and then you glue these pieces a long  $J$ - matrices. Then it is claimed that “since  $A \times \mathbb{S}^1$  is a collar” then the gluing matrix (up to a sign) is  $JH_k J \cdots JH_1 J$ . However, notice that each piece  $A \times \mathbb{S}^1$  has two boundary tori, and they inherit "opposite" orientations. More concretely, the natural radial projection from one boundary torus to the other is orientation reversing. So even, if they are a collar (which they are), they interfere somehow in the gluing. That is why we add the matrices  $\begin{pmatrix} -1 & 0 \\ 0 & 1 \end{pmatrix}$  between each  $J$  and each  $H_k$  matrix.

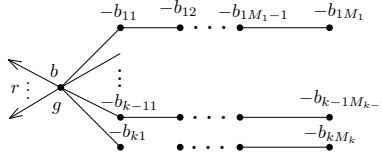
We now state a known proposition that is a consequence of the previous lemma and that is used in Part III. It tells us how to produce a star-shaped plumbing graph that represents a Seifert manifold directly from its invariants. It can be found in several references in the literature. See for example [NR78, Theorem 5.1] or [Neu81, Corollary 5.7].



**Proposition 3.17.** *Let  $M(g, r; (\hat{\alpha}_1, \hat{\beta}_1), \dots, (\hat{\alpha}_k, \hat{\beta}_k))$  be a Seifert fibering. Then it is diffeomorphic as a circle bundle to a Seifert fibering of the form*

$$M(g, r; (1, b), (\alpha_1, \beta_1), \dots, (\alpha_k, \beta_k))$$

where  $0 \leq \beta_i < \alpha_i$  for all  $i = 1, \dots, k$ . If  $r = 0$  then  $b$  is uniquely defined. The corresponding plumbing graph associated to the Seifert manifold is



where the numbers  $b_{ij}$  are the continuous fraction expansion for  $\alpha_i/\beta_i$ , that is

$$\frac{\alpha_i}{\beta_i} = b_{i1} - \frac{1}{b_{i2} - \frac{1}{b_{i3} - \frac{1}{\dots}}}$$

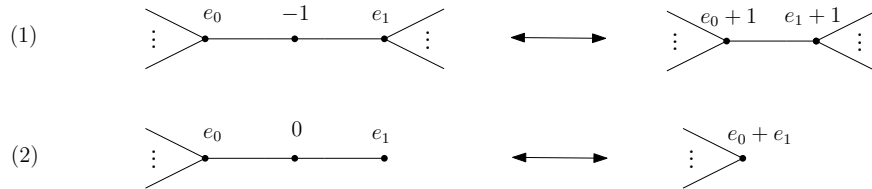
*Proof.* The proof can be found in the cited references before the proposition. We sketch it here.

Observe that we can always introduce an “artificial” Seifert pair  $(1, 0)$  to the given Seifert fibering. Then we use the result of Remark 3.6 (1). More concretely, let  $b_1 \in \mathbb{Z}$  such that  $0 \leq \hat{\beta}_1 + b_1 \hat{\alpha}_1 < \hat{\alpha}_1$ . Now set  $(\alpha_1, \beta_1) := (\hat{\alpha}_1, \hat{\beta}_1 + b_1 \hat{\alpha}_1)$  and change  $(1, 0)$  for  $(1, -b_1)$ . After repeating the process for all  $k$  Seifert pairs, we get that  $0 \leq \beta_i < \alpha_i$  for all  $i$  and that the pair  $(1, 0)$  has turned into  $(1, b) = (1, \sum_i -b_i)$ .

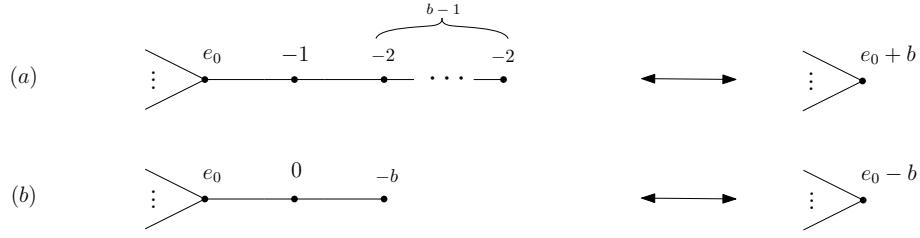
If  $r = 0$ , then we do not need the sum  $\sum_i \beta_i/\alpha_i$  to be constant (see again Remark 3.6 (1)). So, we do not need to make the modification to the pair  $(1, 0)$ . In this case the number  $b$  is not well defined (the proposition is true for any  $b$  in this case). Think now of the case  $r = 0$ . We observe that the  $k_i$  are uniquely determined, so the modifications to the pair  $(1, b)$  are uniquely determined as well. We conclude again by Remark 3.6 (1).

The statement on the plumbing graph that represents the figure follows from using Lemma 3.13 and then applying “plumbing calculus” to the graph (see next remark).  $\square$

**Remark 3.18** (Plumbing calculus). Two plumbing graphs that represent diffeomorphic manifolds are related by a series of “moves”. This is the content of the so-called “plumbing calculus” (see [Neu81] for more). The following are two examples of these moves:



Actually with these two moves, one is able to prove the following equivalence of graphs:



By applying move (1) to (a) iteratively and move (2) to (b) we get the depicted equivalences.

Observe that the arm of the case (a) corresponds to the continued fraction of  $1/b$  when  $b$  is positive, that is, to the Seifert pair  $(1, b)$ . Similarly, the arm of the case (b) corresponds to the continued fraction expansion of  $1/-b$  for  $b$  positive, that is, to the Seifert pair  $(1, -b)$ .

This is enough to complete the proof of the previous lemma.

### Waldhausen graphs and links

We already showed how can a plumbing graph with arrows represents a 3 dimensional manifold together with a link. This inspires the following definition. For more on Waldhausen graphs, see [Wal67, Neu81].

**Definition 3.19.** *Let  $Y$  be a closed graph manifold (see Definition 3.10). A Waldhausen link is a pair  $(Y, L)$  where  $L$  is a disjoint union of Seifert fibers in some Seifert pieces of  $Y$ .*

So a plumbing graph with arrows can be interpreted as a Waldhausen link  $(Y, L)$  (recall 3.11).

**Remark 3.20.** We assume in this work that  $Y$  is oriented and that the fibers of each Seifert piece are also oriented, so this gives an orientation to each connected component  $L_k$  of  $L$ . Observe that we can always invert the orientation of the fibers of a Seifert piece  $Y_n$  if we also invert the orientation on the base space in order to keep global orientation of the manifold.

Using Lemma 3.13 we are able to codify the topology of a graph manifold with another kind of graph: the *Waldhausen graph*. Although it differs from conventions of [Wal67], it contains equivalent information.

Let  $(Y, L)$  be a Waldhausen link. Suppose that we are given a Waldhausen decomposition  $Y = \bigcup_n Y_n$  in Seifert pieces. We are also given a framing of each boundary torus of each Seifert piece and a gluing matrix for each separating torus.

We define  $G(Y, L)$  as follows. Let  $\mathcal{N}$  be the subset of *nodes*, it has an element for each Seifert piece in the given Waldhausen decomposition. Let  $\mathcal{A}$  be the set of arrowheads, it has an element for each connected component of  $L$ . Then  $G(Y, L)$  has as vertex set  $\mathcal{N} \sqcup \mathcal{A}$ . It has an edge  $e$  between two vertices for each separating torus in the Waldhausen decomposition, also attach an edge to a vertex in  $\mathcal{N}$  for each component of  $L$  in that Seifert piece and for each special fiber in that Seifert piece. We give the edges an orientation: for an edge between two nodes, we choose any of the two orientations and for an edge stemming from of a node (corresponding to special fiber or a component of a link) we assign the orientation that goes out of the node.

The graph  $G(Y, L)$  has the following decoration:

- (1) Let  $e$  be an oriented edge.
  - (i) Suppose that  $e$  corresponds to a torus connecting the node  $n_1$  to the node  $n_2$ . Let  $s_i, f_i$  be the section and fiber that form the framing of the node  $n_i$  for  $i = 1, 2$ . Then

$f_1 = bs_2 + df_2$ . We can interpret  $|b|$  as the intersection multiplicity  $f_1 \cdot f_2$  in the boundary torus  $T_e$  with its orientation as boundary of  $Y_1$ . We define

$$\alpha_e = |f_1 \cdot f_2|, \quad \epsilon_e = \text{sign}(f_1 \cdot f_2)$$

we define  $\beta_e$  as the unique integer satisfying  $\alpha_e s_1 + \beta_e f_1 = \epsilon_e f_2$ . Note that if we denote by  $e'$  the edge  $e$  with the opposite orientation, the number  $\alpha_e$  does not change but we get a  $\beta'_e$  that satisfies  $\beta_e \beta'_e \equiv 1 \pmod{\alpha_e}$ .

There exists up to homology a unique choice of sections  $s_1, s_2$  such that the invariants are normalized, i.e  $0 \leq \beta_e, \beta'_e < \alpha_e$ . We weight the edge  $e$  by the normalized triple  $(\alpha_e, \beta_e, \epsilon_e)$ . If the sign is omitted we assume it to be 0.

- (ii) Suppose now that  $e$  corresponds to a Seifert fiber. It has thus associated a well-defined normalized Seifert pair  $(\alpha, \beta)$ . This is the weight that we put to this edge.
  - (iii) If  $e$  corresponds to a component of the link, we assign to it the normalized Seifert pair of the component of the link seen as a Seifert fiber of  $Y$ .
- (2) Each node  $n \in \mathcal{N}$  has an genus weight  $g_n$  which corresponds to the genus of the base space of the Seifert manifold. It also has as weight the Euler number  $b$ . This number can be computed using the method of Proposition 3.17 as follows. Orient all edges as going out of  $n$ . Now consider the unnormalized Seifert invariants (the Seifert invariants computed directly from the given basis at each boundary torus). We interpret all these Seifert pairs as Seifert invariants of fibers of  $Y_n$ . Then we apply the method Proposition 3.17 to normalize the invariants at the cost of introducing a new special fiber  $(1, -b)$  and  $b$  is the corresponding Euler weight.

It is clear that given a graph with the weights as above, we can recover a 3-dimensional manifold which is a graph manifold.

**3.21.** Observe that plumbing graphs can be considered as a special case of Waldhausen graphs in which all the edges have the weight  $(1, 0, \epsilon_e)$  and all the Seifert pieces have no special fibers. By, using Lemma 3.13, we can produce a plumbing graph from a Waldhausen graph. The plumbing graph will have a node for each node in  $\mathcal{N}$  (with the same decoration) and a bamboo for each in  $G(Y, L)$ .

If  $\epsilon_e = +1$ , then the edges of the bamboo corresponding to  $e$  are positive. If  $\epsilon_e = -1$ , then one (or any odd number) of the edges are given a negative sign.

Furthermore, they share the same set of arrowhead vertices  $\mathcal{A}$ . Corresponding to eq. (4.18), we find for any  $v \in \mathcal{V}$

$$-b_v S_v + \sum_e \epsilon_e S_w = 0 \in H_1(Y_n, \mathbb{Z}), \tag{3.22}$$

where the sum ranges over edges adjacent to  $v$ , and  $w$  is the other vertex adjacent to that edge.

**Example 3.23.** Here we see an example of a plumbing graph and a Waldhausen graph representing diffeomorphic 3-manifolds. The translation from one to the other can be extracted from Lemma 3.13.



## Chapter 4

---

# *Graph manifolds fibered over the circle*

This chapter depends on Chapter 3.

Graph manifolds were introduced in Definition 3.10 as those manifolds that can be encoded by a plumbing graph. In this chapter we study fibrations of graph manifolds over the circle and how to encode this information in a combinatorial way. All of this material is known and there are several references on the topic. See for example [Pic01, Neu97, LP05]. However, for the sake of completeness and to fix conventions for Chapter 11 we work out an exposition of these ideas here and provide with proofs for those results for which we could not find an appropriate reference.

The chapter is divided in three sections. In the first section we study horizontal surfaces of Seifert manifolds with non-empty boundary which is the easiest case. In the second section we fully generalize to the case of horizontal open books in closed graph manifolds. In the last section we explain how to obtain the conjugacy and isotopy invariants of the monodromy of a horizontal open book from the combinatorial data that encodes the horizontal open books. This last section is the most useful for Section 12.1.

## 4.1 Horizontal surfaces in Seifert manifolds

In this section, we study and classify horizontal surfaces of Seifert fiberings up to isotopy. We point out [Hat07, Proposition 2.2] which says that horizontal surfaces always exist on a Seifert manifold with non-empty boundary and that horizontal surfaces exist in a closed Seifert manifold if and only if its orbifold Euler number is 0.

We consider only Seifert manifolds that are orientable with orientable base space and with non-empty boundary in this section. Let  $s : Y \rightarrow B$  be a Seifert fibering of a manifold  $Y$  with non-empty boundary and Seifert invariants  $(g, r, (\alpha_1, \beta_1), \dots, (\alpha_k, \beta_k))$ .

**Definition 4.1.** Let  $H$  be a surface with non-empty boundary which is properly embedded in  $Y$  i.e.  $H \cap \partial Y = \partial H$ . We say that  $H$  is a horizontal surface of  $Y$  if it is transverse to all the fibers of  $Y$ .

Horizontal surfaces in a orientable Seifert manifold with orientable base space are always orientable since the map  $s$  restricted to the horizontal surface is a branched cover over the base space. Therefore, by our assumptions, only orientable horizontal surfaces appear in this work.

**Definition 4.2.** Let  $H(Y)$  be the set of all horizontal surfaces of  $Y$ , we define

$$\mathcal{H}(Y) := H(Y) / \sim$$

where two elements  $H_1, H_2 \in H(Y)$  are related  $H_1 \sim H_2$  if their inclusion maps are isotopic.

Let  $n := \text{lcm}(\alpha_1, \dots, \alpha_k)$ . We consider the action of the subgroup of the unitary complex numbers given by the  $n$ -th roots of unity  $c_n := \{e^{2\pi im/n}\}$  with  $m = 0, \dots, n-1$  on the fibers of  $Y$ . The element  $e^{2\pi im/n}$  acts on a typical fiber by a rotation of  $2\pi m/n$  radians and acts on a special fiber with multiplicity  $\alpha_i$  by a rotation of  $2\pi m\alpha_i/n$  radians.

We quotient  $Y$  by the action of this group and denote  $\hat{Y} = Y/c_n$  the resulting quotient space. By definition, the action of  $c_n$  preserves the fibers and is effective. The manifold  $\hat{Y}$  is then a Seifert manifold where we have *killed* the multiplicity of all the special fibers of  $Y$ . Hence it is a locally trivial  $S^1$ -fibration over  $B$  and since  $\partial B \neq \emptyset$ , it is actually a trivial fibration so  $\hat{Y}$  is diffeomorphic to  $B \times S^1$ .

Let  $\pi : Y \rightarrow \hat{Y}$  be the quotient map induced by the action of  $c_n$ . Observe that  $\hat{Y}$ , seen as a Seifert fibering with no special fibers, has the same base space as  $Y$  because the action given by  $c_n$  preserves fibers. In particular we find the following commutative diagram

$$\begin{array}{ccc} Y & \xrightarrow{\pi} & \hat{Y} \\ \downarrow s & \swarrow \hat{s} & \\ B & & \end{array} \quad (4.3)$$

Where  $s$  (resp.  $\hat{s}$ ) is the projection map from the Seifert fibering  $Y$  (resp.  $\hat{Y}$ ) onto its base space  $B$ .

**Definition 4.4.** Let  $H$  be a horizontal surface in  $Y$ . We say that  $H$  is well embedded if it is invariant by the action of  $c_n$ .

A horizontal surface  $H$  defines a linear map  $H_1(Y; \mathbb{Z}) \rightarrow \mathbb{Z}$  by considering its Poincaré dual. If  $H$  intersects a generic fiber  $m$  times, then it intersects a special fiber with multiplicity  $\alpha$ ,  $m/\alpha \in \mathbb{Z}$  times (in particular  $m$  is a multiple of  $n$ ). This is because a generic fiber covers that special fiber  $\alpha$  times. Hence, by isotoping any horizontal surface, we can always find well-embedded representatives  $\hat{H} \in [H]$ .

**Remark 4.5.** Observe that if  $H$  and  $H'$  are two well-embedded surfaces with  $[H] = [H']$ , then we can always find a fiber-preserving isotopy  $h$  that takes the inclusion  $i : H \hookrightarrow Y$  to an homeomorphism  $h(\cdot, 1) : H \rightarrow H'$  such that  $h(H, t)$  is a well-embedded surface for all  $t$ . This helps us prove the following:

**Lemma 4.6.** There is a bijection  $\pi_{\sharp} : \mathcal{H}(Y) \rightarrow \mathcal{H}(\hat{Y})$  induced by  $\pi$ .

*Proof.* Let  $[H] \in \mathcal{H}(Y)$  and suppose that  $H \in [H]$  is a well-embedded representative. Then clearly  $\pi(H) \in H(\hat{Y})$ . If  $H'$  is another well-embedded representative of the same class, then by Remark 4.5 we have that  $[\pi(H)] = [\pi(H')]$  in  $\mathcal{H}(\hat{Y})$ . Hence the map  $\pi_{\sharp}([H]) := [\pi(H)]$  is well defined.

The map  $\pi_{\sharp}$  is clearly surjective because  $\pi^{-1}(\hat{H})$  is a well-embedded surface for any horizontal surface  $\hat{H} \in H(\hat{Y})$  and hence  $\pi_{\sharp}([\pi^{-1}(\hat{H})]) = [\hat{H}]$ .

Now we prove that the natural candidate for inverse  $\pi_{\sharp}^{-1}([\hat{H}]) := [\pi^{-1}(\hat{H})]$  is well-defined. Let  $[\hat{H}] \in \mathcal{H}(\hat{Y})$  with  $\hat{H} \in [\hat{H}]$  a representative of the class. Let  $H := \pi^{-1}(\hat{H})$ . If  $[\hat{H}] = [\hat{H}']$  for some  $\hat{H}'$  in  $H(\hat{Y})$  then  $[\pi^{-1}(\hat{H}')] = [\pi^{-1}(\hat{H})]$  by just pulling back the isotopy between  $\hat{H}$  and  $\hat{H}'$  to  $Y$  by the map  $\pi$ . Hence the map is well defined. By construction, it is clear that for any  $H \in \mathcal{H}(Y)$  we have that  $\pi_{\sharp}^{-1}(\pi_{\sharp}([H]) = [H]$  so we are done.  $\square$

The objective of this section is to study  $\mathcal{H}(Y)$  but because of Lemma 4.6 above, it suffices to study  $\mathcal{H}(\hat{Y})$ .

Fix a trivialization  $\hat{Y} \simeq B \times \mathbb{S}^1$  once and for all. We observe that since  $\partial B \neq \emptyset$ , the surface  $B$  is homotopically equivalent to a wedge of  $\mu = 2g + r - 1$  circles, denote this wedge by  $\tilde{B}$ . Observe that  $\mathcal{H}(Y)$  is in bijection with multisections of  $\tilde{B} \times \mathbb{S}^1 \rightarrow \tilde{B}$  up to isotopy. Multisections are multivalued continuous maps from  $\tilde{B}$  to  $\tilde{B} \times \mathbb{S}^1$ .

**Lemma 4.7.** *The elements in  $\mathcal{H}(\tilde{B} \times \mathbb{S}^1)$  are in bijection with elements of*

$$H^1(\tilde{B} \times \mathbb{S}^1; \mathbb{Z}) = H^1(\tilde{B}; \mathbb{Z}) \oplus \mathbb{Z}$$

*that are not in  $H^1(\tilde{B}; \mathbb{Z}) \oplus \{0\}$ . Oriented horizontal surfaces that intersect positively any fiber of  $\tilde{B} \times \mathbb{S}^1$  are in bijection with elements of  $H^1(\tilde{B}; \mathbb{Z}) \oplus \mathbb{Z}_{>0}$ .*

*Proof.* We have that  $H^1(B; \mathbb{Z}) \oplus \mathbb{Z} = \mathbb{Z}^{\mu} \oplus \mathbb{Z}$ . Take an element

$$(p_1, \dots, p_{\mu}, q) = k((p'_1, \dots, p'_{\mu}, q')) \in \mathbb{Z}^{\mu} \times \mathbb{Z}$$

with  $q \neq 0$  and  $(p'_1, \dots, p'_{\mu}, q')$  irreducible (seeing  $\mathbb{Z}^{\mu} \times \mathbb{Z}$  as a  $\mathbb{Z}$ -module). Let  $\frac{p'_j}{q'} = \frac{k_j p''_j}{k_j q''}$  with  $p''_j/q''$  an irreducible fraction. Consider in each  $S^1_k \times \mathbb{S}^1$ ,  $k_j$  disjoint copies of the closed curve of slope  $p''_j/q''$ . We denote the union of these  $k_j$  copies by  $\tilde{H}_j$ . We observe that  $\tilde{H}_j$  intersects  $C$  in  $k_j q'' = q'$  points for each  $j$ . We can, therefore, isotope the connected components of each  $\tilde{H}_j$  so that  $\bigcup_j \tilde{H}_j$  intersects  $C$  in just  $q'$  points. We do so and consider the set  $\bigcup_j \tilde{H}_j$ . The horizontal surface  $\tilde{H}$  of  $\tilde{B} \times \mathbb{S}^1$  associated to  $k((p'_1, \dots, p'_{\mu}, q'))$  is  $k$  disjoint parallel copies of  $\bigcup_j \tilde{H}_j$ .

On the other direction, given an element  $[H] \in \mathcal{H}(\tilde{B} \times \mathbb{S}^1)$ . Let  $[H]$  denote also the class of any horizontal surface in  $H_1(\tilde{B} \times \mathbb{S}^1; \mathbb{Z})$ . Then  $q = [H] \cdot C$  and  $p_i = [H] \cdot [S^1_i \times \{0\}]$ . That is, the corresponding element in  $H^1(B; \mathbb{Z}) \oplus \mathbb{Z}$  is the Poincaré dual of the class of  $H$  in the homology of  $\tilde{B} \times \mathbb{S}^1$ .  $\square$

**Lemma 4.8.**  *$\tilde{H}$  is connected if and only if the element  $(p_1, \dots, p_{\mu}, q)$  is irreducible in  $H^1(\hat{Y}; \mathbb{Z}) \simeq H^1(\tilde{B}; \mathbb{Z}) \oplus \mathbb{Z}$ .*

*Proof.* We know that by construction  $\tilde{H} \cap C$  are  $q$  points. It is enough to show that these  $q$  points lie in the same connected component since any other part of  $\tilde{H}$  intersects some of these points. We label the points cyclically according to the orientation of  $C$ . So we have  $c_1, \dots, c_q \in C$ . We recall that  $S^1_j \times \mathbb{S}^1 \cap \tilde{H}$  is formed by  $k_j$  parallel copies of the closed curve of slope  $p'_j/q'$  with  $\frac{k_j p'_j}{k_j q'} = \frac{p_j}{q}$ .

Hence the point  $x_i$  is connected by these curves with the points  $c_{i+tk_j \pmod q}$ . Since  $(p_1, \dots, p_\mu, q)$  is irreducible then  $\gcd(p_1, \dots, p_\mu, q) = 1$  and hence  $\gcd(k_1, \dots, k_\mu) = 1$ . Therefore the equation

$$i + t_1 k_1 + \dots + t_\mu k_\mu = j \pmod q$$

admits an integer solution on the variables  $t_1, \dots, t_\mu$  for any two  $i, j \in \{1, \dots, q\}$ . This proves that the points  $c_i$  and  $c_j$  are in the same connected component in  $\tilde{H}$ .

Conversely if the element is not irreducible, then  $(p_1, \dots, p_\mu, q) = k(p'_1, \dots, p'_\mu, q')$  for  $(p'_1, \dots, p'_\mu, q')$  irreducible and  $k > 1$ . Then, by construction,  $\tilde{H}$  is formed by  $k$  disjoint copies of the connected horizontal surface associated to  $(p'_1, \dots, p'_\mu, q')$   $\square$

### Handy model of a Seifert fibering

We describe a particularly handy model of the Seifert fibering that we use in Chapter 11. The idea is taken from a construction in [Hat07]. For each  $i = 1, \dots, k$  let  $x_i \in B$  be the image by  $s : Y \rightarrow B$  of the special fiber  $F_i$ . We pick one boundary component of the base space and denote it by  $L$ . For each  $i = 1, \dots, k$  pick an arc  $l_i$  properly embedded in  $B$  and with the end points in  $L$  (i.e. with  $l_i \cap L = \partial l_i$ ) in such a way that cutting along  $l_i$  cuts off a disk  $D_i$  that contains  $x_i$  and no other point from  $\{x_1, \dots, x_k\}$ . We pick a collection of such arcs  $l_1, \dots, l_k$  pairwise disjoint. We define

$$B' := B \setminus \bigsqcup_i \text{int}(D_i)$$

where  $\text{int}(\cdot)$  denotes the interior. See Figure 4.9 below and observe that  $B$  and  $B'$  are diffeomorphic.

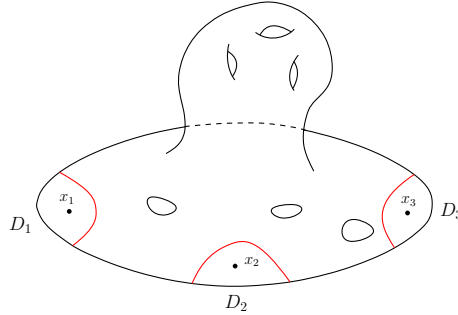


**Figure 4.9:** We see the base space  $B$  of a Seifert manifold. It has genus 3 and 4 boundary components. The 3 points are the image of the special fibers by the projection  $s$  and if we cut along the three red arcs, we get the surface  $B'$ .

Let  $Y' := s^{-1}(B')$ . Since  $Y'$  contains no special fibers and  $\partial B' \neq \emptyset$  then  $Y'$  is diffeomorphic as a circle bundle to  $B' \times \mathbb{S}^1$ . Recall that  $s^{-1}(D_i)$  is a solid torus of type  $(p_i, \alpha_i)$  with  $p_i \beta_i \equiv 1 \pmod{\alpha_i}$  (see Lemma 3.7).

Summarizing, the *handy model* consists of:

- i) A system of arcs  $l_1, \dots, l_k$  as explained.
- ii) A trivialization of  $Y'$ , that is an identification of  $Y'$  with  $B' \times \mathbb{S}^1$ .
- iii) Identifications of  $s^{-1}(D_i)$  with the corresponding model  $T_{p_i, \alpha_i}$  for each  $i = 1, \dots, k$ .

**Remark 4.10.** Let  $A_i$  be the vertical annulus  $s^{-1}(l_i)$ . A properly embedded horizontal disk  $D \subset s^{-1}(D_i)$  intersects  $A_i$  in  $\alpha_i$  disjoint arcs by definition of the number  $\alpha_i$ . Since a horizontal surface  $H$  intersects each typical fiber the same number of times we get that  $H$  must meet each fiber  $t \cdot \text{lcm}(\alpha_1, \dots, \alpha_k) = t \cdot n$  times for some  $t \in \mathbb{Z}_{>0}$ . If a horizontal surface meets  $t \cdot n$  times a typical fiber, then it meets  $t \cdot n/\alpha_i$  times the special fiber  $F_i$ .

**Lemma 4.11.** *There is a bijection between  $\mathcal{H}(Y)$  and  $HS(Y) := \{\gamma \in H^1(Y; \mathbb{Z}) : \gamma([C]) \neq 0\}$  where  $C$  is a generic fiber of  $Y$ .*

*Proof.* Clearly, an element  $[H] \in \mathcal{H}(Y)$  can be seen as the dual of a 1-form  $\gamma$  with  $\gamma_H(C) \neq 0$ .

To see that there is a bijection, take a handy model for  $Y$  (we use notation described there). Then we observe that given a  $\gamma \in HS(Y)$ , it restricts to a 1-form in  $H^1(Y'; \mathbb{Z})$ . The manifold  $Y'$  is diffeomorphic to a product, so by Lemma 4.7, there is a horizontal surface in  $\mathcal{H}(Y')$  representing the restriction of  $\gamma$  to  $Y'$ . It also restricts as a 1-form in  $H^1(s^{-1}(B); \mathbb{Z})$  where we recall that  $s^{-1}(B)$  is a disjoint union of tori, each containing a special fiber of  $Y$ . If  $\gamma([C]) = n$  then,  $\gamma([F_i]) = n/\alpha_i \in \mathbb{Z}$  so we can see the dual of  $\gamma|_{s^{-1}(B)}$  as an union of  $n/\alpha_i$  disks in each of the tori  $s^{-1}(D_i)$  for all  $i$ . Each of these disks intersects  $\alpha_i$  times the annulus  $s^{-1}(l_i)$ . So we can glue the horizontal surface represented by  $\gamma|_{Y'}$  with these disks to produce a horizontal surface in all  $Y$ . By construction, this horizontal surface represents the given  $\gamma \in H^1(Y; \mathbb{Z})$ .  $\square$

**Lemma 4.12.** *Let  $\hat{H}$  be a horizontal surface in  $\hat{Y}$ , that is,  $\hat{H} \in H(\hat{Y})$  and let  $H := \pi^{-1}(\hat{H})$ . Then  $H$  is connected if and only if  $\hat{H}$  is connected.*

*Proof.* If  $H$  is connected, then so is  $\hat{H}$  because  $\pi$  is a continuous map.

Suppose now that  $\hat{H}$  is connected. If  $\pi^{-1}(\hat{H})$  is not connected, then it is formed by parallel copies of diffeomorphic horizontal surfaces. Each of them is sent by  $\pi$  onto  $\hat{H}$  and each of them represents the same element in  $HS(Y)$ . But, by Lemma 4.11  $HS(Y)$  is in bijection with  $\mathcal{H}(Y)$  which, by Lemma 4.6, is in bijection with  $\mathcal{H}(\hat{Y})$ . So we get to a contradiction.  $\square$

By construction, we have established the 1 : 1 correspondences

$$HS(Y) \longleftrightarrow \mathcal{H}(Y) \longleftrightarrow \mathcal{H}(\hat{Y}) \longleftrightarrow H^1(B; \mathbb{Z}) \oplus \mathbb{Z} \setminus H^1(B; \mathbb{Z}) \oplus \{0\} \quad (4.13)$$

Where the first correspondence is Lemma 4.11, the second is Lemma 4.6 and the last one is Lemma 4.7.

Actually if we fix an orientation on the manifold and the fibers and we restrict ourselves to oriented horizontal surfaces that intersect positively the fibers of  $Y$ , these are parametrized by elements in  $H^1(B; \mathbb{Z}) \oplus \mathbb{Z}_{>0}$ . From now on we restrict ourselves to oriented horizontal surfaces  $H$  with  $H \cdot C > 0$ , that is, those whose oriented intersection product with any typical fiber is positive. Also the fibers are assumed to be oriented. This orientation induces a monodromy on each horizontal surface.

**Remark 4.14.** Let  $\Sigma$  be a surface with boundary and  $\phi : \Sigma \rightarrow \Sigma$  a periodic automorphism and let  $\Sigma_\phi$  be the corresponding mapping torus which is a Seifert manifold. The manifold  $\Sigma_\phi$  fibers over  $S^1$  and we can see  $\Sigma$  as a horizontal surface of  $\Sigma_\phi$  by considering any of the fibers of  $f : \Sigma_\phi \rightarrow S^1$ . Now let  $\Sigma^\phi$  be the orbit space of  $\Sigma$  which is also the base space of  $\Sigma_\phi$ . Let  $m$  be the lcm of the multiplicities of the special fibers of the Seifert fibering and let  $\Sigma_\phi/c_m$  be the quotient space resulting from the action of  $c_m$  on  $\Sigma_\phi$ . We observe, as before, that  $\Sigma_\phi/c_m$  is diffeomorphic to  $\Sigma^\phi \times S^1$  but there is not a preferred diffeomorphism between them. A trivialization is given by a choice of a section of  $\Sigma_\phi/c_m \rightarrow \Sigma^\phi$ .



Let  $[S_1], \dots, [S_\mu]$  be a basis of the homology group  $H_1(\Sigma^\phi; \mathbb{Z})$  where each  $S_i$  is a simple closed curve in  $\Sigma^\phi$ . Let  $C$  be any fiber of  $\Sigma_\phi/c_m$ . Let  $w, \hat{w} : \Sigma^\phi \rightarrow \Sigma_\phi/c_m$  be two sections, then we have two different basis of the homology of  $H_1(\Sigma_\phi/c_m; \mathbb{Z})$  induced by these two sections. For instance

$$\{[w(S_1)], \dots, [w(S_\mu)], [C]\} \text{ and } \{[\hat{w}(S_1)], \dots, [\hat{w}(S_\mu)], [C]\}.$$

Let  $\Sigma = f^{-1}(0)$  be the horizontal surface that we are studying and let  $\hat{\Sigma} := \pi(\Sigma)$  where  $\pi$  is the quotient map  $\Sigma_\phi \rightarrow \Sigma_\phi/c_m$ . Then  $\hat{\Sigma}$  is represented with respect to the (duals of the) two basis by integers  $(p_1, \dots, p_\mu, q)$  and  $(\hat{p}_1, \dots, \hat{p}_\mu, q)$  respectively and  $p_i \equiv \hat{p}_i \pmod{q}$  for all  $i = 1, \dots, \mu$  because a section differs from another section in a integer sum of fibers at the level of homology.

So the numbers  $p_1, \dots, p_\mu$  are well defined modulo  $\mathbb{Z}_q$  regardless of the trivialization chosen for  $\Sigma_\phi/c_m$ . Also by the discussion above, we see that if we fix a basis of  $H_1(B; \mathbb{Z})$ , then all the elements of the form  $(p_1 + n_1 q, \dots, p_\mu + n_\mu q, q)$  represent diffeomorphic horizontal surfaces with the same monodromy. That there exists an diffeomorphism of  $Y$  preserving the fibers that sends  $H_1$  to  $H_2$  comes from the fact that on a torus  $S^1 \times S^1$ , there exist a diffeomorphism preserving the vertical fibers  $\{t\} \times S^1$  that sends the curve of type  $(p, q)$  to the curve of type  $(p + kq, q)$  for any  $k \in \mathbb{Z}$ : the  $k$ -th power of a left handed Dehn twist along some fiber  $\{pt\} \times S^1$  that is different from  $C$ .

## 4.2 Horizontal open books in graph manifolds.

In this section we review some theory about graph manifolds and their fibrations over the circle.

The main result in this part is Proposition 4.21 which classifies horizontal fibrations of link complements by those cohomology classes which do not vanish on generic fibers in Seifert pieces. On one hand, this statement is proved in [EN85] when  $Y$  is an integral homology sphere. It is proved there as well that a homotopy class in  $[Y, S^1]$  contains at most one fibration. A criterion is also given in [Neu97] for a graph manifold to fiber over  $S^1$  and have a horizontal surface. On the other hand, the results of [Pic01] provide existence of fibrations of a link complement  $Y \setminus L$ , by constructing  $Y \setminus L$  as the mapping torus of a surface automorphism. For the sake of completeness, we state and prove this result which helps us clarify the setting used in Sections 12.1 and 12.2.

**Definition 4.15.** *We say that  $L$  is a fibered link if there exists a locally trivial fibration  $f : Y \setminus L \rightarrow S^1$  and for each connected component  $L_k \subset L$  there exists a tubular neighborhood  $U_k$  and a trivialization  $\rho_k : \bar{U}_k \rightarrow D^2 \times S^1$  such that the following diagram commutes*

$$\begin{array}{ccc} U_k \setminus L_k & \xrightarrow{\rho_k} & (D^2 \setminus \{0\}) \times S^1 \\ \downarrow f & & \downarrow g \\ S^1 & \xrightarrow{id} & S^1 \end{array} \quad (4.16)$$

where  $g(z, t) = \left(\frac{z}{|z|}\right)^{m_k} \cdot t^{n_k}$ .

We call  $m_k$  the multiplicity of the component  $L_k$ , it coincides with the intersection number of a fiber  $f^{-1}(t)$  and a meridian  $\partial \rho_k^{-1}(D^2 \times \{t\})$  around  $L_k$ . When  $m_k = +1$  for all the components in  $L$ , we call  $f$  an open book decomposition of  $Y$ . We note that  $n_k$  is determined modulo  $m_k$ .

If the fibers  $f^{-1}(t)$  are transverse to the Seifert fibers of each Seifert piece of  $Y \setminus L$ , then we say that it is a horizontal fibration for the pair  $(Y, L)$ . And when  $m_k = +1$  for all the components in  $L$  we say that it is a horizontal open book.

## Waldhausen graphs and horizontal surfaces

Let  $Y$  be a closed oriented graph manifold and let  $L \subset Y$  be a Waldhausen link (recall Definition 3.19). Thus, we have  $Y = \cup_{n \in \mathcal{N}} Y_n$ , where each  $Y_n$  is a Seifert manifold. Decompose  $L$  into connected components as  $L = \cup_{a \in \mathcal{A}} L_a$ . For each  $a \in \mathcal{A}$ , we have an  $n(a) \in \mathcal{N}$  so that  $L_a \subset Y_{n(a)}$  is a Seifert fiber.

Let  $\Sigma_n$  be a horizontal surface (a surface transverse to each Seifert fiber and such that  $\Sigma_n \cap \partial Y_n = \partial \Sigma_n$ ) in  $Y_n \setminus L$ . Such a surface exists, unless  $Y_n$  is a closed Seifert manifold,  $L = \emptyset$  and the orbifold Euler number is nonzero (recall [Hat07, Proposition 2.2]). Let  $S_n$  be a general Seifert fiber of  $Y_n$ .

The intersection number between  $S_n$  and  $\Sigma_n$  is independent of the general Seifert fiber  $S_n$ , call this number  $m_n$ . With a correct orientation, we can assume that  $m_n > 0$  at the cost of introducing  $-$  signs in the corresponding plumbing/Waldhausen graph (this is done by changing the orientation on the fiber at the same time that we change the orientation on the base space of the manifold). Orient  $\Sigma_n \cap T_e$  as the boundary of  $\Sigma_n$ . Orient any edge adjacent to  $n$  as going out of  $n$ . We find  $(\Sigma_n \cap T_e, S_n)_{T_e} = m_n$ . We use this notation for intersections of homology classes to specify which is the ambient space for the intersection.

**Remark 4.17.** In the setting of pseudo-periodic automorphisms arising from mixed tête-à-tête graphs that are defined in Chapter 9, we can safely assume (as we will see) that  $\epsilon_e = +1$  for every edge in the plumbing graph. By assuming that both the multiplicities  $m_n$  and the signs  $\epsilon_e$  are positive, we are only considering horizontal surfaces whose monodromy has only positive fractional Dehn twist coefficients and negative screw numbers. This is derived a posteriori from computation in Lemma 4.24.

Also we can assume that at least some  $L_v \subset L$  has  $m_v = +1$ . This assures that we are in the case of ((1) and (2)) that allow us to use Theorem 10.7 in order to model the monodromy by a mixed tête-à-tête graph.

We find that  $\Sigma_n \cap T_e$  is the sum of  $-m_n \epsilon_e S_{n'}/\alpha_e$  and some multiple of  $S_n$ . Let  $N_L$  be an open tubular neighborhood around  $L$  in  $Y$ . Since  $\partial(\Sigma_n \setminus N_L) = \cup_e \Sigma_n \cap T_e$ , there exists a number  $e_n \in \mathbb{Q}$  so that

$$e_n S_n + \sum_e \frac{\epsilon_e}{\alpha_e} S_{n'} = 0 \in H_1(Y_n; \mathbb{Z}), \quad (4.18)$$

where  $e$  ranges over oriented edges going from  $n$  to any  $n'$ . Since  $m_n \neq 0$ , the fiber  $S_n$  does not represent a torsion element of  $H_1(Y_n; \mathbb{Z})$ , and so  $e_n$  is well defined by this equation. We observe that  $e_n$  is the *orbifold Euler number* associated with  $Y_n$  by interpreting the Seifert invariants of edges as Seifert invariants of fiber of  $Y_n$ . Compare with the expression

$$e_n = -b_n + \sum_e \beta_e / \alpha_e \quad (4.19)$$

where  $b_n$  is the Euler weight of the central node of a star-shaped plumbing graph representation of  $Y_n$ .

We define the *orbifold intersection matrix*  $I^\circ$  by setting

$$I_{n,n}^\circ = e_n, \quad I_{n,n'}^\circ = \sum_e 1/\alpha_e \quad n \neq n',$$

where the sum runs over edges connecting  $n$  and  $n'$ . In the case of a plumbing graph, the orbifold intersection matrix is simply called the *intersection matrix* and is denoted by  $I$ . This is an integral matrix.

**Remark 4.20.** Homotopy classes of maps  $Y \setminus L \rightarrow S^1$  are in bijection with  $H^1(Y \setminus L; \mathbb{Z})$ . It follows from the universal coefficient theorem that  $H^1(Y \setminus L; \mathbb{Z}) = H_1(Y \setminus L; \mathbb{Z})^\vee$ . This bijection  $[Y \setminus L, S^1] \rightarrow H_1(Y \setminus L; \mathbb{Z})^\vee$  is realized by sending  $f : Y \setminus L \rightarrow S^1$  to  $f_* : H^1(Y \setminus L; \mathbb{Z}) \rightarrow H^1(S^1; \mathbb{Z}) = \mathbb{Z}$ . The associated *multiplicities* are defined as  $m_w = f_*([S_w])$  for any  $w \in \mathcal{W}$ .

Note that if the orbifold intersection matrix  $I^\circ$  is invertible, then eq. (4.18) shows that the family  $(m_n)_{n \in \mathcal{N}}$  is determined by  $(m_a)_{a \in \mathcal{A}}$ .

**Proposition 4.21.** *Let  $\gamma : H_1(Y \setminus L; \mathbb{Z}) \rightarrow \mathbb{Z}$  be a linear map. The corresponding element of  $[Y \setminus L, S^1]$  contains a horizontal fibration if and only if, with notation as in Remark 4.20,  $m_n \neq 0$  for all  $n \in \mathcal{N}$ . In this case, the fibration is unique up to isotopy.*

Before proving the proposition, we state the following lemma.

**Lemma 4.22.** *Let  $(Y, L)$  be a Waldhausen link with plumbing graph  $\Lambda$ . Let  $E = Y / \sim$  be the quotient space under the finest equivalence relation  $\sim$  so that any Seifert fiber is contained in an equivalence class. Define the group  $K$  as the set of formal sums as in the left hand side of eq. (3.22). We then have an exact sequence*

$$0 \rightarrow K \rightarrow \mathbb{Z}\langle C_v | v \in \mathcal{V} \rangle \rightarrow H_1(Y \setminus L; \mathbb{Z}) \rightarrow H_1(E; \mathbb{Z}) \rightarrow 0$$

Furthermore,  $H_1(E; \mathbb{Z})$  is a direct sum of free groups  $H_{G(Y, L)}$  and  $H_n$ ,  $n \in \mathcal{N}$ , where

- $H_n = H_n(E_n / \sim; \mathbb{Z})$ , where  $E_n = Y_n / \sim$  is the image of  $Y_n$  in  $E$ . We note that this is an  $r_n$ -punctured surface of genus  $g_n$  where  $r_n$  is the number of components of  $L$  contained in  $Y_n$ . We note that  $H_n$  is contained in the image of  $H_1(Y_n; \mathbb{Z})$  via the inclusion and that  $\text{rk } H_n = 2g_n + \max\{r_n - 1, 0\}$ .
- $H_{G(Y, L)} = H_1(G(Y, L); \mathbb{Z})$ , the map  $H_1(Y \setminus L; \mathbb{Z}) \rightarrow H_{G(Y, L)}$  is obtained by collapsing  $Y \setminus L$  onto  $G(Y, L)$  in the obvious way.

*Proof.* This sequence is in [Ném00, Proposition 2.18]. □

*Proof of Proposition 4.21.* In the case when  $L$  is a union of fibers in a Seifert manifold, this is proved in Section 4.1. The general case then follows from [EN85, Theorem 4.2] We provide here a proof which follows [EN85, Theorem 4.2] but does not depend on some deep theorems cited there due to the horizontal assumption.

Let  $\text{HFib}(Y, L)$  be the set of horizontal fibrations of the complement  $Y \setminus L$ . Let  $H \subset H^1(Y \setminus L; \mathbb{Z})$  be the set of cohomology classes  $\gamma$  satisfying  $\langle \gamma, S_n \rangle \neq 0$  for all  $n \in \mathcal{N}$ . If  $f : Y \setminus L \rightarrow S^1$  is horizontal, then each fiber is transverse to the boundary of the Seifert pieces of  $Y \setminus L$ . In particular,  $f$  restricted to any Seifert piece is a fibration. It follows from the classification given in Section 4.1 that the general fiber has nonzero intersection with any fiber of  $f$ , i.e.  $m_n \neq 0$ . In particular, the correspondence  $f \mapsto f_*$  induces a map  $\text{HFib}(Y, L) \rightarrow H$ . We will construct a map  $H \rightarrow \text{HFib}(Y, L)$ ,  $\gamma \mapsto f_\gamma$  and show that the two maps are inverse to each other.

Let  $\gamma \in H$  and set  $\gamma_n = \gamma|_{Y_n}$  for  $n \in \mathcal{N}$ . As  $m_n \neq 0$ , we know that there exists a fibration  $f_n : Y_n \setminus L \rightarrow S^1$  satisfying  $f_{n,*} = \gamma_n$ , unique up to isotopy. If  $T$  is a torus corresponding to an edge connecting  $n$  and  $n'$ , then  $\gamma_n|_T = \gamma|_T = \gamma_{n'}|_T$ . It follows that we can isotope  $f_n$  and  $f_{n'}$  in a neighborhood around  $T$  to coincide on  $T$ , and to glue together to form a fibration  $f : Y \setminus L \rightarrow S^1$ . The fibration  $f_\gamma$  is obtained by a modification of  $f$  explained below.

Let  $A$  be a spanning tree for  $G(Y, L)$  and let  $\mathcal{E}^A$  be the set of edges in  $G(Y, L)$  not in  $A$ . For each  $e \in \mathcal{E}^A$ , let  $c_e$  be the unique simple circuit in  $G(Y, L)$  containing only  $e$  and edges in  $A$  and let  $p_e : S^1 \rightarrow Y \setminus L$  be a path visiting the vertices and edges of the circuit  $c_e$ .

We define  $f_\gamma : Y \setminus L \rightarrow S^1$  as follows. For any  $e \in \mathcal{E}^A$ , let  $N_e$  be a tubular neighborhood around  $T_e$ . Since the normal bundle of  $T_e \subset Y$  is orientable, it is trivial:  $N_e \cong T_e \times [0, 1]$ ; let  $\pi_e : N_e \rightarrow [0, 1]$  be the projection. We can assume that the intersection  $N_e \cap p_e(S^1)$  is a fiber of the projection onto  $T_e$ , with the orientations coinciding. Define  $h_e = p_{e,*}([S^1]) \in H_1(Y \setminus L; \mathbb{Z})$ . Using a  $C^\infty$  function  $\psi : [0, 1] \rightarrow \mathbb{R}$ , taking constant values 0, 1 in neighborhoods around 0, 1, respectively, define

$$f_\gamma = f \cdot \prod_{e \in \mathcal{E}^A} e^{2\pi i((\gamma, h_e) - f_*(h_e))\psi \circ \pi},$$

where, outside  $N_e$ , the factor corresponding to  $e$  is understood to take the value 1.

It follows from Lemma 4.22 that the quotient of  $H_1(Y \setminus L; \mathbb{Z})$  modulo the images of  $H_1(Y_n \setminus L; \mathbb{Z})$  for  $n \in \mathcal{N}$  is freely generated by the classes  $h_e$  for  $e \in \mathcal{E}^A$ . By construction,  $f_*$ ,  $f_{\gamma,*}$  and  $\gamma$  coincide on these images. It then follows by the above modification of  $f$  that  $f_{\gamma,*}(h_e) = \gamma(h_e)$  for all  $e \in \mathcal{E}^A$ , thus  $f_{*,\gamma} = \gamma$ .

Finally, we must show that, given an  $f \in \text{HFib}(Y, L)$ , the maps  $f$  and  $f_{f_*}$  are isotopic. As above, for all edges  $e$  in  $G(Y, L)$ , the torus  $T_e$  is transverse to all fibers of  $f$ . Then the restrictions of  $f$  and  $f_{f_*}$  to any Seifert piece are horizontal. They are therefore, isotopic by Section 4.1, since  $(f_{f_*})_* = f_*$ . Thus, we may assume that  $f$  and  $f_{f_*}$  coincide outside  $\cup_{e \in \mathcal{E}^A} N_e$ . Thus, up to isotopy, we may assume that  $f/f_{f_*}$  equals 1 outside  $\cup_e N_e$ , whereas, for an oriented edge  $e$ , we have  $f/f_{f_*} = e^{2\pi i t_e \psi \circ \pi}$  on  $N_e$  for some  $t_e \in \mathbb{Z}$ .

Let  $\pi$  be a map obtained by collapsing  $Y_n \setminus \cup_e N_e$  to a point for all  $n \in \mathcal{N}$ , as well as collapsing the fibers of  $\pi_e$  to points. We thus get a map  $\pi : Y \setminus L \rightarrow G(Y, L)$ . Since  $G(Y, L)$  is a graph and  $((f/f_{f_*}) \circ \pi)_* = 0$ , there is an  $h : G(Y, L) \times [0, 1] \rightarrow S^1$  satisfying  $h(\cdot, 0) = (f/f_{f_*}) \circ \pi$  and  $h(\cdot, 1) = 1$ . By multiplication with  $h$ , we obtain an isotopy between  $f$  and  $f_{f_*}$ .  $\square$

## 4.3 Description of the monodromy

The previous section classifies horizontal open books on graph manifolds. However, this does not give us a good understanding of the action of the monodromy on the pages of the open book. This section is devoted to understand the monodromy and produce numerical data that help us construct the desired mixed tête-à-tête graph in Section 12.1.

In [LP05, Lemma 3.1] I. Luengo and A. Pichon include a *dictionary* between horizontal fibrations of Waldhausen links and Nielsen graphs. In this section we start with a horizontal open book of a graph manifold and explain how to get the data of the pseudo-periodic diffeomorphism corresponding to the monodromy in order to produce a mixed tête-à-tête graph whose mapping torus recovers the original graph manifold.

The monodromy may be understood by getting a good grasp of:

- i) The action of the monodromy on the periodic pieces, that is, the number of connected components, the period and the non-trivial isotropy points of each orbit.
- ii) The attaching of the different orbits along annuli.
- iii) The screw numbers of the annuli connecting the periodic pieces.
- iv) The fractional Dehn twist coefficients associated to the components  $L_v$  of the binding of the open book.

The above information allows us to give a model of the page and a pseudo-periodic automorphism of it in a canonical form. Then, we can apply the procedure described in the proof of Theorem 10.7 to build a mixed tête-à-tête graph modeling the automorphism.

### i) Periodic pieces

Let  $Y_j$  be a Seifert piece. The map  $f|_{Y_j}$  induces an element  $(f|_{Y_j})_*$  of  $H^1(Y_j; \mathbb{Z})$  that does not vanish on a generic fiber. Hence we can apply the algorithms described in Chapter 11 to get a description of the topology of the horizontal surface  $\Sigma_j$  and the monodromy acting on it.

### ii) Attaching of orbits along annuli

In order to recover the topology of the page  $\Sigma$  we have to glue some boundary components of the periodic pieces  $\Sigma_j$  constructed above.

We follow the notation of the second part of Proposition 4.21. For each periodic orbit  $\Sigma_j$  choose a connected component and denote it by  $\Sigma_{j,1}$ . Label the rest according to the action of the monodromy by  $\Sigma_{j,2}, \dots, \Sigma_{j,\alpha_j}$ .

Let  $A$  be a spanning tree of  $G(Y, L)$ . First we construct the part of the page  $\Sigma$  contained in the pieces of the spanning tree. For each edge  $e$  in  $A$  connecting vertices  $j, j'$  there corresponds an orbit of annuli  $\mathcal{A}_e$  of the page  $\Sigma$ . This orbit of annuli is in a thickened torus  $N_e$ . Note that since  $A$  is a tree,  $j \neq j'$  and in particular this orbit is not amphidrome.

We glue a boundary component of  $\Sigma_{j,1}$  in  $N_e$  to a boundary component of  $\Sigma_{j',1}$  in  $N_e$ . We glue the rest of boundary components in that torus equivariantly by the monodromy. Since  $A$  is a tree, different choices produce the same surface.

Let  $\mathcal{E}^A$  be the set of edges in  $G(Y, L)$  not in  $A$ . For each edge  $e$  in  $\mathcal{E}^A$ , let  $c_e$  be the circuit in  $G(Y, L)$  that only intersects  $\mathcal{E}^A$  in  $e$ . By choosing an inverse to the last arrow of the exact sequence in Lemma 4.22 we get an splitting

$$H_1(Y \setminus L; \mathbb{Z}) \simeq H_1(E; \mathbb{Z}) \oplus \frac{\mathbb{Z} \langle C_v | v \in \mathcal{V} \rangle}{K}.$$

Which also by Lemma 4.22 factorizes in

$$H_{G(Y,L)} \oplus \frac{\mathbb{Z} \langle C_v | v \in \mathcal{V} \rangle}{K} \bigoplus_{n \in \mathcal{N}} H_n$$

Then  $f_*(c_e)$  is a number  $n_e$  which, up to the choice of splitting, is well defined modulo the greatest common divisor of  $\alpha_{j''}$  for  $j''$  on the circuit  $c_e$ . Then, a boundary component of  $\Sigma_{j,1}$  in  $N_e$  is glued to a boundary component of  $\Sigma_{j',1+n_e}$ .

**Remark 4.23.** The number  $n_e$  contains equivalent data as the *action of the monodromy in the partition graph* in [MM11] or the invariant  $\omega(h)$  in [Pic01].

This completes the construction of the page  $\Sigma$ .

### iii) Screw numbers

We recall that we can easily get the plumbing graph  $\Lambda$  from the Waldhausen graph  $G(Y, L)$ .

**Lemma 4.24.** *Let  $n, n' \in \mathcal{N}$  be joined by an edge  $e$  in  $G(Y, L)$ . Let  $\alpha_e/\beta_e = [b_1, \dots, b_s]$  be the negative continued fraction expansion. Define  $m_0, m_1, \dots, m_{s+1}$  by*

$$m_0 = m_n, \quad m_1 = \frac{\beta_e m_n + m_{n'}}{\alpha_e}, \quad m_{i-1} - b_i m_i + m_{i+1} = 0 \quad i = 1, \dots, s.$$

The screw number  $r_e$  associated to the edge  $e$  in the Nielsen graph of  $\phi$  is

$$-d^2 \sum_{i=0}^s \frac{1}{m_i m_{i+1}}.$$

where  $d = \gcd(m_0, m_1)$  which is equal to  $\gcd(m_i, m_{i+1})$  for all  $i$ .

*Proof.* Let  $A_1, \dots, A_k$  be the annuli in  $\Sigma$  corresponding to the edge  $e$  and let  $v_1, \dots, v_s$  be the vertices on the bamboo joining  $n, n'$  in  $\Lambda$ . The annulus  $A_j$  can be split up into a union of annuli as

$$A_j = A_j^{0,1} \cup A_j^1 \cup A_j^{1,2} \cup A_j^2 \cup \dots \cup A_j^s \cup A_j^{s,s+1}.$$

Here,  $A_j^{i,i+1}$  corresponds to the edge joining  $v_i$  and  $v_{i+1}$ , and  $A_j^i$  is the complement of these annuli inside the plumbed piece corresponding to  $v_i$ . We can assume that  $\phi$  is truly periodic on the pieces  $A_j^i$ , so  $r_e$  is the sum of screw numbers associated to the edges connecting  $v_i$  and  $v_{i+1}$  (where we set  $v_0 = n$  and  $v_{s+1} = m_{s+1}$ ). This reduces the proof to the case when  $\alpha_e = 1$  and  $s = 0$ .

Denote by  $\phi'$  the restriction of  $\phi^k$  to  $A_1$ . It follows from Definition 2.44 that  $\phi$  and  $\phi'$  have the same screw number on  $A_1^{0,1}$ . This reduces the proof to the case when  $\gcd(m_0, m_1) = 1$ .

The annulus  $A = A_1^{0,1}$  is the Milnor fiber of the non-isolated plane curve singularity given by  $x^{m_0} y^{m_1} = 0$ . Let  $F$  be this Milnor fiber and let  $F_{\text{sing}}$  be the *singular Milnor fiber*. In fact, define the total space of the singular Milnor fibration as the closure of the set

$$\{(z, x) \in S^1 \times S^3 \mid f(x)/|f(x)| = z\}$$

The singular fibration is the first projection. Furthermore, the singular fibration contains the trivial fibration with fiber  $L_f$  (the link) given by  $f(x, y) = x^{m_0} y^{m_1} = 0$ . We get the singular monodromy, well defined up to homotopy,  $h_{\text{sing}} : F_{\text{sing}} \rightarrow F_{\text{sing}}$ , satisfying  $h_{\text{sing}}|_{L_f} = \text{id}_{L_f}$ .

Note that the oriented real blowup of the singular fiber space along  $L_f$  is the Milnor fiber. The singular monodromy lifts to a monodromy  $h$  on the Milnor fiber. Although this monodromy is not the identity on the boundary, it gives a well defined screw number. In fact, this representative of the monodromy coincides with  $\phi$  on  $A = F$ .

Next, we describe the singular monodromy for the plane curve  $f(x, y) = x^a y^b$ , assuming  $\gcd(a, b) = 1$ . Define an action of  $\mathbb{R}$  on  $S^3$  by setting

$$t * (x, y) = (e^{2\pi i t |y|/a} x, e^{2\pi i t (1-|y|)/b} y), \quad t \in \mathbb{R}.$$

Note the similarity to the classical computation in Milnor's book for weighted homogeneous polynomials. Since this polynomial is weighted homogeneous for any weight, we can vary the weights. This is done in order to guarantee that the action is trivial on the link  $L_f$ . The link consists of points  $(x, y)$  where either coordinate vanishes. Note that we choose a Milnor ball of radius 1. It follows that this action acts trivially on  $L_f$ . Furthermore, we have  $f(t * (x, y)) = e^{2\pi i t} f(x, y)$ . It follows that the singular monodromy is obtained by acting by 1. We parametrize the Milnor fiber by

$$[0, 1] \times S^1 \rightarrow S^3, \quad (s, \eta) \mapsto \frac{(\eta^b s, \eta^{-a}(s-1))}{\sqrt{s^2 + (s-1)^2}}.$$

Writing  $r(s)^{-1}$  for the denominator, the action of  $t = ab$  on this image is

$$\begin{aligned} r(s)(\eta^{-b}s, \eta^a(1-s)) &\mapsto r(s)(e^{2\pi i(1-s)b}\eta^b s, e^{2\pi ia}\eta^{-a}(1-s)) \\ &= r(s)((e^{-2\pi is}\eta)^b s, (e^{-2\pi is}\eta)^{-a}(1-s)), \end{aligned}$$

i.e.  $(s, \eta) \mapsto (s, e^{-2\pi is}\eta)$ , a right-handed Dehn twist. It follows that the screw number of  $\phi$  is  $-1/ab$ .  $\square$

**Remark 4.25.** Note that the Lemma above recovers [MM11, Theorem 5.1 (5)], which is a number theory result, by using a singularity theoretic point of view and a purely topological technique.

Observe that one can also apply the technique of the previous Lemma to part *i*). In fact, by applying the lemma to an arm of the plumbing graph, we get

**Corollary 4.26.** *Let  $m_0, m_1, \dots, m_s, m_{s+1}$  be the multiplicities of an arm of  $\Lambda$  corresponding to a special fiber of a Seifert piece. Then, the corresponding rotation number of the non-trivial isotropy orbit is*

$$-d^2 \sum_{i=0}^s \frac{1}{m_i m_{i+1}}.$$

$\square$

#### iv) Fractional Dehn twist coefficients at the boundary components fixed by the monodromy

A  $L_v \subset L$  has  $m_v = +1$ , so there exists a well defined representative of the monodromy fixing the corresponding boundary component of the fiber near  $L_v$ . Then, it makes sense to compute the fractional Dehn twist coefficient at that boundary component.

We observe that fractional Dehn twist coefficients can be seen as screw numbers. Let  $C$  be a boundary component of a periodic part  $\Sigma_j$  the fiber. Suppose that  $\phi|_C = \text{id}$ . We can glue an annulus  $A$  to this boundary component and extend  $\phi$  by the identity to all the annulus. Then the fractional Dehn twist of  $\phi$  at  $C$  coincides with minus the screw number of  $\phi$  between the periodic piece  $A$  and the periodic piece  $\Sigma_j$ . Hence, from Lemma 4.24 we get the following

**Corollary 4.27.** *Let  $m_0, m_1, \dots, m_s, m_{s+1}$  be the multiplicities of an arm of  $\Lambda$  ending at an arrowhead (thus  $m_{s+1} = 1$ ). Then, the corresponding fractional Dehn twist coefficient is*

$$d^2 \sum_{i=0}^s \frac{1}{m_i m_{i+1}}.$$

$\square$

By the fact that all multiplicities are positive and the edges have weight  $+1$  (recall Remark 4.17), we get that these fractional Dehn twist coefficients are positive which allows the monodromy to be modeled by a mixed tête-à-tête graph as we will see in Chapter 9.

## Chapter 5

---

# Singularity theory

In this chapter we do a brief review of the concepts of singularity theory that we use in the forthcoming parts. We do not attempt to make a comprehensive introduction here, but rather do a quick overview of the concepts used and provide with references for all the results mentioned.

We do a local study of singularities of maps and sets locally in this work. So we treat with function germs. Let

$$f : (\mathbb{C}^n, 0) \rightarrow (\mathbb{C}, 0)$$

be a holomorphic function germ. Let  $V_f := f^{-1}(0)$  be the analytic set defined by  $f$ . We say that  $f$  has a singularity at a point  $p \in V_f$  if all partial derivatives of  $f$  vanish at  $p$ , i.e. if

$$\frac{\partial f}{\partial z_i}(p) = 0 \text{ for all } i = 1, \dots, n.$$

When  $0 \in V_f$  is the only singular point of a neighborhood of  $0 \in \mathbb{C}^n$  we say that  $f$  has an isolated singularity at 0.

Let  $\mathbb{S}_\epsilon^{2n-1}$  be the sphere of radius  $\epsilon_0 > 0$  centered at 0. In [Mil68], Milnor proved that for  $\epsilon_0$  small enough, the intersection  $K_\epsilon := \mathbb{S}_\epsilon^{2n-1} \cap V_f$  is a smooth manifold for all  $0 < \epsilon < \epsilon_0$  and its topology does not depend on  $\epsilon$ . We call  $K_\epsilon$  the link of the singularity. Furthermore, in that same reference Milnor proved his celebrated theorem. The following is the usual formulation:

**Theorem 5.1** (Milnor's fibration Theorem). *Let  $f : (\mathbb{C}^n, 0) \rightarrow (\mathbb{C}, 0)$  be a holomorphic function germ having a singularity at  $0 \in \mathbb{C}^n$ . Then there exists a small  $\epsilon_0 > 0$  such that for all  $0 < \epsilon \leq \epsilon_0$  the map*

$$\frac{f}{|f|} : \mathbb{S}_\epsilon^{2n-1} \setminus K_\epsilon \rightarrow \mathbb{S}^1$$

*is a locally trivial fibration.*

**Monodromy.** Let  $F \hookrightarrow E \rightarrow B$  be a locally trivial smooth fibration with fiber  $F$ . Fix a base point  $b \in B$ . There is a well-defined action of  $\pi_1(B, b)$  on the mapping class group of  $F$ . The image of  $\pi_1(B, b)$  by this action is known as the geometric monodromy group. A sketch of the construction of the monodromy goes as follows:



- (1) Let  $\beta : [0, 1] \rightarrow B$  be a loop representing an element of  $\pi_1(B)$ . (So  $\beta(0) = \beta(1) = b$ ). We suppose that  $\beta$  is differentiable. The construction is very similar for piecewise differentiable path.
- (2) For each point  $x \in E$ . There is a well defined subspace of  $T_x E$  which is,  $T_x F$ , that is, the tangent space to the fiber  $F$  at the point  $x$ . This gives a vector sub-bundle of the tangent bundle  $TE$ . We choose another vector sub-bundle  $TH$  such that  $T_x E \simeq T_x F \oplus T_x H$ . That is, we choose a vector sub-bundle that complements  $TF$ . This can always be done by pasting local decompositions using a partition of unity. This *horizontal vector bundle*  $TH$  is not unique and is some times called *Ehresmann connection*.
- (3) Now we may use this connection to lift a parametrization of  $\beta$  to a homotopy  $h_t : F_{\beta(0)} \mapsto E$  such that for each  $t$  the map  $h_t$  is a diffeomorphism from the fiber  $F_{\beta(0)}$  over  $\beta(0) = b$  to the fiber over  $\beta(t)$ . The map  $h_1$  is a diffeomorphism from  $F_b$  to itself.
- (4) It can be proved that homotopic paths give isotopic diffeomorphisms. And different connections give as well isotopic diffeomorphisms. Hence, the action is well defined from the fundamental group to the mapping class group.

We show now other versions of Theorem 5.1. In particular there is a formulation of this theorem that is sometimes more useful:

**Theorem 5.2** (Milnor fibration in the tube). *Let  $f : (\mathbb{C}^n, 0) \rightarrow (\mathbb{C}, 0)$  be a holomorphic function germ having a singularity at the origin in  $\mathbb{C}^n$ . Let  $\delta_0 > 0$  be a positive number small enough so that  $\mathbb{S}^{2n-1}$  intersects transversally  $f^{-1}(t)$  for all  $t$  with  $0 < |t| \leq \delta_0$ . Let  $D_\delta \subset \mathbb{C}$  be the disk of radius  $\delta < \delta_0$  and  $B_\epsilon \subset \mathbb{C}^n$  the closed ball of radius  $\epsilon$ . Then*

$$f|_{B_\epsilon \cap f^{-1}(\mathbb{S}_\delta^1)} : B_\epsilon \cap f^{-1}(\mathbb{S}_\delta^1) \rightarrow \mathbb{S}_\delta^1$$

*is a locally trivial fibration and is equivalent to the fibration in Theorem 5.1. The set  $N_{\epsilon, \delta} := B_\epsilon \cap f^{-1}(\mathbb{S}_\delta^1)$  is usually called the Milnor tube.*

Note that the Milnor fiber in the above theorem is a compact manifold with boundary.

Milnor proved the above theorem in [Mil68] in the case when  $f$  has an isolated singularity. It was Lê Dũng Tráng who proved the above theorem. Actually he proved it in [LDuT77] in a greater generality:

**Theorem 5.3** (Milnor-Lê fibration Theorem). *Let  $X$  be an analytic set of an open neighborhood of the origin in  $\mathbb{C}^n$ . Let  $f : (X, 0) \rightarrow (\mathbb{C}, 0)$  be a holomorphic function germ. Let  $V_f := f^{-1}(0)$  be as before. Let  $B_\epsilon$  denote the closed ball of radius  $\epsilon$  in  $\mathbb{C}^n$  centered at the origin and let  $D_\delta^*$  be the punctured disk of radius  $\delta$  in  $\mathbb{C}$ . Then for  $\epsilon > 0$  small enough there exists  $\delta > 0$  small with respect to  $\epsilon$  such that*

$$f : X \cap B_\epsilon \cap f^{-1}(\mathbb{S}_\delta^1) \rightarrow \mathbb{S}_\delta^1$$

*is a locally trivial fibration. We call  $f^{-1}(0) \cap X \cap B_\epsilon$  the link of the Milnor-Lê fibration associated with  $f$ .*

**Remark 5.4.** Given an analytic space germ  $(X, 0)$  and an embedding of  $(X, 0)$  in  $(\mathbb{C}^n, 0)$ . Its *link* is defined as the intersection of  $X$  and a small ball  $B_\epsilon \subset \mathbb{C}^n$  centered at 0. The topological type of the link does not depend neither on the embedding nor on  $n$ . So, in the previous theorem, the topological type of the fibration depends only on  $X$  and on  $f$ .

**Remark 5.5.** (a) If the singularity is isolated, then there exists a representative of the monodromy that fixes the boundary pointwise. This is essentially because the Milnor fibration on the tube trivializes near the boundary of the total space. So, when constructing the connection, we may pick a particular cover by trivializing open sets where one of these open sets contains the boundary of the (closure of the) Milnor fiber.

In this case, the monodromy gives a well-defined element of  $\text{MCG}^+(F, \partial F)$ .

(b) Observe that the base space of the Milnor fibration is a circle and its fundamental group is isomorphic to  $\mathbb{Z}$ . Hence, to give the monodromy group one only needs to give the action of one generator of this group. What is usually called the monodromy, is the mapping class induced by the the lifting of the loop parametrized by  $t \mapsto e^{2\pi t}$ .

## Plane curve singularities

By taking  $n = 2$  we restrict ourselves to the theory known as *plane curve singularities*. This is a classical and very well understood topic in singularity theory. We refer to [BK86] which is a canonical reference on this topic.

Let  $f : (\mathbb{C}^2, 0) \rightarrow (\mathbb{C}, 0)$  be a germ and suppose that we take a representative of it given a convergent series of powers. We observe that  $f$  can be uniquely (up to multiplication by an unity) described as a product of powers of irreducible germs  $f = f_1^{m_1} \cdots f_k^{m_k}$ . When  $m_i = 1$  for all  $i$ , we say that the germ is reduced. When also  $k = 1$ , we say that the germ is irreducible. Hence, by definition, each  $f_i$  is an irreducible germ and its set of zeros is called *branch*.

**Puiseux series.** Let  $f(x, y)$  be an irreducible polynomial with complex coefficients. We consider the equation  $f(x, y) = 0$  and think about the problem of solving the expression for  $y$ . Observe that this problem, in general, does not have a solution in the space of polynomials with complex coefficients, not even in the space of series with complex coefficients. However, if we allow fractional exponents, then it is possible to express  $y$  as a series with complex coefficients and fractional exponents (with bounded denominator) that is convergent in a neighborhood of 0. That is, the equality

$$y = h(x) = \sum_{k \geq n} c_k x^{k/m}$$

holds in a neighborhood of 0. Where  $n$  is the first non-zero coefficient and  $m$  is the bound of the denominators. This series is called Puiseux expansion.

We use Puiseux series to codify the information of the equation  $f(x, y) = \theta$  for small  $|\theta| > 0$ . Which, intersected with a sufficiently small ball center at the origin of  $\mathbb{C}^2$ , is the Milnor fiber (recall Theorem 5.2). All the topological information of the series can be recovered from the exponents of the non-zero coefficients. Which in turn, can be codified by pairs of co-prime numbers: *the Puiseux pairs*. Actually we are interested in a subset of these pairs, called the *characteristic Puiseux pairs* which are enough to recover the topology of the germ. Given a series we do the following to obtain the characteristic Puiseux pairs. Take  $n_1/m_1$  the irreducible fraction for  $n/m$ . The pair  $(n_1, m_1)$  is called the first characteristic Puiseux pair. If  $\text{gcd}(m, n) = 1$ , then we have finished. Otherwise, we have that  $m/m_1 > 1$ . In this case, let

$$k_2 := \min\{k : c_k \neq 0 \text{ and } k \text{ is not divisible by } (m/m_1)\}$$

Take  $(n_2/m_2)$  the irreducible fraction for  $k_2/(m/m_1)$ . The pair  $(n_2, m_2)$  is the second Puiseux pair. If  $m/(m_1 m_2) > 1$  we iterate the process, whereas if  $m/(m_1 m_2) = 1$  the process ends here.

After a finite number of steps, the algorithm ends and we get a sequence of pairs of co-prime natural numbers

$$(n_1, m_1), \dots, (n_g, m_g)$$

which are the characteristic Puiseux pairs.

## Surface singularities

These are singularities of analytic spaces that have generic dimension 2. See [N99] for more on this topic.

**Definition 5.6.** Let  $f_1, \dots, f_k : (\mathbb{C}^n, 0) \rightarrow (\mathbb{C}, 0)$  be a collection of holomorphic function germs. We say that the germ  $(X, 0) := (V_{f_1} \cap \dots \cap V_{f_k}, 0)$  is a surface singularity if the rank of the Jacobian matrix

$$\left( \frac{\partial f_i}{\partial z_j} \right)_{\substack{i=1, \dots, k \\ j=1, \dots, n}}$$

is  $n - 2$  at a any generic point. If the rank is also  $n - 2$  at 0, this is actually a smooth germ. And if the rank is less than  $n - 2$  only at 0, we say that this is an isolated surface singularity.

If any bounded holomorphic function  $X \setminus \{0\} \rightarrow \mathbb{C}$  can be holomorphically extended to  $X$ , we say that  $(X, 0)$  is a normal surface singularity.

**Remark 5.7.** It can be proved (see for example [Lau71]), that any normal surface singularity has, at most, an isolated singularity. That is, it is either isolated or a smooth germ.

As we have seen in the previous section, there is a Milnor-Lê fibration theorem for holomorphic map germs with isolated singularities in these spaces. In [NP07] the authors study criterions for an automorphism of a surface to be the monodromy of the Milnor-Lê fibration of an holomorphic function germ  $f : (X, 0) \rightarrow (\mathbb{C}, 0)$  defined on an isolated surface singularity. The following result is contained in [NP07, Theorem 2.1]. Recall Definitions 3.19 and 4.15.

**Theorem 5.8.** Let  $(Y, L)$  be a Waldhausen link. Then the following two statements are equivalent

- (1)  $(Y, L)$  has the structure of horizontal open book for some  $g : Y \setminus L \rightarrow \mathbb{S}^1$  and some power of the monodromy  $\phi : \Sigma \rightarrow \Sigma$  is a composition of right-handed Dehn twists around disjoint simple closed curves that include all boundary components.
- (2) There exists a complex analytic structure on  $C(Y)$  (the cone of  $Y$ ) with  $(C(Y), 0)$  an isolated surface singularity. And there exists a reduced holomorphic map germ  $f : C(Y) \rightarrow \mathbb{C}$  whose Milnor-Lê fibration realizes  $(Y, L)$ , that is, the link of the Milnor-Lê fibration of  $f$  is  $L$ .

**Remark 5.9.** We make some clarifying observations to the previous theorem.

- (a) If we start with (1), then the monodromy of the Milnor-Lê fibration that we get in (2) coincides with the monodromy given in (1) and the singularity  $(C(Y), 0)$  is normal.
- (b) Given an isolated surface singularity  $(X, 0)$  and a reduced holomorphic map germ  $f : (X, 0) \rightarrow (\mathbb{C}, 0)$ , the monodromy of the Milnor-Lê fibration associated with  $f$  satisfies that some power of it is a product of right-handed Dehn twists around disjoint simple closed curves that include all boundary components.

Observation (a) can be extracted from [NP07]. Observation (b) follows from Grauert's criterion together with the computations of Section 4.3.

Part II

---

**Tête-à-tête graphs and  
twists**



## Chapter 6

---

# Tête-à-tête graphs

Chapter 1 and Chapter 2 (except last section) are the preliminaries for this chapter.

In this chapter, we introduce the main object of this work: *tête-à-tête graphs*. We essentially follow [A'C10]. In particular, Definitions 6.2, 6.6 and 6.13 are contained in the cited work. We also prove some basic properties of these objects that yield a comfortable setting for the rest of the work. This chapter can be followed completely having read Chapter 1.

We start by adding more structure to a relative ribbon graph: we consider *metric* relative ribbon graphs. A metric graph is given by a graph  $\Gamma$  and lengths  $l(e) \in \mathbb{R}$  for every edge  $e \in e(\Gamma)$ . In an edge  $e$ , we take a homogeneous metric that gives  $e$  total length  $l(e)$ . We consider the distance  $d(x, y)$  on  $\Gamma$  given by the minimum of the lengths of the paths joining  $x$  and  $y$ . It is a complete metric space. We denote a metric relative ribbon graph by  $(\Gamma, A, d)$  and when it is clear from context we omit the distance  $d$  in the notation.

**Definition 6.1.** *A walk in a graph  $\Gamma$  is a continuous mapping*

$$\gamma : I \rightarrow \Gamma,$$

*from an interval  $I$ , possibly infinite, and such that for any  $t \in I$  there exists a neighborhood around  $t$  where  $\gamma$  is injective.*

Now we give the first definitions inherent to tête-à-tête graphs, following essentially [A'C10]. The notion of safe walk is central in this work. This is a purely graph theoretical definition.

**Definition 6.2** (Safe walk). *Let  $(\Gamma, A, d)$  be a metric relative ribbon graph. A safe walk for a point  $p$  in the interior of some edge is a walk  $\gamma_p : \mathbb{R}_{\geq 0} \rightarrow \Gamma$  with  $\gamma_p(0) = p$  and such that:*

- (1) *The absolute value of the speed  $|\gamma_p'|$  measured with the metric of  $\Gamma$  is constant and equal to 1. Equivalently, the safe walk is parametrized by arc length, i.e. for  $s$  small enough  $d(p, \gamma_p(s)) = s$ .*
- (2) *When  $\gamma_p$  gets to a vertex, it continues along the next edge in the given cyclic order.*

- (3) If  $p$  is in an edge of  $A$ , the walk  $\gamma_p$  starts running in the direction prescribed by the orientation of  $A$  (recall that this orientation is opposite to the orientation of  $A$  seen as boundary of  $\Sigma$ ). This is sometimes called the relative safe walk or the boundary safe walk.

An  $\ell$ -safe walk is the restriction of a safe walk to the interval  $[0, \ell]$ . If a length is not specified when referring to a safe walk, we understand that its length is  $\pi$ .

The notion in (2) of *continuing along the next edge in the order of  $e(v)$*  is equivalent to the notion of *turning to the right* in every vertex for paths parallel to  $\Gamma$  in  $\Sigma$  in A'Campo's words in [A'C10].

Following A'Campo notation, we treat mainly with  $\pi$ -safe walks. In Chapter 7 we make use of safe walks of different lengths, that is why we introduce it in such a generality here.

**Remark 6.3** (Safe walk via cylinder decomposition). Condition (2) in the previous definition is equivalent to:

- (2) the path  $\gamma$  admits a lifting  $\tilde{\gamma}_p : \mathbb{R}_{\geq 0} \rightarrow \Sigma_\Gamma$  in the cylinder decomposition of  $\Sigma_\Gamma$  (see Notation 1.11), which runs in the opposite direction to the one indicated by the orientation induced on  $\tilde{\Gamma}_i$  seen as boundary of the cylinder  $\tilde{\Sigma}_i$ .

**Remark 6.4.** In fact, from this viewpoint, a safe walk starting from  $p \in \Gamma$  is nothing else than the image by  $g_\Gamma$  of a negative arc-length parametrization of a circle  $\tilde{\Gamma}_i$  (see Notation 1.11) starting from a preimage of  $p$ . This extends Definition 6.2 to safe walks starting at any point  $p$  in the graph  $\Gamma$ .

Each of the equivalent formulations of Property (2) of safe walks has its own virtues. The first is purely described in terms of graphs and is more convenient for defining *General tête-à-tête homeomorphisms* in Section 7.3. The second is more convenient to define *Signed tête-à-tête homeomorphisms* in Chapter 7 and *Mixed tête-à-tête graphs* in Chapter 8.

**Remark 6.5.** Given a relative ribbon graph  $(\Gamma, A)$  with thickening  $(\Sigma, A)$ , we make four observations in order to help fixing ideas:

- (1) Every vertex  $v \in v(\Gamma)$  has as many preimages by  $g_\Gamma$  as its valency  $e(v)$ . These preimages belong to certain  $\tilde{\Gamma}_i \subseteq \tilde{\Sigma}_i$  for certain cylinders  $\tilde{\Sigma}_i$  which could occasionally be the same. An interior point of an edge not included in  $A$  has exactly two preimages. An interior point of an edge included in  $A$  has exactly one preimage.
- (2) For every point  $p \in \Gamma$  and every oriented direction from  $p$  along  $\Gamma$  compatible with the orientation of  $A$  there is a safe walk starting on  $p$  following that direction. This safe walk admits a lifting to one of the cylinders  $\tilde{\Sigma}_i$ .

More clearly:

- (a) For  $p$  an interior point of an edge not belonging to  $A$ , that is for  $p \in \Gamma \setminus (v(\Gamma) \cup A)$ , only 2 starting directions for a safe walk are possible, corresponding to the two different preimages of  $p$  by  $g_\Gamma$ . We will denote the corresponding safe walks by  $\gamma_p$  and  $\omega_p$ . If  $p$  is at the interior of an edge contained in  $A$  only one starting direction for a safe walk at  $p$  is possible: the direction indicated by the orientation of  $A$  (opposite to the orientation of  $A$  seen as boundary of  $\Sigma$ ).
- (b) For a vertex  $v$ , not belonging to  $A$  there are as many starting directions as edges in  $e(v)$ , and for any vertex  $v$  belonging to  $A$ , there are as many starting directions as edges in  $e(v)$  minus 1.

**Definition 6.6** (Tête-à-tête property). *Let  $(\Gamma, A, d)$  be a metric relative ribbon graph without univalent vertices. We say that  $\Gamma$  satisfies the  $\ell$ -tête-à-tête property, or that  $\Gamma$  is an  $\ell$ -tête-à-tête graph if:*

- *For any point  $p \in \Gamma \setminus (A \cup v(\Gamma))$  the two different  $\ell$ -safe walks starting at  $p$  (see Remark 6.5), that we denote by  $\gamma_p, \omega_p$ , satisfy  $\gamma_p(\ell) = \omega_p(\ell)$ .*
- *For a point  $p$  in  $A \setminus v(\Gamma)$ , the end point of the unique  $\ell$ -safe walk starting at  $p$  belongs to  $A$ .*

*If  $\Sigma$  is the regular thickening of the graph  $\Gamma$  and  $A$  denotes the corresponding union of boundary components, we say that  $(\Gamma, A)$  gives a relative  $\ell$ -tête-à-tête structure to  $(\Sigma, (\Gamma, A))$  or that  $(\Gamma, A)$  is a relative  $\ell$ -tête-à-tête graph or spine for  $(\Sigma, (\Gamma, A))$ .*

*If  $A = \emptyset$ , we call it a pure  $\ell$ -tête-à-tête structure or graph.*

**Remark 6.7.** Since by Remark 6.4 there are safe walks starting at any vertex the seemingly stronger notion of the  $\ell$ -tête-à-tête property may be defined:

- For any point  $p \in \Gamma$  all the  $\ell$ -safe walks starting at  $p$  end at the same point.
- If  $p$  belongs to  $A \setminus v(\Gamma)$ , the end point of the unique  $\ell$ -safe walk starting at  $p$  belongs to  $A$ .

**Lemma 6.8** (Lemma and Definition). *For an  $\ell$ -tête-à-tête graph  $(\Gamma, A, d)$ , the following are true:*

- (1) *The conditions stated in Remark 6.7 hold true.*
- (2) *The mapping  $\sigma_\Gamma : \Gamma \rightarrow \Gamma$  defined by  $\sigma_\Gamma(p) = \gamma_p(\ell)$  is a homeomorphism. If  $p$  is a vertex,  $\gamma_p$  denotes any  $\ell$ -safe walk starting at  $p$ .*

*Proof.* A proof in terms of the description of safe walks via images of parametrizations of boundaries of cylinders as in Remark 6.4 is easy: let

$$\sigma : \coprod_i \tilde{\Gamma}_i \rightarrow \coprod_i \tilde{\Gamma}_i$$

be the homeomorphism which restricts to the metric circle  $\tilde{\Gamma}_i$  to the negative rotation of amplitude  $\ell$  (move each point to a point which is at distance  $\ell$  in the negative sense with respect to the orientation). The tête-à-tête property implies that  $\sigma$  is compatible with the gluing  $g_\Gamma$  at any point which is not the preimage of a vertex. By continuity the compatibility extends to all the points. The mapping  $\sigma$  descends to the mapping  $\sigma_\Gamma$ . This proves simultaneously both assertions.

However, for later use in the definition of *general tête-à-tête homeomorphisms* in Section 7.3, we give below a proof using only the combinatorial description of a safe walk.

We note first that if  $q = \gamma_p(s)$  is an interior point of an edge, then we have the equality  $\gamma_q(\ell) = \gamma_{\gamma_p(\ell)}(s)$ .

Take a vertex  $v \in v(\Gamma)$ . Let  $\epsilon > 0$  be smaller than  $\ell$  and than half the length of any edge. For any edge  $e_i \in e(v) = \{e_1, \dots, e_k\}$  take a sequence of points  $\{y_i^n\}_n$  of  $e_i$  such that  $d(y_i^n, v) = \epsilon/n$ . We have that  $d(y_i^n, y_j^m) = \epsilon/n + \epsilon/m$  if  $i \neq j$  because we have chosen  $\epsilon$  small enough. We also have that  $\gamma_{y_i^n}(\epsilon/n + \epsilon/m) = y_{i+1}^m$ . Thus  $d(\gamma_{y_i^n}(\ell), \gamma_{y_{i+1}^m}(\ell)) \leq \epsilon/n + \epsilon/m$ . Then for every  $i = 1, \dots, k$  the Cauchy sequences  $\{\gamma_{y_i^n}(\ell)\}_n$  converge to the same point  $u$ . Similarly the Cauchy sequences  $\{\omega_{y_i^n}(\ell)\}_n$  converge to the same point  $u'$ . By the tête-à-tête property we have the equality  $u = u'$ . It is easy to observe that  $u$  is the image of all the safe walks starting at  $v$ . This proves the first assertion.

We define  $\sigma_\Gamma(v) =: u$ . It is clear that with this definition  $\sigma_\Gamma$  is continuous and that  $u$  is a common vertex of the images by  $\sigma_\Gamma$  of the edges  $e_i$ .



The inverse of  $\sigma_\Gamma$  for a point  $q \in \sigma_\Gamma(\Gamma \setminus v(\Gamma))$  is the end of a walk of length  $\ell$  starting at  $q$  that when approaching a vertex  $v$  turns to the previous edge in the cyclic order of  $e(v)$ . Note that the tête-à-tête property of Definition 6.6 also holds for this type of paths whenever they start in  $\sigma_\Gamma(\Gamma \setminus v(\Gamma))$ . So, we can do the same as in the first part of the proof and see that it extends to the whole  $\Gamma$  and that it is continuous. Then,  $\sigma_\Gamma$  has a continuous inverse.  $\square$

**Remark 6.9.** There is a special and easy case for  $\pi$ -tête-à-tête graphs: when  $\Gamma$  is homeomorphic to  $\mathbb{S}^1$ . The thickening surface is in this case the cylinder. In this case the only possibilities for  $\sigma_\Gamma$  are the identity or the  $\pi$  rotation (for the homogeneous metric on  $\mathbb{S}^1$ ). Then  $\Gamma$  has total length of  $2\pi/n$  for some  $n \in \mathbb{N}$ .

**Corollary 6.10.** *The homeomorphism  $\sigma_\Gamma$  has the following properties:*

- (1) *It is an isometry.*
- (2) *It preserves the cyclic orders of  $e(v)$  for every  $v \in v(\Gamma)$ .*
- (3) *It takes vertices of valency  $k > 2$  to vertices of the same valency.*
- (4) *It has finite order.*

*Proof.* Point (1) follows from the proof of Lemma 6.8 because  $\sigma_\Gamma$  is a homeomorphism that is an isometry restricted to the edges. Point (2) follows also from the proof. Point (3) is immediate since  $\sigma_\Gamma$  is a homeomorphism.

To see that  $\sigma_\Gamma$  has finite order when it is not  $\mathbb{S}^1$ , we observe that  $\sigma_\Gamma$  induces a permutation between edges and vertices of  $\Gamma'$  and is an isometry. Then, it has finite order. When the graph is homeomorphic to  $\mathbb{S}^1$ , it follows from Remark 6.9.  $\square$

**Corollary 6.11.** *The following assertions hold:*

- (1) *If  $\sigma_\Gamma|_e = \text{id}$  for some edge  $e$ , then  $\sigma_\Gamma$  is the identity.*
- (2) *For every  $m \in \mathbb{N}$  the homeomorphism  $\sigma_\Gamma^m$  is also induced by a tête-à-tête graph.*
- (3) *If  $\sigma_\Gamma^m|_e = \text{id}$  for some edge  $e$ , then  $\sigma_\Gamma^m$  is the identity.*

*Proof.* Given  $\sigma_\Gamma$  as in (1), since it preserves the cyclic order at every  $v$ , then it fixes all the edges adjacent to the vertices of  $e$ . Since the graph is connected, this argument extends to the whole graph and the statement follows.

To see (2) and find a tête-à-tête graph for  $\sigma_\Gamma^m$  one can take the same combinatorial graph  $\Gamma$  with edge lengths equal to the ones of  $\Gamma$  divided by  $m$ .

For (3), we have by (2) that the homeomorphism  $\sigma_\Gamma^m$  is also induced by a tête-à-tête graph and then we are in the case of point (1).  $\square$

**Lemma 6.12.** *If  $(\Gamma, A, d)$  is a relative tête-à-tête graph, only modifying the underlying combinatorics (without changing the topological type of  $\Gamma$ ), we can ensure we are in one of the following cases:*

- (1) *Unless  $\Gamma$  is either homeomorphic to  $\mathbb{S}^1$  or contractible, all the vertices have valency  $\geq 3$ .*
- (2) *There are no loops (edges joining a vertex with itself) and there is at the most one edge joining two vertices. In this case the restriction  $\sigma_\Gamma|_{v(\Gamma)}$  determines  $\sigma_\Gamma$ .*
- (3) *All the edges have the same length.*

(4) The graph satisfies properties in (2) and (3) simultaneously.

*Proof.* If  $\Gamma$  is either homeomorphic to  $\mathbb{S}^1$  or contractible, after Remark 6.9, the proof is trivial.

Let's see the case where  $\Gamma$  is neither homeomorphic to  $\mathbb{S}^1$  nor contractible. To get a graph as in (1) we can consider the graph  $\Gamma'$  forgetting the valency-2-vertices of  $\Gamma$  but keeping distances. It is clearly a tête-à-tête graph.

To get a graph as in (2) we consider the graph  $\Gamma$  as in (1). We add as vertices some mid-point-edges  $q_1, \dots, q_m$  to  $\Gamma'$  in order the new graph has no loops and no more than one edge between any pair of vertices. Now, we have to add as vertices any other point  $p$  for which  $\gamma_p(\pi)$ , the end of the safe walk for  $\Gamma$ , is one of these new vertices  $q_i$ . Since  $\sigma_\Gamma$  takes isometrically edges to edges, it will take midpoint edges to midpoint edges of  $\Gamma$ . Then we have to add at the most all the mid point edges of  $\Gamma$  as vertices to reach the desired graph.

Moreover, we note that in a graph as in (2), the image  $\sigma_\Gamma(e)$  of an edge  $e$  joining  $v_i$  and  $v_j$ , has to be the only edge joining  $\sigma_\Gamma(v_i)$  and  $\sigma_\Gamma(v_j)$ . Then,  $\sigma_\Gamma|_{v(\Gamma)}$  determines  $\sigma_\Gamma$ .

To find a tête-à-tête graph as in (3), we start with a graph  $\Gamma$  as in (1). The homeomorphism  $\sigma_\Gamma$  permutes edges. Moreover the tête-à-tête condition says that certain summations of the lengths  $\{l(e)\}_{e \in e(\Gamma)}$  are equal to  $\pi$ . We consider only the summations that come from measuring the lengths of the safe walks that start in vertices of  $\Gamma$ , which are a finite number. We collect all these linear equations in the variables  $l(e)$  in a system  $S$ . We consider the system of equations  $S'$  by replacing the independent term  $\pi$  in the equations of  $S$  by 1. It is clear that there exist positive rational solutions  $l(e)$  of the system  $S'$ . Let  $N$  be a common denominator. We consider the graph  $\Gamma'$  by subdividing every edge  $e$  of  $\Gamma$  into  $N \cdot l(e)$  edges of length  $\pi/N$  obtaining the desired graph.

If  $\Gamma'$  does not satisfy properties in (2), taking  $N = 2N$  you get it. You can also add the middle points of all the edges as vertices and finish as in the proof of (2).  $\square$

A way to obtain relative tête-à-tête graphs from pure ones is A'Campo notion of  $\epsilon$ -blow up.

**Definition 6.13** ( $\epsilon$ -blow up of  $(\Sigma, \Gamma)$  at a vertex of  $\Gamma$ ). *Let  $\Gamma$  be a pure  $l$ -tête-à-tête graph and  $\Sigma$  be its thickening surface. Let  $v$  be a vertex of valency  $p$ . We consider the real blow up of  $\Sigma$  at  $v$ . We denote by  $\Sigma'$  and  $\Gamma'$  the transformations of  $\Sigma$  and  $\Gamma$ . Note that  $\Sigma$  has one more boundary component and  $\Gamma'$  has changed the vertex  $v$  by a circle  $A \cong \mathbb{R}P^1$  with  $p$  edges attached. Away from  $v$ , we consider the metric in  $\Gamma'$  as in  $\Gamma$ . We assign the length  $2\epsilon$  to the new edges in  $\Gamma'$  along  $\mathbb{R}P^1$  and redefine the length of the edges corresponding to each  $e \in e(v)$  by  $length(e) - \epsilon$ . (See figure below Figure 6.14). We do this at every vertex on the orbit of  $v$  by the  $\sigma_\Gamma$  and denote the resulting space by  $Bl_v(\Gamma, \epsilon)$ . We say that it is the result of performing the  $\epsilon$ -blowing up of  $\Gamma$  at  $v$ .*

It is immediate to check that  $(\Gamma', A)$  is a relative tête-à-tête graph and that  $\Sigma'$  is its thickening. we denote it by  $(\Sigma', (\Gamma', A))$ .

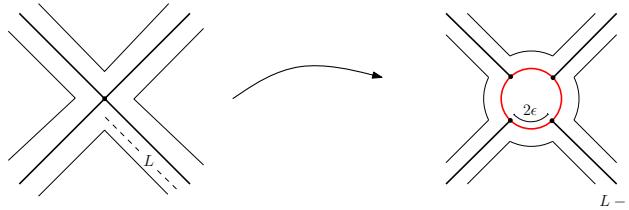


Figure 6.14: Blow-up some vertex  $v$  of valency 4.



## Chapter 7

---

# *Tête-à-tête twists*

Chapter 6 is needed for this chapter. In this chapter we explain how to associate to each tête-à-tête graph a freely periodic automorphism of a surface up to conjugation and isotopy. First we extend a little bit the definitions of Chapter 6 and allow safe walks that *turn left at vertices* instead of turning right. This extension leads to a definition of *signed tête-à-tête graph*. Then we associate to each signed tête-à-tête graph a freely periodic automorphism.

Not every invariant spine obtained in the proof of Lemma 2.13 accepts a tête-à-tête structure such that  $\sigma_\Gamma = \phi|_\Gamma$  (see Examples C.1 and 7.16). In Theorem 7.30 we will see how to find one that accepts it. In Theorem 7.30, which is one of the main results of the present work and appeared first in [FPP17], we prove that the automorphisms that can be modeled by signed tête-à-tête graphs are exactly the freely periodic automorphisms. In Corollary 7.19 we show that the class of automorphisms modeled by tête-à-tête graphs (as defined by A'Campo) is the class of freely periodic automorphisms with strictly positive fractional Dehn twist coefficients.

In the last part of the chapter we study, as a corollary of this theory, the modeling of truly periodic automorphisms by tête-à-tête graphs and obtain analogous results.

## 7.1 Signed tête-à-tête graphs and freely periodic automorphisms

We start recalling a definition and making an extension of Remark 6.5 adding point (b').

Let  $(\Gamma, A)$  be a metric relative ribbon graph. Let  $(\Sigma, A)$  be a thickening, let

$$g_\Gamma : \Sigma_\Gamma \rightarrow \Sigma$$

be the gluing map as in Notation 1.11.

**Remark 7.1** (Definition of  $\gamma_p^-, \omega_p^-, \gamma_p^0, \gamma_p^+$  and  $\omega_p^+$ ).

(b') for every point  $p \in \Gamma \setminus v(G)$  and every of the two possible oriented directions from  $p$  along  $\Gamma$ , there is a walk starting on  $p$  following each of this directions, such that in every vertex  $v$ , the walk continues along the *previous* edge in the cyclic order of  $e(v)$ . We denote by  $\gamma_p^-$  and  $\omega_p^-$  these walks of length  $\pi$  and speed 1. Each of the oriented directions at  $p$  corresponds to a point in  $q \in g_\Gamma^{-1}(p)$ , which lives in a cylinder  $\tilde{\Sigma}_i$ . These walks are the image of the negative sense parametrization of the boundary of  $\tilde{\Sigma}_i$  starting at  $q$ .

We denote by  $\gamma_p^+$  and  $\omega_p^+$  the usual safe walks of Definition 6.2 or Remark 6.5 of length  $\pi$  and speed 1. We call  $\gamma_p^+$  and  $\omega_p^+$  the *positive safe walks* and  $\gamma_p^-$  and  $\omega_p^-$  the *negative safe walks*.

In the case of points in  $A$ , since  $A$  is oriented, we have also a positive and negative sense for a parametrization. Then, for  $p \in A$ , we define  $\gamma_p^+$  (respectively  $\gamma_p^-$ ) as the parametrization from  $p$  that starts along  $A$  in the positive (respectively negative) sense and that when reaching a vertex  $v$  takes the next (respectively previous) edge in the order of  $e(v)$ . We recall, once again, that the orientation on  $A$  is opposite to the orientation induced as boundary of  $\Sigma$ .

We also define a *safe constant walk*  $\gamma_p^0 := p$  (this one is the safest).

Before stating next definition, recall that there is a bijection between the set  $\mathcal{C}$  of boundary components of  $\Sigma$  that are not in  $A$ , and the cylinders  $\tilde{\Sigma}_i$ 's. Given a “sign” map  $\iota : \mathcal{C} \rightarrow \{0, +, -\}$ , we denote by  $\iota(i)$  the image by  $\iota$  of the component that corresponds to  $\tilde{\Sigma}_i$  under the bijection.

**Definition 7.2.** Let  $(\Gamma, A)$  be a metric relative ribbon graph and let  $(\Sigma, A)$  be a thickening. Let  $\mathcal{C}$  denote the set of boundary components of  $\Sigma$  which do not belong to  $A$ . Fix a map

$$\iota : \mathcal{C} \rightarrow \{0, +, -\}.$$

We say that  $(\Gamma, A)$  satisfies the signed tête-à-tête property for  $\iota$  or that  $(\Gamma, A, \iota)$  is a signed relative tête-à-tête graph if given any point  $p$  contained in the interior of an edge the following properties are satisfied:

(1) If  $p$  does not belong to  $A$  and  $p \in g_\Gamma(\tilde{\Sigma}_i) \cap g_\Gamma(\tilde{\Sigma}_j)$  for some  $i, j$ , then we have the equality

$$\gamma_p^{\iota(i)}(\pi) = \omega_p^{\iota(j)}(\pi).$$

(2) If  $p$  belongs to  $A$  and  $p$  belongs to  $g_\Gamma(\tilde{\Sigma}_i)$ , then the ending point  $\gamma_p^{\iota(i)}(\pi)$  of the unique signed safe walk starting at  $p$  belongs to  $A$ .

**Notation 7.3** (Remark and Notation). Observe that the map  $\Gamma \setminus v(\Gamma) \rightarrow \Gamma$  that sends  $p \in \Gamma \setminus v(\Gamma)$  to  $\gamma_p^{\iota(i)}(\pi)$  extends to  $v(\Gamma)$  and defines a homeomorphism of  $\Gamma$  that we denote by  $\sigma_{(\Gamma, \iota)}$ . The proof is as the one of Lemma 6.8.

In the next definition we use Notation 1.11.

**Definition 7.4** (Definition of  $\phi_{(\Gamma, A, \iota)}$ ). Let  $(\Gamma, A, \iota)$  be a signed relative tête-à-tête graph. For every thickening  $(\Sigma, A)$  and for every choice of product structure  $\tilde{\Sigma}_i \approx \tilde{\Gamma}_i \times I$  we consider the homeomorphism

$$\begin{aligned} \psi_i : \tilde{\Gamma}_i \times I &\longrightarrow \tilde{\Gamma}_i \times I \\ (p, s) &\mapsto (\tilde{\gamma}_p^{\iota(i)}(s \cdot \pi), s) \end{aligned} \tag{7.5}$$

where  $\tilde{\gamma}_p^{\iota(i)}$  is the lifting of the safe walk to  $\tilde{\Gamma}_i$ . The homeomorphism  $\psi_i$  of the cylinder can be visualized very easily using the universal covering of the cylinder as in Figure 7.6.

These homeomorphisms glue well due to the signed tête-à-tête graph property satisfied by  $(\Gamma, A, \iota)$  and define a homeomorphism of  $(\Sigma, A)$  that leaves  $\partial^1 \Sigma$  fixed pointwise and  $A$  invariant. We denote by  $\phi_{(\Sigma, \Gamma, A, \iota)}$  the resulting homeomorphism of  $(\Sigma, A)$ . If all the elements on which it depends are clear from the context, we simply denote it by  $\phi_\Gamma$ . We call it the induced tête-à-tête twist.

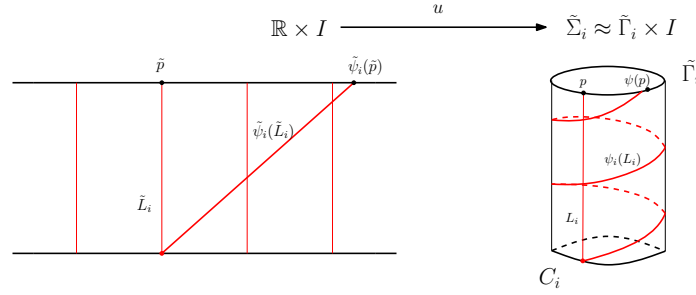


**Figure 7.6:** On the right we see the cylinder  $\tilde{\Sigma}_i \simeq \tilde{\Gamma}_i \times I$  and the action of  $\psi_i$  on a properly embedded segment  $L_i$ . On the left we see the universal cover of the cylinder with the preimages of  $L_i$  and the action  $\tilde{\psi}_i$  (the lifting of  $\psi_i$ ).

**Example 7.7.** Consider the tête-à-tête -structure of the  $K_{p,q}$  of the Example 1.6. In that example we find the formulas for the genus and the boundary components. The induced homeomorphism  $\phi_\Gamma$  has order  $M = \text{lcm}(p, q)$  (and leaves the boundary components invariant by definition). There are two special orbits, the one of  $p$  vertices that are ramification points of order  $M/q$  and another one of  $q$  vertices of ramification order  $M/p$ .

Then, knowing that  $\Sigma^{\phi_\Gamma}$  has also  $D = \text{gcd}(p, q)$  boundary components and using Hurwitz formula we get that the genus of the quotient surface  $\Sigma^{\phi_\Gamma}$  is 0.

If we look at the image of  $\Gamma = K_{p,q}$  by the quotient map  $p : \Sigma \rightarrow \Sigma^{\phi_\Gamma}$  map we obtain the graph in  $\Sigma^{\phi_\Gamma}$  of Figure 7.8.

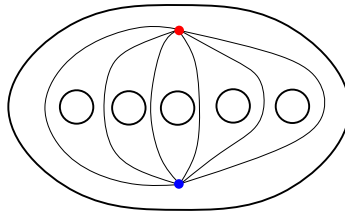


**Figure 7.8:** Drawing of  $p(K_{pq})$  which consists of two vertices (red and blue) corresponding to the two special fibers and  $r$  edges corresponding to the  $D$  boundary components, in the picture  $D = 6$ .

**Remark 7.9.** We can restate the  $\ell$ -tête-à-tête property in terms of boundary Dehn twists (recall Definition 2.49) of length  $\ell$  as follows. Let  $(\Sigma, \Gamma)$  be a thickening surface of a metric ribbon graph  $\Gamma$ . Let  $g_\Gamma : \Sigma_\Gamma \rightarrow \Sigma$  be the gluing map. Consider the pull back metric on  $g^{-1}(\Gamma)$ . Denote by  $\mathcal{D}_\ell$  the composition of the boundary Dehn twists  $\mathcal{D}_\ell$  along each  $\tilde{\Gamma}_j \subset \tilde{\Gamma}$ . Then  $(\Sigma, \Gamma)$  holds the  $\ell$ -tête-à-tête property if and only if  $\mathcal{D}_\ell$  is compatible with the gluing  $g_\Gamma$ . We see from this that the lengths of  $\tilde{\Gamma}_j$  are in  $\ell\mathbb{Q}_+$ .

**Remark 7.10.** We have made some non-canonical decisions in defining  $\phi_\Gamma$ . This ambiguity has the following counterpart.

- For a given product structure, the homeomorphism  $\phi_\Gamma$  is defined up to isotopy.
- Given two different product structures (or equivalently, regular retractions) of the cylinders, the induced tête-à-tête twists are conjugate by a homeomorphism that fixes  $\Gamma$ .
- For two different embeddings of  $\Gamma$  in  $\Sigma$ , the tête-à-tête twists are conjugate by the same homeomorphism of  $\Sigma$  that relates the two embeddings.

We conclude that a relative signed tête-à-tête graph by itself, defines a freely periodic mapping class up to conjugation.

**Remark 7.11.** The homeomorphism  $\phi_{(\Sigma, \Gamma, A, \iota)}$  leaves  $\Gamma$  invariant and by Lemma 2.27 has the following fractional Dehn twist coefficients (see also Figure 7.6):

$$R_i := \text{rot}_{\partial^1}(\phi_{(\Sigma, \Gamma, A, \iota)}, C_i) = \iota(i) \cdot \frac{\pi}{\text{length}(\tilde{\Gamma}_i)}. \quad (7.12)$$

Hence, the homeomorphism  $\psi_i$  of eq. (7.5) equals the linear twist  $\mathcal{D}_{-R_i, 0}$  (recall Notation 2.34). So a tête-à-tête twist induces linear twists  $\psi_i$  on each cylinder  $\tilde{\Sigma}_i$ . By Remark 2.47 the screw number of  $\psi_i$  equals  $-R_i$ .

The following lemma uses results from Section 2.4 and improves Corollary 2.28.

**Lemma 7.13.** *Let  $\phi_0, \phi_1 : \Sigma \rightarrow \Sigma$  be two homeomorphisms that are the identity on  $\partial\Sigma$ . Let  $\Gamma \hookrightarrow \Sigma$  be a spine. Suppose that  $\Gamma$  is invariant by both homeomorphisms, that  $\phi_0|_\Gamma = \phi_1|_\Gamma$  and that their fractional Dehn twist coefficients coincide at each boundary component. Then  $\phi_0$  and  $\phi_1$  are conjugate by an homeomorphism  $h$  isotopic to the identity in  $\text{MCG}^+(\Sigma, \partial\Sigma)$ . In particular, they are isotopic in  $\text{MCG}^+(\Sigma, \partial\Sigma)$ .*

*Proof.* Since  $\phi_0$  and  $\phi_1$  leave  $\Gamma$  invariant, they induce automorphisms  $\psi_i^0, \psi_i^1 : \tilde{\Sigma}_i \rightarrow \tilde{\Sigma}_i$  for each cylinder in  $\Sigma_\Gamma$ . By the first part of Lemma 2.39, these homeomorphisms are, up to isotopy preserving the action on the boundary, linear twists with the same screw number. Now apply the second part of Lemma 2.39 to these twists. We get a collection of homeomorphisms  $h_i$  that conjugate  $\psi_i^0$  and  $\psi_i^1$  and that are isotopic to the identity relative to the boundary. These homeomorphisms glue up to give a homeomorphism  $h : \Sigma \rightarrow \Sigma$  boundary-fixed isotopic to the the identity that conjugates  $\phi_0$  and  $\phi_1$ .  $\square$

**Remark 7.14.** Observe that if  $\iota(i) = 0$  for some  $i$ , then the homeomorphism  $\psi_i$  is the identity and  $\text{rot}_{\partial^1}(\phi_{(\Sigma, \Gamma, A, \iota)}, C_i) = 0$ . In particular, by Corollary 6.11 we find that the signed tête-à-tête twist must be the identity restricted to  $\Gamma$  and hence the fractional Dehn twist coefficient  $\text{rot}_{\partial^1}(\phi_{(\Sigma, \Gamma, A, \iota)}, C_j)$  is an integer for all boundary components. So  $\phi_{\Sigma, \Gamma, A, i}$  equals, up to isotopy, a composition of Dehn twists around boundary parallel curves.

Signed tête-à-tête homeomorphisms are a generalization of Dehn twists. We will call them also *signed tête-à-tête twists*. If all the signs are positive this notion coincides with A'Campo's original notion of tête-à-tête twists (see [A'C10]).

**Example 7.15.** The homeomorphisms induced by the tête-à-tête structures on the  $K_{p,q}$  ribbon graphs given in Example 1.6, were the first examples studied by A'Campo: they model the monodromy fixed at the boundary of the Milnor fibration associated to the singularities  $x^p + y^q = 0$ .

Before going on with the chapter, we note that not every invariant spine admits a metric modeling the corresponding homeomorphism. Indeed, we have the following counterexamples.

**Example 7.16.** In Figure 7.17 we find a spine  $\Gamma$  for the surface of genus 1 with 2 boundary components that is invariant by the  $\pi$ -rotation along the vertical axis.

This ribbon graph does not admit a tête-à-tête structure that models the given rotation. If  $L_1$  and  $L_2$  were the lengths of the edges of the graph that meet both cylinders of  $\Sigma_\Gamma$ , and  $L_3$  the other one, this would imply, by (eq. (7.12)), that  $1/2(L_1 + L_2) = \pi$  and  $1/2(L_1 + L_2 + L_3) = \pi$  which imply  $L_3 = 0$  that is not possible in a tête-à-tête graph.

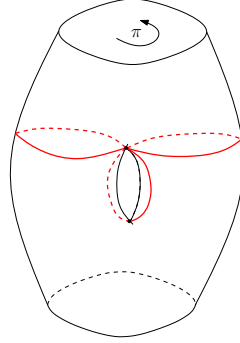


**Figure 7.17:** A spine for the genus-1 surface with one boundary components that is invariant by the  $\pi$ -rotation along the vertical axes.

In Example C.1, it is shown a method to produce examples of invariant ribbon graphs that do not admit a metric that models the automorphism by which it is invariant.

In the next theorem we characterize the homeomorphisms whose mapping class contains a signed tête-à-tête twist. As a corollary, we obtain a characterization of the homeomorphisms whose mapping class contains a tête-à-tête graph in the sense of A'Campo [A'C10]. We deal with the non-relative case first.

**Theorem 7.18.** *Let  $\Sigma$  be an oriented surface with non-empty boundary. Let  $[\phi]_\partial$  be a freely periodic mapping class in  $\text{MCG}^+(\Sigma, \partial\Sigma)$ . Then there exists  $\phi \in [\phi]_\partial$  such that  $\phi$  is periodic outside a collar neighborhood  $U$  of  $\partial\Sigma$  and:*

- (i) *There exists a signed tête-à-tête spine  $(\Gamma, \iota)$  embedded in  $\Sigma$  that is invariant by  $\phi$  such that the restriction of  $\phi$  to  $\Gamma$  coincides with  $\phi_{(\Sigma, \Gamma, \iota)}$ .*
- (ii) *The isotopy classes relative to the boundary  $[\phi]_\partial$  and  $[\phi_{(\Sigma, \Gamma, \iota)}]_\partial$  coincide.*
- (iii) *The homeomorphisms  $\phi$  and  $\phi_{\Gamma, \iota}$  are conjugate by a homeomorphism that fixes the boundary pointwise, fixes  $\Gamma$  and is isotopic to the identity in  $\text{MCG}^+(\Sigma, \partial\Sigma)$ .*

**Corollary 7.19.** *This theorem characterizes the originally defined A'Campo relative tête-à-tête twists as: orientation preserving homeomorphism fixing pointwise  $\partial^1\Sigma$  and freely isotopic to a periodic one  $\hat{\phi}$  with strictly positive fractional Dehn twist coefficients.*

In [HKM07, Definition 2.1], the notion of right-veering diffeomorphism was introduced. In [Gra15, Proposition 6.2.2] Graf characterized right-veering periodic homeomorphisms as the *multi-speed* tête-à-tête twists with non-negative walk lengths. The following corollary strengthens that result because signed tête-à-tête graphs have a unique walk-length for all boundary components.



**Corollary 7.20.** *Let  $(\Gamma, \iota)$  be a signed tête-à-tête graph. The diffeomorphism  $\phi_\Gamma$  is right-veering if and only if the map  $\iota$  doesn't take the value “−” at any boundary component.*

*Proof.* Both statements follow from Theorem 7.18 and [HKM07, Proposition 3.2].  $\square$

*Proof of Theorem 7.18.* We use Notation 1.11, Notation 2.7 and Notation 2.14.

By Lemma 2.23 we can assume that there exists a collar  $U$  of  $\partial\Sigma$  and  $\phi \in [\phi]_\partial$  such that  $\phi' := \phi|_{\Sigma \setminus U}$  is periodic. Let  $n$  be the order of  $\phi'$ . Let  $\Sigma^{\phi'}$  be the quotient surface. By abuse of notation we are writing  $\Sigma^{\phi'}$  instead of  $(\Sigma \setminus U)^{\phi'}$  since  $\Sigma$  and  $\Sigma \setminus U$  are homeomorphic.

We construct the invariant graph  $\Gamma$  as in the proof of Lemma 2.13, that is, as the preimage by the quotient map  $p : \Sigma \rightarrow \Sigma^{\phi'}$  of an appropriate spine  $\Gamma^{\phi'}$  for  $\Sigma^{\phi'}$ . The rest of the proof consists in giving a metric for the spine in  $\Sigma^{\phi'}$  such that the pullback metric in the corresponding invariant graph in  $\Sigma$  solves the problem.

By Corollary 2.28, we need to put a metric on  $\Gamma^{\phi'}$  such that the pullback-metric in  $\Gamma := p^{-1}(\Gamma^{\phi'})$  defines a tête-à-tête metric with  $\gamma_p^{(i)}(\pi) = \phi(p)$  for the signed safe walks along  $\Gamma$  and with the given signed tête-à-tête twist  $\phi_{\Gamma, \iota}$  having the same fractional Dehn twist coefficients as  $\phi$ .

We define

$$R_i := |\text{rot}_{\partial^1}(\phi, C_i)|.$$

The tête-à-tête structure of  $\Gamma$  has to satisfy the equality  $\gamma_p(\pi) = \phi(p)$  and moreover, the fractional Dehn twist coefficient of  $\phi_{\Gamma, \iota}$  at  $C_i$  has to be  $R_i$ . So, by eq. (7.12), we want that for every  $i$  with  $R_i \neq 0$

$$\text{rot}_{\partial^1}(\phi, C_i) \cdot \text{length}(\widetilde{\Gamma}_i) \cdot \iota(i) = \pi \quad (7.21)$$

holds. If  $\text{rot}_{\partial}(\phi, C_i)$  equals 0, by the definition of constant safe walk (see the end of Remark 7.1), we obtain no condition.

By the definition of  $R_i$  and the fact that both  $\text{rot}_{\partial^1}(\phi, C_i)$  and  $\iota(i)$  have the same sign, this equation becomes:

$$R_i \cdot \text{length}(\widetilde{\Gamma}_i) = \pi, \quad (7.22)$$

Moreover, we want the metric on  $\Gamma$  to be invariant by  $\phi'$  so it has to be the pullback of a metric on  $\Gamma^{\phi'}$ . We denote by  $\Sigma_{\Gamma^{\phi'}}$  the surface obtained by cutting  $\Sigma^{\phi'}$  along  $\Gamma^{\phi'}$  and consider the gluing map  $g_{\Gamma^{\phi'}} : \Sigma_{\Gamma^{\phi'}} \rightarrow \Sigma^{\phi'}$  analogously to Notation 1.11. We consider the lifting of  $p : \Sigma \rightarrow \Sigma^{\phi'}$  to the cut surfaces and we denote it by  $\widetilde{p} : \Sigma_\Gamma \rightarrow \Sigma_{\Gamma^{\phi'}}$ . We denote by  $\widetilde{p}(\widetilde{\Gamma}_i)$  the preimage of  $p(\Gamma_i)$  by  $g_{\Gamma^{\phi'}}$ . Since  $\widetilde{p}|_{\widetilde{\Gamma}_i} : \widetilde{\Gamma}_i \rightarrow \widetilde{p}(\widetilde{\Gamma}_i)$  is a  $n : 1$  covering map, we have the equality

$$\text{length}(\widetilde{\Gamma}_i) = n \cdot \text{length}(\widetilde{p}(\widetilde{\Gamma}_i)). \quad (7.23)$$

Note that one can easily read  $\text{length}(\widetilde{p}(\widetilde{\Gamma}_i))$  looking at the lengths of the edges of  $p(\Gamma_i) \subseteq \Gamma^{\phi'}$ .

Putting (eq. (7.22))-(eq. (7.23)) together, we find that what we need is that the equality

$$\text{length}(\widetilde{p}(\widetilde{\Gamma}_i)) = \frac{\pi}{n \cdot R_i} \quad (7.24)$$

holds for all  $i$  with  $R_i \neq 0$ .

Next, we prove that by finding a metric spine  $\Gamma^{\phi'} \hookrightarrow \Sigma^{\phi'}$  whose lengths satisfy (eq. (7.24)) for every  $i$  with  $R_i \neq 0$  we finish the proof of the theorem by taking  $\Gamma := p^{-1}(\Gamma^{\phi'})$  with the pullback metric.

The graph  $\Gamma := p^{-1}(\Gamma^{\phi'})$  is a signed tête-à-tête graph for  $\iota$  defined as  $\iota(i) = \text{sign}(\text{rot}_{\partial^1}(\phi, C_i))$  because the liftings of the safe walks to each cylinder in  $\Sigma_\Gamma$  act by construction as the lifting

of  $\phi'$  to  $\Sigma_\Gamma$  restricted to  $\tilde{\Gamma}$  (because they have the same rotation number). Let  $\phi_{(\Sigma, \Gamma, \iota)}$  be the induced signed tête-à-tête twist. This tête-à-tête structure on  $\Gamma$  induces by construction a rotation  $\tilde{\phi}_{(\Sigma, \Gamma, \iota)}|_{\tilde{\Gamma}_i}$  of rotation number  $|\text{rot}_{\partial^1}(\phi, C_i) - \lfloor \text{rot}_{\partial^1}(\phi, C_i) \rfloor|$  in each  $\tilde{\Gamma}_i$ . It is conjugate to  $\tilde{\phi}|_{\tilde{\Gamma}_i}$  since they have the same rotation number (recall Corollary 2.29). The orbits of  $\tilde{\phi}|_{\tilde{\Gamma}_i}$  are the fibers of  $\tilde{p}|_{\tilde{\Gamma}_i}$ . By the choice of lengths, the orbits of the tête-à-tête rotation in  $\tilde{\Gamma}_i$  are also the fibers of  $\tilde{p}|_{\tilde{\Gamma}_i}$ . By Corollary 2.28 we find that  $\phi'$  and  $\phi_{(\Sigma, \Gamma, \iota)}$  are isotopic since they coincide on  $\Gamma$ .

By first part of Lemma 2.39 we see that, after an isotopy of  $\phi$  fixing  $\Gamma$  and the boundary we can assume that  $\phi$  induces linear twists on the cylinders of  $\tilde{\phi}$ . Then we apply Lemma 7.13 to  $\phi'$  and  $\phi_{(\Sigma, \Gamma, \iota)}$  to prove part (iii) of the statement.

Now we finish the proof showing how to find the appropriate invariant spine  $\Gamma$  and its tête-à-tête metric.

First we prove the case  $g := \text{genus}(\Sigma^{\phi'}) \geq 1$ . To choose a spine in  $\Sigma^{\phi'}$ , we use a planar representation of  $\Sigma^{\phi'}$  as a convex  $4g$ -gon in  $\mathbb{R}^2$  with  $r$  disjoint open disks removed from its convex hull. The sides of the  $4g$ -gon are labelled clockwise like  $a_1 b_1 a_1^{-1} b_1^{-1} a_2 b_2 a_2^{-1} b_2^{-1} \dots a_g b_g a_g^{-1} b_g^{-1}$ , where edges labelled with the same letter (but different exponent) are identified by an orientation reversing homeomorphism. The number  $r$  is the number of boundary components. We number the boundary components  $C_i \subseteq \partial \Sigma$ ,  $1 \leq i \leq r$ . We denote by  $d$  the arc  $a_2 b_2 a_2^{-1} b_2^{-1} \dots a_g b_g a_g^{-1} b_g^{-1}$ . We consider  $l_1, \dots, l_{r-1}$  arcs as in Figure 7.26. We denote by  $c_1, \dots, c_r$  the edges in which  $a_1^{-1}$  (and  $a_1$ ) is subdivided, numbered according to the component  $p(C_i)$  they enclose. We consider the spine  $\Gamma^{\phi'}$  of  $\Sigma^{\phi'}$  given by the union of  $d$ ,  $a_1 b_1 a_1^{-1} b_1^{-1}$  and the  $l_i$ 's. We construct  $\Gamma^{\phi'}$  so that it passes by all the branching points of  $p$ . Then the retraction of  $\Sigma^{\phi'}$  to  $\Gamma^{\phi'}$  lifts to a retraction of  $\Sigma$  to the preimage  $\Gamma := p^{-1}(\Gamma^{\phi'})$ . Hence  $\Gamma$  is a spine of  $\Sigma$ .

We denote by  $D$ ,  $B_1$  and  $C_i$  the lengths of  $d$ ,  $b_1$  and  $c_i$  respectively. We will assume all the  $l_i$  and  $b_1$  of the same length  $L$ . Then the system (eq. (7.24)) for this case can be expressed as follows:

$$\begin{aligned} 2L + 2C_1 &= \frac{\pi}{n \cdot R_1} \\ 2L + 2C_i &= \frac{\pi}{n \cdot R_i} \quad \text{for } i = 2, \dots, r-1 \\ 2L + 2C_r + D &= \frac{\pi}{n \cdot R_r}, \end{aligned} \tag{7.25}$$

which has obviously positive solutions  $C_i$ ,  $D$  after taking, for example,  $L = \min\{\frac{\pi}{4 \cdot n \cdot R_i}\}$ . We assign  $\text{length}(a_i) = \text{length}(b_i) = D/4(g-1)$  for  $i > 1$  to get a metric on  $\Gamma^{\phi}$ . We consider the pullback-metric in  $\Gamma$ . This finishes the case  $\text{genus}(\Sigma^{\phi'}) \geq 1$ .

For the case  $\text{genus}(\Sigma^{\phi'}) = 0$  we proceed a bit differently to choose the spine  $\Gamma^{\phi'}$ . The surface  $\Sigma^{\phi'}$  is a disk with  $r-1$  smaller disjoint disks removed. We cut the surface along an embedded segment that we call  $c$  as we can see in the first image of Figure 7.27. Cutting along  $c$  we get another planar representation of  $\Sigma^{\phi'}$  as in the second image. The exterior boundary corresponds to  $cc^{-1}$ ; we call the exterior boundary  $P$  and denote by  $q_1$  and  $q_2$  the points in  $P$  that come from the two extremes of  $c$ . We look at the graph of the third picture in Figure 7.27. We have drawn  $r-1$  vertical segments  $l_1, \dots, l_{r-1}$  so that  $P$  union with them contains all branch points and is a regular retract of the disk enclosed by  $P$  minus the  $r$  disks.

The rest of the proof follows by cases on the number of boundary components  $r$  and the number of branch points.

If  $r = 1$  and there are no branch points or 1 branch point, then  $\Sigma$  is a disk (this follows from the Hurwitz formula) which is not covered by the statement of the theorem. If there are at least

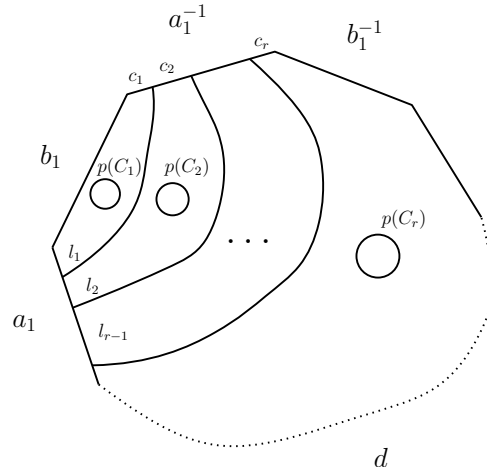


**Figure 7.26:** Planar representation of the surface  $\Sigma^\phi$  of genus  $\geq 1$  and  $r$  boundary components  $p(C_1), \dots, p(C_r)$ . Drawing of  $l_1, \dots, l_r$  and  $c_1, \dots, c_r$ .

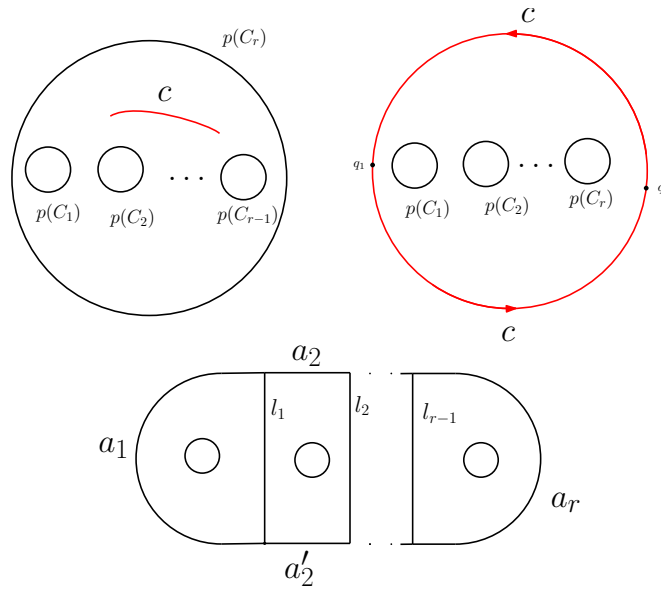


**Figure 7.27:** In the first two pictures we have the disk with  $r - 1$  smaller disks removed. In the third one we forget the identification along the exterior and we draw a spine.

2 branch points, we can get that two branch points lie in  $q_1$  and  $q_2$  so that  $\Gamma$  has no univalent vertices. In this case we set  $length(c) = \frac{\pi}{2nR_1}$ .

Suppose now  $r = 2$ . If there are no branch points, then  $\Sigma$  is a cylinder which is not included in the statement of this theorem.

If there is at least 1 branch point we consider two cases, namely  $R_1 = R_2$  and  $R_1 > R_2$ .

In the case  $R_1 = R_2$ , we choose the graph depicted on the right hand side of Figure 7.28. That is,  $q_1$  and  $q_2$  are exactly  $a_1 \cap a_2$ . In this case we do not care about the location of the branch point

as long as it is contained in the graph. In this case we set  $length(c) = length(l_1) = \frac{\pi}{2nR_1}$

In the case  $R_1 < R_2$ , we choose the graph depicted on the left hand side of Figure 7.28 and we choose the branch point to lie on  $q_1$ , this way, since  $q_1$  is the only vertex of valency 1, we get that the preimage of this graph by  $p$  does not have univalent vertices. We set the lengths,  $length(l_1) = \frac{\pi}{nR_1}$  and  $length(c) = (\frac{\pi}{nR_2} - \frac{\pi}{nR_1})/2$ .

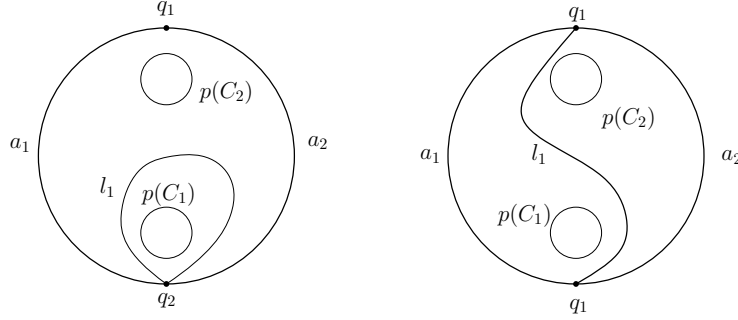


**Figure 7.28:** On the left, the case  $R_1 < R_2$ . On the right the case when  $R_1 = R_2$ .

Suppose now  $r > 2$ .

We are going to assign lengths to every edge in Figure 7.27 and decide how to divide and glue  $P$  in order to recover  $\Sigma^{\phi'}$ . This means that we are going to decide the position of  $q_1$  and  $q_2$  in  $P$ , relative to the position of the ends of the  $l_i$ 's, in order to get a suitable metric spine of the quotient surface  $\Sigma^{\phi'}$ .

To every vertical interior segment  $l_j$  we assign the same length

$$L < \min\left\{\frac{\pi}{2(n \cdot R_i)}\right\}.$$

We look at the segments  $a_1, a_2, a'_2, \dots, a_{r-1}, a'_{r-1}, a_r$  in which  $P$  is divided by the vertical segments (see Figure 7.27) and give lengths  $A_1, A_2, A'_2, \dots, A_{r-1}, A'_{r-1}, A_r$ . The following system corresponds to (eq. (7.24)) for this case:

$$\begin{aligned} A_1 + L &= \frac{\pi}{n \cdot R_1} \\ A_i + A'_i + 2L &= \frac{\pi}{n \cdot R_i} \quad \text{for } i = 2, \dots, r-1 \\ A_r + L &= \frac{\pi}{n \cdot R_r}. \end{aligned} \tag{7.29}$$

It has obviously positive solutions  $A_i$ . We choose  $A_i = A'_i$  for  $i = 2, \dots, r-1$ .

In order this distances can be pullback to the original graph  $\Sigma^{\phi'}$ , there is one equation left: we have to impose equal length to the two paths  $c$  and  $c^{-1}$ , or in other words to place  $q_1$  and  $q_2$  dividing  $P$  in two segments of equal length.

If  $\phi$  has at least two branch points, we choose  $q_1$  and  $q_2$  to be any two of the branch points. Then, we can choose the metric and the vertical segments so that  $q_1$  and  $q_2$  are the middle points of  $a_1$  and  $a_r$ . If we identify the two paths  $c$  and  $c^{-1}$  joining  $q_1$  and  $q_2$  then we recover  $\Sigma^{\phi'}$ , and we get a metric graph on it. Then, the preimage by  $p$  of the resulting metric graph gives a metric graph. We claim that this graph has no univalent vertices. Indeed, a univalent vertex of this graph has to be the preimage of univalent vertices of the graph below, which are only  $q_1$  and  $q_2$ , which are branch points. By Remark 2.8 all their preimages are ramification points and then they are

not univalent vertices. The metric induces a tête-à-tête structure in the graph by construction. Now, we finish the proof as in the case  $\text{genus}(\Sigma^{\phi'}) \geq 1$ .

If  $\phi$  has no ramification points or only one, in the previous construction we could obtain univalent vertices at the preimages of  $q_1$  and  $q_2$ . So we need to do some changes in the assignments of lengths and in the positions of the vertical segments relative to  $q_1$  and  $q_2$  in order that the extremes  $q_1$  and  $q_2$  of  $c$  coincide with vertices of the graph in  $\Sigma^{\phi'}$ .

Assume that  $A_1 \geq A_2 \geq \dots \geq A_r$ .

We choose  $q_1 := a_1 \cap a_2$ . Let  $q_2$  be the antipodal point (so  $q_1$  and  $q_2$  divides  $P$  in two paths of equal length). If  $q_2$  is a vertex we have finished. If it is not, then it is on a segment  $a'_i$ , for some  $i = 2, \dots, r_1$ . We redefine  $A'_i := d(a'_i \cap a'_{i-1}, q_2)$  and  $A_i := A_i + d(q_2, a'_i \cap a'_{i+1})$ . Now the antipodal point of  $q_1$  is  $a_i \cap a_{i+1}$ . We redefine  $q_2 := a_i \cap a_{i+1}$  and identify orientation reversing the two paths joining  $q_1$  and  $q_2$  to recover  $\Sigma^{\phi}$ .

Now the pullback of the resulting metric graph has no univalent vertices and gives a tête-à-tête structure since the corresponding system of equations is satisfied.  $\square$

Now we state the relative case in a simple way:

**Theorem 7.30.** *Let  $\Sigma$  be an oriented surface with non-empty boundary. Let  $\partial^1 \Sigma$  be a non empty union of boundary components. Let  $A$  be the union of the boundary components not contained in  $\partial^1 \Sigma$ . Let  $\phi$  be an orientation preserving homeomorphism fixing pointwise  $\partial^1 \Sigma$  and freely isotopic to a periodic homeomorphism. Then, there exists a signed tête-à-tête spine  $(\Gamma, A, \iota) \hookrightarrow \Sigma$  such that  $\phi_{(\Sigma, \Gamma, A, \iota)}$  is isotopic relative to  $\partial^1 \Sigma$  to  $\phi$ . Moreover, if  $\phi$  is periodic outside a collar of  $\partial^1 \Sigma$ , we have also that  $[\phi]_{\partial, \phi|_{\partial}} = [\phi_{(\Sigma, \Gamma, A, \iota)}]_{\partial, \phi|_{\partial}}$ .*

*Proof.* Apply Alexander's trick to the boundary components in  $A$  in order to obtain a larger surface and a homeomorphism fixing pointwise the boundary. Construct a signed tête-à-tête graph inducing this homeomorphism like in the proof of Theorem 7.18. We can always get that this signed tête-à-tête graph contains as vertices the centers of the disks added by Alexander's trick. Now apply an  $\epsilon$ -blow up (recall Definition 6.13) to these vertices to get the desired signed relative tête-à-tête graph.  $\square$

## 7.2 Truly periodic automorphisms and tête-à-tête graphs

In this section, we prove, as a corollary of the previous section, that periodic homeomorphisms induced by tête-à-tête graphs give rise to all truly periodic homeomorphisms (leaving at least one boundary component invariant) up to isotopy and conjugacy.

**Definition 7.31.** *Replacing the map (eq. (7.5)) in Definition 7.4 by*

$$\begin{aligned} \psi_i : \tilde{\Gamma}_i \times I &\longrightarrow \tilde{\Gamma}_i \times I \\ (p, s) &\mapsto (\tilde{\gamma}_p^+(\pi), s) \end{aligned}$$

*we get a truly periodic homeomorphism that we denote by  $\phi_{\Sigma, \Gamma, A, \iota}^{\text{per}}$ . We call it the induced periodic tête-à-tête twist.*

**Remark 7.32.** Similarly as in Remark 4.14 we get must observe the following ambiguity in the decisions made:

- For two different product structures of the cylinders, the induced periodic tête-à-tête twists are conjugate by a homeomorphism that fixes  $\Gamma$ .
- For two different embeddings in  $\Sigma$ , the periodic tête-à-tête twists are conjugate by the same homeomorphism of  $\Sigma$  that relates the two embeddings.

Note that obviously  $\phi_{\Sigma, \Gamma, A, \iota}^{per}$  is freely isotopic to  $\phi_{(\Sigma, \Gamma, A, \iota)}$  and coincides with it along  $\Gamma$ . Given a periodic homeomorphism  $\phi$ , we can clearly choose a representative  $\phi'$  of  $[\phi]$  that leaves each component in  $\partial^1 \Sigma$  pointwise fixed (by isotoping  $\phi$  near  $\partial^1 \Sigma$  until it is the identity on all of them). Then, we can find a signed tête-à-tête graph  $(\Gamma, A, \iota)$  embedded in  $\Sigma$  to represent it using Theorem 7.18 and Theorem 7.30. Then, we can consider the periodic homeomorphism  $\phi_{\Sigma, \Gamma, A, \iota}^{per}$ . Note that we can always get that  $\phi'$  has all its fractional Dehn twist coefficients positive, which means  $\iota \equiv +$ . Then, we get the following theorem by using Corollary 2.17:

**Theorem 7.33.** *Let  $\Sigma$  be a connected surface with non-empty boundary which is not a disk or a cylinder. Let  $\phi$  be an orientation preserving periodic homeomorphism of  $\Sigma$  that leaves (at least) one boundary component invariant. Let  $A$  be the set containing all boundary components that are not invariant by  $\phi$ . Then there exists a relative tête-à-tête graph  $(\Gamma, A)$  embedded in  $(\Sigma, A)$ , which is invariant by  $\phi$ , such that:*

- We have the equality of boundary-free isotopy classes  $[\phi_{(\Sigma, \Gamma, A, \iota)}^{per}]_{A, \phi|_A} = [\phi]_{A, \phi|_A}$  (recall notation introduced in Definition 2.1).*
- The homeomorphism  $\phi$  is conjugate to  $\phi_{(\Sigma, \Gamma, A, \iota)}^{per}$  by a homeomorphism that fixes  $\Gamma$ .*

**Remark 7.34.** Observe that in order to represent all truly periodic homeomorphisms we do not need the extension to be signed tête-à-tête graphs, A'Campo's original construction is enough.

## 7.3 General tête-à-tête structures

In this section we study any orientation preserving periodic homeomorphism. Let  $\phi : \Sigma \rightarrow \Sigma$  be such a homeomorphism. We realize its boundary-free isotopy type and its conjugacy class in  $\text{MCG}(\Sigma)$  by a generalization of tête-à-tête graphs, using a technique that reduces to the case of homeomorphisms of a larger surface that leave all boundary components invariant.

In contrast with the rest of the work, in this section, we allow ribbon graphs with some *special* univalent vertices.

**Definition 7.35.** *A ribbon graph with boundary is a pair  $(\Gamma, \mathcal{P})$  where  $\Gamma$  is a ribbon graph, and  $\mathcal{P}$  is the set of univalent vertices, with the following additional property: given any vertex  $v$  of valency greater than 1 in the cyclic ordering of adjacent edges  $e(v)$  there are no two consecutive edges connecting  $v$  with vertices in  $\mathcal{P}$ .*

In order to define the thickening of a ribbon graph with boundary we need the following construction:

Let  $\Gamma'$  be a ribbon graph (without univalent vertices) and let  $\Sigma$  be its thickening. Let

$$g_{\Gamma'} : \Sigma_{\Gamma'} \rightarrow \Sigma$$

be the gluing map. The surface  $\Sigma_{\Gamma'}$  splits as a disjoint union of cylinders  $\coprod_i \tilde{\Sigma}_i$ . Let  $w$  be a vertex of  $\Gamma'$ . The cylinders  $\tilde{\Sigma}_i$  such that  $w$  belongs to  $g_{\Gamma'}(\tilde{\Sigma}_i)$  are in a natural bijection with the pairs of consecutive edges  $(e', e'')$  in the cyclic order of the set  $e(w)$  of adjacent edges to  $w$ .

Let  $(\Gamma, \mathcal{P})$  be a ribbon graph with boundary. The graph  $\Gamma'$  obtained by erasing from  $\Gamma$  the set  $E$  of all vertices in  $\mathcal{P}$  and its adjacent edges is a ribbon graph. Consider the thickening surface  $\Sigma$  of  $\Gamma'$ . Let  $e$  be an edge connecting a vertex  $v \in \mathcal{P}$  with another vertex  $w$ , let  $e'$  and  $e''$  be the immediate predecessor and successor of  $e$  in the cyclic order of  $e(w)$ . By the defining property of ribbon graphs with boundary they are consecutive edges in  $e(w) \setminus E$ , and hence determine a unique associated cylinder which will be denoted by  $\tilde{\Sigma}_i(v)$ .

Each cylinder  $\tilde{\Sigma}_i$  has two boundary components, one, denoted by  $\tilde{\Gamma}_i$  corresponds to the boundary component obtained by cutting the graph, and the other, called  $C_i$ , corresponds to a boundary component of  $\Sigma$ . Fix a cylinder  $\tilde{\Sigma}_i$ . Let  $\{v_1, \dots, v_k\}$  be the vertices of  $\mathcal{P}$  whose associated cylinder is  $\tilde{\Sigma}_i$ . Let  $\{e_1, \dots, e_k\}$  be the corresponding edges, let  $\{w_1, \dots, w_k\}$  be the corresponding vertices at  $\Gamma'$ , and let  $\{w'_1, \dots, w'_k\}$  be the set of preimages by  $g_{\Gamma'}$  contained in  $\tilde{\Sigma}_i$ . The defining property of ribbon graphs with boundary imply that  $w'_i$  and  $w'_j$  are pairwise different if  $i \neq j$ . Furthermore, since  $\{w'_1, \dots, w'_k\}$  is included in the circle  $\tilde{\Gamma}_i$ , which has an orientation inherited from  $\Sigma$ , the set  $\{w'_1, \dots, w'_k\}$ , and hence also  $\{e_1, \dots, e_k\}$  and  $\{v_1, \dots, v_k\}$  has a cyclic order. We assume that our indexing respects it.

Fix a product structure  $\mathbb{S}^1 \times I$  for each cylinder  $\tilde{\Sigma}_i$ , where  $\mathbb{S}^1 \times \{0\}$  corresponds to the boundary component  $\tilde{\Gamma}_i$ , and  $\mathbb{S}^1 \times \{1\}$  corresponds to the boundary component of  $C_i$ .

Using this product structure we can embed  $\Gamma$  in  $\Sigma$ : for each vertex  $v \in \mathcal{P}$  consider the corresponding cylinder  $\tilde{\Sigma}_{i(v)}$ , let  $w'$  be the point in  $\tilde{\Gamma}_{i(v)}$  determined above. We embed the segment  $g_{\Gamma'}(w' \times I)$  in  $\Sigma$ .

Doing this for any vertex  $v$  we obtain an embedding of  $\Gamma$  in  $\Sigma$  such that all the vertices  $\mathcal{P}$  belong to the boundary  $\partial\Sigma$ , and such that  $\Sigma$  admits  $\Gamma$  as a regular deformation retract.

**Definition 7.36.** *Let  $(\Gamma, \mathcal{P})$  be a ribbon graph with boundary. We define the thickening surface  $\Sigma$  of  $(\Gamma, \mathcal{P})$  to be the thickening surface of  $\Gamma'$  together with the embedding  $(\Gamma, \mathcal{P}) \subset (\Sigma, \partial\Sigma)$  constructed above. We say that  $(\Gamma, \mathcal{P})$  is a general spine of  $(\Sigma, \partial\Sigma)$ .*

**Definition 7.37** (General safe walk). *Let  $(\Gamma, \mathcal{P})$  be a metric ribbon graph with boundary. Let  $\sigma$  be a permutation of  $\mathcal{P}$ .*

*We define a general safe walk in  $(\Gamma, \mathcal{P}, \sigma)$  starting at a point  $p \in \Gamma \setminus v(\Gamma)$  to be a map  $\gamma_p : [0, \pi] \rightarrow \Gamma$  such that*

- 1)  $\gamma_p(0) = p$  and  $|\gamma'_p| = 1$  at all times.
- 2) when  $\gamma_p$  gets to a vertex of valency  $\geq 2$  it continues along the next edge in the cyclic order.
- 3) when  $\gamma$  gets to a vertex in  $\mathcal{P}$ , it continues along the edge indicated by the permutation  $\sigma$ .

**Definition 7.38** (General tête-à-tête graph). *Let  $(\Gamma, \mathcal{P}, \sigma)$  be as in the previous definition. Let  $\gamma_p, \omega_p$  be the two safe walks starting at a point  $p$  in  $\Gamma \setminus v(\Gamma)$ .*

*We say  $\Gamma$  has the general tête-à-tête property if*

- for any  $p \in \Gamma \setminus v(\Gamma)$  we have  $\gamma_p(\pi) = \omega_p(\pi)$

*Moreover we say that  $(\Gamma, \mathcal{P}, \sigma)$  gives a general tête-à-tête structure for  $(\Sigma, \partial\Sigma)$  if  $(\Sigma, \partial\Sigma)$  is the thickening of  $(\Gamma, \mathcal{P})$ .*

In the following construction we associate to a general tête-à-tête graph  $(\Gamma, \mathcal{P}, \sigma)$  a homeomorphism of  $(\Gamma, \mathcal{P})$  which restricts to the permutation  $\sigma$  in  $\mathcal{P}$ ; we call it the *general tête-à-tête homeomorphism* of  $(\Gamma, \mathcal{P}, \sigma)$ . We construct also a homeomorphism of the thickening surface which leaves  $\Gamma$  invariant and restricts on  $\Gamma$  to the general tête-à-tête homeomorphism of  $(\Gamma, \mathcal{P}, \sigma)$ . We construct the homeomorphism on the graph and on its thickening simultaneously.

Consider the homeomorphism of  $\Gamma' \setminus v(\Gamma)$  defined by

$$p \mapsto \gamma_p(\pi).$$

The same proof of Lemma 6.8 shows that there is an extension of this homeomorphism to a homeomorphism

$$\sigma_\Gamma : \Gamma \rightarrow \Gamma.$$

The restriction of the general tête-à-tête homeomorphism that we are constructing to  $\Gamma'$  coincides with  $\sigma_\Gamma$ . The mapping  $\sigma_\Gamma$  leaves  $\Gamma'$  invariant for being a homeomorphism. Let  $\tilde{\Gamma}'$  be the union of the circles  $\tilde{\Gamma}'_i$ . The homeomorphism  $\sigma_\Gamma|_{\Gamma'}$  lifts to a periodic homeomorphism

$$\tilde{\sigma} : g_{\Gamma'}^{-1}(\tilde{\Gamma}') \rightarrow g_{\Gamma'}^{-1}(\tilde{\Gamma}'),$$

which may exchange circles in the following way. For any  $p \in \tilde{\Gamma}'$ , the points in  $g_{\Gamma'}^{-1}(p)$  corresponds to the starting poing of safe walks in  $\tilde{\Gamma}'$  starting at  $p$ . A safe walk starting at  $p$  is determined by the point  $p$  and an starting direction at an edge containg  $p$ .

As we have seen, if  $(\Gamma, \mathcal{P}, \sigma)$  is a general tête-à-tête structure for  $(\Sigma, \partial\Sigma)$  then the surface  $\Sigma_{\Gamma'}$  is a disjoint union of cylinders. The lifting  $\tilde{\sigma}$  extends to  $\Sigma_{\Gamma'}$ . This extension interchanges some cylinders  $\tilde{\Sigma}_i$  and goes down to an homeomorphism of  $\Sigma$ . We denote it by  $\phi_{(\Gamma, \mathcal{P}, \sigma)}$ . If necessary, we change the embedding of the part of  $\Gamma$  not contained in  $\Gamma'$  in  $\Sigma$  such that it is invariant by  $\phi_{(\Gamma, \mathcal{P}, \sigma)}$ . This is done by an adequate choice of the trivilizations of the cylinders.

**Definition 7.39.** *The homeomorphism  $\phi_{(\Gamma, \mathcal{P}, \sigma)}$  is by definition the homeomorphism of the thickening, and its restriction to  $\Gamma$  the general tête-à-tête homeomorphism of  $(\Gamma, \mathcal{P}, \sigma)$ .*

With the notation and definitions introduced we are ready to state and proof the main result of the work.

**Theorem 7.40.** *Given a periodic homeomorphism  $\phi$  of a surface with boundary  $(\Sigma, \partial\Sigma)$  which is not a disk or a cylinder, the following assertions hold:*

- (i) *There is a general tête-à-tête graph  $(\Gamma, \mathcal{P}, \sigma)$  such that the thickening of  $(\Gamma, \mathcal{P})$  is  $(\Sigma, \partial\Sigma)$ , the homeomorphism  $\phi$  leaves  $\Gamma$  invariant and we have the equality  $\phi|_\Gamma = \phi_{(\Gamma, \mathcal{P}, \sigma)}|_\Gamma$ .*
- (ii) *We have the equality of boundary-free isotopy classes  $[\phi|_\Gamma] = [\phi_{(\Gamma, \mathcal{P}, \sigma)}]$ .*
- (iii) *The homeomorphisms  $\phi$  and  $\phi_{(\Gamma, \mathcal{P}, \sigma)}$  are conjugate.*

*Proof.* In the first part of the proof we extend the homeomorphism  $\phi$  to a homeomorphism  $\hat{\phi}$  of a bigger surface  $\hat{\Sigma}$  that leaves all the boundary components invariant. Then, we find a tête-à-tête graph  $\hat{\Gamma}$  for  $\hat{\phi}$  such that  $\hat{\Gamma} \cap \Sigma$ , with a small modification in the metric and a suitable permutation, is a general tête-à-tête graph for  $\phi$ .

Let  $n$  be the order of the homeomorphism. Consider the permutation induced by  $\phi$  in the set of boundary components. Let  $\{C_1, \dots, C_m\}$  be an orbit of cardinality strictly bigger than 1, numbered such that  $\phi(C_i) = C_{i+1}$  and  $\phi(C_m) = C_1$ . Take an arc  $\alpha \subset C_1$  small enough so that it



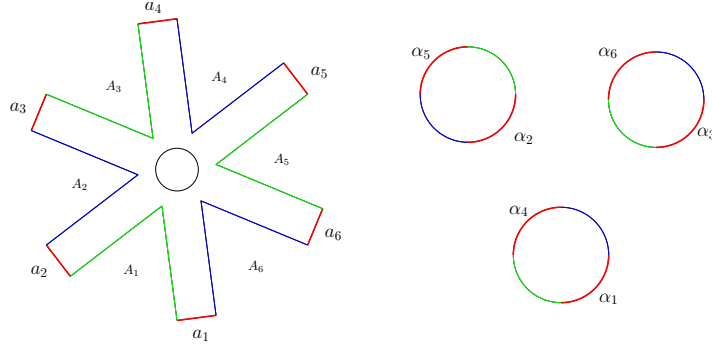


**Figure 7.41:** Example of a star-shaped piece  $S$  with 6 arms on the left and boundary components on the right. The arcs along which the two pieces are glued, are marked in red. In blue and red are the boundaries of the two disks that we used to cap off the new boundaries.

is disjoint from all its iterations by  $\phi$ . Define the arcs  $\alpha^i := \phi^i(\alpha)$  for  $i \in \{0, \dots, n-1\}$ , which are contained in  $\cup_i C_i$ . Obviously we have the equalities  $\alpha^{i+1} = \phi(\alpha^i)$  and  $\phi(\alpha^{n-1}) = \alpha^0 = \alpha$ .

We consider a star-shaped piece  $S$  of  $n$  arms as in Figure 7.41. We denote by  $D$  the central boundary component. Let  $a^0, \dots, a^{n-1}$  be the boundary of the arms of the star-shaped piece labelled in the picture, oriented counterclockwise. We consider the rotation  $r$  of order  $n$  acting on this piece such that  $r(a^i) = a^{i+1}$ . Note that this rotation leaves  $D$  invariant.

We consider the surface  $\hat{\Sigma}$  obtained by gluing  $\Sigma$  and  $S$  identifying  $a^i$  with  $\alpha^i$  reversing the orientation, and such that  $\phi$  and the rotation  $r$  glue to a periodic homeomorphism  $\hat{\phi}$  in the resulting surface.

The boundary components of the new surface are precisely the boundary components of  $\Sigma$  different from  $\{C_1, \dots, C_m\}$ , the new boundary component  $D$ , and the boundary components  $C'_1, \dots, C'_k$  that contain the part of the  $C_i$ 's not included in the union  $\cup_{i=0}^{n-1} \alpha^i$ .

The homeomorphism  $\hat{\phi}$  leaves  $D$  invariant and may interchange the new boundary components  $C'_1, \dots, C'_k$ . We cup each component  $C'_i$  with a disk  $D_i$  and extend the homeomorphism by the Alexander trick, obtaining a homeomorphism  $\hat{\phi}$  of a bigger surface  $\hat{\Sigma}$ . The only new ramification points that the action of  $\hat{\phi}$  may induce are the centers  $t_i$  of these disks. We claim that, in fact, each of the  $t_i$ 's is a ramification point.

Denote the quotient map by

$$p : \hat{\Sigma} \rightarrow \hat{\Sigma}^{\hat{\phi}}.$$

In order to prove the claim notice that the difference  $\hat{\Sigma} \setminus \Sigma$  is homeomorphic to a closed surface with  $m+1$  disks removed. On the other hand the difference of quotient surfaces  $\hat{\Sigma}^{\hat{\phi}} \setminus \Sigma^{\phi}$  is homeomorphic to a cylinder. Since  $m$  is strictly bigger than 1, Hurwitz formula for  $p$  forces the existence of ramification points. Since  $p$  is a Galois cover each  $t_i$  is a ramification point.

The new boundary component of  $\hat{\Sigma}^{\hat{\phi}}$  corresponds to  $p(D)$ , where  $D$  is invariant by  $\hat{\phi}$ . The point  $q_1 := p(t_1)$  is then a branch point of  $p$ .

We do this operation for every orbit of boundary components in  $\Sigma$  of cardinality greater than 1. Then we get a surface  $\hat{\Sigma}$  and an extension  $\hat{\phi}$  of  $\phi$  that leaves all the boundary components invariant. The quotient surface  $\hat{\Sigma}^{\hat{\phi}}$  is obtained from  $\Sigma^{\phi}$  attaching some cylinders  $\mathcal{C}_j$  to some boundary components. Let

$$p : \hat{\Sigma} \rightarrow \hat{\Sigma}^{\hat{\phi}}$$

denote the quotient map. Comparing  $p|_{\Sigma}$  and  $p|_{\hat{\Sigma}}$ , we see that we have only one new branching point  $q_j$  in every cylinder  $\mathcal{C}_j$ .

Now we construct a tête-à-tête graph for  $\hat{\phi}$  modifying slightly the construction of Theorem 7.18.

To fix ideas we consider the case in which the genus of the quotient  $\hat{\Sigma}^{\hat{\phi}}$  is positive. The modification of the genus 0 case is exactly the same. As in Theorem 7.18 we use a planar representation of  $\Sigma^{\phi}$  as a convex  $4g$ -gon in  $\mathbb{R}^2$  with  $r$  disjoint open disks removed from its convex hull and whose edges are labelled clockwise like

$$a_1 b_1 a_1^{-1} b_1^{-1} a_2 b_2 a_2^{-1} b_2^{-1} \dots a_g b_g a_g^{-1} b_g^{-1}.$$

We number the boundary components  $C_i \subset \partial\Sigma$ ,  $1 \leq i \leq r$ , we denote by  $d$  the arc  $a_2 b_2 a_2^{-1} b_2^{-1} \dots a_g b_g a_g^{-1} b_g^{-1}$ , and we consider  $l_1, \dots, l_{r-1}$  arcs as in Figure 7.42. We denote by  $c_1, \dots, c_r$  the edges in which  $a_1^{-1}$  (and  $a_1$ ) is subdivided according to the component  $p(C_i)$  they enclose.

We impose the further condition that each of the regions in which the polygon is subdivided by the  $l_i$ 's encloses not only a component  $p(C_i)$ , but also the branching point  $q_i$  that appears in the cylinder  $\mathcal{C}_i$ . We assume that the union of  $d$ ,  $a_1 b_1 a_1^{-1} b_1^{-1}$  and the  $l_i$ 's contains all the branching points of  $p$  except the  $q_i$ 's.

In order to be able to lift the retraction we need that the spine that we draw in the quotient contains all branching points. In order to achieve this we add an edge  $s_i$  joining  $q_i$  and some interior point  $q'_i$  of  $l_i$  for  $i = 1, \dots, r-1$  and joining  $q_r$  with some interior point  $q'_r$  of  $l_{r-1}$ . We may assume that  $q'_i$  is not a branching point. We consider the circle  $p(C_i)$  and ask  $s_i$  to meet it transversely to it at only 1 point. See Figure 7.43. We consider the graph  $\Gamma'$  as the union of the previous segments and the  $s_i$ 's. Clearly the quotient surface retracts to it. Since it contains all branching points its preimage  $\hat{\Gamma}$  is a spine for  $\hat{\Sigma}$ . It has no univalent vertices since the  $q_i$ 's are branching points of a Galois cover.

In order to give a metric in the graph we proceed as follows. We give the segments  $d$  and  $C_i$ 's the same length they had in the proof of Theorem 7.18. We impose every  $s_i$  to have length some small enough  $\epsilon$  and the part of  $s_i$  inside the cylinder  $\mathcal{C}_i$  to have length  $\epsilon/2$  (see Figure 7.43). We give each segment  $l_i$  length  $L - 2\epsilon$ . It is easy to check that the preimage graph  $\hat{\Gamma}$  with the pullback metric is tête-à-tête.

Now we consider the graph  $\Gamma := \hat{\Gamma} \cap \Sigma$  with the restriction metric, except on the edges meeting  $\partial\Sigma$  whose length is redefined to be  $\epsilon$ . Along the lines of the proof of Theorem 7.18 we get that  $\phi_{(\Gamma, \mathcal{P}, \sigma)}$  and  $\phi$  are isotopic and conjugate. If we denote by  $\mathcal{P}$  the set of univalent vertices of  $\Gamma$ , it is an immediate consequence of the construction that  $(\Gamma, \mathcal{P}, \sigma)$  with the obvious permutation  $\sigma$  of  $\mathcal{P}$  is a general tête-à-tête graph with  $\phi_{(\Gamma, \mathcal{P}, \sigma)}|_{\Gamma} = \phi|_{\Gamma}$ .  $\square$

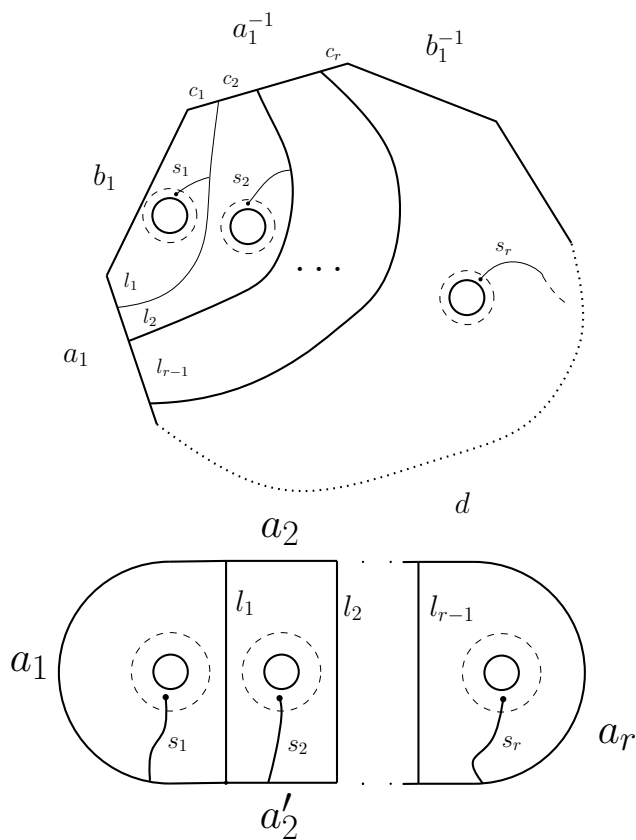


**Figure 7.42:** Drawing of  $\Gamma'$  for the case  $genus(\hat{\Sigma}^{\hat{\phi}}) \geq 1$  in the first image and  $genus(\hat{\Sigma}^{\hat{\phi}}) = 0$  in the second.

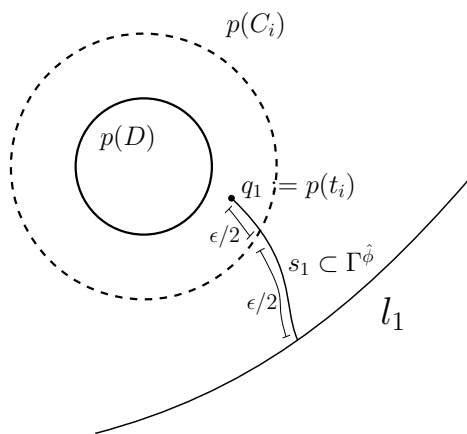


**Figure 7.43:** Neighbourhood of  $q_1 = p(t_i)$  in  $\hat{\Sigma}^{\hat{\phi}}$  and edge  $s_1$  joining  $q_1$  and  $l_1$ .

## Chapter 8

---

# *Mixed tête-à-tête graphs*

Chapter 7 is needed for this chapter. With pure, relative and general tête-à-tête graphs we model freely periodic homeomorphisms. In this chapter, we extend the notion of tête-à-tête graph and introduce *mixed tête-à-tête graphs* with the aim to model some pseudo-periodic homeomorphisms in Chapter 9. We use the theory and notation of Section 2.4. The content of this chapter is purely of a graph-theoretical nature and appeared before on [FPP17] and [PS17].

Let  $(\Gamma^\bullet, A^\bullet)$  be a decreasing filtration on a connected relative metric ribbon graph  $(\Gamma, A)$ . That is

$$(\Gamma, A) = (\Gamma^0, A^0) \supset (\Gamma^1, A^1) \supset \dots \supset (\Gamma^d, A^d)$$

where  $\supset$  between pairs means  $\Gamma^i \supset \Gamma^{i+1}$  and  $A^i \supset A^{i+1}$ , and where  $(\Gamma^i, A^i)$  is a (possibly disconnected) relative metric ribbon graph for each  $i = 0, \dots, d$ . We say that  $d$  is the depth of the filtration  $\Gamma^\bullet$ . We assume each  $\Gamma^i$  does not have univalent vertices and is a subgraph of  $\Gamma$  in the usual terminology in Graph Theory. We observe that since each  $(\Gamma^i, A^i)$  is a relative metric ribbon graph, we have that  $A^i \setminus A^{i+1}$  is a disjoint union of connected components homeomorphic to  $\mathbb{S}^1$ .

For each  $i = 0, \dots, d$ , let

$$\delta_i : \Gamma^i \rightarrow \mathbb{R}_{\geq 0}$$

be a locally constant map (so it is a map constant on each connected component). We put the restriction that  $\delta_0(\Gamma^0) > 0$ . We denote the collection of all these maps by  $\delta_\bullet$ .

Let  $p \in \Gamma$ , we define  $c_p$  as the largest natural number such that  $p \in \Gamma^{c_p}$ .

**Definition 8.1** (Mixed safe walk). *Let  $(\Gamma^\bullet, A^\bullet)$  be a filtered relative metric ribbon graph. Let  $p \in \Gamma \setminus A \setminus v(\Gamma)$ . We define a mixed safe walk  $\gamma_p$  starting at  $p$  as a concatenation of paths defined iteratively by the following properties*

- i)  $\gamma_p^0$  is a safe walk of length  $\delta_0(p)$  starting at  $p_0^\gamma := p$ . Let  $p_1^\gamma := \gamma^0(\delta_0)$  be its endpoint.*
- ii) Suppose that  $\gamma_p^{i-1}$  is defined and let  $p_i^\gamma$  be its endpoint.*
  - If  $i > c_p$  or  $p_i^\gamma \notin \Gamma^i$  we stop the algorithm.*
  - If  $i \leq c_p$  and  $p_i^\gamma \in \Gamma^i$  then define  $\gamma_p^i : [0, \delta_i(p_i)] \rightarrow \Gamma^i$  to be a safe walk of length  $\delta_i(p_i^\gamma)$  starting at  $p_i^\gamma$  and going in the same direction as  $\gamma_p^{i-1}$ .*

iii) Repeat step ii) until algorithm stops.

Finally, define  $\gamma_p := \gamma_p^k \star \cdots \star \gamma_p^0$ , that is, the mixed safe walk starting at  $p$  is the concatenation of all the safe walks defined in the inductive process above.

As in the pure case, there are two safe walks starting at each point on  $\Gamma \setminus (A \cup v(\Gamma))$ . We denote them by  $\gamma_p$  and  $\omega_p$ .

**Definition 8.2** (Boundary mixed safe walk). *Let  $(\Gamma^\bullet, A^\bullet)$  be a filtered relative metric ribbon graph and let  $p \in A$ . We define a boundary mixed safe walk  $b_p$  starting at  $p$  as a concatenation of a collection of paths defined iteratively by the following properties*

i)  $b_{p_0}^0$  is a boundary safe walk of length  $\delta_0(p)$  starting at  $p_0 := p$  and going in the direction indicated by  $A$  (as in the relative tête-à-tête case). Let  $p_1 := b_{p_0}^0(\delta_0)$  be its endpoint.

ii) Suppose that  $b_{p_{i-1}}^{i-1}$  is defined and let  $p_i$  be its endpoint.

– If  $i > c_p$  or  $p_i \notin \Gamma^i$  we stop the algorithm.

– If  $i \leq c(p)$  and  $p_i \in \Gamma^i$  then define  $b_{p_i}^i : [0, \delta_i(p_i)] \rightarrow \Gamma^i$  to be a safe walk of length  $\delta_i(p_i)$  starting at  $p_i$  and going in the same direction as  $b_{p_{i-1}}^{i-1}$ .

iii) Repeat step ii) until algorithm stops.

Finally, define  $b_p := b_{p_k}^k \star \cdots \star b_{p_0}^0$ , that is, the boundary mixed safe walk starting at  $p$  is the concatenation of all the safe walks defined in the inductive process.

**Notation 8.3.** We call the number  $k$  in Definition 8.1 (resp. Definition 8.2), the *order* of the mixed safe walk (resp. boundary mixed safe walk) and denote it by  $o(\gamma_p)$  (resp.  $o(b_p)$ ).

We denote by  $l(\gamma_p)$  the *length* of the mixed safe walk  $\gamma_p$  which is the sum

$$\sum_{j=0}^{o(\gamma_p)} \delta_j(p_j^?)$$

of the lengths of all the walks involved. We consider the analogous definition  $l(b_p)$ .

As in the pure case, two mixed safe walks starting at  $p \in \Gamma \setminus v(\Gamma)$  exist. We denote by  $\omega_p$  the mixed safe walk that starts at  $p$  but in the opposite direction to the starting direction of  $\gamma_p$ .

Observe that since the safe walk  $b_{p_0}^0$  is completely determined by  $p$ , for a point in  $A$  there exists only one boundary safe walk.

Now we define the relative mixed tête-à-tête property.

**Definition 8.4** (Relative mixed tête-à-tête property). *Let  $(\Gamma^\bullet, A^\bullet)$  be a filtered relative metric ribbon graph and let  $\delta_\bullet$  be a set of locally constant mappings  $\delta_k : \Gamma^k \rightarrow \mathbb{R}_{\geq 0}$ . We say that  $(\Gamma^\bullet, A^\bullet, \delta_\bullet)$  satisfies the relative mixed tête-à-tête property or that it is a relative mixed tête-à-tête graph if for every  $p \in \Gamma - (v(\Gamma) \cup A)$*

I) The endpoints of  $\gamma_p$  and  $\omega_p$  coincide.

II)  $c_{\gamma_p(l(\gamma_p))} = c_p$

and for every  $p \in A$ , we find that

III)  $b_p(l(b_p)) \in A^{c_p}$

As a consequence of the two previous definitions we have:

**Lemma 8.5.** *Let  $(\Gamma^\bullet, A^\bullet, \delta_\bullet)$  be a mixed relative tête-à-tête graph, then*

- a)  $o(\omega_p) = o(\gamma_p) = c_p$
- b)  $l(\gamma_p) = l(\omega_p)$  for every  $p \in \Gamma \setminus v(\Gamma)$ .

*Proof.* a) By Definition 8.1 ii), we find that  $o(\gamma_p) \leq c_p$  for all  $p \in \Gamma \setminus v(\Gamma)$ . Suppose that for some  $p$ , we find that  $o(\gamma_p) = k < c_p$ . This means, that while constructing the mixed safe walk we stopped after constructing the path  $\gamma_p^k$  either because  $k > c_p$  which contradicts the supposition, or because the endpoint  $p_k^\gamma$  of  $\gamma_p^k$  is not in  $\Gamma^k$  which contradicts that  $c_p = c_{\gamma_p(l(\gamma_p))}$ . This proves the equality  $o(\gamma_p) = c_p$ . In order to prove  $o(\omega_p) = c_p$  use the equality  $\gamma_p(l(\gamma_p)) = \omega_p(l(\omega_p))$  and repeat the same argument.

b) Let  $q$  be the endpoint of  $\gamma_p$  and  $\omega_p$ . Since the image of the safe walks  $\gamma_p^{c_p}$  and  $\omega_p^{c_p}$  lies on the same connected component of  $\Gamma^{c_p}$  we find that their starting points  $p_{c_p}^\gamma$  and  $p_{c_p}^\omega$  also lie on that same connected component. Therefore  $\delta_{c_p}(p_{c_p}^\gamma) = \delta_{c_p}(p_{c_p}^\omega)$ .

Suppose now that  $p_i^\gamma$  and  $p_i^\omega$  lie on the same connected component of  $\Gamma^i$  (and so  $\delta_i(p_i^\gamma) = \delta_i(p_i^\omega)$ ). Then the image of the safe walks  $\gamma_p^{i-1}$  and  $\omega_p^{i-1}$  lies on the same connected component of  $\Gamma^{i-1}$  and we find that their starting points  $p_{i-1}^\gamma$  and  $p_{i-1}^\omega$  also lie on that same connected component. So  $\delta_{i-1}(p_{i-1}^\gamma) = \delta_{i-1}(p_{i-1}^\omega)$ .

We conclude that  $\delta_j(p_j^\gamma) = \delta_j(p_j^\omega)$  for all  $j = 0, \dots, d$  which concludes the proof.  $\square$

An purely graph-theoretical example is worked out in Example C.9.



## Chapter 9

---

# Mixed tête-à-tête twists

Chapter 8 and last section of Chapter 2 are the preliminaries for this chapter. In this chapter, we associate a mapping class of pseudo-periodic automorphisms to each mixed tête-à-tête graph and we prove several properties about these automorphisms.

**Notation 9.1.** Let  $g_{\Gamma^i} : \Sigma_{\Gamma^i} \rightarrow \Sigma$  be the gluing map as in Notation 1.11. Let  $\Gamma_{\Gamma^i}$  be the preimage of  $\Gamma$  by  $g_{\Gamma^i}$ . We also denote by  $g_{\Gamma^i}$  its restriction  $g_{\Gamma^i} : \Gamma_{\Gamma^i} \rightarrow \Gamma$ . The union of the boundary components of  $\Sigma_{\Gamma^i}$  that come from  $\Gamma^i$  is denoted by  $\tilde{\Gamma}^i$ . Observe that a single connected component of  $\Gamma^i$  might produce more than one boundary component in  $\Sigma_{\Gamma^i}$ .

It's clear that  $g_{\Gamma^i}$  factorizes as follows:

$$\Sigma_{\Gamma^i} \rightarrow \Sigma_{\Gamma^{i+1}} \rightarrow \dots \rightarrow \Sigma.$$

We denote these mappings by  $g_j : \Sigma_{\Gamma^j} \rightarrow \Sigma_{\Gamma^{j+1}}$  for  $j = 0, \dots, d-1$  and also their restrictions  $g_j : \Gamma_{\Gamma^j} \rightarrow \Gamma_{\Gamma^{j+1}}$ .

**Remark 9.2.** Observe that by Definition 8.4, each connected component of the relative metric ribbon graph  $(\Gamma_{\Gamma^1}, \tilde{\Gamma}^1)$  has the relative tête-à-tête property for safe walks of length  $\delta_0(\Gamma)$ .

Let  $\phi_{\Gamma,0} : \Sigma_{\Gamma^1} \rightarrow \Sigma_{\Gamma^1}$  be the tête-à-tête homeomorphism fixing each boundary component that is not in  $\tilde{\Gamma}^1$  as in Definition 7.4. It is the homeomorphism induced by the relative tête-à-tête property of each connected component of  $(\Gamma_{\Gamma^1}, \tilde{\Gamma}^1)$  for some choice of product structures on  $(\Sigma_{\Gamma^1})_{\Gamma_{\Gamma^1}}$ .

Also according to Definition 7.4, observe that since we do not specify anything, we assume that the sign  $\iota$  is constant  $+1$ .

Now we continue to define inductively the homeomorphism  $\phi_{\Gamma}$ .

**Notation 9.3.** Let

$$\mathcal{D}_{\delta_i} : \Sigma_{\Gamma^i} \rightarrow \Sigma_{\Gamma^i}$$

be the homeomorphism consisting of the composition of all the boundary Dehn twists  $\mathcal{D}_{\delta_i(g_{\Gamma^i}(C))}(C)$  for all connected components  $C$  in  $\tilde{\Gamma}^i$  (recall Definition 2.49). Where  $\delta_i(g_{\Gamma^i}(C))$  means  $\delta_i(p)$  for any  $p \in (g_{\Gamma^i}(C))$ .



**Lemma 9.4.** *The homeomorphism*

$$\tilde{\phi}_{\Gamma,1} := \mathcal{D}_{\delta_1} \circ \phi_{\Gamma,0} : \Sigma_{\Gamma^1} \rightarrow \Sigma_{\Gamma^1}$$

is compatible with the gluing  $g_1 : \Sigma_{\Gamma^1} \rightarrow \Sigma_{\Gamma^2}$ .

*Proof.* We use the notation introduced in Definition 8.1.

Since  $g_1$  only identifies points in  $\tilde{\Gamma}^1$ , we must show that if  $x, y$  are different points in  $\tilde{\Gamma}^1$  such that  $g_1(x) = g_1(y) \in \Gamma^1$ , then  $g_1(\tilde{\phi}_{\Gamma,1}(x)) = g_1(\tilde{\phi}_{\Gamma,1}(y))$ .

So let  $x, y \in \tilde{\Gamma}^1$  be such that  $g_1(x) = g_1(y) = p$ . In particular,  $c_p = 1$  and we find that  $\gamma_p = \gamma_p^1 \star \gamma_p^0$  and  $\omega_p = \omega_p^1 \star \omega_p^0$  by Lemma 8.5 *a*). So the mixed safe walks end in a connected component of  $\Gamma^1$ . Denote by  $\hat{p}$  their endpoint. By Definition 8.4 *II*) we find that  $c_{\hat{p}} = 1$ .

Observe that  $\phi_{\Gamma,0}(x) = b_x(\delta_0(p))$  where  $b_x : [0, \delta_0(p)] \rightarrow \Gamma_{\Gamma^1}$  is the boundary safe walk of length  $\delta_0(p)$  given by the relative tête-à-tête structure on  $(\Gamma_{\Gamma^1}, \tilde{\Gamma}^1)$ . Analogously  $\phi_{\Gamma,0}(y) = b_y(\delta_0(p))$ . So we have  $g_1(\phi_{\Gamma,0}(x)) = \gamma_p(\delta_0(p))$  and  $g_1(\phi_{\Gamma,0}(y)) = \omega_p(\delta_0(p))$ .

It is clear that  $(\mathcal{D}_{\delta_1}(\phi_{\Gamma,0}(x))) = \tilde{\gamma}_p^0(\delta_1(\phi_{\Gamma,0}(x)) + \delta_0(p))$  with  $\tilde{\gamma}_p$  the safe walk in  $\tilde{\Gamma}^1$ . It is also clear that  $\tilde{\gamma}_p$  is the actual lifting of  $\gamma_p$  along  $\Gamma$ . Then,

$$g_1(\mathcal{D}_{\delta_1} \circ \phi_{\Gamma,0}(x)) = \gamma_p(\delta_1(\phi_{\Gamma,0}(x)) + \delta_0(p)) = \gamma_p(\delta_1(\gamma_p^0(\delta_0(p))) + \delta_0(p)) = \gamma_p(l(\gamma_p))$$

and analogously  $g_1(\mathcal{D}_{\delta_1} \circ \phi_{\Gamma,0}(y)) = \omega_p(l(\omega_p))$ .

By property *I*) of a mixed tête-à-tête graph we conclude.  $\square$

Now, we consider the homeomorphism induced by  $\tilde{\phi}_{\Gamma,1}$  and we denote it by

$$\phi_{\Gamma,1} : \Sigma_{\Gamma^2} \rightarrow \Sigma_{\Gamma^2}.$$

The same argument applies inductively to prove that each map

$$\tilde{\phi}_{\Gamma,i} := \mathcal{D}_{\delta_i} \circ \phi_{\Gamma,i-1} : \Sigma_{\Gamma^i} \rightarrow \Sigma_{\Gamma^i} \tag{9.5}$$

is compatible with the gluing  $g_i$  and hence it induces a homeomorphism

$$\phi_{\Gamma,i} : \Sigma_{\Gamma^{i+1}} \rightarrow \Sigma_{\Gamma^{i+1}}. \tag{9.6}$$

In the end we get a map

$$\phi_{\Gamma} := \phi_{\Gamma,d} : \Sigma \rightarrow \Sigma \tag{9.7}$$

which we call the mixed tête-à-tête homeomorphism induced by  $(\Gamma^\bullet, \delta_\bullet)$ .

**Notation 9.8.** We can extend the notation introduced before by defining  $\phi_{\Gamma,-1} := id$  and  $\tilde{\phi}_{\Gamma,0} := \mathcal{D}_{\delta_0} \circ \phi_{\Gamma,-1} = \mathcal{D}_{\delta_0}$ .

Then we can restate Remark 9.2 by saying that  $\tilde{\phi}_{\Gamma,0}$  is compatible with the gluing  $g_0$  and induces the homeomorphism  $\phi_{\Gamma,0}$ .

**Remark 9.9.** After the description of the construction of the mixed tête-à-tête map above and the diagram (9.10), we observe that satisfying *I*) and *II*) of the mixed tête-à-tête property in Definition 8.4 is equivalent to satisfying:



Now we consider  $\tilde{\phi}_{\Gamma,i} := \mathcal{D}_{\delta_i} \circ \phi_{\Gamma,i-1}$  as in (eq. (9.5)). The curves  $\mathcal{C}_{j,k}^i = \eta_{j,k}^i(\mathbb{S}^1 \times \{0\})$  are invariant by  $\tilde{\phi}_{\Gamma,i}$ . These curves separate  $\Sigma_{\Gamma^i}$  in two pieces:  $\mathcal{U}^i$  and its complementary that we call  $\mathcal{B}$ . After quotienting by  $g_i$ , we get a  $\phi_{\Gamma,i}$ -invariant piece that is  $g_i(\mathcal{B}) \approx \mathcal{B}$  and another one that is  $g_i(\mathcal{U}^i)$ . The restriction of  $\phi_{\Gamma,i}$  to  $g_i(\mathcal{B})$  is conjugate to  $\phi_{\Gamma,i-1}$  and then pseudo-periodic. The restriction to  $g_i(\mathcal{U}^i)$  has an invariant spine that is  $g_i(\tilde{\Gamma}^i)$  and then, by Lemma 2.13, it is boundary free isotopic to a periodic one. Then, we have seen that  $\phi_{\Gamma,i}$  is pseudo-periodic.  $\square$

**Remark 9.13.** The screw number associated to the orbit of an invariant annuli at the curve  $\mathcal{C}_{j,k}^i$  that appears in the previous proof is

$$s(\mathcal{C}_{j,k}^i) = - \sum_k \delta_{j,k}^1 / \ell(\tilde{\Gamma}_{j,1}^1). \quad (9.14)$$

We check this by giving a more elaborated construction that the one in the proof of Proposition 9.12 from which the computation of the screw number follows easily.

Let  $\tilde{\Gamma}_{j,1}^i, \dots, \tilde{\Gamma}_{j,\alpha_j}^i$  be a set of boundary components of  $\Sigma_{\Gamma^i}$  contained in  $\tilde{\Gamma}^i$  and cyclically permuted by  $\phi_{\Gamma,i-1}$ . Let  $\mathcal{A}_{j,k}^i$  annular neighborhoods of them as in the previous proof such that  $\phi_{\Gamma,i-1}(\mathcal{U}_{j,k}^i) = \mathcal{U}_{j,k+1}^i$ .

Since  $\phi_{\Gamma,i-1}^\alpha |_{\mathcal{U}_{j,1}^i}$  is periodic, we can choose coordinates/parametrization  $r_{j,1}^i$  from  $\mathbb{S}^1 \times [0, 1]$  (with  $\mathbb{S}^1 \approx \mathbb{R}/\mathbb{Z}$  of total length 1) to  $\mathcal{U}_{j,1}^i$  with respect to which  $\phi_{\Gamma,i-1}^\alpha |_{\mathcal{U}_{j,1}^i}$  is a rotation of the annulus, that is

$$(r_{j,1}^i)^{-1} \circ \phi_{\Gamma,i-1}^\alpha \circ r_{j,1}^i(x, t) = (x + \tau_{i-1}, t),$$

where  $\tau_{i-1}$  is the rotation number  $rot(\phi_{\Gamma,i-1}^\alpha |_{\tilde{\Gamma}_{j,i}^i})$  (note that  $\tau_{i-1}$  depends on the considered orbit of annuli, not only on  $i$ ). Assume  $\tilde{\Gamma}_{j,k}^i = r_{j,k}^i(\mathbb{S}^1 \times \{1\})$ . Let  $\ell(\tilde{\Gamma}_{j,k}^i)$  be the length of  $\tilde{\Gamma}_{j,k}^i$ . We assume without loss of generality that  $r_{j,k}^i |_{\mathbb{S}^1 \times \{1\}}$  is a homothety of ratio  $\ell(\tilde{\Gamma}_{j,k}^i)$  onto  $\tilde{\Gamma}_{j,k}^i$ . Define  $r_{j,k}^i := \phi_{\Gamma,0}^{k-1} \circ r_{j,1}^i$  for  $k = 2, \dots, \alpha_j - 1$ .

Define now  $\mathcal{A}_{j,k}^i := r_{j,k}^i(\mathbb{S}^1 \times [0, 1/2])$  and  $\mathcal{C}_{j,k}^i := r_{j,k}^i(\mathbb{S}^1 \times \{1/4\})$  (note that this system of curves  $\mathcal{C}_{j,k}^i$  is different from that of the previous proof but isotopic to it). We choose a representative of the boundary Dehn twists  $\mathcal{D}_{\delta_i}$  (defined up to isotopy fixing the boundary) performing *all the twisting* in the annuli  $\mathcal{A}_{j,k}^i$ . More precisely we can assume  $\mathcal{D}_{\delta_i}$  is expressed on  $\mathcal{U}_{j,k}^i$  in the coordinates  $r_{j,k}^i$  as follows:

$$(r_{j,k+1}^i)^{-1} \circ \mathcal{D}_{\delta_i} \circ r_{j,k}^i(x, t) := \begin{cases} (x + 2 \cdot t \cdot \delta_{j,k}^i / \ell(\tilde{\Gamma}_{j,k}^i), t) & \text{if } 0 \leq t \leq 1/2 \\ (x + \delta_{j,k}^i / \ell(\tilde{\Gamma}_{j,k}^i), t) & \text{if } 1/2 \leq t \leq 1 \end{cases}$$

where we denote by  $\delta_{j,k}^i := \delta_i(g_i(\tilde{\Gamma}_{j,k}^i))$  with  $g_i : \Sigma_{\Gamma^i} \rightarrow \Sigma_{\Gamma^{i+1}}$  the gluing function.

Then, we find that  $\tilde{\phi}_{\Gamma,i} := \mathcal{D}_{\delta_i} \circ \phi_{\Gamma,i-1}$  satisfies that

$$(r_{j,1}^i)^{-1} \circ \tilde{\phi}_{\Gamma,i} \circ r_{j,1}^i(x, t) = \begin{cases} (x + \tau_{i-1} + 2 \cdot t \cdot \sum_k \delta_{j,k}^i / \ell(\tilde{\Gamma}_{j,1}^i), t) & \text{if } 0 \leq t \leq 1/2 \\ (x + \tau_{i-1} + \sum_k \delta_{j,k}^i / \ell(\tilde{\Gamma}_{j,1}^i), t) & \text{if } 1/2 \leq t \leq 1 \end{cases} \quad (9.15)$$

where  $\tau_{i-1} = rot(\phi_{\Gamma,i-1}^\alpha |_{\tilde{\Gamma}_{j,i}^i})$  is the rotation number of  $\phi_{\Gamma,i-1}^\alpha$  at  $\tilde{\Gamma}_{j,1}^i$ . Recall that this rotation number is computed orienting  $\tilde{\Gamma}_{j,1}^i$  with the orientation induced by relative safe walks, that is, the opposite as the orientation that it inherits as boundary component of  $\Sigma_{\Gamma^i}$ .

From the expression in (eq. (9.15)) we see that the restriction of  $\tilde{\phi}_{\Gamma,i}^{\alpha_j}$  to  $\mathcal{A}_{j,k}^i$  is conjugated to  $\mathcal{D}_{s,\tau_{i-1}}$  (note that we have to re-parametrize  $t = t/2$  in order to get the expression of  $\mathcal{D}_{s,\tau_{i-1}}$  which is defined in  $\mathbb{S}^1 \times [0, 1]$ ) with  $s$  the opposite of the expression in (eq. (9.14)). Applying Definition 2.44, we get that the screw number at  $\mathcal{A}_{j,k}^i$  are given exactly by the expression (eq. (9.14)).

By Definition 2.44 this computes the screw number at  $\mathcal{C}_{j,k}^i$  since the mapping  $\tilde{\phi}_{\Gamma,i}$ , after taken the quotient by  $g_i$ , goes down to a homeomorphism that is periodic restricted to  $g_i(\mathcal{U}_j^i \setminus \mathcal{A}_j^i)$  where  $\mathcal{U}_j^i = \cup_k \mathcal{U}_{j,k}^i$  and  $\mathcal{A}_j^i = \cup_k \mathcal{A}_{j,k}^i$ , and to pseudo-periodic homeomorphism of  $\Sigma_{\Gamma^i} \setminus \mathcal{U}^i \subseteq \Sigma_{\Gamma^{i+1}}$  in a almost-canonical form (see Remark 2.33).

**Corollary 9.16.** *A mixed tête-à-tête twist has strictly positive fractional Dehn twists and negative screw numbers.*

*Proof.* The statement on the fractional Dehn twists follows from the fact that pure tête-à-tête graph have positive fractional Dehn twist coefficients. And the statement on the screw numbers follow from the previous Remark 9.13.  $\square$

**Remark 9.17.** Let  $(\Gamma^\bullet, A^\bullet, \delta_\bullet)$  be a mixed tête-à-tête graph. Let  $\Sigma$  be a relative thickening of  $(\Gamma, A)$ , that is, an embedding  $(\Gamma, A) \hookrightarrow (\Sigma, \partial\Sigma)$  such that  $\Sigma$  regular retracts to  $\Gamma$ . Let  $\partial^1\Sigma$  be the union of the boundary components of  $\Sigma$  not contained in  $A$ .

For the sake of simplicity in notation we have worked out the construction of  $\phi_\Gamma$   $A^\bullet = \emptyset$  during the construction. But the general case is completely analogous. That is, a relative mixed tête-à-tête graph embedded in its thickening defines, up to isotopy fixing  $\partial^1\Sigma$ , and also relative to the action on  $A$ , a pseudo-periodic homeomorphism  $\phi_\Gamma$  of  $\Sigma$ .

We state three more remarks that are useful for the next chapter.

**Remark 9.18.** We make the following observation that is used in Theorem 10.7.

Let  $(\Gamma^\bullet, A^\bullet, \delta_\bullet)$  be a relative mixed tête-à-tête graph. For any choice of product structures on  $(\Sigma_{\Gamma^1})_{\Gamma^1}$ , the relative tête-à-tête homeomorphism  $\phi_{\Gamma,0} : \Sigma_{\Gamma^1} \rightarrow \Sigma_{\Gamma^1}$  is, by definition, an isometry restricted to  $\tilde{\Gamma}^1 \cup (A^0 \setminus A^1)$ . Recall that in the construction, for simplicity of notation, we assumed  $A = \emptyset$  but it is not always the case.

Observe now that  $\mathcal{D}_{\delta_1}|_{\tilde{\Gamma}^1}$  is also an isometry by definition of boundary Dehn twist. Also  $\mathcal{D}_{\delta_1}|_{A^0 \setminus A^1} = id$ . We can conclude that the induced  $\phi_{\Gamma,1}|_{A^0 \setminus A^2}$  is an isometry. The same argument extends to the rest of the filtered graph, so we conclude that for any choice of product structure, the mixed tête-à-tête homeomorphism  $\phi_\Gamma$  satisfies that its restriction to the relative boundaries  $\phi_\Gamma|_A$  is an isometry.

**Remark 9.19.** Observe that if  $(\Gamma^\bullet, \delta_\bullet)$  is a mixed tête-à-tête graph. Then for each  $i = 1, \dots, \ell$  there is an induced filtration on  $\Gamma_{\Gamma^i}$  of depth  $i$  such that  $(\Gamma_{\Gamma^{i+1}}, \tilde{\Gamma}^{i+1})$  is a relative mixed tête-à-tête graph with the functions  $\delta_0, \dots, \delta_i$ .

**Remark 9.20.** Note that for mixed tête-à-tête graphs it is not true that  $p \mapsto \gamma_p(\delta(p))$  gives a continuous mapping from  $\Gamma$  to  $\Gamma$ .

However, there is a similar result for each *level* of the filtration. The map

$$\sigma_i : \Gamma_{\Gamma^{i+1}}^i \rightarrow \Gamma_{\Gamma^{i+1}}^i$$

that sends a point  $p \in \Gamma_{\Gamma^{i+1}}^i$  to the end point of its mixed safe walk in the relative mixed tête-à-tête graph  $(\Gamma_{\Gamma^{i+1}}, \tilde{\Gamma}^{i+1})$  is periodic. This can be proved using the argument that showed that the map  $\sigma_\Gamma$  is periodic in a pure tête-à-tête graph (it is contained in Lemma 6.8 (2) and Corollary 6.10 (4)) together with Remark 9.18.

In Examples C.11, C.19 and C.38, one can find detailed examples of mixed tête-à-tête graphs embedded in their thickenings so that they produce mixed tête-à-tête twists. Some of these examples use the main theorem of the next chapter in the construction. Nevertheless, one can skip directly to the description of the graph, lengths and  $\delta$  functions to check that it is actually a mixed tête-à-tête graph.

## Chapter 10

---

# Realization theorem

Chapter 9 is the main requirement for this chapter and we recall that the last section of Chapter 2 is also heavily used. On the other hand Chapter 5 contains the basic definitions to understand the corollary to the main theorem of this chapter.

In this chapter we prove Theorem 10.7 which is the main result of this work. It appeared previously in a joint work with Baldur Sigurðsson in [PS17]. This result characterizes the pseudo-periodic mapping classes that can be realized by mixed tête-à-tête graphs as those that have positive fractional Dehn twists at all fixed boundary components and negative screw numbers at all separating annuli.

As noted in the introduction, this theorem is a major improvement of a theorem that first appear in the joint work [FPP17] where we proved that mixed tête-à-tête twists are enough to model a restricted class of pseudo-periodic automorphisms that include all monodromies of plane branches. The specific improvements and what is essentially new of this theorem with respect to the previous one is detailed in Remark 10.8 after some notation has been introduced. It is worth noting that the expected scope of mixed tête-à-tête graphs when we gave the definition was to model monodromies of isolated plane curves.

Let  $\phi : \Sigma \rightarrow \Sigma$  be a pseudo-periodic automorphism. For the remaining of this work we impose the following restrictions on  $\phi$ :

- (1) The screw numbers are all negative.
- (2) It leaves at least one boundary component pointwise fixed and the fractional Dehn twist coefficients at these boundary components are positive.

Denote by  $\partial^1 \Sigma \subset \partial \Sigma$  the union of the boundary components pointwise fixed by  $\phi$ . We assume that  $\phi$  is given in some almost-canonical form as in Remark 2.33.

**Notation 10.1.** We define a graph  $G(\phi)$  associated to a given almost-canonical form:

- (1) It has a vertex  $v$  for each subsurface of  $\Sigma \setminus \mathcal{A}$  whose connected components are cyclically permuted by  $\phi$ . Let  $\mathcal{N}$  denote the set of vertices of  $G(\phi)$ .

- (2) For each set of annuli in  $\mathcal{A}$  permuted cyclically it has an edge connecting the vertices corresponding to the surfaces on each side of the collection of annuli.

**Definition 10.2.** We say that a function  $L : \mathcal{N} \rightarrow \mathbb{Z}_{\geq 0}$  is a *filtering function* for  $G(\phi)$  if it satisfies:

- (1) If  $v, v' \in \mathcal{N}$  are connected by an edge, then  $L(v) \neq L(v')$ .
- (2) If  $v \in \mathcal{N}$ , then either  $v$  has a neighbor  $v' \in \mathcal{N}$  with  $L(v) > L(v')$ , or  $L(v) = 0$  and  $\Sigma_v$  contains a component of  $\partial^1 \Sigma$ .

Condition (2) above implies that for  $L$  to be a filtering function,  $L^{-1}(0)$  must only contain vertices corresponding to subsurfaces of  $\Sigma \setminus \mathcal{A}$  that contain some component of  $\partial^1 \Sigma$ . That same condition assures us that  $L^{-1}(0)$  is non-empty.

**Definition 10.3.** Define the *distance function*  $D : \mathcal{N} \rightarrow \mathbb{Z}_{\geq 0}$  as follows:

- (1)  $D(v) = 0$  for all  $v$  with  $\Sigma_v \cap \partial^1 \Sigma \neq \emptyset$ .
- (2)  $D(v)$  is the distance to the set  $D^{-1}(0)$ , that is the number of edges of the smallest bamboo in  $G(\phi)$  connecting  $v$  with some vertex in  $D^{-1}(0)$ .

**Remark 10.4.** Take some  $\phi : \Sigma \rightarrow \Sigma$  in canonical form and observe that the function  $D$  might not be a filtering function. It can happen that there are two adjacent vertices  $v, v' \in \mathcal{N}$  with  $D(v) = D(v')$  or even that there is a vertex with a loop based at it (see Example C.38). When this happens, we can modify the canonical form into an almost-canonical form for which the function  $D$  is a filtering function:

Let  $\phi : \Sigma \rightarrow \Sigma$  be an automorphism in canonical form such that  $D(v) = D(v')$  for some adjacent  $v, v' \in \mathcal{N}$ . Take one edge joining  $v$  and  $v'$ , this edge corresponds to a set of annuli  $\mathcal{A}_1, \dots, \mathcal{A}_k$  being permuted cyclically by  $\phi$ . For each  $i = 1, \dots, k$ , let  $\eta_i : \mathbb{S}^1 \times I \rightarrow \mathcal{A}_i$  be parametrizations as in Lemma 2.45 if  $\phi^k$  does not interchange boundary components, and parametrizations as in Lemma 2.48 if  $\phi^k$  does exchange boundary components. Let  $\mathcal{C}_i \subset \mathcal{A}_i$  be the core curves of the annuli. We distinguish what we do in the two cases:

- (1) The core curves are not amphidrome. By Remark 2.35 we can isotope  $\phi$  on the annuli  $\mathcal{A}_i$  to a automorphism  $\tilde{\phi}$  without changing the action of  $\phi$  on  $\partial \mathcal{A}_i$  so that in the annuli  $\eta_i(\mathbb{S}^1 \times [\frac{1}{3}, \frac{2}{3}])$  it is periodic. In doing so, we can redefine the canonical form to an almost-canonical form as follows.
  - (a) For each  $i = 1, \dots, k$  take  $\mathcal{C}_i$  out from the set  $\mathcal{C}$  and include  $\eta_i(\mathbb{S}^1 \times \{\frac{1}{6}\})$  and  $\eta_i(\mathbb{S}^1 \times \{\frac{5}{6}\})$ .
  - (b) For each  $i = 1, \dots, k$  take  $\mathcal{A}_i$  out of  $\mathcal{A}$  and include  $\eta_i(\mathbb{S}^1 \times [0, 1/3])$  and  $\eta_i(\mathbb{S}^1 \times [\frac{2}{3}, 1])$ .

It is clear that this new set of data defines an almost-canonical form for  $\tilde{\phi}$  and that on the corresponding  $G(\tilde{\phi})$  the vertices  $v$  and  $v'$  are no longer adjacent since a new vertex corresponding to the surface  $\bigcup_i \eta_i(\mathbb{S}^1 \times [\frac{1}{3}, \frac{2}{3}])$  appears between them.

- (2) The core curves are amphidrome. This case is completely analogous to case (1) with the advantage that by definition of  $\tilde{\mathcal{D}}_s$  in Notation 2.41, it is already periodic in the central annuli.

It is clear that after performing (1) or (2) (accordingly) for all pairs of adjacent vertices  $v, v'$  with  $D(v) = D(v')$  we provide  $\phi$  with an almost-canonical whose distance function  $D$  is a filtering function.

**Remark 10.5.** We observe that orbits of amphidrome annuli  $\mathcal{A}_1, \dots, \mathcal{A}_i$  correspond to loops in  $G(\phi)$ . So we find that after performing the modification of Remark 10.4, the almost-canonical form of  $\phi$  does not have any amphidrome annuli in  $\mathcal{A}$ . However, some of the surfaces of  $\Sigma \setminus \mathcal{A}$  are now amphidrome annuli.

**Notation 10.6.** We assume  $\phi$  is in the almost-canonical form induced from the canonical form after performing the modification described in Remark 10.4. We denote by  $\hat{\Sigma}$  the closure of  $\Sigma \setminus \mathcal{A}$  in  $\Sigma$ . Let  $\hat{G}(\phi)$  be a graph constructed as follows:

- (1) It has a vertex for each connected component of  $\Sigma \setminus \mathcal{C}$ .
- (2) There are as many edges joining two vertices as curves in  $\mathcal{C}$  intersect the two surfaces corresponding to those vertices.

We observe that the previously defined  $G(\phi)$  is nothing but the quotient of  $\hat{G}(\phi)$  by the action induced by  $\phi$  on the connected components of  $\Sigma \setminus \mathcal{A}$ .

Let  $\hat{\mathcal{N}}$  be the set of vertices of  $\hat{G}(\phi)$ . Since  $\phi$  permutes the surfaces in  $\hat{\Sigma}$ , it induces a permutation of the set  $\hat{\mathcal{N}}$  which we denote by  $\sigma_\phi$ . We label the set  $\hat{\mathcal{N}}$ , as well as the connected components of  $\hat{\Sigma}$  and the connected components of  $\mathcal{A}$  in the following way:

- (1) Label the vertices that correspond to surfaces containing components of  $\partial^1 \Sigma$  by  $v_{1,1}^0, v_{2,1}^0, \dots, v_{\beta_0,1}^0$ . Let  $V^0$  be the union of these vertices. Note that  $\sigma_\phi(v_{j,1}^0) = v_{j,1}^0$  for all  $j = 1, \dots, \beta_0$ .
- (2) Let  $\hat{D} : \hat{\mathcal{N}} \rightarrow \mathbb{Z}_{\geq 0}$  be the distance function to  $V^0$ , that is,  $\hat{D}(v)$  is the number of edges of the smallest path in  $\hat{G}(\phi)$  that joins  $v$  with  $V^0$ . Let  $V^i := \hat{D}^{-1}(i)$ . Observe that the permutation  $\sigma_\phi$  leaves the set  $V^i$  invariant. There is a labeling of  $V^i$  induced by the orbits of  $\sigma_\phi$ : suppose it has  $\beta_i$  different orbits. For each  $j = 1, \dots, \beta_i$ , we label the vertices in that orbit by  $v_{j,k}^i$  with  $k = 1, \dots, \alpha_j$  so that  $\sigma_\phi(v_{j,k}^i) = v_{j,k+1}^i$  and  $\sigma_\phi(v_{j,\alpha_j}^i) = v_{j,1}^i$ .

Denote by  $\Sigma_{j,k}^i$  the surface in  $\hat{\Sigma}$  corresponding to the vertex  $v_{j,k}^i$ . Denote by  $\Sigma^i$  the union of the surfaces corresponding to the vertices in  $V^i$ . We denote by  $\Sigma^{\leq i}$  the union of  $\Sigma^0, \dots, \Sigma^i$  and the annuli in between them. We recall that  $\alpha_j$  is the smallest positive number such that  $\phi^{\alpha_j}(\Sigma_{j,k}^i) = \Sigma_{j,k}^i$ .

**Theorem 10.7.** *Let  $\phi : \Sigma \rightarrow \Sigma$  be a pseudo-periodic automorphism satisfying assumptions (1) and (2) at the beginning of this chapter. Then there exists a relative mixed tête-à-tête graph  $(\Gamma^\bullet, A^\bullet, \delta_\bullet)$  with  $\Gamma$  embedded in  $\Sigma$  such that:*

- (1)  $\delta_i$  is a constant function for each  $i = 1, \dots, d$ .
- (2)  $[\phi]_{\partial^1 \Sigma} = [\phi_\Gamma]_{\partial^1 \Sigma}$ .
- (3)  $\phi|_{\partial \Sigma \setminus \partial^1 \Sigma} = \phi_\Gamma|_{\partial \Sigma \setminus \partial^1 \Sigma}$ .
- (4) Filtration indices are induced by the distance function  $D$  for the almost-canonical form induced from the canonical form by Remark 10.4.

**Remark 10.8.** As said in the introduction, in [FPP17] it was proved a similar but weaker result that had as a consequence that the class of automorphisms modeled by mixed tête-à-tête twists included monodromies of isolated plane branches.

More concretely, [FPP17, Theorem 9.4] proves the statement of Theorem 10.7 adding the hypothesis:



- (i) That (in the notation of this article) the graph  $\hat{G}(\phi)$  is a tree. Observe that this is a strong condition on the automorphism  $\phi$  that implies, for example, that  $G(\phi)$  is also a tree. In particular, amphidrome curves do not appear in those automorphisms.
- (ii) That all the boundary components in  $\partial^1 \Sigma$  are contained in a single component of  $\Sigma \setminus \mathcal{C}$ .

One can check in [A'C73] that the monodromy of a plane branch clearly satisfies (i) and (ii). Also, the condition (1) that the functions  $\delta_i$  are constant is not imposed in [FPP17].

Now we state and prove Lemma 10.9 and Lemma 10.10 which are used in the proof of Theorem 10.7.

**Lemma 10.9.** *Let  $\phi : \Sigma \rightarrow \Sigma$  be a periodic automorphism of order  $n$ . Let  $C = C_1 \sqcup \cdots \sqcup C_k$  be a non-empty collection of boundary components of  $\Sigma$  such that  $\phi(C_i) = C_i$ , that is, each one is invariant by  $\phi$ . For each  $i$  let  $m_i$  be a metric on  $C_i$  invariant by  $\phi$ . Then there exists a relative metric ribbon graph  $(\Gamma, A) \hookrightarrow (\Sigma, \partial \Sigma \setminus C)$  and parametrizations  $r_i : \mathbb{S}^1 \times I \rightarrow \tilde{\Sigma}_i$  of the cylinders of  $\Sigma_\Gamma$  such that:*

(i)  $\phi(\Gamma) = \Gamma$  and the metric of  $\Gamma$  is also invariant by  $\phi$ .

(ii)  $l(\tilde{\Gamma}_i) = l(C_i)$ .

(iii) The projection from  $C_i$  to  $\tilde{\Gamma}_i$  induced by  $r_i$  is an isometry, that is, the map

$$r(\theta, 0) \mapsto r(\theta, 1)$$

is an isometry.

(iv)  $\phi$  sends retractions lines (i.e.  $\{\theta\} \times I$ ) to retractions lines.

*Proof.* The proof uses essentially the same technique used in the proof of Theorems 7.18 and 7.30.

Let  $\Sigma^\phi$  be the orbit surface and suppose it has genus  $g$  and  $r \geq k$  boundary components. Let  $p : \Sigma \rightarrow \Sigma^\phi$  be the induced branch cover.

Take any relative spine  $\Gamma^\phi$  of  $\Sigma^\phi$  that:

- (1) Contains all branch points of the map  $p$ .
- (2) Contains the boundary components  $p(\partial \Sigma \setminus C)$ .
- (3) Admits a metric such that  $p(C_i)$  retracts to a part of the graph of length  $l(C_i)/n$ .

We observe that conditions (1) are (2) are trivial to get. Condition 3) follows because of the proof of Theorems 7.18 and 7.30. There, the conditions on the metric of the graph  $\Gamma^\phi$  come from the fractional Dehn twist coefficients of  $\phi$ , however, we do not use that these numbers come from  $\phi$  in finding the appropriate graph so exactly the same argument applies imposing the metric conditions with any other positive numbers.

Observe that since the metric on  $C_i$  is invariant by  $\phi$ , there is a metric induced on  $p(C_i)$  for  $i = 1, \dots, k$ . Now choose any parametrizations (or product structures) of the cylinders in  $\Sigma_{\Gamma^\phi}^\phi$  such that their retractions lines induce an isometry from  $p(C_i)$  to  $\tilde{\Gamma}_i^\phi$ .

Define  $\Gamma := p^{-1}(\Gamma^\phi)$ . By construction, this graph satisfies (i) and (ii). The preimage by  $p$  of retraction lines on  $\Sigma^\phi$  gives rise to parametrizations of the cylinders in  $\Sigma_\Gamma$  satisfying (iii) and (iv).  $\square$

**Lemma 10.10.** *Let  $(\Gamma^\bullet, B^\bullet, \delta_\bullet)$  be a relative mixed tête-à-tête graph embedded in a surface  $\Sigma$  and let  $C_1, \dots, C_k \subset B$  be a set of relative boundary components cyclically permuted by  $\phi$ . Suppose that all the vertices in these boundary components are of valency 3. Then we can modify the metric structure of the graph to produce a mixed tête-à-tête graph  $(\hat{\Gamma}^\bullet, \hat{B}^\bullet, \delta_\bullet)$  with  $l(C_i)$  as small as we want and with  $[\phi_\Gamma]_{\partial^1 \Sigma} = [\phi_{\hat{\Gamma}}]_{\partial^1 \Sigma}$ .*

*Proof.* Let  $e_1, \dots, e_m$  be the edges comprising  $C_1$ , where  $e_j$  has length  $l_j$ . Let  $v_1, \dots, v_m$  be the vertices of these edges, so that  $e_i$  connects  $v_i$  and  $v_{i+1}$  (here, indices are taken modulo  $m$ ). Let  $f_{i,j}$ , for  $j = 1, \dots, n_i$  be the edges adjacent to  $v_i$ , other than  $e_i, e_{i+1}$ , in such a way that the edges have the cyclic order  $e_{i+1}, e_i, f_{i,1}, \dots, f_{i,n_i}$ . Let  $\epsilon < l(C_1)$ . We would like to replace  $C_1$  with a circle of length  $l(C_1) - \epsilon$ . We assume that  $l_1 = \min_i l_i$ .

If  $\epsilon/m \leq l_1$ , then we do the following:

- Each edge  $e_i$  is modified to have length  $l_i - \epsilon/m$ .
- For any  $i$  with  $n_i = 1$ , the length of  $f_{i,1}$  is increased by  $\epsilon/2m$ .
- For any  $i$  with  $n_i > 1$ , extrude an edge  $g_i$  from the vertex  $v_i$  of length  $\epsilon/2m$  so that one end of  $g_i$  is adjacent to  $e_i, e_{i+1}$  and  $g_i$ , and the other is adjacent to  $f_{i,1}, \dots, f_{i,n_i}$  and  $g_i$ , with these cyclic orders.

In the case when  $\epsilon/m > l_1$ , we execute the above procedure with  $\epsilon$  replaced by  $m \cdot l_1$ , which results in a circle made up of fewer edges. After finitely many steps, we obtain the desired length for  $C_1$ .

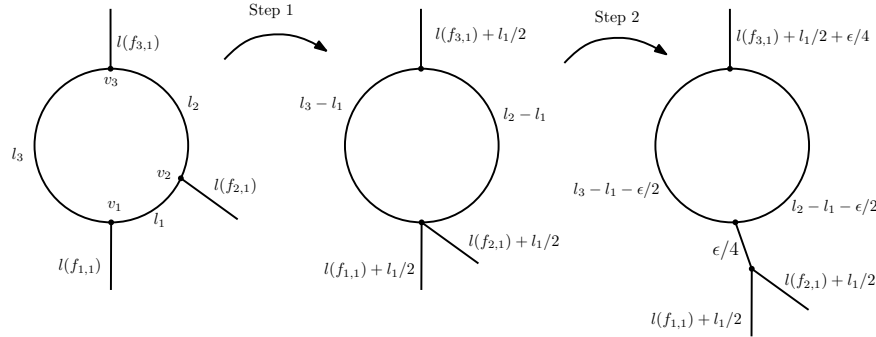


**Figure 10.11:** Example of modification at a boundary component. Suppose that  $l_1 < l_2 < l_3$ . In step 1 we reduce the length of the circle by  $l_1$ . In step 2 we reduce it by  $\epsilon$ .

□

*Proof of Theorem 10.7.* By definition, all surfaces corresponding to vertices in  $D^{-1}(0)$  are connected because they are invariant by  $\phi$ . We have that  $\phi|_{\Sigma_{j,1}^0} : \Sigma_{j,1}^0 \rightarrow \Sigma_{j,1}^0$  is periodic outside a neighborhood of  $\partial^1 \Sigma \cap \Sigma_{j,1}^0$  and that the fractional Dehn twist coefficients with respect to all the components in  $\partial^1 \Sigma \cap \Sigma_{j,1}^0$  are positive. Denote  $B_{j,1}^0 := \partial \Sigma_{j,1}^0 \setminus \partial^1 \Sigma$ . By Theorem 7.30 for each  $j = 1, \dots, \beta_0$ , there is a relative tête-à-tête graph  $(\Gamma_{j,1}^0, B_{j,1}^0)$  embedded in  $\Sigma_{j,1}^0$  modeling  $\phi|_{\Gamma_{j,1}^0}$ . Denote  $\Gamma[0] := \bigsqcup_j \Gamma_{j,1}^0$  and  $B[0] := \bigsqcup_j B_{j,1}^0$ . Then  $(\Gamma[0], B[0], \delta_0)$  is a relative mixed tête-à-tête graph of depth 0 for  $\Sigma^{\leq 0}$  (it is just a relative tête-à-tête graph) such that:

- (1)  $\delta_0|_{\Sigma_{j,1}^0} = \pi$  for all  $j = 1, \dots, \beta_0$ .
- (2)  $[\phi|_{\Sigma^0}]_{\partial^1 \Sigma^0} = [\phi_{\Gamma[0]}]_{\partial^1 \Sigma^0}$ .

- (3)  $\phi|_{B[0]} = \phi_{\Gamma[0]}|_{B[0]}$ .  
 (4) All the vertices on  $B[0]$  have valency 3.

Suppose that we have a relative mixed tête-à-tête graph  $(\Gamma[a-1]^\bullet, B[a-1]^\bullet, \delta[a-1]_\bullet)$  of depth  $a$  embedded as a spine in  $\Sigma^{\leq a}$  and with  $B[a-1] = \partial\Sigma^{\leq a-1} \setminus \partial^1\Sigma$  such that:

- (1)  $\delta[a-1]_i$  is a constant function for each  $i = 0, \dots, a-1$   
 (2)  $[\phi|_{\Sigma^{\leq a-1}}]_{\partial^1\Sigma^{\leq a-1}} = [\phi_{\Gamma[a-1]}]_{\partial^1\Sigma^{\leq a-1}}$   
 (3)  $\phi|_{B[a-1]} = \phi_{\Gamma[a-1]}|_{B[a-1]}$ .  
 (4) All the vertices on  $B[a-1]$  have valency 3.

We recall that  $\phi_{\Gamma[a-1]}$  denotes the mixed tête-à-tête automorphism induced by  $(\Gamma[a-1]^\bullet, B[a-1]^\bullet, \delta[a-1]_\bullet)$ . We extend  $\Gamma[a-1]$  to a mixed tête-à-tête graph  $\Gamma[a]$  satisfying (1) - (4). This proves the theorem by induction. We focus on a particular orbit of surfaces. Fix  $j \in \{1, \dots, \beta_a\}$  and consider the surfaces  $\Sigma_{j,1}^a, \dots, \Sigma_{j,\alpha_j}^a \subset \Sigma^a$  with  $\phi(\Sigma_{j,k}^a) = \Sigma_{j,k+1}^a$  and  $\phi(\Sigma_{j,\alpha_j}^a) = \Sigma_{j,1}^a$ .

For each  $j$ , we distinguish two types of boundary components in the orbit  $\bigsqcup_k \Sigma_{j,k}^a$ :

Type I) Boundary components that are connected to an annulus whose other end is in  $\Sigma^{a-1}$ , we denote these by  $\partial^I$

Type II) The rest: boundary components that are in  $\partial\Sigma$  and boundary components that are connected to an annulus whose other end is in  $\Sigma^{a+1}$ , we denote these by  $\partial^{II}$

Since we are doing the construction for an orbit, we use *local notation* in which not all the indices are specified so that the formulae is easier to read.

Let  $\mathcal{A}^I$  denote the union of annuli connected to boundary components in  $\partial^I$ . These annuli are permuted by  $\phi$ . Suppose that there are  $r'$  different orbits of annuli  $\mathcal{A}_1, \dots, \mathcal{A}_{r'}$ , and let  $\ell_i \in \mathbb{N}$  be the length of the orbit  $\mathcal{A}_i$ . Let  $s_i$  be the screw number of the orbit  $\mathcal{A}_i$  (recall Definition 2.44 and Remark 2.47). Let  $\mathcal{B}_{i,1}, \dots, \mathcal{B}_{i,\ell_i}$  be the orbit of boundary components of  $\Sigma^{a-1}$  that are contained in the orbit  $\mathcal{A}_i$ . The metric of  $\Gamma[a-1]$  gives lengths to these boundary components and all the boundary components in the same orbit have the same length  $l(\mathcal{B}_{i,1}) \in \mathbb{R}_+$ . Consider the positive real numbers

$$\frac{s_1}{\ell_1} l(\mathcal{B}_{1,1}), \dots, \frac{s_{r'}}{\ell_{r'}} l(\mathcal{B}_{r',1}) \quad (10.12)$$

Using Lemma 10.10, we modify the metric structure of  $\Gamma[a-1]$  near each orbit  $\mathcal{B}_i$  so that

$$\frac{s_1}{\ell_1} l(\mathcal{B}_{1,1}) = \dots = \frac{s_{r'}}{\ell_{r'}} l(\mathcal{B}_{r',1}).$$

This is possible since we can make  $l(\mathcal{B}_{i,1})$  as small as needed.

For each  $i = 1, \dots, r'$ , let  $\mathcal{A}_{i,1}, \dots, \mathcal{A}_{i,\ell_i}$  be the annuli in the orbit  $\mathcal{A}_i$  and let  $\mathcal{B}'_{i,1}, \dots, \mathcal{B}'_{i,\ell_i}$  be the boundary components that they share with  $\Sigma^a$ . Take parametrizations  $\eta_{i,1}, \dots, \eta_{i,\ell_i}$  given by Lemma 2.45. The metric on the boundary components of  $B[a-1]$  and the parametrizations induce a metric on all the boundary components in  $\partial^I$  that is invariant by  $\phi$ .

We observe that  $\phi^{\alpha_j}|_{\Sigma_{j,1}^a} : \Sigma_{j,1}^a \rightarrow \Sigma_{j,1}^a$  is periodic and  $\partial^I \cap \Sigma_{j,1}^a$  is a subset of boundary components that have a metric. So we can apply Lemma 10.9 and we get a relative metric ribbon graph  $(\Gamma_{j,1}^a, \partial^{II} \cap \Gamma_{j,1}^a)$  and parametrizations of each cylinder in  $(\Sigma_{j,1}^a)_{\Gamma_{j,1}^a}$  with properties  $i), \dots, iv)$  in the Lemma. We can translate this construction by  $\phi$  to the rest of the surfaces  $\Sigma_{j,2}^a, \dots, \Sigma_{j,\alpha_j}^a$ . So we get graphs  $\Gamma_{j,k}^a \hookrightarrow \Sigma_{j,k}^a$  and parametrizations for the cylinders in  $(\Sigma_{j,k}^a)_{\Gamma_{j,k}^a}$

for all  $k = 1, \dots, \alpha_j$ . The construction assures us that  $\phi|_{\Sigma_{j,\alpha_j}^a} : \Sigma_{j,\alpha_j}^a \rightarrow \Sigma_{j,1}^a$  sends  $\Gamma_{j,\alpha_j}^a$  to  $\Gamma_{j,1}^a$  isometrically and that it takes retraction lines of the parametrizations in  $\Sigma_{j,\alpha_j}^a$  to retraction lines in  $\Sigma_{j,1}^a$ .

We proceed to extend  $\Gamma[a-1]$  to the orbit of  $\Sigma_{j,1}^a$ . For each  $i = 1, \dots, r'$  do the following:

Step 1. Remove  $\mathcal{B}_{i,1}, \dots, \mathcal{B}_{i,\ell_i}$  from  $\Gamma[a-1]$ .

Step 2. Take  $\epsilon > 0$  small enough. Decrease by  $\epsilon$  the metric on all the edges of  $\Gamma[a-1]$  adjacent to vertices in  $\mathcal{B}_{i,1}, \dots, \mathcal{B}_{i,\ell_i}$ .

Step 3. Add to the graph the retraction lines of the parametrizations  $\eta_{i,1}, \dots, \eta_{i,\ell_i}$  that were adjacent to vertices in  $\mathcal{B}_{i,1}, \dots, \mathcal{B}_{i,\ell_i}$ . That is, if  $v \in \mathcal{B}_{i,1} \subset \mathcal{A}_{i,1}$  include  $\eta_{i,1}(\{v\} \times I)$ . Define the length of these segments as  $\epsilon/2$ .

Step 4. Add to the graph the retraction lines of the parametrizations of the cylinders  $(\Sigma_{j,k}^a)_{\Gamma_{j,k}^a}$  that start at the ends of the lines added in the previous step. Define the length of these segments as  $\epsilon/2$ .

Step 5. Add to the graph the graphs  $\Gamma_{j,1}^a, \dots, \Gamma_{j,\alpha_j}^a$ .

We repeat this process for all orbits of surfaces in  $\Sigma^a$  and so we extend the graph  $\Gamma[a-1]$  to all  $\Sigma^a$ . Denote

$$\Gamma[a]^a := \bigsqcup_{j,k} \Gamma_{j,k}^a.$$

Denote the resulting graph by  $\Gamma[a]$ .

We make the following observation:  $(\Gamma[a]_{\Gamma[a]^a}, \tilde{\Gamma}[a]^a)$  is by construction isometric to  $(\Gamma[a-1], \mathcal{B}[a-1])$ . We denote the induced relative mixed tête-à-tête automorphism by  $\phi_{\Gamma[a]_{\Gamma[a]^a}}$  which acts on  $\Sigma_{\tilde{\Gamma}[a]^a}^{\leq a}$ . By the previous observation there is an induced filtration on  $\Gamma[a]$ :

$$\Gamma[a] = \Gamma[a]^0 \supset \Gamma[a]^1 \supset \dots \supset \Gamma[a]^{a-1} \supset \Gamma[a]^a$$

and similarly for the relative parts. We define  $\delta_a : \Gamma[a]^a \rightarrow \mathbb{R}_{\geq 0}$  to be the constant function equal to the numbers  $eq$ . (10.12) (which are by construction the same number).

By the choice of  $\delta_a$  and the parametrizations on the annuli that join  $\Sigma^{a-1}$  with  $\Sigma^a$  we find that

$$\mathcal{D}_{\delta_a} \circ \phi_{\Gamma[a]} : \Sigma_{\Gamma[a]^a} \rightarrow \Sigma_{\Gamma[a]^a}$$

is compatible with the gluing  $g_{a+1}$ . So that  $(\Gamma[a], \mathcal{B}[a])$  is a relative mixed tête-à-tête graph follows from  $I'$  in Remark 9.9.

We have already made sure in the construction that (1) and (4) hold in  $\Gamma[a]$ .

Let's show that (2) and (3) also hold. Observe that by construction  $\phi$  leaves  $\Gamma[a]$  invariant so there is an automorphism  $\tilde{\phi}_a : \Sigma_{\Gamma[a]^a} \rightarrow \Sigma_{\Gamma[a]^a}$  induced. This automorphism coincides with  $\mathcal{D}_{\delta_a} \circ \phi_{\Gamma[a]}$  on  $\tilde{\Gamma}[a]$  by the choice of the parametrizations of the annuli  $\mathcal{A}$  and by the choice of the number  $\delta_a$ . Also, by the choice of  $\delta_a$  and Remark 9.13 we see that they have the same screw numbers on the annuli connecting the level  $a-1$  and the level  $a$ . From this discussion we get (2) and (3) and finish the proof.  $\square$

**Remark 10.13.** From the proof we get as an important consequence that a more restrictive definition of a mixed tête-à-tête graph is valid: it is enough to consider mixed tête-à-tête graphs where  $\delta_i$  is a constant function (i.e. a number) for all  $i = 0, \dots, \ell$ .

**Corollary 10.14.** *The monodromy associated with a reduced holomorphic function germ defined on an isolated surface singularity is a mixed tête-à-tête twist. Conversely, let  $C(\Gamma)$  be the cone over the open book associated with a mixed tête-à-tête graph. Then there exists a complex structure on  $C(\Gamma)$  and a reduced holomorphic function germ  $f : C(\Gamma) \rightarrow \mathbb{C}$  inducing  $\phi_\Gamma$  as the monodromy of its Milnor fibration.*

*Proof.* The plumbing graph associated to a reduced holomorphic function germ has positive signs at all edges and induces positive multiplicity weights (this just follows from the computation of the resolution graph of the singularity). Then by Lemma 4.24, we find that this monodromy has negative screw numbers and positive fractional Dehn twist coefficients. Therefore, we conclude the first part of the statement from Theorem 10.7.

The second part of the statement follows from Theorem 10.7 and [NP07, Theorem 2.1] (the relevant part of this theorem is in Theorem 5.8 in this work).  $\square$

**Remark 10.15.** In B.2 we give an explicit mixed tête-à-tête graph for any given isolated plane curve singularity, so we actually prove that mixed tête-à-tête graph model monodromies on reduced plane branches without using Theorem 10.7. The graph that we produce in the appendix is different from the graph produced by the construction of Theorem 10.7.

Part III



**Algorithms**



## Chapter 11

---

# *Tête-à-tête graphs and Seifert manifolds*

The first part of Chapters 3 and 4 are the preliminaries for this chapter.

The homeomorphism type of mapping torus of an automorphism  $\phi : \Sigma \rightarrow \Sigma$  depends only on the conjugacy class of the mapping class  $[\phi]$ . In [Eps72] Epstein proved that a 3-manifold is a Seifert manifold if and only if it admits a foliation by circles. From this, we can conclude that the mapping torus of a periodic mapping class is a Seifert manifold. On the other hand, given an oriented surface  $\Sigma$  properly embedded in a fibered-oriented Seifert manifold  $Y$  and transverse to all the fibers, has a monodromy induced on it (by following the flow of the fibers). Since the fibers are circles, this monodromy is periodic.

In this chapter we describe an algorithm that, given a general, relative or pure tête-à-tête graph, produces a star-shaped plumbing graph together with a the horizontal surface. We also describe the algorithm that goes in the opposite direction.

## 11.1 From general tête-à-tête graph to star-shaped plumbing graph

Let  $(\Gamma, \mathcal{P}, \sigma)$  be a general tête-à-tête graph. For simplicity, we suppose that  $\Gamma$  is connected. This includes as particular cases pure tête-à-tête graphs and relative tête-à-tête graphs. Let  $\phi_\Gamma$  be a truly periodic representative of the tête-à-tête automorphism and let  $\Sigma_{\phi_\Gamma}$  be the mapping torus of the the diffeomorphism  $\phi_\Gamma : \Sigma \rightarrow \Sigma$ . The mapping torus given by a periodic diffeomorphism of a surface is a Seifert manifold. We describe an algorithm that takes  $(\Gamma, \mathcal{P}, \sigma)$  as input and returns as output:



- (1) The invariants of a Seifert manifold:

$$M(g, r; (1, b), (\alpha_1, \beta_1), \dots, (\alpha_k, \beta_k))$$

diffeomorphic to the mapping torus  $\Sigma_{\phi_\Gamma}$ . It is represented by a star-shaped plumbing graph  $\Lambda$  corresponding to the Seifert manifold.

- (2) A tuple
- $(p_1, \dots, p_\mu, q)$
- with
- $p_i \in \mathbb{Z}/q\mathbb{Z}$
- and
- $q \in \mathbb{Z}_{>0}$
- representing the horizontal surface given by
- $\Sigma$
- with respect to some basis of the homology
- $H_1(B; \mathbb{Z}) \simeq \mathbb{Z}^\mu$
- of the base space
- $B$
- of
- $Y$
- .

**Step 1.** We consider  $\Gamma^{\phi_\Gamma}$ , that is the quotient space  $\Gamma / \sim$  where  $\sim$  is the equivalence relation induced by the action of the safe walks on the graph. This graph is nothing but the image of  $\Gamma$  by the projection of the branched cover  $p : \Sigma \rightarrow \Sigma^{\phi_\Gamma}$  onto the orbit space.

The map  $p|_\Gamma : \Gamma \rightarrow \Gamma^{\phi_\Gamma}$  induces a ribbon graph structure on  $\Gamma^{\phi_\Gamma}$ . We can easily get the genus  $g$  and number of boundary components  $r$  of the thickening of  $\Gamma^{\phi_\Gamma}$  from the combinatorics of the graph. This gives us the first two invariants of the Seifert manifold.

**Step 2.** Let  $sv(\Gamma)$  be the set of points with non trivial isotropy subgroup in  $\langle \phi_\Gamma \rangle$ . This is the set of branch points of  $p : \Sigma \rightarrow \Sigma^{\phi_\Gamma}$  by definition.

Let  $v \in sv(\Gamma)$ . Then there exists  $m < n$  with  $n = m \cdot s$  such that  $v$  is a fixed point of  $\phi_\Gamma^m$  (take  $m$  the smallest natural number satisfying that property). We can therefore use Corollary 3.8. We get that  $\phi_\Gamma^m$  acts as rotation with rotation number  $p/s$  in a small disk centered at  $v$ . So around the fiber corresponding to the vertex  $v$ , the Seifert manifold is diffeomorphic fiberwise to a  $p, s$ -torus. and the corresponding Seifert pair  $(\alpha_v, \beta_v)$  is given by  $(\alpha_v, \beta_v) = (s, -b)$  with  $bp \equiv 1 \pmod{q}$ .

We do this for every vertex in  $sv(\Gamma)$  and we get all the Seifert pairs.

**Step 3.** Since we have already found a complete set of Seifert invariants, we have that

$$M(g, r; (\alpha_1, \beta_1), \dots, (\alpha_k, \beta_k))$$

is diffeomorphic to the mapping torus of the pair  $(\Sigma, \phi_\Gamma)$ .

Now we use Proposition 3.17 to get the normalized form of the plumbing graph associated to the Seifert manifold.

**Step 4.** For this step, recall Section 4.1 and notation introduced there. Fix a basis  $[S_1^1], \dots, [S_\mu^1]$  of  $H_1(B; \mathbb{Z})$  where  $S_i^1$  is a simple closed curve contained in  $\Gamma^{\phi_\Gamma}$ .

Let  $m := \text{lcm}(\alpha_1, \dots, \alpha_k)$ . Observe that necessarily  $m|n$  so  $n = m \cdot q$  (with  $n$  the order of  $\phi_\Gamma$ ).

This number  $q$  that we have found is the last term of the cohomology element we are looking for. Of course, it is also the oriented intersection number of  $\hat{\Gamma} = \pi(\Gamma)$  with  $C$ . (recall  $\pi$  was the projection  $Y \rightarrow Y/c_m =: \hat{Y}$ ).

Pick any basis of  $H_1(B; \mathbb{Z})$  by picking a collection of circles  $S_1^1, \dots, S_k^1$  contained in the orbit graph  $\Gamma^{\phi_\Gamma} \subset B$  that generate the homology of the graph.

Now if we intersect the graph  $\Gamma/c_m \cap S_i^1 \times C$  with the torus over one of the representatives of the basis, we get a collection of  $k_i$  closed curves, each one isotopic to the curve of slope  $p'_i/q'_i$  where  $q'_i \cdot k_i = q$  and  $p_i = p'_i \cdot k_i = p_i$ . This number,  $p_i$ , is the  $i$ -th coordinate of the cohomology element with respect to the fixed basis.

We can compute  $p_1, \dots, p_k$  directly. Let  $S_i^1$  be one of the generators of  $H_1(\Gamma^{\phi_\Gamma}; \mathbb{Z})$ . Let  $\hat{S}_i^1 := \Gamma/c_m \cap S_i^1 \times \mathbb{S}^1$  where  $S_i^1 \times \mathbb{S}^1 \subset \Gamma^{\phi_\Gamma} \times \mathbb{S}^1$ ; and let  $\tilde{S}_i^1 := p|_\Gamma^{-1}(\hat{S}_i^1)$ . Observe that  $\hat{S}_i^1$  consists of  $k_i$  disjoint circles and that  $k_i$  divides  $q$ . Let  $q'_i = q/k_i$ .

Pick a point  $z \in S_i^1$  which is not in the image by  $\pi$  of a special fiber. Then  $\hat{\pi}^{-1}(z) \cap \Gamma/c_m$  consists of  $q$  points lying in the  $k_i$  connected components of  $\hat{S}_i^1$ . Pick one of these connected components and enumerate the corresponding  $q'_i$  points in it using the orientation induced on that

connected component by the given orientation of  $S_i^1$ . Then we have the points  $z_1, \dots, z_{q'_i}$ . We observe that by construction, these points lie on the same fiber in  $\hat{Y}$  and this fiber is oriented. Follow the fiber from  $z_1$  in the direction indicated by the orientation, the next point is  $z_{t_i}$ , with  $t_i \in \{1, \dots, q'_i\}$ . We therefore find that this connected component of  $\hat{S}_i^1$  lies in  $S_i^1 \times \mathbb{S}^1$  as the curve with slope  $(t_i - 1)/q'_i$  and so  $p_i = (t_i - 1) \cdot k_i$ .

## 11.2 From star-shaped plumbing graph to tête-à-tête graphs

The input that we have is:

- i) A Seifert fibering of a manifold  $Y$ .
- ii) A horizontal surface given by an element in  $H^1(B \times \mathbb{S}^1; \mathbb{Z})$  that does not vanish on a typical Seifert fiber.

The output is:

- (1) A general, relative or pure tête-à-tête graph such the induced mapping torus is diffeomorphic to the given plumbing manifold in the input. And such that the thickening of the graph, represents the horizontal surface given.

**Step 1.** We start with a Seifert fibering  $M(g, r; (\alpha_1, \beta_1, \dots, \alpha_k, \beta_k))$ .

We fix a model of the Seifert fibering as in Section 4.1. We recall that the model consists of the following data:

- i) The Seifert fibering  $s : Y \rightarrow B$  where  $B$  is a surface of genus  $g$  and  $r$  boundary components.
- ii) A collection of arcs  $\{l_i\}$  with  $i = 1, \dots, k$  properly embedded in  $B$  where the boundary of these arcs lie in one chosen boundary component of  $B$ . These satisfy that when we cut along one of them, say  $l_i$  we cut off a disk denoted by  $D_i$  from  $B$  that contains the image of exactly one special fiber, we denote the image of this fiber by  $x_i$ .
- iii) We have an identification of each solid torus  $s^{-1}(D_i)$  with the corresponding fibered solid torus  $T_{p_i, q_i}$  with  $q_i = \alpha_i$  and  $-p_i \beta_i \equiv 1 \pmod{\alpha_i}$  and  $0 < p_i < q_i$ .

**Step 2.** Observe that  $B$  is homotopic to a wedge of  $\mu = 2g - r + 1$  circles that does not contain any  $x_i$  for  $i = 1, \dots, k$ . We can see this wedge as a spine embedded in  $B$ . Denote by  $c$  the common point of all the circles. Now we embed disjoint segments  $e_i$  with  $i = 1, \dots, k$  where each one satisfies that one of its ends lies in the spine and the other end lies in  $x_i$ . Also, they do not intersect the wedge of circles at any other point and they also  $e_i$  does not intersect any  $D_j$  for  $j \neq i$ . We denote the union of the wedge and these segments by  $\tilde{\Lambda}$  and observe that  $\tilde{\Lambda}$  is a spine of  $B$ .

**Step 3.** We suppose that the element in  $H^1(\hat{Y}; \mathbb{Z})$  given is irreducible, otherwise if it is of the form  $k(p'_1, \dots, p'_\mu, q')$  with  $(p'_1, \dots, p'_\mu, q')$  irreducible, we take the irreducible part, carry out the following construction of the corresponding horizontal surface and then take  $k$  parallel copies of this surface.

Recall diagram 4.3 for the definition of the maps  $s, \hat{s}$  and  $\pi$ .

Once and for all, fix a trivialization  $\hat{Y} \simeq B \times \mathbb{S}^1$ . We assume that the element  $(p_1, \dots, p_\mu, q) \in H^1(\hat{Y}; \mathbb{Z})$  is expressed with respect to the dual basis  $[S_1], \dots, [S_\mu], [C]$  where the first  $\mu$  are circles of the wedge embedded in  $B$  and  $[C]$  is the homology class of  $C := \hat{s}^{-1}(c)$ .

For each  $i = 1, \dots, \mu$ , consider the torus  $\hat{s}^{-1}(S_i)$  which is naturally trivialized by the trivialization of  $\hat{Y}$ . We pick in it  $k_i$  copies of the curve of slope  $p'_i/q'$  where  $p_i/q = k_i p'_i/k_i q'$ . For each  $i$ , the curves constructed this way in  $\hat{s}^{-1}(S_i)$  intersect  $q$  times the curve  $C$ . Hence we can isotope them so that all of them intersect  $C$  in the same  $q$  points. We denote the union of these curves by  $\hat{\Lambda}'$ . We assume that  $\hat{\Lambda}'$  projects to  $\tilde{\Lambda} \setminus \bigcup e_i$  by  $B \times \mathbb{S}^1 \rightarrow B$ .

By construction,  $\hat{\Lambda}'$  is a ribbon graph for the surface horizontal surface  $\hat{H} \subset \hat{Y}$ . Observe that  $s(\hat{\Lambda}') \neq \tilde{\Lambda}$ . However  $s(\hat{\Lambda}')$  is also a spine of  $B$  (it coincides with the wedge of circles in  $B$ ).

Define  $\Lambda' := \pi^{-1}(\hat{\Lambda}')$ . By the definition of  $\pi$ , this graph can also be constructed by taking in each of the tori  $\pi^{-1}(\hat{s}^{-1}(S_i)) = \hat{s}^{-1}(S_i)$ ,  $k_i$  copies of the curve of slope  $p'_i/n$ . Which by construction all intersect in  $n$  points in  $s^{-1}(c)$ .

**Step 4.** Now we describe  $\pi^{-1}(\hat{s}^{-1}_{\hat{H}}(e_i))$  for each  $i = 1, \dots, k$ . First we observe that it is equal to  $s|_H^{-1}(e_i)$  which is a collection of  $q \cdot n/\alpha_i$  disjoint star shaped graphs. Each star-shaped piece has  $\alpha_i$ . To find out the gluings of these arms with  $\Lambda'$  one looks as the structure of  $s^{-1}(D_i)$  as a  $(c, \alpha_i)$ -solid torus. To visualize it, place the  $q \cdot n/\alpha_i$  star-shaped pieces in a solid cylinder  $D^2 \times [0, 1]$  and identify top with bottom by a  $c/\alpha_i$  rotation. The fibers of the fibered torus give the monodromy on the end of the arms and the attaching to  $\Lambda'$ .

We define  $\Lambda$  as the union of  $\Lambda'$  with these star-shaped pieces

**Step 5.** The embedding of  $H$  in the Seifert manifold defines a diffeomorphism  $\phi : H \rightarrow H$  in the following way. Let  $x \in H$  and follow the only fiber of the Seifert manifold that passes through  $x$  in the direction indicated by its orientation, we define  $\phi(x)$  as the next point of intersection of that fiber with  $H$ .

To describe  $\phi$  up to isotopy it is enough to give the rotation numbers of  $\phi$  around each boundary component of  $H$  plus some spine invariant by  $\phi$ . By construction  $\Lambda$  is an invariant graph. The fibers of the Seifert fibering give us an automorphism on the graph  $\Lambda$ . To get the rotation numbers, we cut the thickening  $H$  along  $\Lambda$  and we get a collection of cylinders  $\Lambda_j \times [0, 1]$  with  $j = 1, \dots, r'$ .

Now we invoke Theorem 7.33 if the monodromy leaves at least 1 boundary component invariant and we invoke Theorem 7.40 if the monodromy does not leave any boundary component invariant. This gives us a constructive method to find a graph (which in general will be different from  $\bigcup_{i=1}^{\mu} S_i \cup_{j=1}^k e_j$ ) containing all branch points in  $B$  such that it is a retract of  $B$  and such that it admits a metric that makes its preimage a tête-à-tête graph.

# *Mixed tête-à-tête graphs and graph manifolds*

The previous Chapter 11 and the last part of Chapters 3 and 4 are the preliminaries for this chapter.

The mapping torus of a pseudo-periodic mapping class is a graph manifold. On the other hand, a horizontal surface of a fibered-oriented graph manifold has a pseudo-periodic monodromy induced on it. In this chapter we use the machinery developed in Chapter 4 to provide with algorithms that travel between the world of mixed tête-à-tête graphs and certain fibrations of graph manifolds over  $\mathbb{S}^1$ .

## 12.1 From open books to mixed tête-à-tête graphs

Suppose we are given:

- (1) A graph manifold  $Y$  given by a plumbing graph  $\Lambda$ .
- (2) A Waldhausen link  $L \subset Y$ .
- (3) A homomorphism  $\gamma : H_1(Y \setminus L, \mathbb{Z}) \rightarrow \mathbb{Z}$  that does not vanish on the classes of generic Seifert fibers of all Seifert pieces and whose associated system of multiplicities satisfies that  $m_v = +1$  for all components  $L_v$  of  $L$ .

Section 4.3 provides the combinatorial data associated with the monodromy  $\phi$  of the fibration  $f$  so that  $f_* = \gamma$ . Now, Theorem 10.7 produces a mixed tête-à-tête graph inducing  $\phi$ . This construction is made explicit in the proof of the theorem. This is done by first choosing relative tête-à-tête graphs for those pieces in  $Y$  which contain a component of  $L$ . An iterative process follows: choose an invariant spine of each neighboring piece; then the screw number of each orbit of connecting annuli produces a parametrization of these annuli and some retraction lines of these

parametrizations are used to connect the previously constructed graph with the new invariant spines. This produces the desired mixed tête-à-tête graph.

## 12.2 From mixed tête-à-tête graphs to open books

In this section we describe an algorithm that works in the reverse direction of the previous algorithm. That is, we start with a mixed tête-à-tête graph  $(\Gamma^\bullet, \delta_\bullet)$  with a thickening  $\Sigma$ , and the algorithm produces:

- (1) A graph manifold  $Y$  represented by a plumbing graph  $\Lambda$ .
- (2) A Waldhausen link  $(Y, L)$  such that  $Y \setminus L$  is diffeomorphic to the mapping torus of the mixed tête-à-tête automorphism  $\phi_\Gamma$ .
- (3) An element  $f_* \in H^1(Y \setminus L; \mathbb{Z})$  given by a horizontal open book  $f : Y \setminus L \rightarrow \mathbb{S}^1$  that has fiber diffeomorphic to  $\Sigma$  and whose monodromy is conjugate to that of  $\phi_\Gamma$ .

First we are going to obtain the information about the Seifert pieces of  $Y$ . Recall that  $\phi_{\Gamma,i}|_{\Gamma_{\Gamma^{i+1}}^i} : \Gamma_{\Gamma^{i+1}}^i \rightarrow \Gamma_{\Gamma^{i+1}}^i$  is a periodic automorphism. For each  $p \in \Gamma_{\Gamma^{i+1}}^i \subset \Gamma_{\Gamma^{i+1}}$  we recall that  $\phi_{\Gamma,i}(p)$  is, by definition, the last point of the walk resulting from the concatenation  $\gamma_p^i \star \cdots \star \gamma_p^0$ .

Let  $\ell$  be the depth of the filtration of  $\Gamma^\bullet$ . For each  $i = 0 \dots, \ell$  we find that the graph  $\Gamma_{\Gamma^{i+1}}^i$  and the restriction  $\phi_{\Gamma,i}|_{\Gamma_{\Gamma^{i+1}}^i}$  give us

- (1) The number of Seifert pieces that lie on the  $i$ -th level of the filtration. This is the number of orbits of  $\phi_{\Gamma,i}$  on the set of connected components of  $\Gamma_{\Gamma^{i+1}}^i$ . For each Seifert piece, there will be a node on  $\Lambda$ .
- (2) The number of connected components in each orbit.
- (3) The multiplicity  $m_n$  corresponding to the node  $n$  of the corresponding Seifert piece which is the order of  $\phi_{\Gamma,i}|_{\Gamma_{\Gamma^{i+1}}^i}$  restricted to the corresponding orbit.
- (4) By applying Steps 1-4 of the algorithm *From general tête-à-tête graphs to star-shaped plumbing graphs* in Chapter 11, we get the decoration corresponding to the Euler numbers of the arms of each Seifert piece.

Note that we leave the nodes without the Euler number decoration until the end.

**12.1.** We recall a piece of the algorithm in Chapter 11 which is be useful now. Suppose that  $\phi_{\Gamma,i}|_{\Gamma_{\Gamma^{i+1}}^i}$  has order  $n$ . If  $x \in \Gamma_{\Gamma^{i+1}}^i$  is a point with non-trivial isotropy in  $\langle \phi_{\Gamma,i}|_{\Gamma_{\Gamma^{i+1}}^i} \rangle$ , then there exists a natural number  $0 < k < n$  such that  $\phi_{\Gamma,i}|_{\Gamma_{\Gamma^{i+1}}^i}^k(x) = x$  and in this case,  $\phi_{\Gamma,i}|_{\Gamma_{\Gamma^{i+1}}^i}^k$  is a rotation in a disk around  $x$ . Suppose that this rotation has rotation number  $p/q$  with  $q = n/k$ . The rotation number is measured at the boundary of the disk with the orientation induced as boundary of the disk. Then the Seifert fiber over  $x$  has Seifert invariants  $(\alpha, \beta) = (q, -b)$  with  $bp \equiv 1 \pmod{q}$  and  $0 < -b < q$ . By Corollary 3.8 and discussion before in that same work, the attaching matrix is

$$([s][f]) = ([m][l]) \begin{pmatrix} a & p \\ b & q \end{pmatrix} \quad (12.2)$$

where  $[s], [f]$  (section, fiber) is a positive basis of the boundary torus in the circle bundle of the corresponding node; and  $[m], [l]$  (meridian, longitude) is a basis on the boundary torus of the solid torus  $D^2 \times \mathbb{S}^1$  that is attached. Each of the boundaries of the  $k$  disks is glued to a meridian of this solid torus. By extending the fibration on the node to the attached solid torus, we get a  $(p, q)$ -fibered torus which induces a rotation with rotation number  $p/q$  on each of the  $k$  boundary components.

The decoration of the Euler numbers in the arm corresponding to that Seifert fiber is given by the continued fraction of  $q/-b$ .

**12.3.** Now we describe the Euler weights of the arms of the plumbing graph that end at arrowheads with multiplicity  $(1)$ . These correspond to boundary components of  $\Sigma$  that are fixed by  $\phi_\Gamma$ . Let  $p/q$  be the fractional Dehn twist at a boundary component (note that possibly  $p > q$ ). Let  $b$  be as before, i.e.  $bp \equiv 1 \pmod{q}$  and  $0 < -b < q$ . Then the Euler numbers of the vertices of the arm correspond to the continued fraction expansion of  $-p/a$  with  $a = (pb - 1)/q$ . The reason is that by the construction of an open book, we need to attach a solid torus  $D^2 \times \mathbb{S}^1$  to the mapping torus of  $\phi_\Gamma$  matching  $pt \times \mathbb{S}^1$  with the boundary of the surface. This corresponds to change the matrix from eq. (3.2) to

$$\begin{pmatrix} 0 & 1 \\ 1 & 0 \end{pmatrix} \begin{pmatrix} a & p \\ b & q \end{pmatrix} = \begin{pmatrix} b & q \\ a & p \end{pmatrix} \quad (12.4)$$

Hence, by using Lemma 3.13, we find that the decoration of the Euler numbers in the arm corresponding to that Seifert fiber is given by the continued fraction expansion of  $-p/a$ . The arm ends with an arrow with multiplicity weight equal to  $(1)$ .

**12.5.** Finally we describe the bamboos joining nodes in the plumbing graph. To each orbit of annuli in the almost-canonical form defined by a mixed tête-à-tête graph there corresponds a bamboo in the plumbing graph. Remark 9.13 gives us a simple formula for the screw number associated with an orbit of annuli that corresponds to components  $\tilde{\Gamma}_{j,1}^i, \dots, \tilde{\Gamma}_{j,\alpha_j}^i$  of  $\tilde{\Gamma}^i$ . We have that the screw number is  $\sum_k -\delta_{j,k}^i / l(\tilde{\Gamma}_{j,1}^i)$ .

The maps  $\phi_{\Gamma,i}|_{\Gamma_{\Gamma^{i+1}}^i}$  and  $\phi_{\Gamma,i+1}|_{\Gamma_{\Gamma^{i+2}}^{i+1}}$  give us the rotation numbers of  $\phi_\Gamma^{\alpha_j}$  restricted to each boundary component of the annuli  $\mathcal{A}_{j,1}^i$ . These rotation numbers are  $p_0/q_0$  and  $p_1/q_1$ . The screw number can then be written as  $1 - p_0/q_0 - p_1/q_1 + t$  with  $t \in \mathbb{Z}$ . Then, the gluing matrix from the Seifert piece corresponding to the node  $n_0$  to the Seifert piece corresponding to the node  $n_1$  is the composition of three matrices. The first matrix corresponds to performing a twist of fractional Dehn twist coefficient equal to  $p_0/q_0 - 1 - t$  near the boundaries of  $n_0$ ; the second matrix  $\begin{pmatrix} -1 & 0 \\ 0 & 1 \end{pmatrix}$  represents the gluing of boundary components from  $n_0$  to boundary components in  $n_1$  (the  $-1$  on the top left is because boundaries inherit opposite orientations); and the last matrix has the same meaning as the first, but the remaining amount of twisting is  $p_1/q_1$ . Hence, the gluing matrix is:

$$\begin{aligned} & \begin{pmatrix} a_1 & p_1 \\ b_1 & q_1 \end{pmatrix}^{-1} \begin{pmatrix} -1 & 0 \\ 0 & 1 \end{pmatrix} \begin{pmatrix} a_0 & p_0 - (t+1)q_0 \\ b_0 & q_0 \end{pmatrix} = \\ & = \begin{pmatrix} q_1 a_0 + p_1 b_0 & q_1(p_0 - (t+1)q_0) + p_1 b_0 \\ * & * \end{pmatrix} \end{aligned} \quad (12.6)$$

Where  $b_1 p_1 \equiv 1 \pmod{q_1}$  and  $0 < -b_1 < q_1$ ; and  $b_0(p_0 - (t+1)q_0) \equiv 1 \pmod{q_0}$  and  $0 < -b_0 < q_0$ . And numbers  $a_0$  and  $a_1$  are defined by the property that the matrices have determinant  $-1$ . If  $q_i = 1$ , then we take  $b_i = 0$  and hence  $a_i = -1$ , for  $i = 0, 1$ .

Hence, again using Lemma 3.13 we find that the Euler number weights corresponding to the bamboo are given by the continued fraction expansion of

$$-\frac{q_1(p_0 - (t+1)q_0) + p_1b_0}{q_1a_0 + p_1b_0}.$$

In case the denominator is 0, this correspond to an empty bamboo or just an edge joining the two nodes.

Summarizing we already have a plumbing graph  $\Lambda$  of which we know:

- (1) The genus number for all vertices.
- (2) The Euler number of all the vertices in the bamboos.
- (3) The multiplicities at the nodes and the arrowheads.

Since we know the Euler numbers of the bamboos, the multiplicities everywhere and that the multiplicities at the nodes are non-zero, we can recover the Euler number weights of the nodes using Equation (4.18). Which completes all the information about the plumbing graph.

Note that this is a plumbing graph with arrows, so there is an associated closed graph manifold coming from forgetting the arrows. This is  $Y$  and the arrows correspond to the Waldhausen link  $L$ .

The multiplicities at the nodes together with the Euler number weights, determine a system of multiplicities on the whole graph. However, this information does not, in general, fully determine a horizontal fibration.

We also know the number of connected components of each periodic part. The only piece of information missing to recover the horizontal open book up to diffeomorphism, is the invariant defined in Section 4.3 *ii*). That is, we need to give an element on  $H_G^\vee(Y, L)$ . Let  $c$  be a cycle in  $H_G(Y, L)$ , pick a path  $p_c$  in  $\Gamma$  which is a lift of  $c$ . There exists a number  $k_c$  such that the image by  $\phi_\Gamma^{k_c}$  of end point of  $p_c$  is in the same connected component as the starting point of  $p_c$ . This is the missing invariant.

# *Bibliography*

- [A’C73] Norbert A’Campo. Sur la monodromie des singularités isolées d’hypersurfaces complexes. *Invent. Math.*, 20:147–169, 1973.
- [A’C10] Norbert A’Campo. Tête-à-tête twists and geometric monodromy. Preprint, 2010.
- [BK86] Egbert Brieskorn and Horst Knörrer. *Plane algebraic curves*. Modern Birkhäuser Classics. Birkhäuser/Springer Basel AG, Basel, 1986. Translated from the German original by John Stillwell, [2012] reprint of the 1986 edition.
- [CB88] Andrew J. Casson and Steven A. Bleiler. *Automorphisms of surfaces after Nielsen and Thurston*, volume 9 of *London Mathematical Society Student Texts*. Cambridge University Press, Cambridge, 1988.
- [EN85] David Eisenbud and Walter D. Neumann. *Three-dimensional link theory and invariants of plane curve singularities.*, volume 110 of *Annals of Mathematics Studies*. Princeton University Press, 1985.
- [Eps72] D. B. A. Epstein. Periodic flows on three-manifolds. *Ann. of Math. (2)*, 95:66–82, 1972.
- [FM12] Benson Farb and Dan Margalit. *A primer on mapping class groups*, volume 49 of *Princeton Mathematical Series*. Princeton University Press, Princeton, NJ, 2012.
- [FPP17] J. Fernandez de Bobadilla, M. P. Pereira, and P. Portilla Cuadrado. Representation of surface homeomorphisms by tête-à-tête graphs. *ArXiv e-prints*, June 2017.
- [Gra15] Christian Graf. Tête-à-tête twists: Periodic mapping classes as graphs. Jul 2015.
- [Hat07] Allen Hatcher. Notes on basic 3-manifold topology, 2007.
- [HKM07] Ko Honda, William H. Kazez, and Gordana Matić. Right-veering diffeomorphisms of compact surfaces with boundary. *Invent. Math.*, 169(2):427–449, 2007.
- [HNK71] F. Hirzebruch, W. D. Neumann, and S. S. Koh. *Differentiable manifolds and quadratic forms*. Marcel Dekker, Inc., New York, 1971. Appendix II by W. Scharlau, Lecture Notes in Pure and Applied Mathematics, Vol. 4.
- [JN83] Mark Jankins and Walter D. Neumann. *Lectures on Seifert manifolds*, volume 2 of *Brandeis Lecture Notes*. Brandeis University, Waltham, MA, 1983.



- [Lau71] Henry B. Laufer. *Normal two-dimensional singularities*. Princeton University Press, Princeton, N.J.; University of Tokyo Press, Tokyo, 1971. Annals of Mathematics Studies, No. 71.
- [LDuT77] Lê Dũng Tráng. Some remarks on relative monodromy. pages 397–403, 1977.
- [LP05] Ignacio Luengo and Anne Pichon. Lê’s conjecture for cyclic covers. In *Singularités Franco-Japonaises*, volume 10 of *Sémin. Congr.*, pages 163–190. Soc. Math. France, Paris, 2005.
- [Mil68] John Milnor. *Singular points of complex hypersurfaces*. Annals of Mathematics Studies, No. 61. Princeton University Press, Princeton, N.J.; University of Tokyo Press, Tokyo, 1968.
- [MM11] Yukio Matsumoto and José María Montesinos-Amilibia. *Pseudo-periodic maps and degeneration of Riemann surfaces*, volume 2030 of *Lecture Notes in Mathematics*. Springer, Heidelberg, 2011.
- [N99] A. Némethi. Five lectures on normal surface singularities. In *Low dimensional topology (Eger, 1996/Budapest, 1998)*, volume 8 of *Bolyai Soc. Math. Stud.*, pages 269–351. János Bolyai Math. Soc., Budapest, 1999. With the assistance of Ágnes Szilárd and Sándor Kovács.
- [Ném00] András Némethi. Resolution graphs of some surface singularities. I: Cyclic coverings. In *Singularities in algebraic and analytic geometry.*, pages 89–128. Providence, RI: American Mathematical Society (AMS), 2000.
- [Neu81] Walter D. Neumann. A calculus for plumbing applied to the topology of complex surface singularities and degenerating complex curves. *Trans. Amer. Math. Soc.*, 268(2):299–344, 1981.
- [Neu97] Walter D. Neumann. Commensurability and virtual fibration for graph manifolds. *Topology*, 36(2):355–378, 1997.
- [Nie43] Jakob Nielsen. Abbildungsklassen endlicher Ordnung. *Acta Math.*, 75:23–115, 1943.
- [NP07] Walter D. Neumann and Anne Pichon. Complex analytic realization of links. In *Intelligence of low dimensional topology 2006, Hiroshima, Japan July 22–26, 2006*, pages 231–238. Hackensack, NJ: World Scientific, 2007.
- [NR78] Walter D. Neumann and Frank Raymond. Seifert manifolds, plumbing,  $\mu$ -invariant and orientation reversing maps. In *Algebraic and geometric topology (Proc. Sympos., Univ. California, Santa Barbara, Calif., 1977)*, volume 664 of *Lecture Notes in Math.*, pages 163–196. Springer, Berlin, 1978.
- [Ped09] Helge Moller Pedersen. *Splice diagrams. Singularity links and universal abelian covers*. ProQuest LLC, Ann Arbor, MI, 2009. Thesis (Ph.D.)–Columbia University.
- [Pic01] Anne Pichon. Fibrations sur le cercle et surfaces complexes. *Ann. Inst. Fourier (Grenoble)*, 51(2):337–374, 2001.
- [Por17] P. Portilla Cuadrado. General tête-à-tête graphs and Seifert manifolds. *ArXiv e-prints*, December 2017.
- [PS17] P. Portilla Cuadrado and B. Sigurdsson. Mixed tête-à-tête twists as monodromies associated with holomorphic function germs. *ArXiv e-prints*, December 2017.

- [RS77] Frank Raymond and Leonard L. Scott. Failure of Nielsen's theorem in higher dimensions. *Arch. Math. (Basel)*, 29(6):643–654, 1977.
- [Wal67] F. Waldhausen. Eine Klasse von 3-dimensionalen Mannigfaltigkeiten. I, II. *Invent. Math.*, 3:308–333, 1967.



# Appendices



## Appendix A

---

# Mixed tête-à-tête structures on filtered metric ribbon graphs

Given a filtered metric ribbon graph  $\Gamma^\bullet$  (with some *regularity* condition) we give a complete description in Proposition A.22 of all the possible  $\delta_\bullet$  functions that make it a mixed tête-à-tête graph  $(\Gamma^\bullet, \delta_\bullet)$ . For that, we will define a computable number, the  $\tau$  number, that codifies the obstruction to extend a homeomorphism on  $\Sigma_\Gamma^{i+1}$  to  $\Sigma_{\Gamma^{i+2}}$  to the next level of the filtration. The appendix ends with an example of a filtered metric ribbon graph of depth 1 in which we apply this result.

We start studying all the possible  $\ell$ -tête-à-tête structures for a ribbon graph. From now on, we only consider metric ribbon graphs where the length of each edge is in  $\pi\mathbb{Q}_+$  where  $\mathbb{Q}_+$  denotes the positive rational numbers. This does not restrict us in the set of elements in  $\text{MCG}^+(\Sigma, \partial\Sigma)$  that we can model since by the proof of Theorem 7.18 and by the proof of Theorem 10.7, we can always get that the lengths of the edges of the constructed graphs lie in  $\pi\mathbb{Q}_+$ .

We fix a natural notion of isomorphism between two metric ribbon graphs.

**Definition A.1.** *Let  $\Gamma$  and  $\Gamma'$  be two metric ribbon graphs. We say that  $\Gamma$  and  $\Gamma'$  are isomorphic as metric ribbon graphs if there exists a map  $f : \Gamma \rightarrow \Gamma'$  such that*

- i)  $f$  is an isometry.*
- ii)  $f$  preserves the cyclic order at each vertex.*

*Similarly, given two relative metric ribbon graphs  $(\Gamma, A)$  and  $(\Gamma', A')$  we say that they are isomorphic as relative metric ribbon graphs if there exists a map  $f : \Gamma \rightarrow \Gamma'$  such that i) and ii) hold plus*

- iii)  $f(A) = A'$ .*

Clearly not every metric ribbon graph is a pure  $\pi$ -tête-à-tête graph.

**Definition A.2.** *Let  $\Gamma$  be a metric ribbon graph. We define  $\pi_\Gamma$  as the smallest number in  $\pi\mathbb{Q}_+$  such that  $\Gamma$  satisfies the  $\pi_\Gamma$ -tête-à-tête property.*

**Lemma A.3.** *The number  $\pi_\Gamma$  is well defined for every metric ribbon graph  $\Gamma$ .*

*Proof.* We prove that the set

$$\mathcal{R} := \{r \in \pi\mathbb{Q}_+ : \Gamma \text{ is a tête-à-tête graph for safe walks of length } r\}$$

is nonempty and discrete.

Let  $\tilde{\Gamma} = \{\tilde{\Gamma}_1, \dots, \tilde{\Gamma}_s\}$  be the set of boundary components in  $\Sigma_\Gamma$  that come from cutting  $\Sigma$  (the thickening of  $\Gamma$ ) along  $\Gamma$ . And let  $l(\tilde{\Gamma}_i)$  be the length of  $\tilde{\Gamma}_i$  for  $i = 1, \dots, s$ . Since  $l(\tilde{\Gamma}_i) \in \pi\mathbb{Q}_+$ , we find that  $l(\tilde{\Gamma}_i)/\pi = p_i/q_i$ . The number

$$r := \text{lcm}(p_1, \dots, p_s) \cdot \pi$$

is clearly in  $\mathcal{R}$  and the homeomorphism that it induces is the identity on the graph. So the set is nonempty.

The set is discrete: take  $m(\Gamma) = \min_{e \in e(\Gamma)} l(e)$ . Clearly, if  $r \in \mathcal{R}$ , no number  $x$  with  $|x - r| < m(\Gamma)/2$  can be in  $\mathcal{R}$ .

Note that  $\mathcal{R}$  is bounded below by 0, so its minimum exists and, by definition, coincides with  $\pi_\Gamma$ .  $\square$

Let  $\Gamma$  be tête-à-tête graph for safe walks of length  $r$  and  $\Sigma$  its thickening. Let  $\tilde{\Gamma} = \{\tilde{\Gamma}_1, \dots, \tilde{\Gamma}_b\}$  be the collection of boundary components of  $\Sigma_\Gamma$  that come from cutting along  $\Gamma$ . Recall Notation 1.11. Denote by  $\phi_\Gamma$  the tête-à-tête map that fixes the boundary pointwise (for some choice of retraction lines) and by  $\tilde{\phi}_\Gamma$  the homeomorphism induced on  $\Sigma_\Gamma$ .

**Remark A.4** (Remark on orientation conventions.). In these two appendices we always orient the connected components of  $\tilde{\Gamma}$  with the opposite orientation to the one that they inherit as boundary of  $\Sigma_\Gamma$ . That is, whenever we are computing a rotation number, we put the orientation given by the direction that a relative safe walk would take on this component.

Let  $t \in \mathbb{Q}_+$ . Denote by  $t\Gamma$  the metric ribbon graph resulting from multiplying the lengths of every edge in  $\Gamma$  by  $t$ .

In the next lemma we list some easy properties derived from the definitions in this section.

**Lemma A.5.** *Suppose that  $\Gamma$  is a  $r$ -tête-à-tête graph. The following properties hold:*

- (1)  $r/l(\tilde{\Gamma}_i) = \text{rot}(\tilde{\phi}_\Gamma|_{\tilde{\Gamma}_i}) + m$  with  $m \in \mathbb{N} \cup \{0\}$ .
- (2) If  $\Gamma$  is also a tête-à-tête graph for safe walks of length  $R$ , then it is a tête-à-tête graph for safe walks of length  $|mR + nr|$  for any  $m, n \in \mathbb{Z}$ .
- (3) There exists a natural number  $m \in \mathbb{N}$  such that  $r = m\pi_\Gamma$ .
- (4)  $t \cdot \pi_\Gamma = \pi_{t\Gamma}$
- (5)  $\frac{\pi}{\pi_\Gamma} \cdot \Gamma$  is a pure  $\pi$ -tête-à-tête graph.
- (6) Suppose now that  $\Sigma$  has only one boundary component. Let  $f : \Gamma \rightarrow \Gamma$  be any isomorphism of  $\Gamma$  and  $\tilde{f} : \tilde{\Gamma} \rightarrow \tilde{\Gamma}$  the induced map. Then there exists  $m \in \mathbb{N}$  such that

$$\text{rot}(\tilde{f}|_{\tilde{\Gamma}}) \cdot l(\tilde{\Gamma}) = m\pi_\Gamma$$

*Proof.* (1), (2) and (4) are direct consequences from their respective definitions. (5) is a direct application of (4).

For (3) we use (2): If  $r = \pi_\Gamma$ , then  $m = 1$  and we have finished. Suppose that  $r > \pi_\Gamma$ . Then  $\Gamma$  satisfies the tête-à-tête property for safe walks of length  $r_1 := r - \pi_\Gamma$ . In general, define  $r_k := r_{k-1} - \pi_\Gamma$ . At each step we have that  $r_j < r_{j-1}$ . By definition it can never happen that  $0 < r_j < \pi_\Gamma$  so there exists  $m$  such that  $r_m = 0$ . Then  $r = m\pi_\Gamma$ .

Now we prove (6). Suppose that  $\text{rot}(\tilde{f}|_{\tilde{\Gamma}}) = p/q$ . Then  $\Gamma$  is a tête-à-tête graph for safe walks of length  $\frac{p}{q} \cdot l(\tilde{\Gamma})$ . Conclude by (3).  $\square$

And as a consequence:

**Corollary A.6.** *Every ribbon graph admits a metric that makes it a  $\pi$ -tête-à-tête graph.*

Observe that the metric given by the Corollary above might give a mapping class that is the identity in  $\text{MCG}^+(\Sigma)$ , however it is never the identity in  $\text{MCG}^+(\Sigma, \partial\Sigma)$ .

## A.1 The $\tau$ number.

**Remark A.7.** Let  $a, b \in \mathbb{R}$  with  $b > 0$ . We denote by  $a \bmod b$  the only number in  $[0, b)$  which is congruent with  $a$  modulo integer multiples of  $b$ . For example, with Definition 2.15 of rotation number we have

$$\text{rot}(f \circ g) \bmod 1 = (\text{rot}(f) + \text{rot}(g)) \bmod 1$$

and

$$(-\text{rot}(f)) \bmod 1 = (\text{rot}(f^{-1})) \bmod 1.$$

**Definition A.8.** Let  $\Gamma$  be a metric ribbon graph and let  $\Sigma$  be its thickening. Suppose that  $\Sigma$  has only 1 boundary component. Let  $\tilde{\Gamma}$  be the boundary component in  $\Sigma_{\tilde{\Gamma}}$  that comes from cutting along  $\Gamma$ . Let  $\tilde{f} : \tilde{\Gamma} \rightarrow \tilde{\Gamma}$  be an orientation preserving periodic isometry. We define the number

$$\tau(\tilde{f}, \Gamma) := \left( -\text{rot}(\tilde{f}) \cdot l(\tilde{\Gamma}) \right) \bmod \pi_\Gamma$$

and we call it the tau number of  $\tilde{f}$  with respect to  $\Gamma$ .

Note that if  $\tilde{f}$  and  $\tilde{g}$  are both orientation preserving periodic isometries of  $\tilde{\Gamma} \approx \mathbb{S}^1$ , by Remark A.7 we have that

$$\tau(\tilde{g} \circ \tilde{f}, \Gamma) - \tau(\tilde{f}, \Gamma) - \tau(\tilde{g}, \Gamma) \in \pi_\Gamma \cdot \mathbb{Z} \tag{A.9}$$

**Lemma A.10.** Let  $\Gamma$  be a metric ribbon graph and let  $\Sigma$  be its thickening. Suppose that  $\Sigma$  has only 1 boundary component. Let  $\tilde{\Gamma}$  be the boundary component in  $\Sigma_\Gamma$  that comes from cutting along  $\Gamma$ . Let  $\tilde{f} : \tilde{\Gamma} \rightarrow \tilde{\Gamma}$  be an orientation preserving periodic isometry. Then  $\tilde{f}$  is compatible with the gluing  $g_\Gamma$  if and only if

$$\tau(\tilde{f}, \Gamma) = 0.$$

Moreover, the homeomorphism

$$\tilde{f}' := \mathcal{D}_{\tau(\tilde{f}, \Gamma)}(\tilde{\Gamma}) \circ \tilde{f} : (\Sigma)_\Gamma \rightarrow (\Sigma)_\Gamma$$

is compatible with the gluing  $g_\Gamma$ .



*Proof.* If  $\tau(\tilde{f}, \Gamma) = 0$ , then  $-\text{rot}(\tilde{f}) \cdot l(\tilde{\Gamma}) = m\pi_\Gamma$  for some  $m \in \mathbb{Z}$ . Since  $\text{rot}(\tilde{f}) > 0$  we find that  $m < 0$ . By definition of  $\pi_\Gamma$ , we have that  $\Gamma$  is a tête-à-tête graph for safe walks of length  $-m\pi_\Gamma$  and we conclude that  $f$  is compatible with the gluing  $g_\Gamma$ .

Suppose now that  $\tilde{f}$  is compatible with the gluing. This means that it induces an isomorphism  $f$  of  $\Gamma$ . So by (Lemma A.5 (6)) we have that  $-\text{rot}(\tilde{f}) \cdot l(\tilde{\Gamma}) = m\pi_\Gamma$  for some  $m \in \mathbb{Z}$  and hence  $\tau(\tilde{f}, \Gamma) = 0$ .

For the second part, just observe that by (eq. (A.9)) we find that  $\tau(\tilde{f}', \Gamma) = 0$ .  $\square$

As a consequence, we find that if  $\tilde{f}$  and  $\tilde{g}$  are both orientation preserving periodic isometries of  $\tilde{\Gamma}$ , and  $\tilde{g}$  is compatible with the gluing, then

$$\tau(\tilde{g} \circ \tilde{f}, \tilde{\Gamma}) = \tau(\tilde{f}, \tilde{\Gamma}) \quad \text{and} \quad \tau(\tilde{f} \circ \tilde{g}, \tilde{\Gamma}) = \tau(\tilde{f}, \tilde{\Gamma}). \quad (\text{A.11})$$

Then, the following definition makes sense:

**Definition A.12.** Let  $\Gamma_1$  and  $\Gamma_2$  be two isomorphic metric ribbon graphs whose thickenings have 1 boundary component. Let  $\tilde{\phi} : \tilde{\Gamma}_1 \rightarrow \tilde{\Gamma}_2$  be an orientation preserving isometry such that there exists at least one isomorphism  $g : \Gamma_2 \rightarrow \Gamma_1$  with  $\tilde{g} \circ \tilde{\phi}$  periodic. Then we define

$$\tau(\tilde{\phi}, \Gamma_2) := \tau(\tilde{g} \circ \tilde{\phi}, \Gamma_1)$$

To check it is well defined, one has only to see that given  $g$  and  $g'$  as in the definition, we find that  $\tilde{g}' \circ \tilde{g}^{-1}$  is a periodic isometry and apply (eq. (A.11)) to check

$$\tau(\tilde{g} \circ \tilde{\phi}, \Gamma_1) = \tau((\tilde{g}' \circ \tilde{g}^{-1}) \circ \tilde{g} \circ \tilde{\phi}, \Gamma_1) = \tau(\tilde{g}' \circ \tilde{\phi}, \Gamma_1).$$

The following corollary shows the setting in which we use the previously defined  $\tau$  number. It is the key part in the proof of Proposition A.22.

**Corollary A.13.** Let  $\Gamma_1$  and  $\Gamma_2$  be two isomorphic metric ribbon graphs whose thickenings have 1 boundary components. Let  $\tilde{\phi} : (\Sigma_1)_{\Gamma_1} \rightarrow (\Sigma_2)_{\Gamma_2}$  be an orientation preserving homeomorphism that restricts as an isometry  $\tilde{\phi}|_{\tilde{\Gamma}_1} : \tilde{\Gamma}_1 \rightarrow \tilde{\Gamma}_2$  and such that there exists at least one isomorphism  $g : \Gamma_2 \rightarrow \Gamma_1$  with  $\tilde{g} \circ \tilde{\phi}|_{\tilde{\Gamma}_1}$  periodic. Then  $\tilde{\phi}$  is compatible with the gluings  $g_{\Gamma_1}$  and  $g_{\Gamma_2}$  if and only if

$$\tau(\tilde{\phi}|_{\tilde{\Gamma}_1}, \Gamma_2) = 0. \quad (\text{A.14})$$

Moreover, the homeomorphism

$$\tilde{\phi}' := \mathcal{D}_{\tau(\tilde{\phi}|_{\tilde{\Gamma}_1}, \Gamma_2)}(\tilde{\Gamma}_1) \circ \tilde{\phi} : (\Sigma_1)_{\Gamma_1} \rightarrow (\Sigma_2)_{\Gamma_2}$$

is compatible with the gluings  $g_{\Gamma_1}$  and  $g_{\Gamma_2}$ .

*Proof.* If  $\tilde{\phi}|_{\tilde{\Gamma}_1}$  is compatible, then  $\tilde{g} \circ \tilde{\phi}|_{\tilde{\Gamma}_1}$  is compatible for any isomorphism  $g : \Gamma_2 \rightarrow \Gamma_1$ . Then by Lemma A.10, we have (eq. (A.14)).

Suppose now that (eq. (A.14)) holds, then there exists some isomorphism  $g : \Gamma_2 \rightarrow \Gamma_1$  with  $\tilde{g} \circ \tilde{\phi}|_{\tilde{\Gamma}_1}$  periodic such that  $\tilde{g} \circ \tilde{\phi}|_{\tilde{\Gamma}_1}$  is compatible with the gluing  $g_{\Gamma_1}$ . Let  $\phi_g : \Gamma_1 \rightarrow \Gamma_1$  be the induced mapping. Then it is clear that the lifting of  $g^{-1} \circ \phi_g$  coincides with  $\tilde{\phi}|_{\tilde{\Gamma}_1}$ . Then,  $\tilde{\phi}|_{\tilde{\Gamma}_1}$  induces a mapping from  $\Gamma_1$  to  $\Gamma_2$  and is compatible with both  $g_{\Gamma_1}$  and  $g_{\Gamma_2}$  as desired.

For the last statement, it is clear that  $\tau(\tilde{\phi}', \tilde{\Gamma}) = 0$  and then  $\tilde{\phi}'$  is compatible.  $\square$

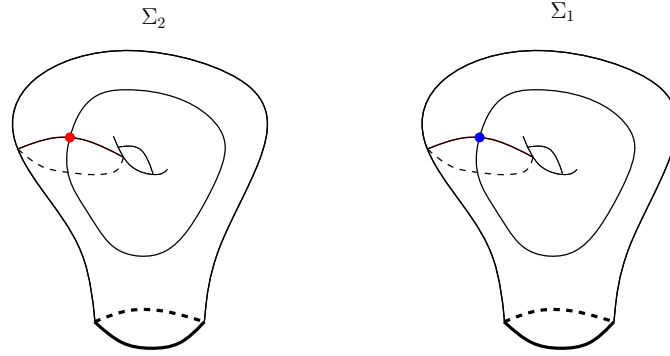


**Figure A.16:** We see two copies of  $\Sigma$  with an embedded metric ribbon graph. In one copy the only vertex is in red and in the other in blue.

We illustrate the use of these definitions and properties in the following example.

**Example A.15.** Let  $\Sigma$  be the one-holed torus which is the thickening of the depicted embedded graph in Figure A.16.

We set that the length of each edge is  $\pi$ . With this metric, the graph satisfies the pure  $\pi$ -tête-à-tête property and the induced homeomorphism has order 4 when restricted to the graph.

In the Figure A.17 is depicted the action of a homeomorphism  $\tilde{\phi} : (\Sigma)_\Gamma \rightarrow (\Sigma)_\Gamma$  which restricts as an isometry  $\tilde{\phi}|_{\tilde{\Gamma}} : \tilde{\Gamma} \rightarrow \tilde{\Gamma}$ .

We pick any isomorphism  $f : \Gamma \rightarrow \Gamma$ . For example, in the picture the induced map  $\tilde{f} : \tilde{\Gamma} \rightarrow \tilde{\Gamma}$  sends  $\hat{v}_i$  to  $v_i$  and is an isometry. The map  $\tilde{f} \circ \tilde{\phi}$  is a rotation with rotation number equal to  $7/12$ .

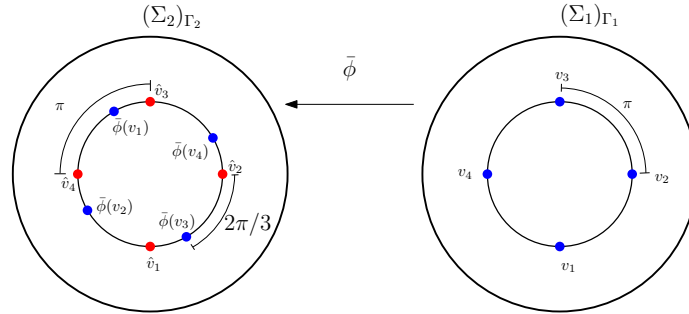


**Figure A.17:** In blue we see the four preimages (by the gluing  $g_\Gamma$ ) of the only vertex in  $\Gamma$ . On the left side of the figure we see in red the preimages of the vertex in  $\Gamma$  and in blue the images by  $\tilde{\phi}$  of the points in  $\tilde{\Gamma}$ .

Now we compute the corresponding tau number.

$$\tau(\tilde{\phi}|_{\tilde{\Gamma}}, \Gamma) = \left( -\frac{7}{12} \cdot 4\pi \pmod{\pi} \right) = \frac{2}{3}\pi$$

We observe also in the picture that  $\mathcal{D}_{2\pi/3} \circ \tilde{\phi}$  is compatible with the gluings.

**Remark A.18** (Relative tête-à-tête versions). Observe that for relative metric ribbon graphs there exists a version for each of the results and definitions in this section. Just substitute metric ribbon graph  $\Gamma$  for relative metric ribbon graph  $(\Gamma, A)$  in each statement.

We define the number defined in Definition A.2 for a relative metric ribbon graph  $(\Gamma, A)$  in the same way and we will denote it by  $\pi_\Gamma$ . It will always be clear from the context that  $\Gamma$  is a relative tête-à-tête graph without specifying the relative part.

For the statements in Lemma A.5 (6), Definition A.8 change the condition that imposes that  $\Sigma$  has only one boundary component and instead impose that  $\Sigma$  has only one boundary component apart from the boundary components in  $A$ .

## A.2 Mixed tête-à-tête structures on filtered metric ribbon graphs

Let  $\Gamma^\bullet$  be a filtration of depth  $d$  on a metric ribbon graph. We analyze which functions  $\delta_\bullet$  make it a mixed tête-à-tête graph.

We address this question in the case of a particular class of filtered metric ribbon graphs that satisfy a certain “regularity” condition.

**Definition A.19.** We say that a filtered metric ribbon graph  $\Gamma^\bullet$  of depth  $d$  is regular if for every  $i = 0, \dots, d$ , the graph  $\Gamma^i$  has the same number of connected components as  $\tilde{\Gamma}^i$ . We will say that  $(\Gamma^\bullet, \delta_\bullet)$  is a regular mixed tête-à-tête graph if it is a regular filtered metric ribbon graph that satisfies the mixed tête-à-tête property.

**Remark A.20.** We observe that a filtered metric ribbon graph  $\Gamma^\bullet$  of depth  $d$  is regular if and only if for every  $i = 0, \dots, d$  it happens that when we cut  $\Sigma$  along a connected component of  $\Gamma^i$  only one boundary component appears.

For example, the graph constructed in Example C.11 is regular. Also all the mixed tête-à-tête graphs corresponding with monodromies of irreducible plane branches in Chapter B.

For each  $\Gamma^i$  we enumerate its connected components  $\Gamma_1^i, \dots, \Gamma_{d_i}^i$ . We denote by  $(\Gamma_j^i)_{\Gamma^{i+1}}$  the result of cutting  $\Gamma_j^i$  along  $\Gamma^{i+1} \cap \Gamma_j^i$ . By regularity of the graph it makes sense the following notation for the connected components of  $\Gamma_{\Gamma^{i+1}}^i$

$$\{(\Gamma_1^i)_{\Gamma^{i+1}}, \dots, (\Gamma_{d_i}^i)_{\Gamma^{i+1}}\},$$

and if we denote by  $\tilde{\Gamma}_j^i$  the boundary component in  $\Gamma_{\Gamma^i}$  that comes from cutting along  $\Gamma_j^i$  we can write as well

$$\{\tilde{\Gamma}_1^i, \dots, \tilde{\Gamma}_{d_i}^i\}.$$

for the connected components of  $\tilde{\Gamma}^i$

**Definition A.21.** We say that a permutation of  $\mathcal{C}(\tilde{\Gamma}^i)$  given by a permutation  $\lambda$  on the indices  $\{1, \dots, d_i\}$  is admissible if

$$\left( (\Gamma_j^i)_{\Gamma^{i+1}}, \tilde{\Gamma}^{i+1} \cap (\Gamma_j^i)_{\Gamma^{i+1}} \right) \simeq \left( (\Gamma_{\lambda(j)}^i)_{\Gamma^{i+1}}, \tilde{\Gamma}^{i+1} \cap (\Gamma_{\lambda(j)}^i)_{\Gamma^{i+1}} \right)$$

for every  $j = 1, \dots, d_i$ . Where  $\simeq$  denotes isomorphism as relative metric ribbon graphs.

Let  $\Gamma^\bullet$  be a filtration of depth  $d$  on a metric ribbon graph. Let  $\hat{\delta}_\bullet$  be a set of functions such that  $(\Gamma_{\Gamma^i}^\bullet, (\tilde{\Gamma}^i)^\bullet, \hat{\delta}_\bullet)$  is a relative mixed tête-à-tête graph with relative mixed tête-à-tête map  $\phi_{\Gamma_{\Gamma^i}}$ . And let  $\lambda_i$  be the permutation induced on  $\{1, \dots, d_i\}$  by  $\phi_{\Gamma_{\Gamma^i}}|_{\tilde{\Gamma}^i}$ .

**Proposition A.22.** *We can extend the collection  $\hat{\delta}_\bullet$  to a collection of functions  $\delta_\bullet$  such that*

$$(\Gamma_{\Gamma^{i+1}}^\bullet, (\tilde{\Gamma}^{i+1})^\bullet, \delta_\bullet)$$

*is a relative mixed tête-à-tête graph if and only if  $\lambda_i$  is admissible.*

*Moreover, if  $\lambda_i$  is admissible then all the possible values of  $\delta_i$  for each connected component of  $\Gamma^i$  are*

$$\delta_i|_{(\Gamma_j^i)_{\Gamma^{i+1}}} = \tau \left( \phi_{\Gamma_{\Gamma^i}}|_{\tilde{\Gamma}_{\lambda_i^{-1}(j)}^i}, (\Gamma_j^i)_{\Gamma^{i+1}} \right) + n\pi_{(\Gamma_j^i)_{\Gamma^{i+1}}} \quad (\text{A.23})$$

*where  $\pi_{(\Gamma_j^i)_{\Gamma^{i+1}}}$  is the number in Definition A.2 (see also Remark A.18) of the relative metric ribbon graph  $((\Gamma_j^i)_{\Gamma^{i+1}}, \tilde{\Gamma}^{i+1} \cap (\Gamma_j^i)_{\Gamma^{i+1}})$  and  $n \in \mathbb{N}$ .*

*Proof.* Suppose that we can extend the collection  $\hat{\delta}_\bullet$  to a collection  $\delta_\bullet$  so that

$$(\Gamma_{\Gamma^{i+1}}^\bullet, (\tilde{\Gamma}^{i+1})^\bullet, \delta_\bullet)$$

is a relative mixed tête-à-tête graph. This means that  $\mathcal{D}_{\delta_i} \circ \phi_{\Gamma_{\Gamma^i}}$  is compatible with  $g_i$ , so in particular  $\lambda_i$  was admissible.

Suppose now that  $\lambda_i$  is admissible. In particular it means that  $\phi_{\Gamma_{\Gamma^i}}$  restricts as an isometry between  $\tilde{\Gamma}_j^i$  and  $\tilde{\Gamma}_{\lambda_i(j)}^i$  whose gluings by  $g_i$  are isomorphic relative metric ribbon graphs.

The first term of the right hand side of eq. (A.23)

$$\tau \left( \phi_{\Gamma_{\Gamma^i}}|_{\tilde{\Gamma}_{\lambda_i^{-1}(j)}^i}, (\Gamma_j^i)_{\Gamma^{i+1}} \right)$$

is the length of a boundary Dehn twist that makes the map

$$\mathcal{D}_{\tau(\phi_{\Gamma_{\Gamma^i}}|_{\tilde{\Gamma}_{\lambda_i^{-1}(j)}^i}, \Gamma_{\Gamma^{i+1}}^i)} \circ \phi_{\Gamma_{\Gamma^i}}$$

compatible with the gluing  $g_i$  (this follows from Corollary A.13).

The second term  $n\pi_{(\Gamma_j^i)_{\Gamma^{i+1}}}$  of the right hand side of equation eq. (A.23) tells us all the possible lengths of safe walks that make  $((\Gamma_j^i)_{\Gamma^{i+1}}, \tilde{\Gamma}^{i+1} \cap (\Gamma_j^i)_{\Gamma^{i+1}})$  a relative tête-à-tête graph (this follows from Lemma A.5 (6) and from the Definition A.2).

So we can conclude that equation eq. (A.23) describes all possible values of  $\delta_i|_{(\Gamma_j^i)_{\Gamma^{i+1}}}$  such that the map  $\mathcal{D}_{\delta_i|_{(\Gamma_j^i)_{\Gamma^{i+1}}}} \circ \phi_{i-1}$  is compatible with the gluings.  $\square$

We use the previous lemma to analyze the situation in Example C.51.

The following lemma tells us how to redistribute the  $\delta$  numbers on a regular mixed tête-à-tête graph.

**Lemma A.24.** *Let  $(\Gamma^\bullet, \delta_\bullet)$  be a regular mixed tête-à-tête graph which is a spine of a surface  $\Sigma$ . And let  $\phi_\Gamma : \Sigma \rightarrow \Sigma$  be a representative of the mixed tête-à-tête homeomorphism induced. Let  $\tilde{\Gamma}_{j,1}^i, \dots, \tilde{\Gamma}_{j,\alpha_j}^i$  be a collection of connected components of  $\tilde{\Gamma}^i$  cyclically exchanged by  $\phi_{\Gamma, i-1}$  and so,*

also by  $\tilde{\phi}_{\Gamma,i} = \mathcal{D}_{\delta_i} \circ \phi_{\Gamma,i-1}$ . Let  $\delta_{j,k}^i := \delta_i(g_i(\tilde{\Gamma}_{j,k}^i))$ . And let  $\delta'_{j,1}, \dots, \delta'_{j,1}$  be positive real numbers such that  $\sum_k \delta'_{j,k} = \sum_k \delta_{j,k}^i$ . Then there exists a mixed tête-à-tête graph  $(\Gamma^\bullet, \delta'_\bullet)$  of the same depth as  $\Gamma$  embedded in  $\Sigma$  such that:

- i) The graph  $\Gamma_{\Gamma^i}$  is isometric to  $\Gamma'_{\Gamma^i}$ .
- ii) The graph  $\Gamma^i$  is isometric to  $\Gamma'^i$ .
- iii) The functions  $\delta'_\bullet$  all coincide with the functions  $\delta_\bullet$  except that  $\delta'_{j,k}|_{\Gamma'^i} = \delta'_{j,k}$  for all  $k = 1, \dots, \alpha_j$ .
- iv)  $[\phi_\Gamma]_{\partial^1 \Sigma} = [\phi_{\Gamma'}]_{\partial^1 \Sigma}$ .

Observe that i) and ii) in particular give an bijection of the connected components of each level of the filtration so iii) makes sense.

*Proof.* By definition

$$\mathcal{D}_{\delta_i} = \mathcal{D}_{\delta_{j,\alpha_j}^i} \circ \dots \circ \mathcal{D}_{\delta_{j,1}^i}$$

where each boundary Dehn twist is around the corresponding boundary component.

Define  $r_1 := \delta'_{j,1} - \delta_{j,1}^i \in \mathbb{R}$ . Now we define

$$\mathcal{D}'_{\delta_i} = \mathcal{D}_{\delta_{j,\alpha_j}^i} \circ \dots \circ \mathcal{D}_{\delta_{j,2}^i - r_1} \circ \mathcal{D}_{\delta_{j,1}^i}$$

that is, we take the same composition of boundary Dehn twists, modifying the first one and the second. The homeomorphism  $\mathcal{D}'_{\delta_i}$  is not necessarily compatible with the gluing

$$g_i : \Sigma_{\Gamma^i} \rightarrow \Sigma_{\Gamma^{i+1}}.$$

But it is compatible with the gluing

$$g'_i := g_i \circ \mathcal{D}_{r_1}(\tilde{\Gamma}_{j,2}^i) \circ \mathcal{D}_{r_1}^{-1}(\tilde{\Gamma}_{j,1}^i)$$

So we have a filtered metric ribbon graph  $\Gamma' := g_\ell \circ \dots \circ g_{i+1} \circ g'_i(\Gamma_{\Gamma^i})$  embedded in  $\Sigma$  that satisfies i) and ii) by construction. And if we take as  $\delta'$  functions for this new graph, the same functions as before but changing  $\delta_{j,1}^i$  for  $\delta'_{j,1}$  and  $\delta_{j,2}^i$  for  $\delta_{j,2}^i - r_1$ . Then  $(\Gamma^\bullet, \delta'_\bullet)$  is a mixed tête-à-tête graph satisfying iv). Well, we might have a problem: that  $\delta_{j,2}^i - r_1 < 0$ ; recall that our definition of mixed tête-à-tête graph only allows non-negative  $\delta$  functions. But if we iterate this construction e.g. now we modify the gluing and boundary Dehn twists on  $\tilde{\Gamma}_{j,2}^i$  and  $\tilde{\Gamma}_{j,3}^i$  and so on. After  $\alpha_j - 1$  iterations we get a mixed tête-à-tête graph  $\Gamma$  that satisfies i) – iv).  $\square$

## *Appendix B*

---

# *$\Lambda$ -blow up*

In this second appendix, we introduce the  $\Lambda$ -blow up operation, where  $\Lambda$  is a filtered metric ribbon graph  $\Lambda^\bullet$ . The  $\Lambda$ -blow up of a tête-à-tête graph  $\Gamma$  gives a filtered metric ribbon graph that is denoted by  $Bl_p(\Gamma, \Lambda, \epsilon)^\bullet$  where  $p$  is a vertex of  $\Gamma$  and  $\epsilon$  has to be properly chosen. In Lemma B.16 we find numbers  $\delta_\bullet$  such that, assuming  $\Lambda^\bullet$  has a mixed tête-à-tête structure, we find that  $(Bl_p(\Gamma, \Lambda, \epsilon)^\bullet, \Delta^\bullet)$  is a mixed tête-à-tête graph. In Section B.2 we use this to find a mixed tête-à-tête graph for the monodromy of a plane branch recursively from the Puiseux pairs. For that we use the description of the monodromy of [A'C73].

Loosely speaking, assume  $\phi : \Sigma \rightarrow \Sigma$  to be a periodic homeomorphism on a surface  $\Sigma$  of order  $n$  and  $\psi : H \rightarrow H$  a pseudo-periodic homeomorphism on a surface  $H$  with 1 boundary component, we can pick an orbit of  $\phi$ , cut disks around each point in the orbit and glue a copy of  $H$  to each of the new boundary components. Let  $S$  be the resulting surface. We will construct a pseudo-periodic homeomorphism  $\varphi$  on  $S$ . The homeomorphism  $\varphi$  will behave as  $\phi$  on the part of the surface that corresponds to  $\Sigma$  minus the disks, and  $\varphi^n$  will behave as  $\psi$  on each of the copies of  $H$  that we glued. We will define this operation in terms of metric ribbon graphs.

Let  $\Lambda$  and  $\Gamma$  be two metric ribbon graphs and let  $H$  and  $\Sigma$  be their respective thickenings. Suppose that  $\Gamma$  is a tête-à-tête graph for safe walks of length  $r$  and let  $\phi_\Gamma : \Gamma \rightarrow \Gamma$  be the induced tête-à-tête homeomorphism fixing the boundary pointwise as in Chapter 9. Suppose also that  $H$  has only 1 boundary component.

Since  $H$  has only 1 boundary component, we find that  $H_\Lambda$  is a cylinder that comes with a gluing map  $g_\Lambda : H_\Lambda \rightarrow H$ . Let  $\tilde{\Lambda}$  be the boundary component of  $H_\Lambda$  that comes from cutting along  $\Lambda$ . This boundary component has naturally a marked set of points  $M_{\tilde{\Lambda}} := g_\Lambda^{-1}(v(H))$  which are the preimage by  $g_\Lambda$  of the vertices in  $H$ . We call this set of points the *marking* induced by  $\Lambda$ . Let  $l(\tilde{\Lambda})$  be the length of  $\tilde{\Lambda}$ .

Let  $p \in \Gamma$  be a vertex of valency  $v(p)$  and let  $m(p) := \min_{e \in e(p)} l(e)$  where  $l(e)$  denotes the length of the edge  $e$ .

Suppose that the condition

$$l(\tilde{\Lambda}) < m(p)v(p) \tag{B.1}$$

holds. When this is the situation, we can define the  $\Lambda$ -Blow up as follows.

Let  $p^{\phi_\Gamma} := \{p_0, p_1, \dots, p_t\}$  be the orbit of an arbitrary point  $p \in \Gamma$  by  $\phi_\Gamma$ , with  $\phi_\Gamma^j(p) = p_j$  and the convention that  $\phi_\Gamma^0 = id$ . In this setting we can perform a blow-up of any length

$$\epsilon < m(p)/2 \tag{B.2}$$

in the sense of A'Campo (see Definition 6.13) at the vertex  $p$ . We denote the resulting relative tête-à-tête graph by  $(Bl_p(\Gamma, \epsilon), \mathcal{C})$ , where  $\mathcal{C} := \{C_0, \dots, C_t\}$  are the new boundary components coming from the blow-up. We denote by  $\phi_{Bl_p(\Gamma, \epsilon)}$  the induced relative tête-à-tête map on  $(Bl_p(\Gamma, \epsilon), \mathcal{C})$ .

We fix

$$\epsilon = l(\tilde{\Lambda})/2v(p) \tag{B.3}$$

which, by eq. (B.1), is strictly less than  $m(p)/2$  so condition eq. (B.2) is satisfied. In this way for each  $j = 0, \dots, t$  we find that

$$l(C_j) = 2\epsilon v(p) = l(\tilde{\Lambda}) \tag{B.4}$$

Since  $l(C_0) = l(\tilde{\Lambda})$ , we can pick an orientation preserving isometry

$$\psi : C_0 \rightarrow \tilde{\Lambda}$$

This gives us a way to close each  $C_j$ : we glue  $x, y \in C_j$  if

$$g_\Lambda \circ \psi \circ \phi_{Bl_p(\Gamma, \epsilon)}^{-j}(x) = g_\Lambda \circ \psi \circ \phi_{Bl_p(\Gamma, \epsilon)}^{-j}(y) \tag{B.5}$$

with the convention that  $\phi_{Bl_p(\Gamma, \epsilon)}^0 = id$ .

After gluing all the boundary components  $C_j$  we get a new metric ribbon graph that we denote by

$$Bl_p(\Gamma, \Lambda, \epsilon)$$

We say that it is a  $\Lambda$ -Blow up of length  $\epsilon$  at  $p \in \Gamma$  or just the  $\Lambda$ -blow up of  $\Gamma$  at  $p$ .

This construction defines as well a gluing map

$$\hat{g} : Bl_p(\Gamma, \epsilon) \rightarrow Bl_p(\Gamma, \Lambda, \epsilon) \tag{B.6}$$

that sends two or more points to the same point if equality eq. (B.5) holds for them.

We denote by  $M_i$  the marking on the boundary component  $C_i$ , that is

$$M_i := \phi_{Bl_p(\Gamma, \epsilon)}^j \circ \psi^{-1}(M_\Lambda) \tag{B.7}$$

Since  $H_\Lambda$  is a cylinder, we can extend  $\psi^{-1}$  to a homeomorphism  $\hat{\psi}^{-1}$  from  $H_\Lambda$  to a whole collar neighborhood  $\hat{H}_0$  of  $C_0$ . Let  $\hat{H}_i := \phi_{Bl_p(\Gamma, \epsilon)}^i(\hat{H}_0)$ . We denote by  $H_i$  the surface resulting from closing the cylinder  $\hat{H}_i$  according to eq. (B.5). We see that  $H_i$  is by construction homeomorphic to  $H$ . Hence the thickening  $S$  of  $Bl_p(\Gamma, \Lambda, \epsilon)$  is homeomorphic to removing a disc around each point in the orbit  $p^{\phi_\Gamma}$  and glue a copy of  $H$  along the boundary circle .

**Notation B.8.** For further reference, we denote by  $\rho_i : H \rightarrow H_i$  each of the homeomorphisms fixed above. Also see Figure B.10.

**Remark B.9.** Observe that once we have the metric ribbon graphs  $\Gamma$  and  $\Lambda$ , and the point  $p \in \Gamma$ , the number  $\epsilon$  is completely determined (by eq. (B.3)), yet we explicit it in the notation of the  $\Lambda$ -blow up.

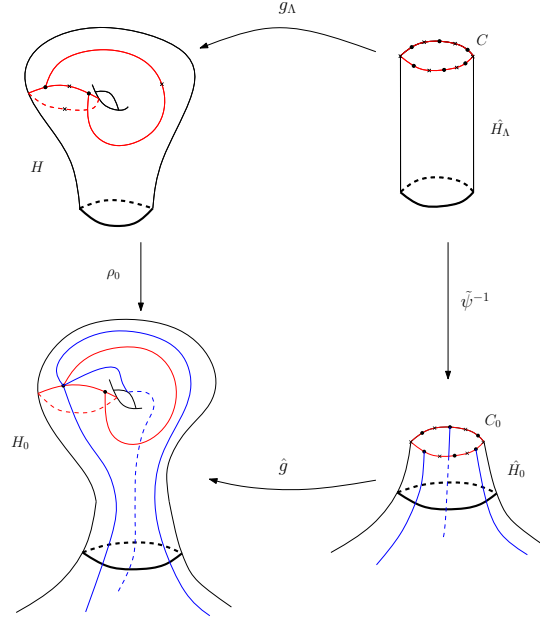


**Figure B.10:** We see what happens at one point of a  $K_{2,3}$ -Blow up on a graph  $\Gamma$ . In red the  $K_{2,3}$  tête-à-tête graph. In blue a part of  $\Gamma$ . On the lower-right part we can see the embedded cylinder that is denoted by  $\hat{H}_0$ . The marking  $M_0$  on  $C_0$  tell us how to close this cylinder to get a surface homeomorphic to  $H$ .

**Remark B.11.** If  $\Lambda$  is a filtered metric ribbon graph of depth  $\ell$ , the construction of the  $\Lambda$ -blow up naturally induces a filtration on  $Bl_p(\Gamma, \Lambda, \epsilon)$  of depth  $\ell + 1$ . Where the level 0 of the filtration is the whole graph and the level  $i$  of the filtration corresponds to the level  $i - 1$  of the copies of  $\Lambda$ .

**Notation B.12.** We introduce the notation for the pieces of each level of the filtration  $Bl_p(\Gamma, \Lambda, \epsilon)^\bullet$  in the case  $\Lambda^\bullet$  is a regular filtered metric ribbon graph.

We identify  $\Lambda$  with  $\hat{g}(C_0)$  (remember that  $\tilde{\Lambda}$  was identified with  $C_0$  by the isometry  $\psi$ ). Now we give a name to the corresponding parts of the filtration by

$$(Bl_p(\Gamma, \Lambda, \epsilon)_{j,k}^{i+1})^0 := \Lambda_{j,k}^i \subset \hat{g}(C_0) \tag{B.13}$$

where for each  $i = 0, \dots, \ell$ , the index  $j$  runs along  $1, \dots, \beta_i$ , and for each  $j$ , the index  $k$  runs along  $1, \dots, \alpha_j$ . The superindex  $i + 1$  indicates the level of the filtration, and the shift in 1 compared to the right hand side of the expression corresponds to Remark B.11. The superindex 0 outside the parenthesis indicates that the corresponding piece is in  $\hat{g}(C_0)$ .

The relative tête-à-tête map  $\phi_{Bl_p(\Gamma, \epsilon)}$  induced by the relative tête-à-tête property of  $(Bl_p(\Gamma, \epsilon), \mathcal{C})$  for safe walks of length  $r$  induces a labelling of the rest of the connected components of each level  $Bl_p(\Gamma, \Lambda, \epsilon)^i$  for all  $i = 1, \dots, \ell + 1$  by taking the pieces that we have already named and setting for each  $s = 1, \dots, t$  the name

$$(Bl_p(\Gamma, \Lambda, \epsilon)_{j,k}^i)^s := \hat{g}(\phi_{Bl_p(\Gamma, \epsilon)}^s(\hat{g}^{-1}((Bl_p(\Gamma, \Lambda, \epsilon)_{j,k}^i)^0))) \tag{B.14}$$

Which is well defined by the construction of the  $\Lambda$ - blow up (see eq. (B.5)).

For each  $i = 0, \dots, \ell + 1$  we denote



$$Bl_p(\Gamma, \Lambda, \epsilon)^{i+1} := \left\{ (Bl_p(\Gamma, \Lambda, \epsilon)_{j,k}^{i+1})^s : s = \{0, \dots, t\} \text{ and } i, j, k \text{ are such that } \Lambda_{j,k}^i \subset \Lambda^i \right\} \quad (\text{B.15})$$

Observe that since  $\Gamma$  was connected,  $Bl_p(\Gamma, \Lambda, \epsilon)^0$  consists of one connected component which is the whole  $Bl_p(\Gamma, \Lambda, \epsilon)$ .

This notation gives a name to every connected component of every level of the filtration  $Bl_p(\Gamma, \Lambda, \epsilon)^\bullet$ .

Assuming  $(\Lambda^\bullet, \delta^\bullet)$  is a regular mixed tête-à-tête graph, we describe in the next lemma how to put a mixed tête-à-tête structure on  $Bl_p(\Gamma, \Lambda, \epsilon)^\bullet$ . We use the results from Chapter A.

**Lemma B.16.** *Let  $(\Lambda^\bullet, \delta^\bullet)$  be a regular mixed tête-à-tête graph whose filtration has depth  $\ell$  and suppose that the thickening  $H$  of  $\Lambda$  has one boundary component. Let  $\Gamma$  be a connected tête-à-tête graph for safe walks of length  $r$  and let  $p \in \Gamma$  be a point whose orbit has order  $t+1$ . Suppose that the condition eq. (B.1) is satisfied. Then there exists a collection of functions  $\Delta_\bullet$ , defined in equations eq. (B.18), eq. (B.19) and eq. (B.20) such that*

- (1)  $(Bl_p(\Gamma, \Lambda, \epsilon)^\bullet, \Delta_\bullet)$  is a mixed tête-à-tête graph of depth  $\ell+1$ .
- (2) We have the following equality of relative tête-à-tête homeomorphisms

$$\phi_{Bl_p(\Gamma, \Lambda, \epsilon), 0} = \phi_{Bl_p(\Gamma, \epsilon)}$$

where  $\phi_{Bl_p(\Gamma, \Lambda, \epsilon), 0}$  follows the notation of eq. (9.10) and we have identified the graph  $Bl_p(\Gamma, \Lambda, \epsilon)_{Bl_p(\Gamma, \Lambda, \epsilon)^1}$  with  $Bl_p(\Gamma, \epsilon)$  in the notation previous to this theorem.

- (3) For every  $q \in \Lambda$  we find that

$$\phi_{Bl_p(\Gamma, \Lambda, \epsilon)}^{t+1}(q) = \phi_\Lambda(q),$$

where  $\phi_{Bl_p(\Gamma, \Lambda, \epsilon)} : S \rightarrow S$  and  $\phi_\Lambda : H \rightarrow H$  be the associated mixed tête-à-tête homeomorphisms of the thickening  $S$  and  $H$  of  $Bl_p(\Gamma, \Lambda, \epsilon)$  and  $\Lambda$  respectively. Recall that we have an identification  $\rho_0 : H \rightarrow H_0$  (Notation B.8) which gives an inclusion  $\Lambda \hookrightarrow H_0 \subset S$ .

*Proof.* For practical purposes, since the expressions involved in the proof of this lemma are rather cumbersome, we will use the notation

$$\Omega := Bl_p(\Gamma, \Lambda, \epsilon)$$

to make them more legible. Also keep in mind Figure B.22. We denote by  $g_{\Omega, i} : \Omega_{\Omega^i} \rightarrow \Omega_{\Omega^{i+1}}$  and  $g_{\Lambda, i} : \Lambda_{\Lambda^i} \rightarrow \Lambda_{\Lambda^{i+1}}$  the gluing functions of the two filtered metric ribbon graphs involved in the lemma and  $\hat{g}_{\Omega, i} = g_{\Omega, \ell+1} \circ \dots \circ g_{\Omega, i}$  and equivalently for  $\hat{g}_{\Lambda, i}$ . For the rest, we are using Notation B.12. In particular, remember that  $\Lambda$  is identified with  $\hat{g}_\Omega(C_0)$ .

We also recall the labelling on the connected components of  $\Lambda^i$  induced by the mixed tête-à-tête structure  $(\Lambda^\bullet, \delta^\bullet)$

$$\Lambda_{1,1}^i, \dots, \Lambda_{1,\alpha_1}^i, \Lambda_{2,1}^i, \dots, \Lambda_{2,\alpha_2}^i, \dots, \Lambda_{\beta_i,1}^i, \dots, \Lambda_{\beta_i,\alpha_{\beta_i}}^i \quad (\text{B.17})$$

related with the orbit structure of  $\tilde{\phi}_{\Lambda, i-1}$ . By the regularity of  $\Lambda$  we find that  $\Lambda_{j,k}^i := g_{\Gamma_i}(\tilde{\Lambda}_{j,k}^i)$  is a whole connected component.

On the first part of the proof we define a collection of functions  $\Delta_\bullet$ . After that, we will prove that these functions make  $(\Omega^\bullet, \Delta_\bullet)$  a mixed tête-à-tête graph with property (2) of the statement.

To recover the homeomorphism induced on  $\Omega_{\Omega^1}$  by the relative tête-à-tête property of  $(Bl_p(\Gamma, \epsilon), \mathcal{C})$  for safe walks of length  $r$ , we set

$$\Delta_0(\Omega^0) := r$$

which proves (3).

We define

$$\Delta_{i+1}|_{(\Omega_{j,k}^{i+1})^0} := \delta_i|_{\Lambda_{j,k}^i} \quad (\text{B.18})$$

where for each  $i = 0, \dots, \ell$  the index  $j$  runs along  $j = 1, \dots, \beta_i$  and for each  $j$  the index  $k$  runs along  $k = 1, \dots, \alpha_j$ ; except for the index  $(i, j, k) = (0, 1, 1)$ .

We denote by  $(\tilde{\Omega}_{j,k}^i)^s$  the boundary component in  $\Omega_{\Omega^i}$  that comes from cutting along  $(\Omega_{j,k}^i)^s$ .

Consider the map

$$\phi_{Bl_p(\Gamma, \epsilon)}^{t+1}|_{(\tilde{\Omega}_{1,1}^1)^0} : (\tilde{\Omega}_{1,1}^1)^0 \rightarrow (\tilde{\Omega}_{1,1}^1)^0$$

and let  $rot(\phi_{Bl_p(\Gamma, \epsilon)}^{t+1}|_{(\tilde{\Omega}_{1,1}^1)^0})$  be its rotation number Definition 2.15 where we are orienting  $(\tilde{\Omega}_{1,1}^1)^0$  with the opposite direction as the one it inherits as boundary component.

Then we set

$$\Delta_1((\Omega_{1,1}^1)^0) := \begin{cases} \delta_0 - rot\left(\phi_{Bl_p(\Gamma, \epsilon)}^{t+1}|_{(\tilde{\Omega}_{1,1}^1)^0}\right) \cdot l((\tilde{\Omega}_{1,1}^1)^0) & \text{if it is positive} \\ \left(1 - rot\left(\phi_{Bl_p(\Gamma, \epsilon)}^{t+1}|_{(\tilde{\Omega}_{1,1}^1)^0}\right)\right) \cdot l((\tilde{\Omega}_{1,1}^1)^0) + \delta_0 & \text{otherwise.} \end{cases} \quad (\text{B.19})$$

Note that  $(\Omega_{1,1}^1)^0$  corresponds to the index  $(i, j, k) = (0, 1, 1)$  that we excluded before.

Finally, for all  $i, j, k$  and  $s = 1, \dots, t$ , we set the functions

$$\Delta_i((\Omega_{j,k}^i)^s) := 0 \quad (\text{B.20})$$

Now we have defined a value of  $\Delta_i$  for each connected component of  $\Omega^i$  for all  $i = 0, \dots, \ell + 1$ .

To prove the statements (1) and (2) of the lemma we will prove inductively the following statements for each  $i = 0, \dots, \ell + 1$ .

- a)  $(\Omega_{\Omega^{i+1}}^\bullet, (\tilde{\Omega}^{i+1})^\bullet, \Delta_\bullet)$  is a relative mixed tête-à-tête graph (whose relative mixed tête-à-tête map we will denote by  $\phi_{\Omega_{\Omega^{i+1}}}$ ). Note that it is of depth less than  $i + 1$ .
- b)

$$D_{\Delta_{i+1}} \circ \phi_{\Omega_{\Omega^{i+1}}}^{t+1}(p) = D_{\delta_i} \circ \phi_{\Lambda, i-1}(p)$$

for every  $p \in \tilde{\Lambda}^i \subset \Omega_{\Omega^{i+1}}$ .

Observe that the relative mixed tête-à-tête homeomorphism  $\phi_{\Omega_{\Omega^{n+1}}}$  coincides by construction with  $\phi_{\Omega, n}$  in the notation of (9.10). We will use this last observation throughout the proof.

First we note that that (1) on the statement follows from a) for  $i = \ell + 1$  since the set  $\Omega^{\ell+2}$  is empty and then a) means that  $(\Omega^\bullet, \Delta_\bullet)$  is a mixed tête-à-tête graph.

Statement (2) follows from statements b) for  $i = 1, \dots, \ell + 1$ . They mean that the homeomorphism  $\phi_{\Omega_{\Omega^{i+1}}}^{t+1}(p)$  is the map induced by the compatibility of  $D_{\Delta_i} \circ \phi_{\Omega_{\Omega^i}}^{t+1}$  with the gluing  $g_{\Omega, i}$  and that  $\phi_{\Lambda, i-1}$  is the map induced by the compatibility of  $D_{\delta_{i-1}} \circ \phi_{\Lambda, i-2}$ . Also observe that  $g_{\Omega, i}|_{(\tilde{\Omega}_{j,k}^i)^0} = g_{\Lambda, i-1}|_{\tilde{\Lambda}_{j,k}^{i-1}}$ .

In order to prove a) – b), we use the equivalence of Remark 9.9 and its notation.

Suppose  $i = 0$ .

Then  $a$ ) is automatic since  $(\Omega_{\Omega^1}, \tilde{\Omega}^1)$  is a relative tête-à-tête graph for safe walks of length  $\Delta_0(\Omega^0) = r$  by construction.

Now we prove  $b$ ).

On the right hand side of the expression we have

$$D_{\delta_0} \circ \phi_{\Lambda, -1} = D_{\delta_0}$$

which induces a rotation of length  $\delta_0$  on  $(\tilde{\Omega}_{1,1}^1)^0$ . On the left hand side of the equation we have

$$D_{\Delta_1} \circ \phi_{\Omega_{\Omega^1}}^{t+1}.$$

Observe that  $\phi_{\Omega_{\Omega^1}}^{t+1}|_{(\tilde{\Omega}_{1,1}^1)^0}$  induces a rotation of length  $rot(\phi_{\Omega_{\Omega^1}}^{t+1}|_{(\tilde{\Omega}_{1,1}^1)^0}) \cdot l((\tilde{\Omega}_{1,1}^1)^0)$  and recall eq. (B.19). Therefore, if

$$\delta_0 - rot(\phi_{\Omega_{\Omega^1}}^{t+1}|_{(\tilde{\Omega}_{1,1}^1)^0}) \cdot l((\tilde{\Omega}_{1,1}^1)^0)$$

is positive, then it satisfies the equality with the left hand side of the equation. If it is negative, the length of the rotation of  $\phi_{\Omega_{\Omega^1}}^{t+1}|_{(\tilde{\Omega}_{1,1}^1)^0}$  exceeds  $\delta_0$ . Since we want to use positive Dehn twists, we compose first with the positive Dehn twist of length  $(1 - rot(\phi_{\Omega_{\Omega^1}}^{t+1}|_{(\tilde{\Omega}_{1,1}^1)^0})) \cdot l((\tilde{\Omega}_{1,1}^1)^0)$  which completes 1 whole loop along  $(\tilde{\Omega}_{1,1}^1)^0$ . After that, we compose with the Dehn twist of length  $\delta_0$  and we also get the equality with the left hand side of the equation in  $b$ ).

Suppose that we know  $a$ ) and  $b$ ) for  $i = d$ . And let  $i = d + 1$ .

First we prove  $a$ ). By hypothesis of induction on  $a$ ), it is enough to prove that  $D_{\Delta_{d+1}} \circ \phi_{\Omega, d}$  is compatible with the gluing  $g_{\Omega, d+1}$ . On one hand, when  $s = 0, \dots, t-1$ , by definition of  $\Lambda$ -blow up, the values  $\Delta_{d+1}((\Omega_{j,d}^s)^s) = 0$  make the map compatible with  $g_{d+1}$ . When  $s = t$ , by definition of  $\Lambda$ -blow up, it is equivalent to prove the compatibility of  $D_{\Delta_{d+1}} \circ \phi_{\Omega, d}^{t+1}$ . But by hypothesis of induction on  $b$ ) we know that  $D_{\Delta_{d+1}} \circ \phi_{\Omega, d}^{t+1} = D_{\delta_d} \circ \phi_{\Lambda, d-1}$ . And the right hand side of the equation above is a map compatible with  $g_{\Omega, d+1} = g_{\Lambda, d}$  because  $(\Lambda^\bullet, \delta_\bullet)$  is a mixed tête-à-tête graph.

Now we prove  $b$ ). We have to prove

$$D_{\Delta_{d+2}} \circ \phi_{\Omega_{\Omega^{d+2}}}^{t+1}(p) = D_{\delta_{d+1}} \circ \phi_{\Lambda, d}(p)$$

for every  $p \in \tilde{\Lambda}^{d+1} \subset \Omega_{\Omega^{d+2}}$ . Observe that  $\phi_{\Omega_{\Omega^{d+2}}}^{t+1}$  is by definition the homeomorphism induced by the compatibility of  $D_{\Delta_{d+1}} \circ \phi_{\Omega_{\Omega^{d+1}}}^{t+1}$  with the gluing  $g_{\Omega, d+1}$ . And  $\phi_{\Lambda, d}$  is the homeomorphism induced by the compatibility of  $D_{\delta_d} \circ \phi_{\Lambda, d-1}$  with the gluing  $g_{\Lambda, d}$  but by hypothesis of induction we know that

$$D_{\Delta_{d+1}} \circ \phi_{\Omega_{\Omega^{d+1}}}^{t+1}(p) = D_{\delta_d} \circ \phi_{\Lambda, d-1}(p)$$

for all  $p \in \tilde{\Lambda}^d$ , and hence  $\phi_{\Lambda, d} = \phi_{\Omega_{\Omega^{d+2}}}^{t+1}$ . To finish the proof we just have to observe that by definition  $\Delta_{d+1}((\Omega_{j,k}^{d+1})^0) = \delta_d(\Lambda_{j,k}^d)$ . So  $b$ ) follows.  $\square$

**Remark B.21.** We observe that (2) of the lemma above implies that  $\phi_{Bl_p(\Gamma, \Lambda, \epsilon)}^{t+1}|_\Lambda$  is isotopic to  $\phi_\Lambda$  because their actions coincide on a spine of  $H$ .

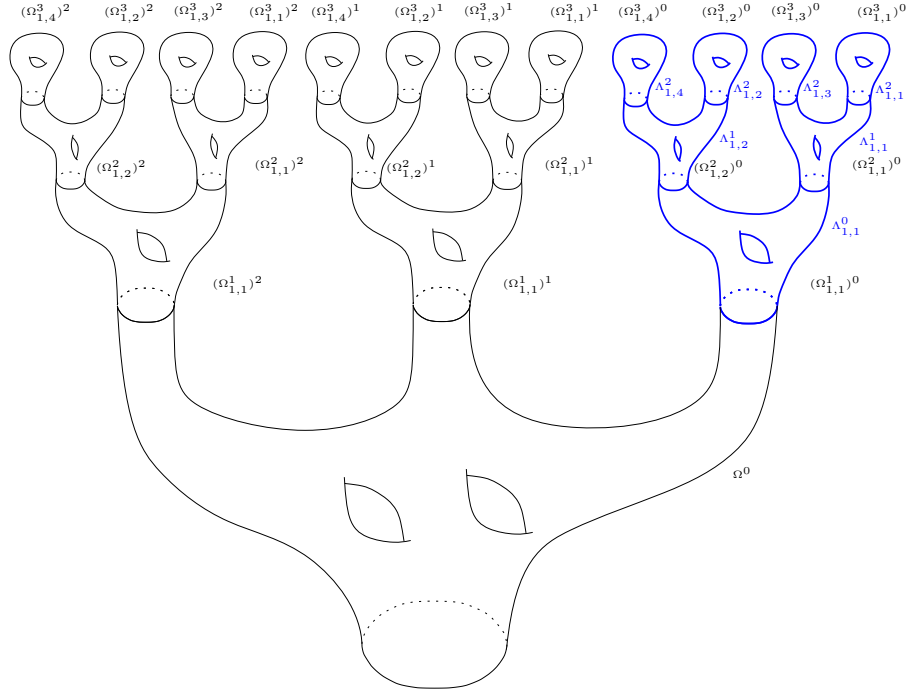


**Figure B.22:** An example of  $\Lambda$ -blow up. In this case  $t + 1 = 3$ , the depth of the filtration of  $\Lambda$  is 2 and hence, the depth of the filtration of  $\Omega$  is 3. As explained in Lemma B.16,  $\Lambda$  is identified with the closing of  $(\widetilde{\Omega}_{1,1}^1)^0$ , that is with  $H_0$  (in blue in the figure). Note that the labelling denotes the part of the graph whose thickening comprehends from the connected piece where the label is to the top of the figure. Using the notation of Lemma B.16, in this figure we have that  $\alpha_0 = 1$ ,  $\alpha_1 = 2$  and  $\alpha_2 = 3$ , also  $\hat{\alpha}_0 = 1$ ,  $\hat{\alpha}_1 = 3$ ,  $\hat{\alpha}_2 = 6$  and  $\hat{\alpha}_3 = 12$ ; and  $\beta_i = 1$  for all  $i = 0, 1, 2, 3$ .

## B.1 Brieskorn-Pham singularities

In this subsection, we outline a description given by A'Campo and discuss some properties of the bipartite complete graphs that model Milnor fibers of Brieskorn-Pham singularities. That is, we describe a model of the Milnor fiber of  $x^p + y^q$ . Consider two parallel vertical lines in  $\mathbb{R}^2$ , let  $L$  be the line on the left and  $R$  the line on the right. We mark  $p$  different points in  $L$  and  $q$  different points in  $R$ .

Consider the projection on the plane of the bipartite complete graph  $K_{p,q}$  resulting from taking the joint of the set of  $p$  points in one line with the set of  $q$  points in the other. If we give the cyclic orientation to the edges incident at each vertex induced by the orientation of the plane, the corresponding thickening is homeomorphic to the Milnor Fiber of the singularity  $x^p + y^q$ .

If we set that the length of each edge is  $\pi/2$ , this graph satisfies the  $\pi$ -tête-à-tête property. Let  $\phi$  be the corresponding tête-à-tête homeomorphism.

Let  $x_0$  be one of the  $p$  vertices of valency  $q$  and let  $x_i := \phi^i(x_0)$  for  $i = 1, \dots, p - 1$ ; similarly take one of the  $q$  vertices of valency  $p$ , denote it by  $y_0$  and denote  $y_i := \phi^i(y_0)$ .

Since  $\phi^p(x_0) = x_0$ , there exists a small disk  $D_0$  around  $x_0$  invariant by  $\phi^p$ . Take a point  $z_0$

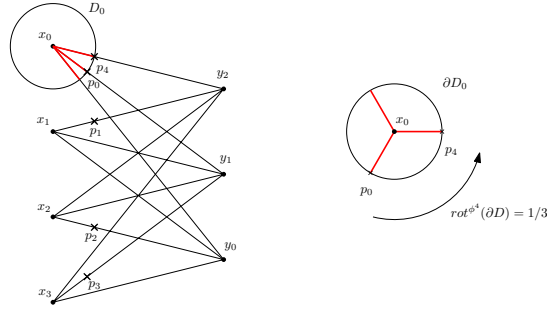


**Figure B.23:** We see a  $K_{3,4}$  graph with each edge of length  $\pi/2$ . If  $\phi$  is the tête-à-tête map, then the disk  $D$  is an invariant disk by the map  $\phi^4$ . The rotation number of  $\phi^4|_{\partial D}$  is  $\hat{p}/4$  where,  $\hat{p}$  is the smallest positive solution to  $\hat{p} \equiv 4 \pmod 3$ ; in this case  $\hat{p} = 3$ .

near  $x_0$  lying on the edge that joins  $x_0$  with  $y_i$ , then  $z_1 = \phi(z_0)$  will lie near  $x_1$  on the edge that joins  $x_1$  with  $y_{i+1}$ , where  $i + 1$  is taken  $\pmod q$  (see Figure B.23) and  $\phi^p(z_0)$  will lie in the line that joins  $x_0$  with  $y_{i+p}$  with  $i + p$  taken  $\pmod q$ . So  $\phi^p|_{\partial D_0}$  has a rotation number of

$$\hat{p}/q \tag{B.24}$$

where  $\hat{p}$  is the smallest positive natural number such that  $\hat{p} \equiv p \pmod q$ . Equivalently for a small disk around any  $y_i$ .

When  $\gcd(p, q) = 1$ , this surface has one boundary component, hence when we cut it along  $\widetilde{K}_{p,q}$  we get a cylinder. And the length of  $\widetilde{K}_{p,q} = 2pq\pi/2 = pq\pi$ . As noted in 7.9, a boundary Dehn twist of length  $\pi$  is compatible with the corresponding gluing. This Dehn twist has a rotation number on  $\widetilde{K}_{p,q}$  of

$$\frac{\pi}{pq\pi} = \frac{1}{pq} \tag{B.25}$$

## B.2 Mixed tête-à-tête graph for isolated plane curve singularities

Let  $f : (\mathbb{C}^2, 0) \rightarrow (\mathbb{C}, 0)$  be an isolated irreducible plane curve singularity and let

$$\hat{S} := \{(m_0, n_0), \dots, (m_a, n_a)\}$$

be its characteristic Puiseux pairs.

We start this Section building a mixed tête-à-tête graph  $(\Gamma(S)^\bullet, \Delta(S)_\bullet)$  using Lemma B.16 whose thickening is homeomorphic to the Milnor fiber of  $f = 0$ . In Proposition Proposition B.28 we prove that the induced homeomorphism is isotopic relative to the boundary to the monodromy of the Milnor fiber. This construction is inspired by the construction depicted in [A'C73] as we see in B.28.

Consider the associated sequence

$$S := \{(\lambda_0, n_0), \dots, (\lambda_a, n_a)\}$$

computed by setting  $\lambda_0 = m_0$  and

$$\lambda_{i+1} = m_{i+1} - m_n n_{i+1} + \lambda_i n_i n_{i+1}.$$

That is, the sequence of the Newton pairs of the singularity.

**Remark B.26.** It is known that the Puiseux pairs satisfy

1.  $\gcd(m_i, n_i) = 1$
2.  $m_i > n_i \cdot m_{i-1}$

and from there, it can be easily deduced that the Newton pairs satisfy

1.  $\gcd(\lambda_i, n_i) = 1$
2.  $\frac{1}{\lambda_i n_i} > \frac{n_{i+1}}{\lambda_{i+1}}$

We will use these properties.

Now we define inductively  $a + 1$  numbers. First, let  $l_a \in \pi\mathbb{Q}_+$  be any positive rational multiple of  $\pi$ . Suppose that we have already defined  $l_{a-s+1}$ . We define

$$l_{a-s} := \frac{1}{k_{a-s}} \frac{\lambda_{a-s+1} l_{a-s+1}}{\lambda_{a-s} n_{a-s}} \tag{B.27}$$

where  $k_{a-s}$  is any natural number greater than 2. We do this for  $s = 1, \dots, a$ .

Let  $K_{\lambda_i, n_i}$  be the complete bipartite graph of type  $(\lambda_i, n_i)$ . We set a metric by declaring that each edge of length  $l_i$ , then it satisfies the tête-à-tête property for safe walks of length  $2l_i$ . We denote the corresponding tête-à-tête map by  $\phi_{\lambda_i, n_i}$ .

We define  $\hat{\Gamma}^a := K_{\lambda_0, n_0}$ . Now we consider the  $n_1$  vertices of valency  $\lambda_1$  in  $K_{\lambda_1, n_1}$  which form an orbit by  $\phi_{\lambda_1, n_1}$  and perform a  $\hat{\Gamma}^a$ -blow up of length  $\epsilon_0 = \frac{\lambda_0 n_0 l_0}{\lambda_1}$  on that orbit. That is

$$Bl_v(K_{\lambda_1, n_1}, \hat{\Gamma}^a, \epsilon_0)$$

that we denote by  $\hat{\Gamma}^{a-1}$ . According to the definition of  $\Lambda$ -blow up we need to check a couple of things so that the above expression makes sense.

First we check that that

$$\epsilon_0 < \frac{l_1}{2}.$$

Indeed,

$$\epsilon_0 = \frac{\lambda_0 n_0 l_0}{\lambda_1} = \left( \frac{\lambda_0 n_0}{\lambda_1} \right) \left( \frac{\lambda_1 l_1}{k_0 \lambda_0 n_0} \right) = \frac{l_1}{k_0} < \frac{l_1}{2}$$

so eq. (B.2) holds and it makes sense to consider a blow-up of length  $\epsilon_0$  in the sense of A'Campo.

Secondly we have to check that eq. (B.4) holds. That is, that the length of  $\widetilde{\Gamma}^a$  coincides with the length of each new boundary component in the graph  $Bl_v(K_{\lambda_1, n_1}, \epsilon_0)$ . The length of  $\widetilde{\Gamma}^a$  is just  $2\lambda_0 n_0 l_0$ . And the length of each boundary component of  $Bl_v(K_{\lambda_1, n_1}, \epsilon_0)$  in the graph

$$2\lambda_1 \epsilon_0 = 2\lambda_1 \frac{\lambda_0 n_0 l_0}{\lambda_1} = 2\lambda_0 n_0 l_0$$

so eq. (B.4) holds and it makes sense to consider the  $\hat{\Gamma}^a$ -blow up of length  $\epsilon_0$ .

We denote by  $C_1^1, \dots, C_{n_1}^1$  the boundary components in  $Bl_v(K_{\lambda_1, n_1}, \epsilon_0)$  coming from the blow up. We observe that by eq. (B.24) and using that  $n_1 < \lambda_1$

$$rot(\tilde{\phi}_{\lambda_1, n_1}^{n_1} |_{C_1^1}) = \frac{n_1}{\lambda_1}$$

where  $\tilde{\phi}_{\lambda_1, n_1}$  is the relative tête-à-tête map of  $Bl_v(K_{\lambda_1, n_1}, \epsilon_0)$ .

Using the notation introduced in Lemma B.16, we observe that in this first step  $\Lambda$  is a tête-à-tête graph for safe walks of length  $2l_0$  (which is a special case of a regular mixed tête-à-tête graph with filtration of depth 0) and  $\Gamma$  is a tête-à-tête graph of length  $2l_1$ .

We apply the method used in that lemma to put a mixed tête-à-tête structure on  $\Omega := Bl_v(K_{\lambda_1, n_1}, \hat{\Gamma}^a, \epsilon_0)$ . We set:

- $\Delta_0^1 := 2l_1$
- $\Delta_1^1((\Omega_{1,1}^1)^0) := 2l_0 - \frac{n_1}{\lambda_1} 2\lambda_0 n_0 l_0$  which corresponds to eq. (B.19). We also note that this number equals  $\left(\frac{1}{\lambda_0 n_0} - \frac{n_1}{\lambda_1}\right) 2\lambda_0 n_0 l_0$ . This will be useful for Proposition B.28.
- $\Delta_1^1((\Omega_{1,k}^1)^t) := 0$  for the rest of  $k, t$ .

The upper index 1 indicates that this is the first step of the induction. Now, for  $1 \leq s \leq a$  we proceed similarly as in the first case and define by recursion

$$\hat{\Gamma}^{a-s} := Bl_v(K_{\lambda_s, n_s}, \hat{\Gamma}^{a-s+1}, \epsilon_{s-1})$$

where  $v$  is any of the  $n_s$  vertices of valency  $\lambda_s$  and

$$\epsilon_{s-1} := \frac{\lambda_{s-1} n_{s-1} l_{s-1}}{\lambda_s}$$

By similar calculations as in the first step, we can check that eq. (B.2) is satisfied:

$$\epsilon_{s-1} = \frac{\lambda_{s-1} n_{s-1} l_{s-1}}{\lambda_s} = \left(\frac{\lambda_{s-1} n_{s-1}}{\lambda_s}\right) \left(\frac{\lambda_s l_s}{k_{s-1} \lambda_{s-1} n_{s-1}}\right) = \frac{l_s}{k_{s-1}} < \frac{l_s}{2}$$

and also we check that the length of  $\hat{\Gamma}^{a-s+1}$ , which is  $2\lambda_{s-1} n_{s-1} l_{s-1}$ , coincides with the length of each new boundary component that comes from the blow-up of length  $\epsilon_{s-1}$  at a vertex  $v$  of valency  $\lambda_s$  in  $K_{\lambda_s, n_s}$  which is

$$2\lambda_s \epsilon_{s-1} = 2\lambda_s \frac{\lambda_{s-1} n_{s-1} l_{s-1}}{\lambda_s} = 2\lambda_{s-1} n_{s-1} l_{s-1}$$

And again, we apply Lemma B.16 to get a mixed tête-à-tête structure and keeping in mind that in this step  $\hat{\Gamma}^{a-s}$  plays the role of  $\Lambda$  and  $K_{\lambda_s, n_s}$  plays the role of  $\Gamma$ .

We set:

- $\Delta_0^s := 2l_s$
- $\Delta_1^s((\Omega_{1,1}^s)^0) := 2l_{s-1} - \left(\frac{n_s}{\lambda_s}\right) 2\lambda_{s-1} n_{s-1} l_{s-1}$ . Again we observe that this number equals  $\left(\frac{1}{\lambda_{s-1} n_{s-1}} - \frac{n_s}{\lambda_s}\right) 2\lambda_{s-1} n_{s-1} l_{s-1}$ .
- $\Delta_i^s((\Omega_{1,1}^s)^0) := \Delta_{i-1}^{s-1}((\Omega_{j,1}^{i-1})^0) = 2l_{s-2} - \left(\frac{n_{s-1}}{\lambda_{s-1}}\right) 2\lambda_{s-2} n_{s-2} l_{s-2}$  which corresponds to eq. (B.18).
- $\Delta_i^s((\Omega_{j,k}^s)^d) := 0$  for the rest of indices.

This construction iterated  $\ell$  steps produces a graph  $\Gamma$  which is naturally filtered

$$\Gamma = \Gamma^0 \supset \dots \supset \Gamma^a$$

with  $\Gamma^j$  being  $m_s = n_{a-j+1}n_{a-j+2} \cdots n_a$  copies of  $\hat{\Gamma}^j$  (for  $j > 0$ ).

Given the sequence  $S := \{(\lambda_0, n_0), \dots, (\lambda_a, n_a)\}$  we denote by

$$(\Gamma(S)^\bullet, \Delta(S)_\bullet)$$

the regular mixed tête-à-tête structure defined by induction as we just did.

**Proposition B.28.** *For a given sequence of Newton pairs  $S = \{(\lambda_0, n_0), \dots, (\lambda_a, n_a)\}$  associated to the characteristic Puiseux pairs of an isolated singularity with Milnor fiber  $\Sigma$ . Then, the homeomorphism induced by  $(\Gamma(S)^\bullet, \Delta(S)_\bullet)$  is a model of the monodromy  $h : \Sigma \rightarrow \Sigma$  of the singularity. That is, the thickening  $\Sigma(\Gamma)$  of  $\Gamma$  is homeomorphic to the Milnor fiber  $F$ , and the mixed tête-à-tête homeomorphism  $\phi_\Gamma$  is isotopic relative to the boundary to the monodromy of the singularity.*

*Proof.* By looking at the description of A'Campo [A'C73] (page 157-158) one can see that our construction produces a homeomorphic surface and an isotopic homeomorphism.

We will reproduce the construction of A'Campo and show how each step of our constructions corresponds to one step of his.

Let  $G_{\lambda_i, n_i}$  be the Milnor fiber of the singularity  $x^{\lambda_i} + y^{n_i}$  and let  $f_{\lambda_i, n_i}$  be a representative of the monodromy of the singularity which is the identity on a neighborhood of the boundary of the Milnor fiber and periodic elsewhere.

In our construction, this Milnor fiber corresponds to the thickening of the complete bipartite graph  $K_{\lambda_i, n_i}$ . The monodromy  $f_{\lambda_i, n_i}$  is isotopic (relative to the boundary) to the homeomorphism that fixes boundary given by the tête-à-tête structure on  $K_{\lambda_i, n_i}$ .

Where the monodromy is periodic, every point has an orbit consisting on  $\lambda_i \cdot n_i$  points, except for a set of  $\lambda_i$  points that are permuted and a set of  $n_i$  points that are also permuted cyclically by the monodromy. Now let  $\tilde{G}_{\lambda_i, n_i}$  be the surface resulting from removing a small disk around each of this  $n_i$  points in such a way that  $f_{\lambda_i, n_i}$  permutes these disks. We call the resulting surface  $\tilde{G}_{\lambda_i, n_i}$  and the restricted homeomorphism  $\tilde{f}_{\lambda_i, n_i}$ .

In our construction this corresponds to the blowing up of the tête-à-tête graph at the  $n_i$  vertices which form an orbit. The homeomorphism  $\tilde{f}_{\lambda_i, n_i}$  corresponds to our induced relative tête-à-tête homeomorphism on the new graph.

Let  $F^{(0)}$  be a disk and let  $f^{(0)}$  be the identity on the disk. Suppose we have already defined the surface  $F^{(s-1)}$  and the homeomorphism  $f^{(s-1)}$  which is the identity in a collar neighborhood of  $\partial F^{(s-1)}$ . Now let  $b_i : \mathbb{S}^1 \rightarrow \partial G_{\lambda_s, n_s}$ , for  $i = 1, \dots, n_s - 1$ , be an orientation preserving homeomorphism identifying each of the boundary components of  $\tilde{G}_{\lambda_s, n_s}$  with  $\mathbb{S}^1$ . In such a way that  $b_{i+1} = \tilde{f}_{\lambda_s, n_s} \circ b_i$ . Now let  $F_{far}^{(s)} = F_1^{(s-1)} \sqcup \dots \sqcup F_{n_s}^{(s-1)}$ , that is the disjoint union of  $n_s$  copies of  $F^{(s-1)}$ . Let  $a_i : \mathbb{S}^1 \rightarrow \partial F_{far}^{(s-1)} = \partial F_i^{(s-1)}$  be an identification of the boundary of each copy with  $M\mathbb{S}^1$ . Finally, let  $\phi : \partial F_{far}^{(s)} \rightarrow \partial \tilde{G}_{\lambda_s, n_s}$  be an orientation reversing homeomorphism on the boundary such that for each  $i$  we have  $\phi \circ a_i = b_i$ . Then we define  $F^{(s)} := \tilde{G}_{\lambda_s, n_s} \cup_\phi F_{far}^{(s)}$ .

In our construction, this corresponds to the process of closing each boundary component of the blow up. More concretely, the operation

$$Bl_v(K_{\lambda_s, n_s}, \hat{\Gamma}^{a-s+1}, \epsilon_{s-1})$$

defines a filtered metric ribbon graph whose thickening is naturally homeomorphic to  $F^{(s)}$  by the construction of A'Campo.

The homeomorphism  $f^{(s)}$  is defined by



- (a)  $f^{(s)}|_{\widetilde{G}_{\lambda_s, n_s}} = \widetilde{f}_{\lambda_s, n_s}$
- (b)  $f^{(s)}|_{F_i^{(s-1)}}$  sends  $F_i^{(s-1)}$  to  $F_{i+1}^{(s-1)}$  by the identity for  $i = 1, \dots, n_s - 1$
- (c)  $f^{(s)}|_{F_{n_s}^{(s-1)}} = f^{(s-1)}$

In our construction this corresponds (respectively) to:

- (a')  $\widetilde{f}_{\lambda_s, n_s}$  is just the homeomorphism induced by the relative tête-à-tête property on  $Bl_p(K_{\lambda_s, n_s}, \epsilon_{s-1})$ .
- (b') That  $f^{(s)}|_{F_i^{(s-1)}}$  sends  $F_i^{(s-1)}$  to  $F_{i+1}^{(s-1)}$  by the *identity* for  $i = 1, \dots, n_s - 1$  corresponds in our construction to the description of the graph of the  $\Lambda$ -blow up  $Bl_v(K_{\lambda_s, n_s}, \widehat{\Gamma}^{a-s+1}, \epsilon_{s-1})$  and the fact that all the new  $\Delta$  numbers are 0 except for one component.
- (c')  $f^{(s)}|_{F_{n_s}^{(s-1)}} = f^{(s-1)}$  This corresponds in our construction to the adjustment made on the component by setting the corresponding  $\Delta$  number to

$$\left( \frac{1}{\lambda_{s-1} n_{s-1}} - \frac{n_s}{\lambda_s} \right) 2\lambda_{s-1} n_{s-1} l_{s-1}.$$

We just observe that the number is the difference between the rotation number of the action of  $f^{(s-1)}$  on the (only) boundary of  $F^{(s-1)}$  and the action of  $\widetilde{f}^{(s)}$  on one of the boundaries that appear after blowing up  $K_{\lambda_s, n_s}$  so it induces a rotation of  $\frac{1}{\lambda_{s-1} n_{s-1}}$  which after gluing, recovers the monodromy of the Newton pair  $(\lambda_{s-1}, n_{s-1})$  (see also the second part of the statement of Lemma B.16)

□

**Example B.29** (Iomdin series). The singularity  $(x^2 + y^3)^2$  is non-isolated, its critical locus has complex dimension 1. We consider the isolated singularities  $f_k(x, y) = (x^2 + y^3)^2 + x^{2k-1}$  with  $k \in \mathbb{N}$ . The associated characteristic Puiseux pairs are  $(3, 2)(6k - 12, 2)$  we compute the sequence of the associated pairs

$$S_k = \{(3, 2)(6(k - 1), 2)\}$$

Then, by the previous construction, delta function  $\delta$  is defined by

$$\delta_1|_{\widehat{\Gamma}_{1,1,1}^1} = 0$$

and

$$\delta_1|_{\widehat{\Gamma}_{1,2}^1} = \left( \frac{1}{6} - \frac{2}{6k - 12} \right) \cdot l(\widehat{\Gamma}_{1,2}^1)$$

and so  $(\Gamma(S_k)^\bullet, \delta(S_k)_\bullet)$  models the fiber and the monodromy of the singularity defined by  $f_k(x, y) = 0$ .

We observe that the thickening of  $\Gamma^1$  consists of two copies  $F_1, F_2$  of the Milnor fiber of the singularity  $(x^2 + y^3)$  and that when  $k \rightarrow \infty$ , the homeomorphism  $\phi_\Gamma|_{\Gamma^1}$  converges to that of  $(x^2 + y^3)^2$ , that is: a periodic homeomorphism that sends  $F_1$  to  $F_2$  by the identity and  $F_2$  to  $F_1$  by a periodic representative of the monodromy of  $x^2 + y^3$  which rotates its only boundary with rotation number  $1/6$  measured with the orientation on the boundary component induced by the orientation of the Milnor fiber.

## Appendix C

---

# Examples

**Example C.1.** Consider the complete bipartite graph  $K_{2,4}$  with the cyclic ordering at each vertex given by the projection on the plane depicted on the left part of Figure C.2. The thickening  $\Sigma$  of this graph is the surface of genus 1 and 2 boundary components.

Giving a length of  $\pi/2$  to each edge, we provide the graph with a tête-à-tête structure such that the corresponding periodic homeomorphism has order 4. We denote a periodic representative of the induced mapping class by  $\phi_{K_{2,4}}$ . We get that the red vertices have trivial isotropy group while the blue vertices have isotropy group of order 2.

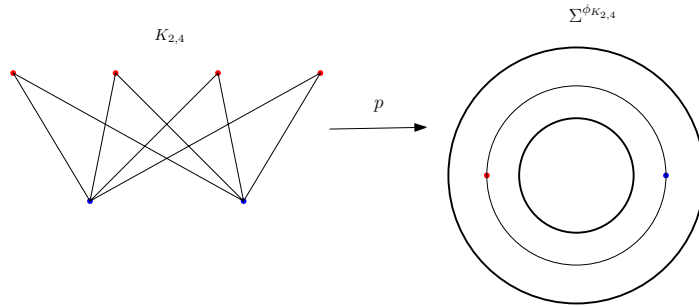


**Figure C.2:** On the left we see  $K_{2,3}$ . On the right we see the orbit surface  $\Sigma^{\phi_{K_{2,4}}}$ .

The orbit surface  $\Sigma^{\phi_{K_{2,4}}}$  has genus 0 and 2 boundary components. It is depicted on the right side of the figure together with the image by the projection map  $p : \Sigma \rightarrow \Sigma^{\phi_{K_{2,4}}}$  of the graph  $K_{2,4}$ .

We perturb this graph as in the right side of Figure C.3. Observe that the vertex of valency 1 on this graph corresponds to a branch point of the map  $p$ .

Now we take the preimage by  $p$  of this graph. This is depicted on the left part of Figure C.3.

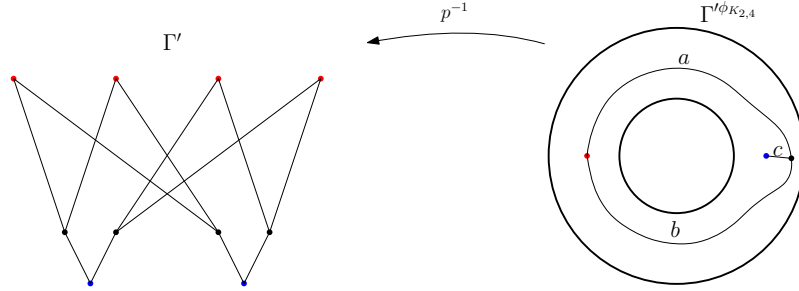


**Figure C.3:** On the left we see  $K_{2,3}$ . On the right we see the orbit surface  $\Sigma^{\phi_{K_{2,4}}}$ .

We make the following observation. The length of all the edges in  $\Gamma'$  is determined by the length of the edges of  $\Gamma^{\phi_{K_{2,4}}}$ . The fractional Dehn twist coefficient of  $\phi$  at each of the two boundary components is  $1/4$ . If  $l(a), l(b)$  and  $l(c)$  denotes the length of the edges of  $\Gamma^{\phi_{K_{2,4}}}$ , by the observation made in this paragraph, we must have

$$l(a) + l(b) = l(a) + l(b) + 2l(c)$$

which is impossible since there can be no edges with length 0.

**Example C.4.** We show an example of construction of a general tête-à-tête graph from a periodic automorphism of a surface permuting all its boundary components.

Let  $\Sigma$  be the surface of genus 1 and 3 boundary components  $C_0, C_1, C_2$  embedded in  $\mathbb{R}^3$  as in the picture C.5. Let  $\phi : \Sigma \rightarrow \Sigma$  be the restriction of the space rotation of order 3 that exchanges the 3 boundary components. We observe that in particular  $\phi^3|_{C_i} = id$  for  $i = 0, 1, 2$ .

We consider the star-shaped piece  $S$  with 3 arms together with the order 3 rotation  $r$  that exchanges the arms (see the picture Figure C.5).

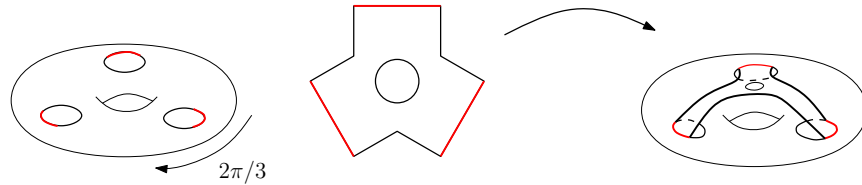


**Figure C.5:** On the left, the torus  $\Sigma$  with 3 disks removed and the orbit of an arc marked, that is, 3 arcs in red. In the center, the star-shaped piece  $S$  with 3 arms to be glued to the torus along those arcs. On the right, the surface we get after gluing, with 2 boundary components, one of them invariant by the induced homeomorphism.

We glue  $S$  to  $\Sigma$  as the theorem indicates: we mark a small arc  $\alpha^0 \subset C_2$  and all its iterated images by the rotation. Then we glue  $\alpha^0, \alpha^1, \alpha^2$  to  $a^0, a^1, a^2$  respectively by orientation reversing homeomorphisms. We get a new surface  $\hat{\Sigma} := \Sigma \cup S$  with 2 boundary components. We cap the boundary component that intersects  $C_0 \cup C_1 \cup C_2$  with a disk  $D^2$  and extend the homeomorphism to the interior of the disk getting a new surface  $\hat{\Sigma}$  and a homeomorphism  $\hat{\phi}$ .

Using Hurwitz formula  $2 - 2g - 4 = 0 - 2$  we get that the surface we are gluing to  $\Sigma$  has genus 0 and hence it is a sphere with 4 boundary components. See picture Figure C.6. Three of them are identified with  $C_0, C_1, C_2$ , and the 4-th is called  $C$  and is the only boundary component of  $\hat{\Sigma}$ .

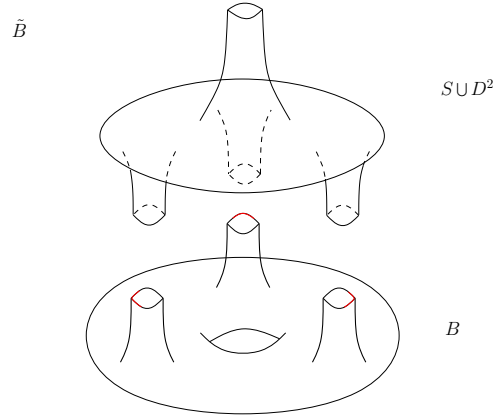


**Figure C.6:** On the left, the torus with 3 disks removed and 3 the orbit of an arc marked. On the right, the star-shaped piece with 3 arms to be glued to the torus along those arcs.

We compute the orbit space  $\hat{\Sigma}^{\hat{\phi}}$  by the extended homeomorphism  $\hat{\phi}$  and get a torus with 1 boundary component. We consider the graph  $\Gamma'$  as in picture Figure C.7. We put a metric in this graph. We set every edge of the hexagon to be  $\pi/6 - \epsilon/3$  long and the path joining the hexagon with the branch point to be  $\epsilon$  long. In this way, if we look at the result of cutting  $\hat{\Sigma}^{\hat{\phi}}$  along the graph  $\hat{\phi}$  we see that the only boundary component that maps to the graph by the gluing map has length  $6(\pi/6 - \epsilon/3) + 2\epsilon = \pi$ .

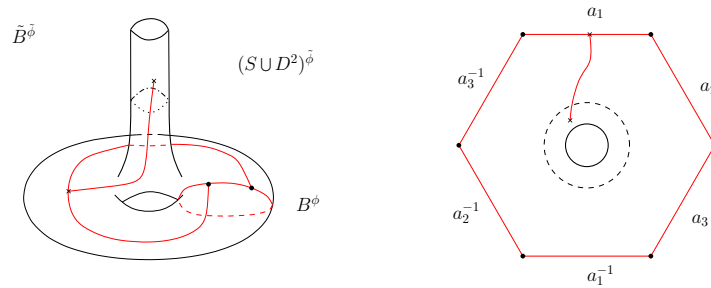


**Figure C.7:** On the lower part we have the original surface. On the upper part we have the surface that we attach, in this case a sphere with 4 holes removed.

The preimage  $\hat{\Gamma}$  of  $\Gamma'$  by the quotient map is a tête-à-tête graph whose thickening is  $\hat{\Sigma}$ . Its associated homeomorphism  $\hat{\phi}$  leaves  $\Sigma$  invariant and its restriction to it coincides with the rotation  $\phi$ . Moreover  $(\hat{\Gamma} \cap \Sigma, \hat{\Gamma} \cap \partial\Sigma)$  is a general spine of  $(\Sigma, \partial\Sigma)$ . Modifying the induced metric in  $\hat{\Gamma} \cap \Sigma$  as in the proof of the Theorem and adding the order 3 cyclic permutation to the valency 1 vertices we obtain a tête-à-tête graph whose associated homeomorphism equals  $\phi$ .

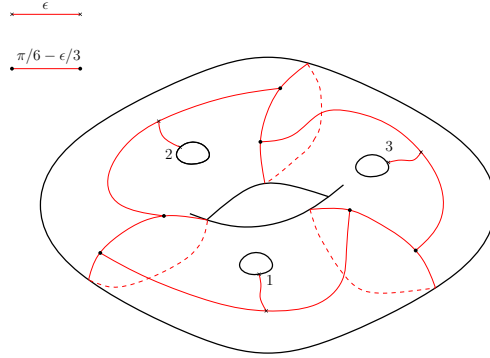


**Figure C.8:** On the left, the torus with 3 disks removed and 3 the orbit of an arc marked. On the right, the star-shaped piece with 3 arms to be glued to the torus along those arcs.

**Example C.9.** This is an example of a mixed tête-à-tête graph. It is given purely in graph terms, meaning that no embedding of the graph in a surface is constructed.

The graph is that of Figure C.10. The blue part is  $\Gamma \setminus \Gamma^1$  and the red part is  $\Gamma^1$ .

The lengths and cyclic orders at each vertex are indicated and one can check that the functions

$$\delta_0 = \pi, \quad \delta_1 = \pi/18$$

make  $(\Gamma^\bullet, \delta_\bullet)$  a mixed tête-à-tête graph. One also can check that its thickening is the oriented surface of genus 2 and 1 boundary component.

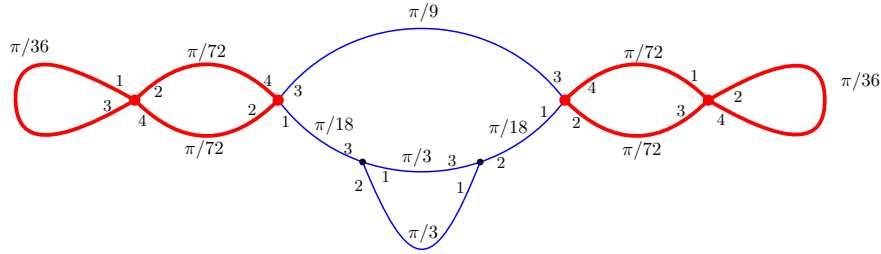


**Figure C.10:** Mixed tête-à-tête graph with  $\Gamma_1$  in red.

**Example C.11.** Let  $\Sigma$  be the surface of Figure C.13. Suppose it is embedded in  $\mathbb{R}^3$  with its boundary component being the unit circle in the  $xy$ -plane. Consider the rotation of  $\pi$  radians around the  $z$ -axis and denote it by  $R_\pi$ . By the symmetric embedding of the surface, it leaves the surface invariant. Isotope the rotation so that it is the identity on  $z \leq 0$ . More concretely, let  $T : \mathbb{R}^3 \rightarrow \mathbb{R}^3$  defined by

$$T(r, \theta, z) := \begin{cases} (re^{i(\theta+\pi)}, z) & \text{if } z \leq \epsilon \\ (re^{\theta+\frac{z}{\epsilon}\pi}, z) & \text{if } 0 \leq z \leq \epsilon \\ \text{id} & \text{if } z \leq 0 \end{cases} \quad (\text{C.12})$$

With  $(r, \theta)$  polar coordinates on the  $xy$ -plane and  $\epsilon > 0$  small.

Let  $D_i$  be a full positive Dehn twist on  $\mathcal{A}_{1,k}^1$ ,  $k = 1, 2$ . We define the homeomorphism

$$\phi := D_2 \circ D_1^{-2} \circ T|_\Sigma.$$

We apply Theorem 10.7 to construct a mixed tête-à-tête graph embedded in  $\Sigma$  modeling  $\phi$ .

It is clear that  $\phi$  is a pseudo-periodic homeomorphism and it is already in canonical form (recall Theorem 2.32). Also we observe that  $[\phi|_{\Sigma \setminus \mathcal{A}}]$  has order 2.

Clearly,  $G(\phi, \Sigma)$  is the graph depicted in Figure C.13 and is a tree. Also, since  $\Sigma$  has only 1 boundary component, there is only one possible root of  $G(\phi, \Sigma)$ . So we root the graph and label the corresponding parts as in the cited figure.

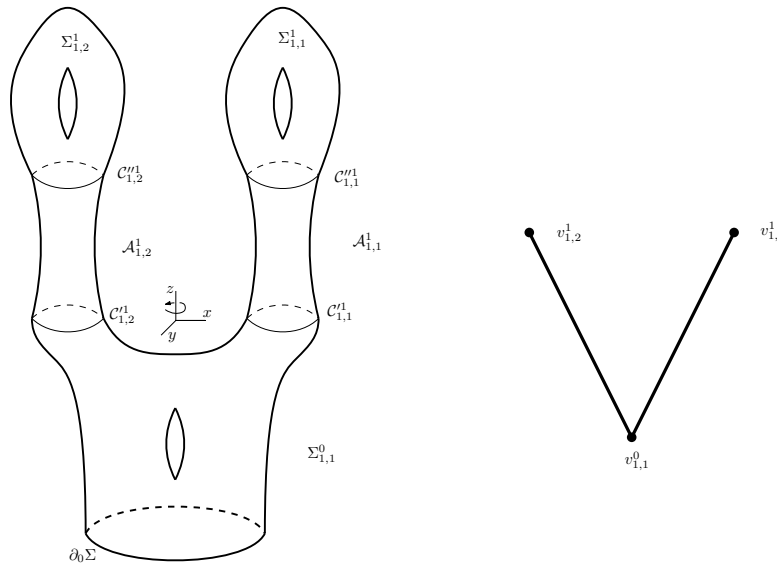


**Figure C.13:** The surface  $\Sigma$ . The axis are also depicted in the figure. The rotation around the  $z$ -axis is isotoped near the boundary of the surface so that it leaves the boundary fixed. On the right, the corresponding  $G(\phi, \Sigma)$  rooted at the only vertex at which is possible to root it.

On Figure C.14 we see the relative tête-à-tête graph  $(\Gamma^0, B^0)$  (in blue). This corresponds to the first iteration of the induction process. In the figure it is indicated the lengths of the edges. The lengths that are not indicated can be deduced knowing that the metric is invariant by  $\phi$ .

Clearly, we only need to iterate once more to construct the final mixed tête-à-tête graph.

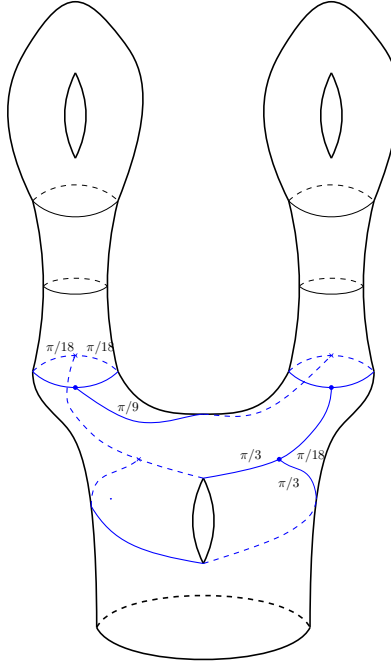


**Figure C.14:** In blue, we see the relative tête-à-tête graph  $(\Gamma^0, B^0)$  for  $\phi|_{\Sigma^0}$ . The graph is embedded in  $\Sigma$ .

On Figure C.15 we see a choice of parametrization  $\eta_{1,1}^1$  of  $\mathcal{A}_{1,1}^1$  on the right and we also see in green  $\eta_{1,1}^1(I \times \{p\})$  and  $\eta_{1,1}^1(I \times \{q\})$ . On the left we see two copies of  $\mathcal{A}_{1,2}^1$ : on the upper copy we can see the image by  $\phi$  of the two retraction lines in  $\mathcal{A}_{1,1}^1$ ; on the lower copy we can see the two retraction lines given by  $\eta_{1,2}^1$ . The latter ones are the ones that are going to be part of the final mixed tête-à-tête graph.

On Figure C.17 we see the following:

- On the upper part, we see  $\Sigma^1$  and the graphs  $\Gamma_{1,1}^1$  and  $\Gamma_{1,2}^1 = \phi(\Gamma_{1,1}^1)$  (in red).
- On the lower part we can see  $\Sigma_{\Gamma^1}$ . Also 4 (in green) retraction lines have been added concatenating with the previous 4 added segments.

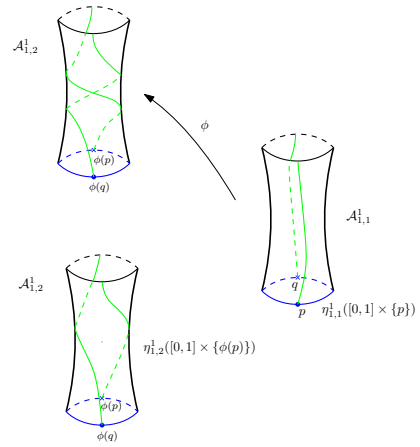


Figure C.15: Choosing the retraction lines in Step 1.

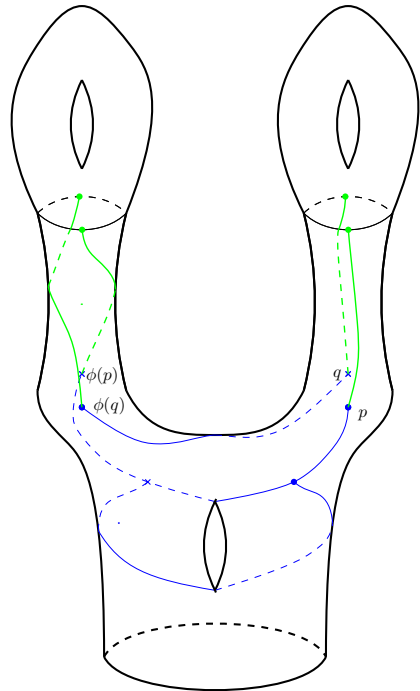
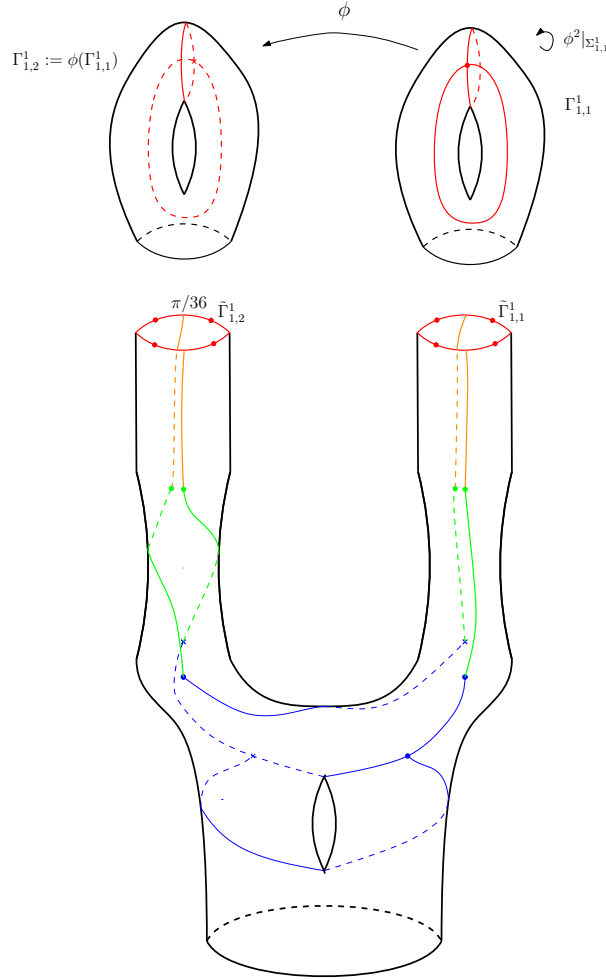


Figure C.16: The retraction lines chosen embedded in the surface  $\Sigma$ .





**Figure C.17:** On the upper part of the figure we see  $\Gamma_{1,1}^1$  and  $\Gamma_{1,2}^1$  in red. The surface on the lower part of the figure is  $\Gamma_{\Gamma^1}$ . We see in blue the relative tête-à-tête graph of the first iteration of the induction process minus its relative boundary components. We see in green the retraction lines added on STEP 1. In orange we see the retraction lines contained in  $\Sigma_{\Gamma^1}^1$  that we add on STEP 2. In red we see  $\tilde{\Gamma}^1$ .

By the lengths chosen on  $\Gamma_{1,1}^1$  which are  $\pi/36$  for each of the two edges, we find that  $l(\tilde{\Gamma}_{1,1}^1) = 4 \cdot \pi/36 = \pi/9$  which coincides with  $l(\mathcal{C}_{1,1}^{\prime\prime 1}) = 2 \cdot \pi/18 = \pi/9$ .

By the construction on Theorem 10.7, we set the length of each of the orange and green lines to be  $\epsilon/2$  and we also redefine the length of the blue edges where the green lines are attached to be  $\pi/9 - \epsilon$ .

On Figure C.18 we see the whole graph.

Now we compute the  $\delta$  numbers. In our case we find that the only screw number is  $-1$ . Since  $\alpha_1 = 2$ , we find that  $\delta_1$  is the constant function  $l(\tilde{\Gamma}_{1,1}^1)/2$ . Also, we have by definition that  $\delta_0 = \pi$ .

This completes the construction.

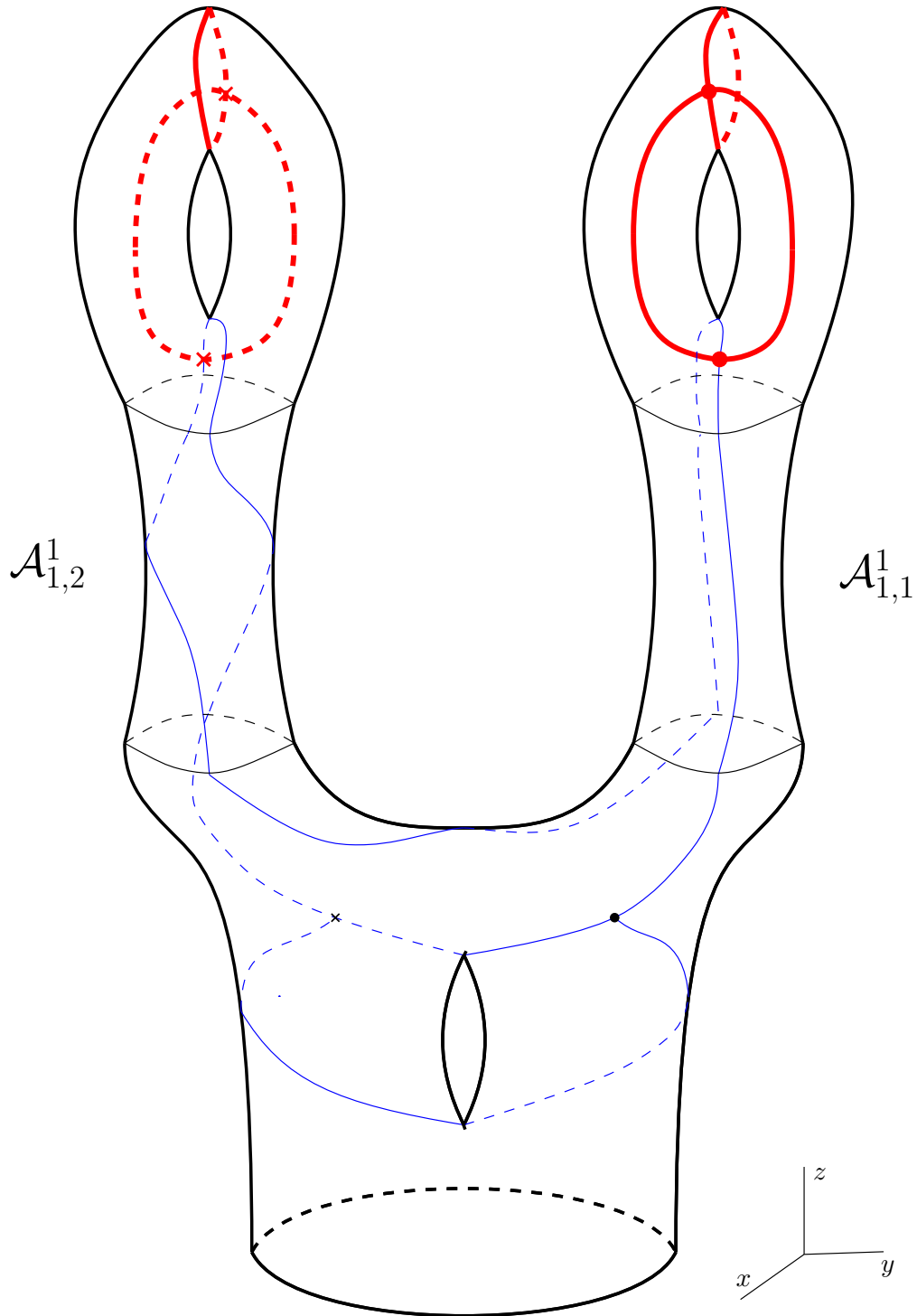


**Figure C.18:** The whole graph  $\Gamma \supset \Gamma^1$  whose associated mixed tête-à-tête homeomorphisms models  $T$ . The red part corresponds to  $\Gamma^1$ .

**Example C.19.** We describe an example of a mixed tête-à-tête graph with a filtration of depth 2:

$$\Gamma \supset \Gamma^1 \supset \Gamma^2.$$

The thickening of  $\Gamma$  is a surface of genus 7, see Figure C.26 and 1 boundary component.

We start by describing first  $\Gamma_{\Gamma^1}$ . Consider the complete bipartite graph of type 2, 3 that we denote by  $K_{2,3}$ . By putting the length of each edge to be  $\pi/2$ , we make it into a tête-à-tête graph. Now perform a blow up of length  $\epsilon_1 < \pi/2$  (in the sense of A'Campo) on the orbit formed by the vertices of valency 2. See Figure C.20. Summarizing, we define  $\Gamma_{\Gamma^1} := Bl_v(K_{2,3}, \epsilon)$ .

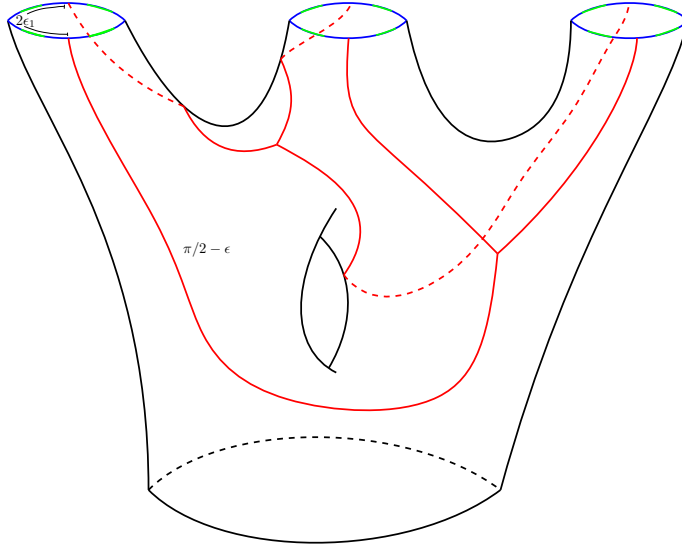


**Figure C.20:** The figure corresponds to  $\Gamma_{\Gamma^1}$ . It equals to  $Bl_v(K_{2,3}, \epsilon_1)$  where  $v$  is any of the three vertices of valency 2 and  $\epsilon_1 < \pi/2$ . It is a relative tête-à-tête graph whose tête-à-tête homeomorphism has order 6. The three boundary components that come from the blowing-up correspond to  $\tilde{\Gamma}^1$  (when  $\Gamma^1$  is defined). The four green arcs in each of these boundary components correspond to the part in  $\tilde{\Gamma}^1$  that is sent to  $\tilde{\Gamma}^2$  by  $g_{\Gamma,1}$  when these are defined (see the following figures).

Let's describe  $\Gamma_{\Gamma^2}^1$ . It consists of three copies of the same relative metric ribbon graph. The graph and the lengths are given in Figure C.21.

In Figure C.22, we see one of the connected components of  $\tilde{\Gamma}^1$ .

We observe that the length of each connected component of  $\tilde{\Gamma}^1$  is  $4\epsilon_1$  which coincides with the length of the relative boundary components of Figure C.20 that come from the blowing up. Therefore, we can pick an isometry from one connected component of  $\tilde{\Gamma}^1$  to one of the boundary components of Figure C.20. We do so as indicated in Figure C.20 by the marked green arcs.

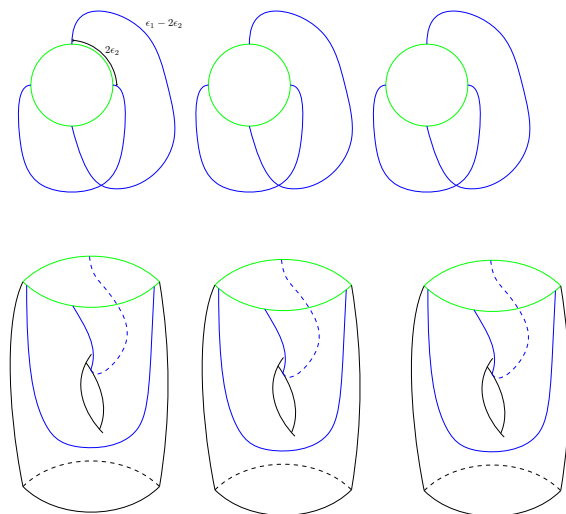


**Figure C.21:** The upper part of the picture is  $\Gamma_{\Gamma^2}^1$ . The lower part of the picture is  $\Sigma_{\Gamma^2}^1$ . The three green circles will correspond to  $\tilde{\Gamma}^2$  (when they are defined).

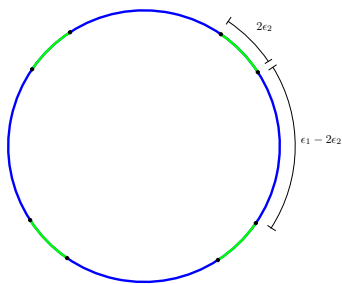


**Figure C.22:** We see one of the connected components of  $\tilde{\Gamma}^1$ . The green part corresponds to the part of  $\Gamma_{\Gamma^2}^1$  that is in  $\tilde{\Gamma}^2$ .

Now we describe  $\Gamma^2$ . It is exactly the graph  $K_{3,3}$  where each edge is of length  $2\epsilon_2/3$ . See Figure C.23. On that picture we also observe its thickening and the result of cutting its thickening along  $K_{3,3}$ .

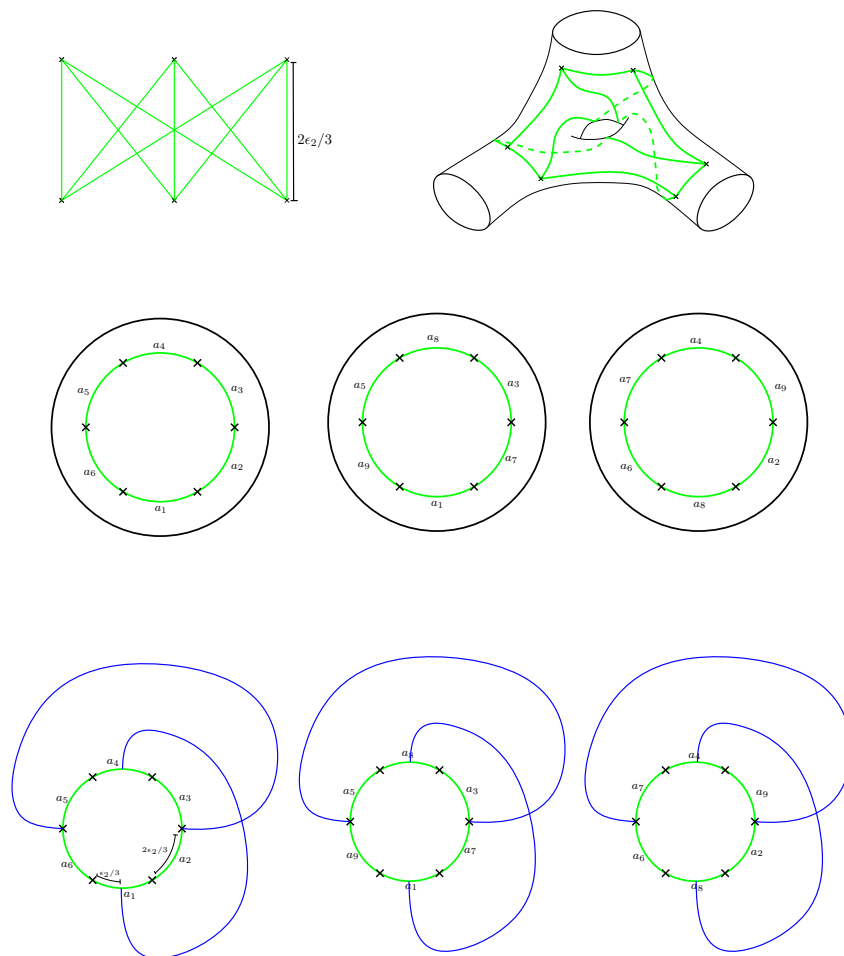


**Figure C.23:** We see the graph  $\Gamma^2 := K_{3,3}$  and its thickening. On the lower part of the figure we see the three cylinders of  $\Sigma_{K_{3,3}}^2$ . The labels on the edges indicate that two edges with the same label should be glued by an orientation reversing isometry to recover  $K_{3,3}$ . On the lower part of the picture, we see the chosen isometries with the boundary components of  $\Gamma_{\Gamma^2}^1$ .

We note that the length of each of the boundary components of  $\Sigma_{K_{3,3}}^3$  that come from cutting, has length  $4\epsilon_2$  which coincides with the lengths of the boundary components of  $\Sigma_{\Gamma^2}^1$  contained in the graph (see Figure C.21). So we can pick isometries that identify the three boundary components with the three boundary components of  $\Gamma_{\Gamma^2}^1$ . We do so as depicted in the lower part of figure Figure C.23

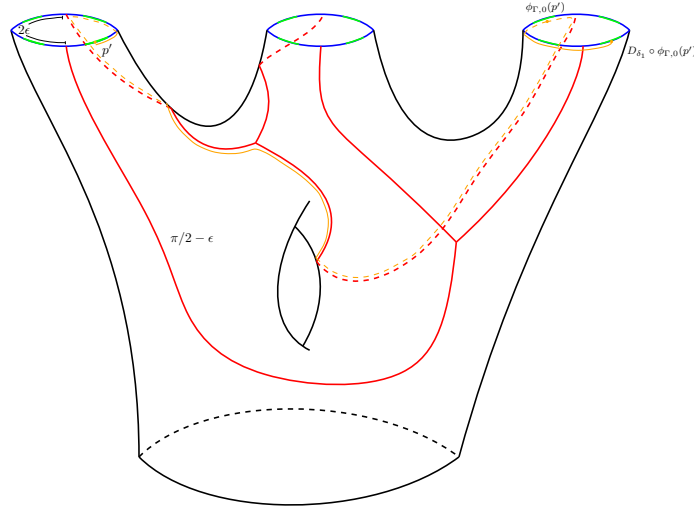


**Figure C.24:** Let  $p'$  be one of the preimages by  $\tilde{g}_{\Gamma,1}$  of  $p$ . We see its image by the relative tête-à-tête homeomorphism  $\phi_{\Gamma,0}$  and we also see its image after composing the relative tête-à-tête homeomorphism with  $\mathcal{D}_{\delta_1}$ .

With this information we have constructed a filtered metric ribbon graph (see Figure C.26).

We observe (see Figure C.26) that  $\Gamma^0, \Gamma^1$  and  $\Gamma^2$  are connected. Hence, the functions  $\delta_0, \delta_1$  and  $\delta_2$  take only one value each. We define them by

$$\begin{aligned} \delta_0 &:= \pi \\ \delta_1 &:= 2\epsilon_1 \\ \delta_2 &:= 2\epsilon_2 \end{aligned} \tag{C.25}$$

It can be checked easily that with these values  $(\Gamma^\bullet, \delta_\bullet)$  is a mixed tête-à-tête graph.

We can picture the construction of the mixed tête-à-tête homeomorphism. We pick a point  $p$  with  $c_p = 2$  so that the corresponding mixed safe walk is formed by the concatenation of three safe walks. Let  $p'$  be one of the preimages of  $p$  by  $\tilde{g}_{\Gamma,1}$ .

In Figure C.24, we see the action of the homeomorphism  $\mathcal{D}_{\delta_1} \circ \phi_{\Gamma,0}$  on  $p'$ .

Finally, in figures Figure C.27 and Figure C.28 we see the two mixed safe walks starting at a point  $p$  with  $c_p = 2$ . One can easily check, using the metric put on the graph, that these are actually the mixed safe walks and that they end at the same point.

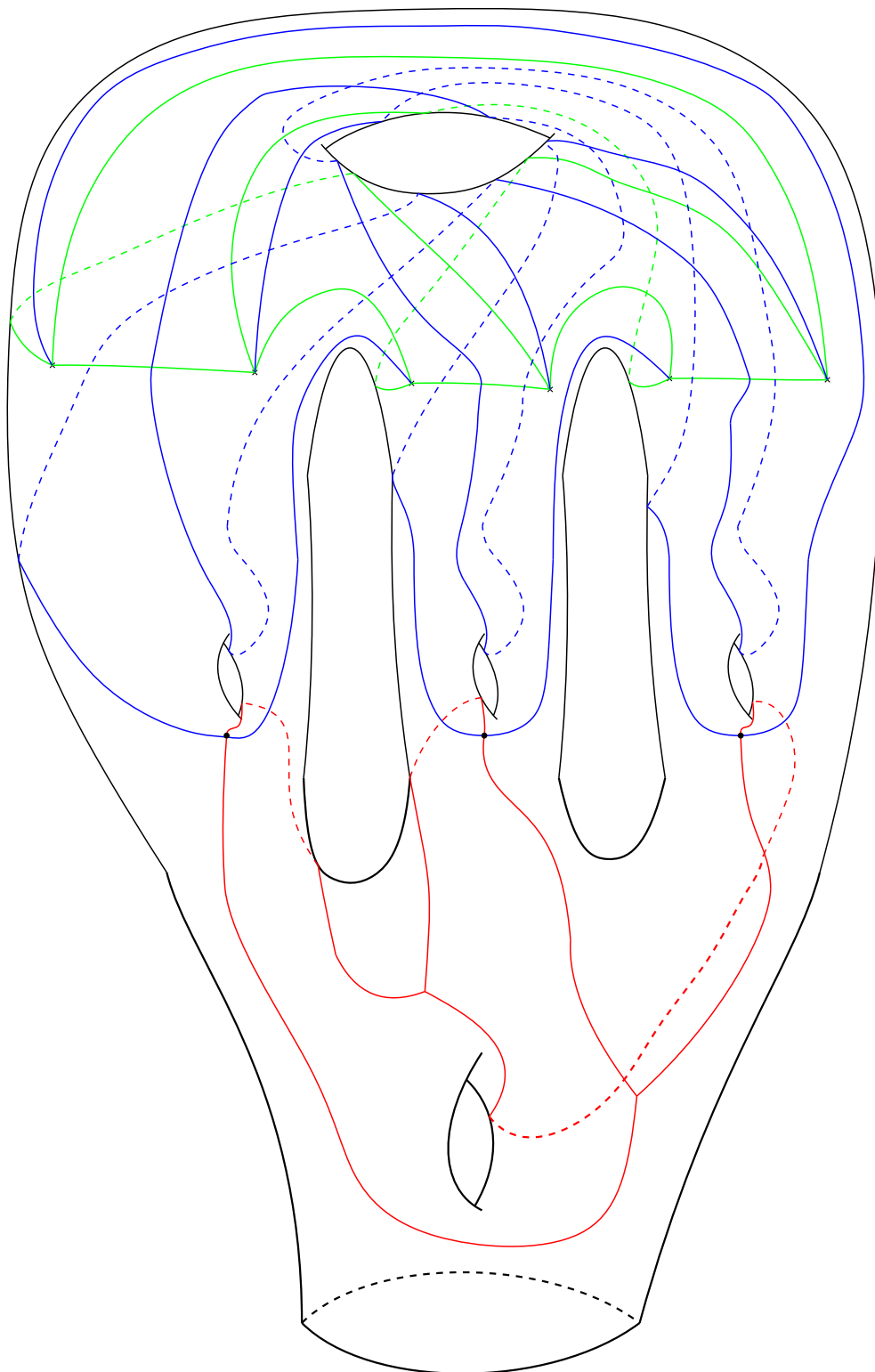


**Figure C.26:** We see the graph  $\Gamma$ . In red we see  $\Gamma \setminus \Gamma^1$ . In blue we see  $\Gamma^1 \setminus \Gamma^2$  and in green we see  $\Gamma^2$ . We observe that, since  $\Gamma^2$  is connected, so is  $\Gamma^1$ , unlike  $\Gamma_{\Gamma^2}^1$  that has 3 connected components.

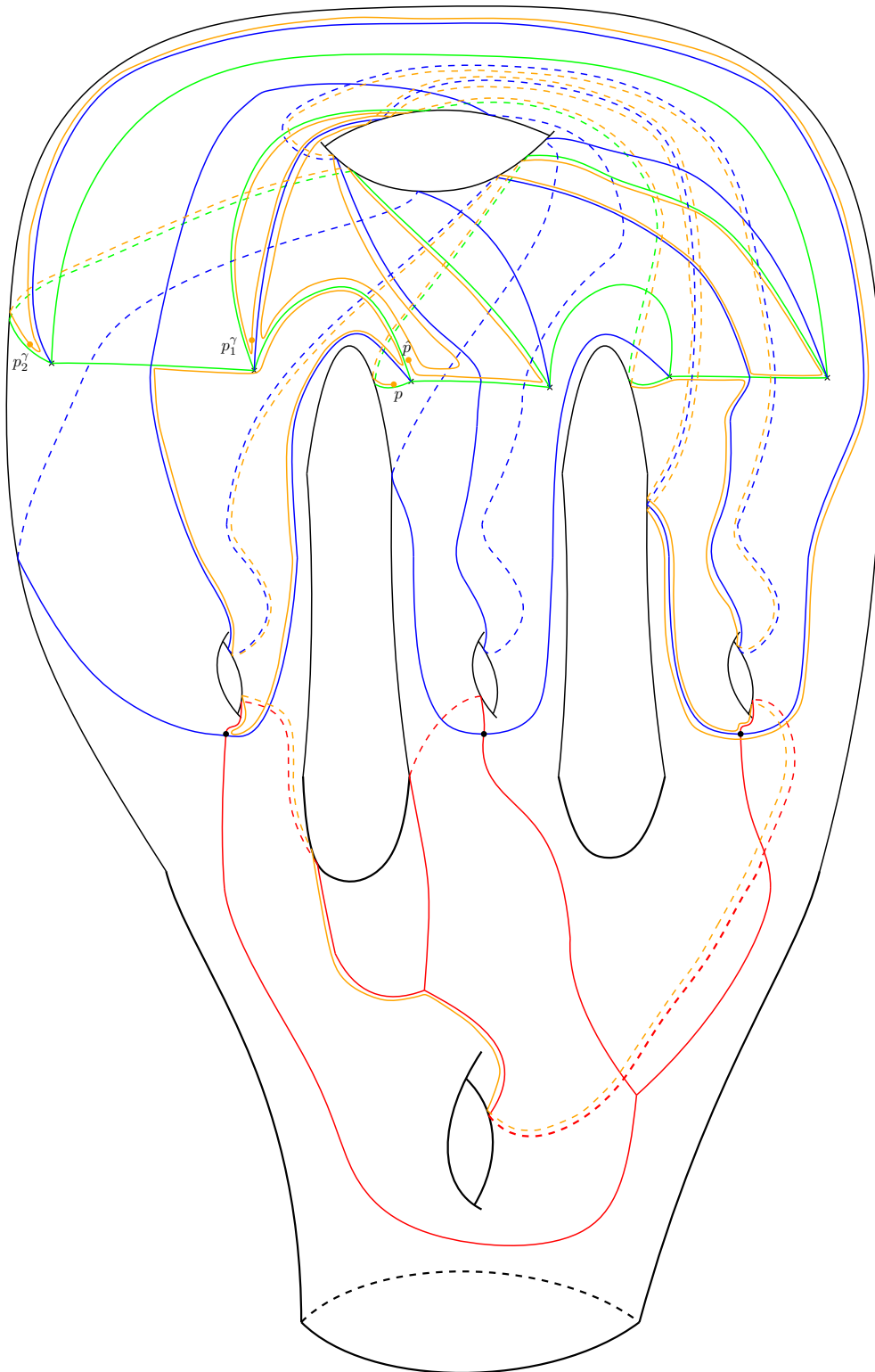


**Figure C.27:** We the see  $\Sigma$  with the embedded graph  $\Gamma$ . In orange we see the mixed safe walk  $\gamma_p$ . We have denoted by  $\hat{p}$  the end of the mixed safe walk.



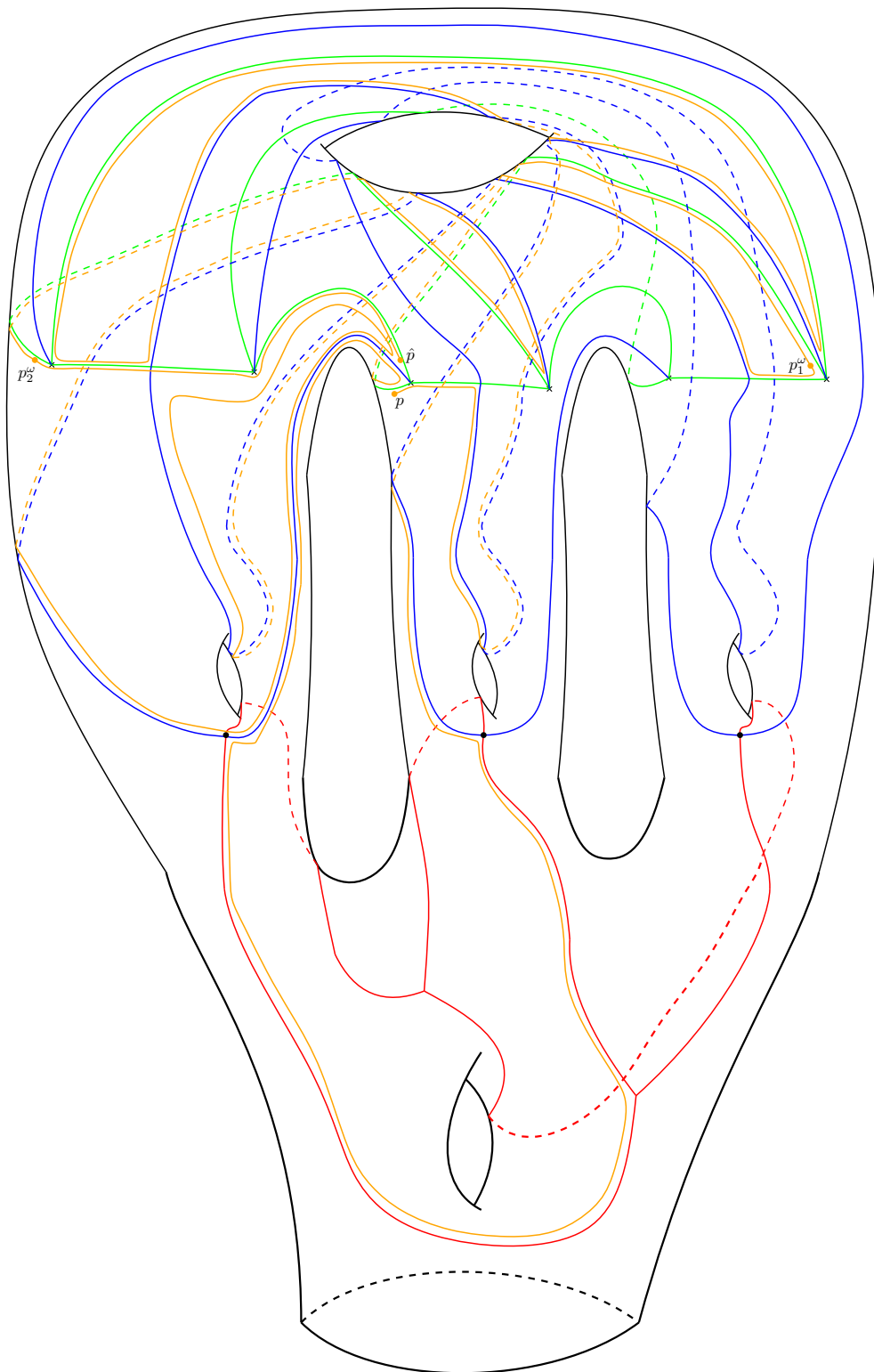


**Figure C.28:** We see  $\Sigma$  with the embedded graph  $\Gamma$ . In orange we see the mixed safe walk  $\omega_p$ .

**Example C.29.** Suppose we are given the bipartite complete graph  $\Gamma$  of type 4, 11 with the cyclic order induced by placing 4 and 11 vertices in two horizontal parallel lines in the plane and taking the joint of the two sets in that plane. Give each edge length  $\pi/2$ . This metric makes it into a tête-à-tête graph as we already know. Let  $\phi_\Gamma$  be a periodic representative of the mapping class induced by the tête-à-tête structure.

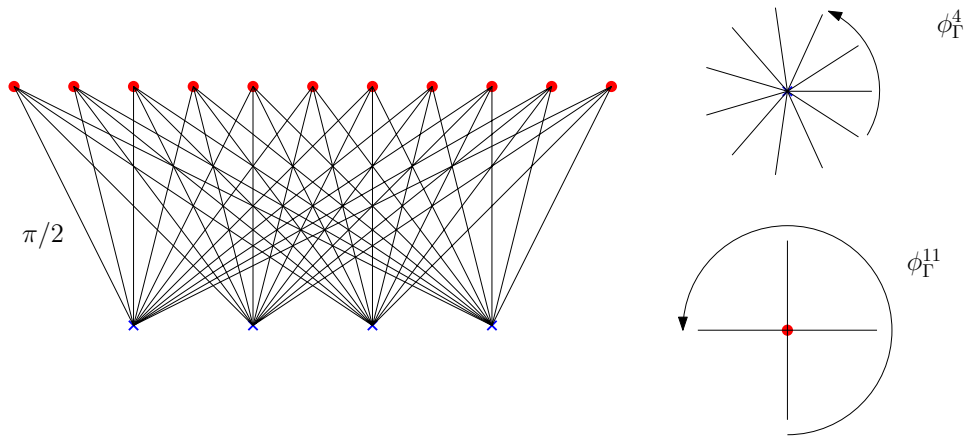


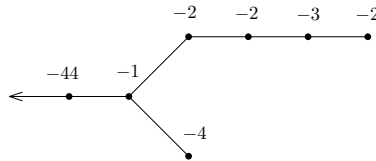
**Figure C.30:** On the left we see the tête-à-tête graph  $K_{4,11}$ . On the right we see a small neighborhood of a vertex of valency 11 where  $\phi_\Gamma^4$  acts as the rotation  $r_{4/11}$  radians. Equivalently, for a vertex of valency 4, we see that  $\phi_\Gamma^{11}$  acts as the rotation  $r_{3/4}$ .

Let's find the associated invariants. One can easily check that the orbit graph is just a segment joining the only two branch points so the orbit surface is a disk and hence  $g = 0$  and  $r = 1$ .

The map  $p : \Sigma \rightarrow \Sigma^{\phi_\Gamma}$  has two branch points that correspond to two Seifert pairs. Let  $r_1$  be the branch point in which preimage lie the 4 points of valency 11. We choose any of those 4 points and denote it  $p_1$ , now  $\phi^4$  acts as a rotation with rotation number  $4/11$  in a small disk around  $p_1$ . Hence, the associated normalized Seifert pair is  $(11, 8)$ . Note that  $8 \cdot 4 \equiv -1 \pmod{11}$  and that  $0 < 8 < 11$ . Equivalently for the other point we find that  $\phi_\Gamma^{11}$  is a rotation with rotation number  $3/4$  when restricted to a disk around any of the 11 vertices of valency 4. Hence, the corresponding normalized Seifert pair is  $(4, 1)$ .

Computing the continued fraction we find that  $\frac{11}{8} = [2, 2, 3, 2]$  and  $\frac{4}{1} = [4]$ . For computing the number  $b$  we think of the surface resulting from extending the periodic automorphism to a disk capping off the only boundary component of  $\Sigma$ . By a similar argument, since the rotation number induced on the boundary is  $-1/44$ , this would lead to a new Seifert pair  $(44, 1)$ . Since these are normalized Seifert invariants, the new manifold is closed and admits a horizontal surface, we can use Proposition 3.17 and compute the number  $b$  as  $-1/4 - 8/11 - 1/44 = -1$ .

So the plumbing diagram corresponding to the mapping torus of  $\Sigma$  by  $\phi_\Gamma$  is the following.



which, up to contracting the bamboo that ends in the arrowhead, coincides with the dual graph

of the resolution of the singularity of  $x^4 + y^{11}$  at 0.

Finally, we are going to compute the element that the surface  $\Sigma$  represents in the homology group  $H_1(\Sigma^{\phi_r}) \oplus \mathbb{Z}$ . First observe that since  $\Sigma^{\phi_r}$  is a disk, the group is isomorphic to  $0 \oplus \mathbb{Z}$ . This tells us that the only possible choices of multisections in the bundle  $\Sigma^{\phi_r} \times \mathbb{S}^1$  are classified (up to isotopy) by the elements  $(0, k)$  with  $k \neq 0$ . The element  $(0, k)$  corresponds to  $k$  parallel copies of the disk  $\Sigma^{\phi_r}$ . In our case, there is only one such disk so the element is  $(0, 1)$ .

**Example C.31.** Suppose we are given the following plumbing graph:

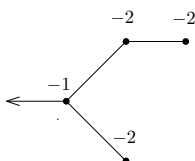


Figure C.32

We are indicated two of the invariants of the Seifert manifold: the genus of the base space  $g = 0$  and its number of boundary components  $r = 2$ . The base space  $B$  is therefore an annulus.

We compute the Seifert invariants by interpreting the weights on the two bamboos of the plumbing graph as numbers describing continued fractions. We get  $[2, 2] = 3/2$  and  $[2] = 2$  so the Seifert pairs are  $(3, 2)$  and  $(2, 1)$ . So the corresponding Seifert fibering  $s : M \rightarrow B$  has two special fibers  $F_1$  (for the pair  $(2, 1)$ ) and  $F_2$  (for the pair  $(3, 2)$ ). Using Lemma 3.7 we find that the Seifert fiber corresponding to the pair  $(3, 2)$  has a tubular neighborhood diffeomorphic to the fibered solid torus  $T_{1,3}$ ; this is because  $-2 \cdot 1 \equiv 1 \pmod{3}$ . Analogously, the fiber corresponding to the Seifert pair  $(2, 1)$  has a tubular neighborhood diffeomorphic to the fibered solid torus  $T_{1,2}$ .

Now we fix a model for our Seifert manifold. Take an annulus as in Figure C.33. Now we use the kind of model explained in Figure 4.9; we choose a boundary component and we pick properly embedded arcs (with their boundaries lying on the chosen boundary component) in such a way that cutting along one of them cuts off a disk containing only one of the two images by  $s$  of the special fibers; over those disks in  $M$  lie the two corresponding fibered solid tori. Let  $d$  be the point lying under  $\pi(F_1)$  and let  $a$  be the point lying under the fiber  $\pi(F_2)$ . We pick an embedded graph which is a spine of  $B$  as in Figure C.33 below, that is, the graph is the union of: a circle whose class generates the homology of the base space. We denote it by  $S$ ; a segment joining a point  $c \in S$  with the vertex  $d$ . We denote this segment by  $D$  and a segment joining a point  $b \in S$  with the vertex  $a$ . We denote this segment by  $A$ . See Figure C.33.

We denote this graph by  $\tilde{\Lambda}$ .

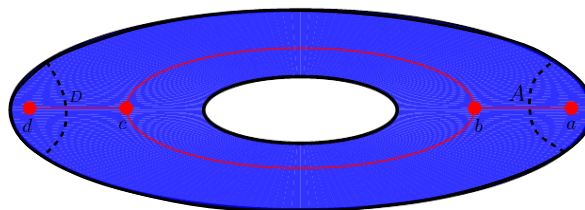


**Figure C.33:** This is the base space  $B$  of the Seifert fibering. In red we see  $\tilde{\Lambda}$  which is formed by a circle and two segments attached to it that end at the image by  $s$  of the special fibers. The dashed lines represents the properly embedded arcs

Now we consider  $\hat{M}$  which is diffeomorphic to  $B \times \mathbb{S}^1$  which is homotopically equivalent to  $\tilde{\Gamma} \times \mathbb{S}^1$ . We denote the projection on  $B$  by  $\hat{s} : \hat{M} \rightarrow B$ . The map  $\pi : M \rightarrow \hat{M}$  satisfies that  $\hat{s} \circ \pi = s$ .

The piece of information missing from the input is the horizontal surface. Suppose we are given the element  $(1, 2) \in H^1(B; \mathbb{Z}) \oplus \mathbb{Z}$  with respect to the basis formed by the class of  $S$ . Then, the intersection of the horizontal surface  $\hat{H} \subset \hat{M}$  with the torus  $\hat{S} := \hat{s}^{-1}(S)$  is a curve of slope  $1/2$ . We also have that  $\hat{s}^{-1}(A)$  consists of two segments, as well as  $\hat{s}^{-1}(D)$ . See figure Figure C.34.

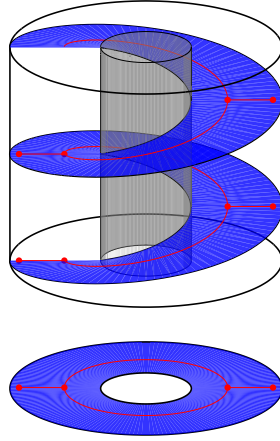


**Figure C.34:** This is  $\hat{M}$  together with the base space under it. Lying over the graph  $\tilde{\Gamma}$  we can see the graph  $\hat{G}$  whose thickening is the horizontal surface  $\hat{H}$  (the blue helicoidal ramp on the figure). Also we see that lying over the circle of  $\tilde{\Gamma}$  lies the closed curve in  $\hat{\Gamma}$  that is a curve of slope  $1/2$  in the torus  $\hat{s}^{-1}(S_1)$ .

The horizontal surface that we are looking for is  $H := \pi^{-1}(\hat{H})$  that is the thickening of  $\pi^{-1}(\hat{\Gamma})$ . To know the topology of  $H$  and the action on it of the monodromy, we construct the ribbon graph  $\pi^{-1}(\hat{\Gamma})$ . We observe that  $\text{lcm}(2, 3) = 6$  so  $\pi^{-1}(\hat{S})$  is the curve of slope  $1/12$  on the torus  $s^{-1}(S)$ . We also have that  $s^{-1}(a) = (\pi \circ \hat{s})^{-1}(a)$  consists of 4 and  $s^{-1}(A)$  consists of 12 segments separated in groups giving valency 3 to each of the points in points. Equivalently  $s^{-1}(d)$  consists of 6 vertices and  $s^{-1}(D)$  of 12 segments naturally separated by pairs. The fact that  $s^{-1}(S)$  is a curve of slope  $1/12$ , give us the combinatorics of the graph. Using notation of C.35, and the rotation numbers associated to each of the two Seifert pairs, we find that the graph is that of Figure C.35.

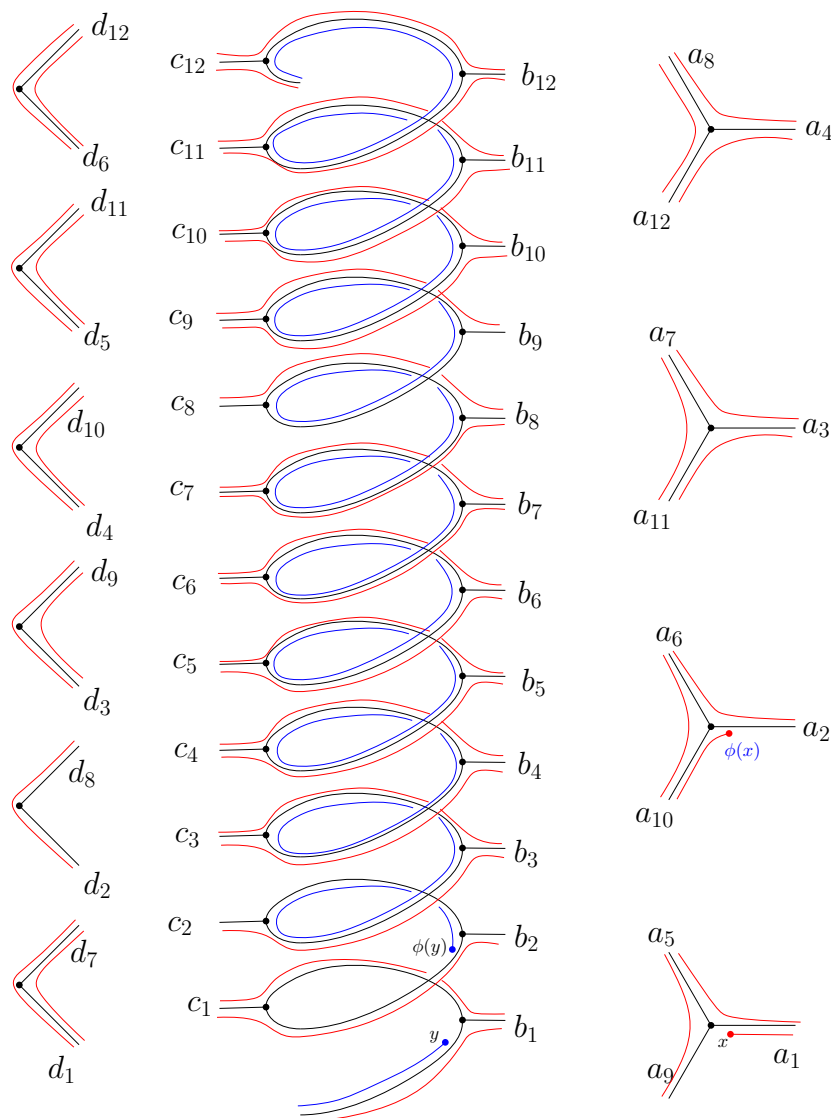


**Figure C.35:** The graph  $\pi^{-1}(\hat{\Lambda})$  in black. The letters with subindexes are interpreted like this: the vertex  $a_i$  is glued to the vertex  $b_i$  and the vertex  $d_i$  is glued to the vertex  $d_i$ . In red we see a path from  $x$  to  $\phi(x)$  used to compute the rotation number of  $\phi$  with respect to the outer boundary component; we observe that the outer boundary component retracts to 72 edges (each edge is counted twice if the boundary component retracts to both sides of the edge), and the red path covers 66 of these edges.

You can easily compute from the ribbon graph that the surface has 2 boundary components and genus 7. Since it has only two boundary components, each of them is invariant by the action of the monodromy induced by the orientation on the fibers.

We compute their rotation numbers as explained on Step 5 of the algorithms. We observe that the "outer" boundary component retracts to 72 edges where an edge is counted twice if the boundary component retracts to both sides of it. We pick a point  $x$  and observe that the

monodromy indicated by the orientation of the fibers takes it to the point immediately above it  $\phi(x)$ . Now we consider a path "turning right" starting at  $x$  and observe that it goes along 66 edges before reaching  $\phi(x)$ . Hence, the rotation number of  $\phi$  with respect to this boundary component is  $11/12$ . Similarly, we observe that the other boundary component retracts to 24 edges and by a similar procedure we can check that  $\phi$  also has a rotation number  $11/12$  with respect to this other boundary component. See figure Figure C.35.

Following the construction in Theorem 7.18, we should put a metric on  $\hat{G}$  so that the part where the outer boundary component retracts has a length of  $\pi/11$  and the same for the other boundary component. But this is impossible given the combinatorics of the graph. That means that this graph does not accept a tête-à-tête metric. However theorem Theorem 7.18 gives us a procedure to find a graph admitting a tête-à-tête metric producing the given monodromy. In this case, it is enough to consider the following graph.

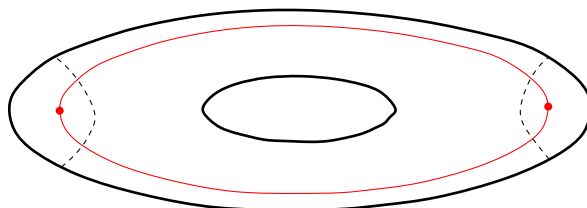


**Figure C.36:** Graph  $\tilde{\Gamma}$  that admits a tête-à-tête metric.

If we call this graph  $\tilde{\Gamma}$  we see that that  $\Gamma := p^{-1}(\tilde{\Gamma})$  is the graph of Figure C.37. By declaring that each of the two edges of the circle  $\tilde{\Gamma}$  has length  $\pi/22$ , then  $\Gamma$  is a pure tête-à-tête graph modeling the action of the monodromy on the horizontal surface  $H$ .

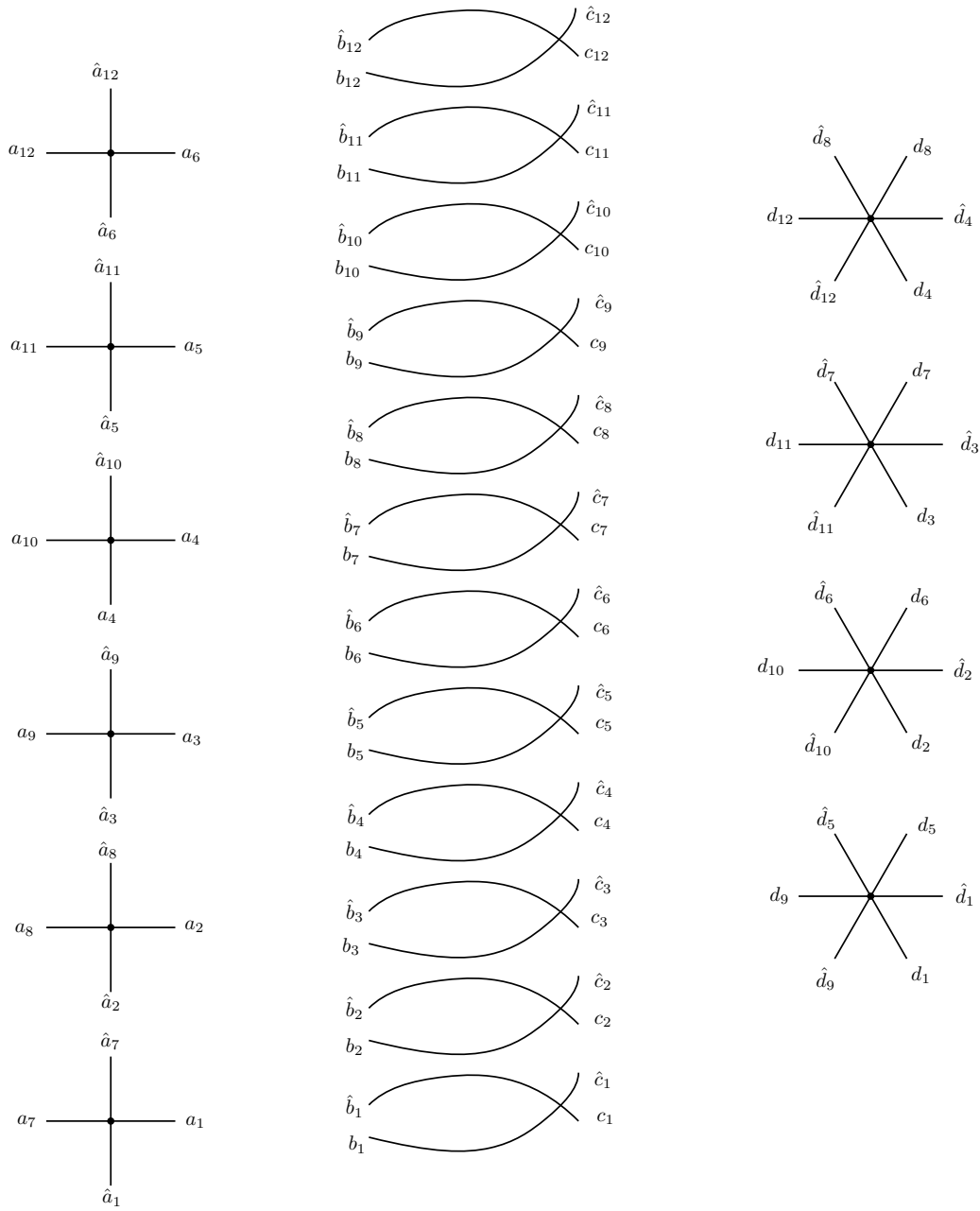


**Figure C.37:** The tête-à-tête graph  $\Gamma$ . The notation means that  $a_i$  is glued to  $b_i$ ,  $\hat{a}_i$  to  $\hat{b}_i$ ,  $c_i$  to  $d_i$  and  $\hat{c}_i$  to  $\hat{d}_i$  for all  $i = 1, \dots, 12$ .

**Example C.38.** Let  $\Sigma$  be the surface of Figure C.39. Suppose it is embedded in  $\mathbb{R}^3$  with its boundary component being the unit circle in the  $xy$ -plane. Consider the rotation of  $\pi$  radians around the  $z$ -axis and denote it by  $R_\pi$ . By the symmetric embedding of the surface, it leaves the surface invariant. Isotope the rotation so that it is the identity on  $z \leq 0$  and it has fractional Dehn twist coefficient equal to  $1/2$ . We denote the isotoped automorphism by  $T$ .

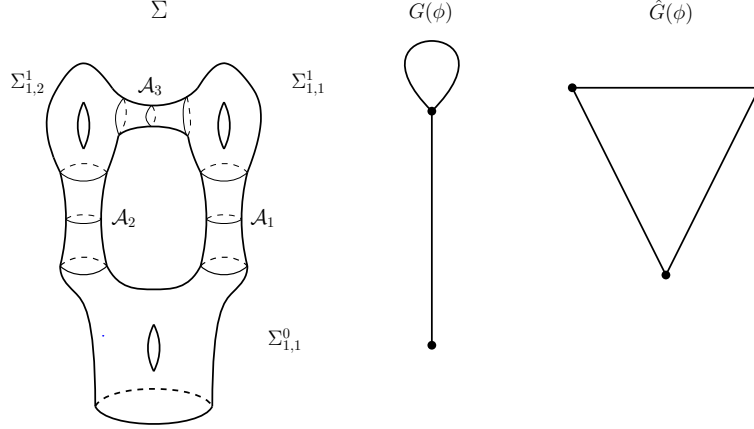


**Figure C.39:** On the left we see the surface  $\Sigma$ . On the right we see the corresponding graphs  $\hat{G}(\phi)$  and  $G(\phi)$  for the depicted canonical form.

More concretely, let  $T : \mathbb{R}^3 \rightarrow \mathbb{R}^3$  defined by

$$T(r, \theta, z) := \begin{cases} (re^{i(\theta+\pi)}, z) & \text{if } z \leq \epsilon \\ (re^{\theta+\frac{z}{\epsilon}\pi}, z) & \text{if } 0 \leq z \leq \epsilon \\ \text{id} & \text{if } z \leq 0 \end{cases} \tag{C.40}$$

With  $(r, \theta)$  polar coordinates on the  $xy$ -plane and  $\epsilon > 0$  small.

Let  $D_i$  be a full positive Dehn twist on the annuli  $\mathcal{A}_i$ ,  $k = 1, 2, 3$  (See Figure C.39). We define the automorphism

$$\phi := \mathcal{D}_3^{-1} \circ \mathcal{D}_2 \circ \mathcal{D}_1^{-2} \circ T|_\Sigma.$$

The automorphism comes already in canonical form. We construct the corresponding Nielsen graph  $\hat{G}(\phi)$  and we observe that the corresponding distance function  $D$  is not a filtering function since there is 1 loop on  $\hat{G}(\phi)$ . So we apply Remark 10.4 and we get the almost-canonical form and graphs of figure Figure C.41.



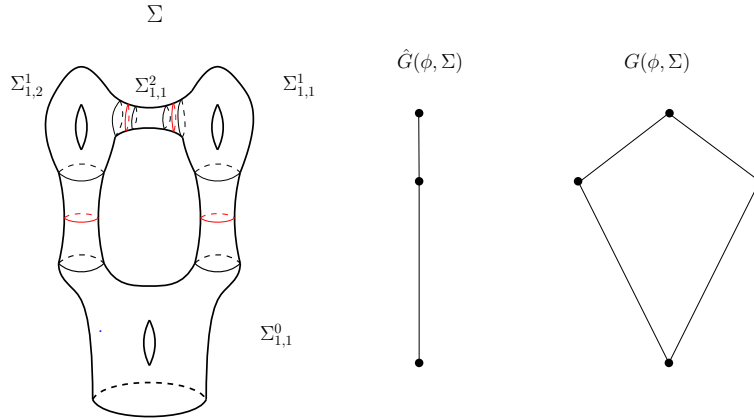


**Figure C.41:** On the left we see the surface  $\Sigma$ . On the right we see the corresponding graphs  $\hat{G}(\phi)$  and  $G(\phi, \Sigma)$  for the depicted almost-canonical form. In red we see the core curves of the annuli in  $\mathcal{A}$ .

Now there are 4 annuli in  $\mathcal{A}$  in this almost-canonical form. The annuli,  $\mathcal{A}_1$  and  $\mathcal{A}_2$  are exchanged by the monodromy, the Dehn twists  $\mathcal{D}_1^{-2}$  and  $\mathcal{D}_2$  indicate that the screw number of this orbit is  $-1$ . And the annuli  $\mathcal{A}_{3,1}$  and  $\mathcal{A}_{3,2}$  that were originally contained in  $\mathcal{A}_3$ ; these annuli are also exchanged by the monodromy. We get that the screw number on this orbit is  $-1$ .

We start the construction process following Theorem 10.7. We construct a relative tête-à-tête graph  $(\Gamma[0], \mathcal{B}[0])$  for  $\phi|_{\Sigma^0} : \Sigma^0 \rightarrow \Sigma^0$ . We use [FPP17, Theorem 5.22] for this. In Figure C.42 we can see this graph in blue.

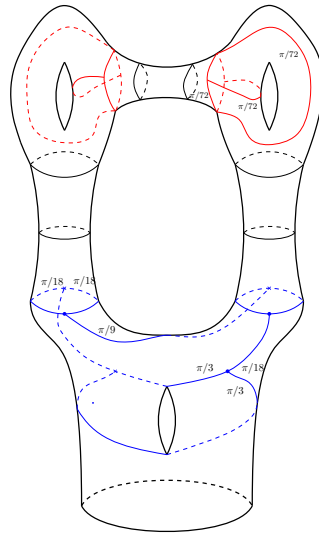


**Figure C.42:** The relative tête-à-tête graph  $(\Gamma[0], \mathcal{B}[0])$  embedded in  $\Sigma^0 \subset \Sigma$ . The lengths are indicated on a few edges and the rest is obtained by symmetry of the graph. We can also see in red an invariant relative spine for  $\Sigma^1$ .

In the next step we construct relative metric ribbon graphs for  $\Sigma^1$ . In this case  $\Sigma^1$  consist of two connected surfaces that are exchanged. Each surface is a torus with two disks removed and

one of the boundary components is glued to an annulus connecting it with  $\Sigma^2$ . This graph will correspond with  $\Gamma_{\Gamma^2}^1$  in the final mixed tête-à-tête graph. In the notation of the theorem we are using, it is  $\Gamma[1]^1$ . In Figure C.42 we can see these relative metric ribbon graphs in red. In this step we also choose an invariant product structure on  $\Sigma_{\Gamma^1}^1$

Now we proceed to find the parametrizations  $\eta_1$  and  $\eta_2$ . We pick any parametrization  $\eta_1$  for  $\mathcal{A}_1$ . On the right part of Figure C.43 we can see the two retraction lines of the parametrization starting at the two vertices  $p$  and  $q$  of the corresponding boundary component in  $B[0]$ . On the left part of that figure we see two annuli, the upper one shows the image of the two retraction lines by  $\phi$ , on the lower annulus we see the retraction lines that we choose according to Lemma 2.45.

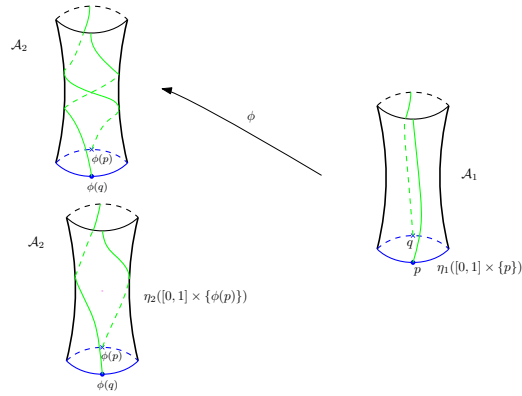


**Figure C.43:** The orbit of annuli  $\mathcal{A}_1$  and  $\mathcal{A}_2$ . On the right part we see  $\mathcal{A}_1$  with a chosen product structure and on the left part we see two copies of  $\mathcal{A}_2$ , the lower one with the parametrization given by Lemma 2.45.

We concatenate the chosen retraction lines of the annuli (green in C.44) with the corresponding retraction lines of the product structure in  $\Sigma^1$  (orange in the the picture).

The metric on the red part is chosen so that each of the two components of  $\tilde{\Gamma}^1$  has the same length as the two relative components in  $\mathcal{B}[0]$ , that is equal to  $\pi/9$ . Since the screw number is  $-1$  and there are two annuli in the orbit we get that  $\delta_1$  is the constant function  $\pi/18$ .

Similarly to the construction of the graph  $(\Gamma[1], \mathcal{B}[1])$ , we construct  $\Gamma[2] = \Gamma$ . We observe that  $\Sigma^2$  is an annulus whose boundary components are permuted by  $\phi$ . It is attached along an orbit of annuli  $\mathcal{A}_{3,1}$  and  $\mathcal{A}_{3,2}$  to  $\Sigma^2$ . It has total length equal to  $4\pi/72 = \pi/18$ . Since this orbit of annuli has screw number  $-1/2$ , we get that  $\delta_2$  is the constant function  $\pi/144$ .

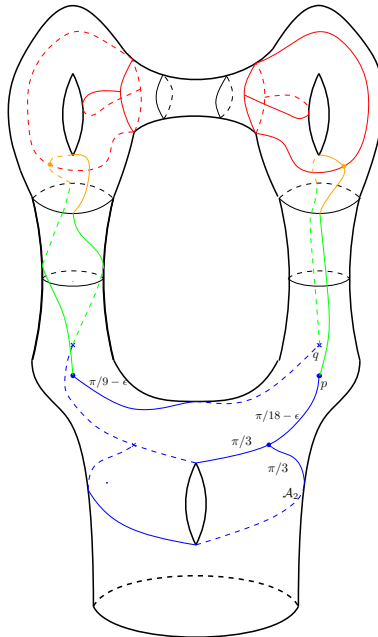


**Figure C.44:** The relative tête-à-tête graph  $(\Gamma[1], \mathcal{B}[1])$  embedded in  $\Sigma^1 \subset \Sigma$ . The lengths are indicated. The green lines correspond to retraction lines of the corresponding product structures  $\eta_1$  and  $\eta_2$  and the orange lines correspond to retraction lines of the product structures chosen for the cylinders  $\Sigma^2_{\Gamma[1]¹}$

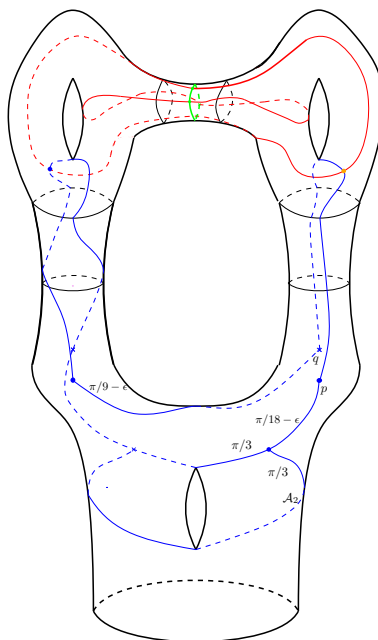


**Figure C.45:** The final mixed tête-à-tête graph  $(\Gamma^\bullet, \delta_\bullet)$ . In green we have  $\Gamma^2$ ; in red we have  $\Gamma^1 \setminus \Gamma^2$  and in blue  $\Gamma \setminus \Gamma^1$ .

**Example C.46.** In this example, we take the mixed tête-à-tête graph  $(\Gamma^\bullet, \delta_\bullet)$  described in Example C.38 and compute the corresponding plumbing graph and associated element of cohomology describing the horizontal surface given by the thickening  $\Sigma$  of  $\Gamma$ . We will use notation from the cited example.

First we observe that since the depth of the graph is 2, and on each level there is only one orbit of surfaces, the plumbing manifold  $Y$  will have 3 Seifert pieces and hence 3 nodes. These correspond exactly to  $\Sigma^0, \Sigma^1$  and  $\Sigma^2$ .

Now we look for the combinatorial information to get the plumbing graph. We observe the following:

- (1) The piece corresponding to  $\Sigma^0$  has three fixed points with rotation number  $1/2$ . The genus of the orbit space is 0 and the automorphism has periodic order 2 restricted to it.
- (2) The boundary has fractional Dehn twist coefficient equal to  $1/2$ .
- (3) The two different orbit of annuli have screw number equal to  $-1$ .
- (4) The Seifert piece corresponding to  $\Sigma^1 \setminus \Sigma^2$  has no points with non-trivial isotropy. The genus of the orbit space is 1 and the automorphism has periodic order 2 restricted to it.
- (5) The Seifert piece corresponding to  $\Sigma^2$  has two fixed points with rotation number  $1/2$ . The genus of the orbit space is 0 and the automorphism has periodic order 2 restricted to it.

By using 12.1, 12.3 and 12.5 we get the decoration of the plumbing graph. For example blue node has multiplicity 2, it has three arms coming out of it with only one vertex each with Euler weight  $-2$  (corresponding to the continued fraction of  $1/2$ ). Since they are fixed points, they have multiplicity weight  $(1)$ . There is an arrowhead coming out of the blue node corresponding to the only boundary component. The fractional Dehn twist at this boundary component is  $1/2$  so by using 12.3 we get that the arm ending in an arrowhead has no vertices. Similarly we get the rest of the decoration of the graph.

Since the graph is contractible, we find that the homology of the Waldhausen graph  $H_1(G; \mathbb{Z}) = 0$  does not contribute to the classification of horizontal fibrations. All the information that's left to determine the horizontal fibration is the number of connected components on each node which is: one connected component on  $\Sigma^0$ , two on  $\Sigma^1$  and one on  $\Sigma^2$ . In the next example, we analyze the only other possibility of pseudo-periodic automorphism whose mapping torus gives the same plumbed manifold and Waldhausen graph.

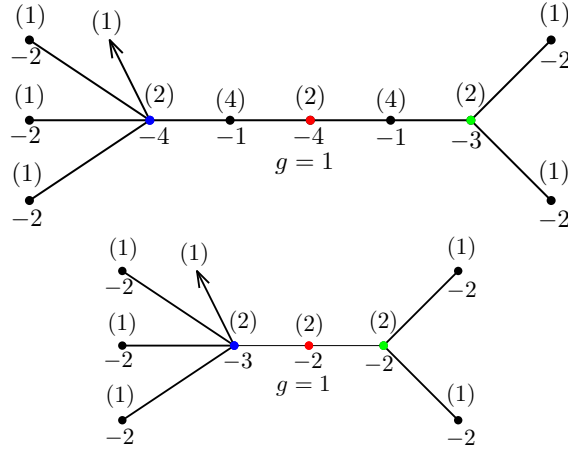


**Figure C.47:** The plumbing graph, the colors indicate which Seifert piece they represent according to C.47. The second figure represents the plumbing graph after plumbing calculus.

**Example C.48.** On this example we show an application of the algorithm that takes a 3-dimensional graph manifold with a Waldhausen link and a horizontal fibration as input and returns a mixed tête-à-tête graph as output.

We use the plumbing graph of the previous example Figure C.47. We consider the same system of multiplicities. The arrowhead on the blue node determines that  $\Sigma^0$  is connected. On the red node, we have exactly two choices since the gcd of its multiplicity and its neighbours multiplicities is 2. The previous example corresponds to the horizontal fibration with two connected components forming  $\Sigma^1$ .

In this example, we construct the mixed tête-à-tête graph corresponding to the horizontal open book whose periodic piece corresponding to the red node has one connected component instead of two.

First we observe that since there are no arms coming out of the node, there are no points with non-trivial isotropy. The multiplicity on the node indicates that the periodic automorphism has order 2. Hence, there is an unramified cover of degree 2 from the piece in the horizontal surface to the orbit space, which is a surface with 2 boundary components and genus 1. Hence, the piece in the horizontal surface has 4 boundary components and genus 1. Also, since there are no arms coming out of that vertex, we get that there are no points with non-trivial isotropy.

In Figure C.49 we see the surface and the periodic automorphism corresponding with the above information.

The surfaces  $\Sigma^0$  and  $\Sigma^2$  are exactly the same. Hence, by following again Theorem 10.7 and figure Figure C.49 we get the following mixed tête-à-tête graph (see Figure C.50) where the lengths of the edges are indicated in the figure.

Finally, the  $\delta$  functions are  $\delta_0 = \pi$ ,  $\delta_1 = \pi/18$  and  $\delta_2 = \pi/198$ .

**Example C.51.** Fix  $0 < \epsilon < \pi/4$  rational multiple of  $\pi$ . First consider two non-isomorphic metric ribbon graphs with homeomorphic thickenings as in Figure C.52.

Consider the following relative metric ribbon graph with the lengths of each edge indicated in the picture Figure C.53 and the cyclic orientation at each vertex induced by the given projection on the plane. The relative boundaries are the four circles. The markings on the circles mean that they should be glued according to Figure C.52, that is, by taking each of the arcs between two contiguous red vertices (resp. blue vertices) and identifying them with opposite arcs in the same

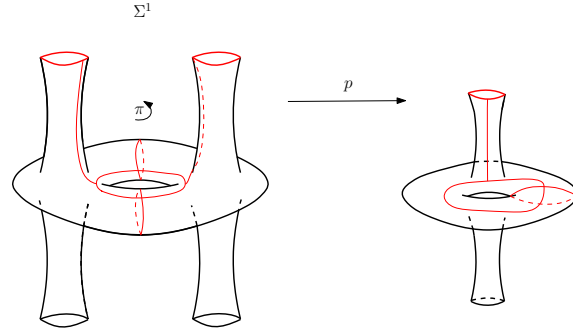


**Figure C.49:** On the left we see the surface  $\Sigma^1$  with the chosen invariant spine by the  $\pi$ -rotation around the vertical axis. On the right we see the orbit space with a spine whose preimage by the cover  $p$  gives the invariant spine.

circle by an orientation reversing isometry. When we glue the four circles we get a metric ribbon graph. We denote by  $\Gamma^1$  the union of the image by the gluing of the four circles. The graph is then filtered by

$$\Gamma = \Gamma^0 \supset \Gamma^1$$

Denote by  $g_1 : \Gamma_{\Gamma^1} \rightarrow \Gamma$  be the gluing function. Now we proceed to find possible  $\delta_0$  numbers. A priori, the possible values are those that make  $(\Gamma_{\Gamma^1}, \tilde{\Gamma}^1)$  a relative tête-à-tête graph which by Lemma A.5 (3) are

$$\delta_0(\Gamma) = n\pi_{\Gamma_{\Gamma^1}}$$

for  $n \in \mathbb{N}$ .

Let  $K_{2,4}$  be the complete bipartite graph of type 2, 4 where each edge is set to be of length  $\pi/2$ . We know that this makes it a tête-à-tête graph. Now observe that  $(\Gamma_{\Gamma^1}, \tilde{\Gamma}^1)$  is  $Bl_v(K_{2,4}, \epsilon)$  (recall Definition 6.13) where  $v$  is one of the 4 vertices of valency 2 in  $K_{2,4}$ . This tells us that  $\pi_{\Gamma_{\Gamma^1}} = \pi$ . We note that the homeomorphism induced on  $Bl_v(K_{2,4}, \epsilon)$  by safe walks of length  $\pi$  has order  $\text{lcm}(2, 4) = 4$ .

Enumerate the circles in the picture from right to left by  $\{1, 2, 3, 4\}$  and denote by  $\lambda_{0,n}$  the permutation induced by setting  $\delta_0(\Gamma) = n\pi$ . We see that

$$\lambda_{0,n} = \begin{cases} (1)(2)(3)(4) & \text{if } n \equiv 0 \pmod{4} \\ (1\ 2\ 3\ 4) & \text{if } n \equiv 1 \pmod{4} \\ (1\ 3)(2\ 4) & \text{if } n \equiv 2 \pmod{4} \\ (1\ 4\ 3\ 2) & \text{if } n \equiv 3 \pmod{4} \end{cases}$$

Where the notation  $(a_1\ a_2\ \dots\ a_k)$  indicates  $\lambda_{0,n}(a_i) = a_{i+1}$  and  $\lambda_{0,n}(a_k) = a_1$ . And the permutations are always written as product of disjoint cycles.

Let  $\Gamma_i^1 := g_1(\tilde{\Gamma}_i^1)$ . The graphs  $\Gamma_1^1$  and  $\Gamma_3^1$  are isomorphic, and  $\Gamma_2^1$  and  $\Gamma_4^1$  are isomorphic and there are no more isomorphism classes in  $\Gamma^1$ . Therefore, by Proposition A.22, we can exclude the cases when  $n \equiv 1 \pmod{4}$  and  $n \equiv 3 \pmod{4}$ . The other two are admissible permutations.

**Case 1.** Suppose  $n \equiv 0 \pmod{4}$  and hence  $\lambda_{0,n} = (1)(2)(3)(4) = id$ . We look at the formula eq. (A.23) specialized at  $i = 1$  and observe that  $\Gamma^2$  is empty in this case since the filtration has depth 1. So the possible values of  $\delta_1$  in each connected component of  $\Gamma^1$  are

$$\delta_1|_{\Gamma_j^1} = \tau(\phi_{\Gamma,0}|_{\tilde{\Gamma}_j^1}, \Gamma_j^1) + m_j \pi_{\Gamma_j^1} \tag{C.54}$$

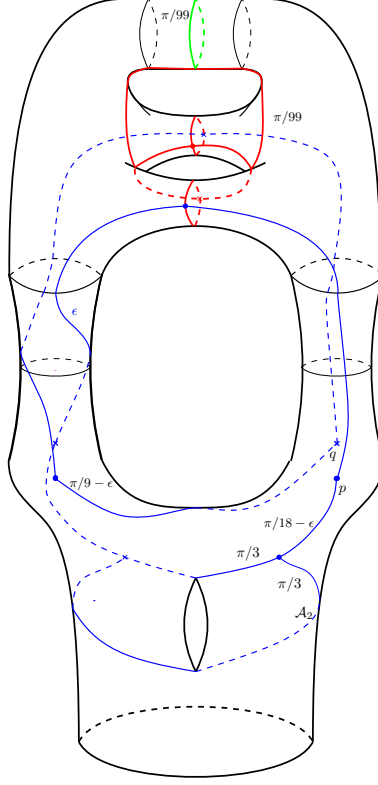


**Figure C.50:** The final mixed tête-à-tête graph  $\Gamma$ . Each red edge has length  $\pi/99$ , the green circle also has length  $\pi/99$ , the for blue edges that go from  $\Sigma^0$  to  $\Sigma^1$  have length  $\epsilon$ . The rest of the edges is the same as in the previous example.

for  $j = 1, 2, 3, 4$  and  $m_j \in \mathbb{N}$ .

Since the relative tête-à-tête map induced by the graph  $K_{2,4}$  has order 4 we see that in all these cases the map induced by  $\phi_{\Gamma,0} : \Sigma_{\Gamma^1} \rightarrow \Sigma_{\Gamma^1}$  on  $\tilde{\Gamma}^1$  is the identity. So  $\phi_{\Gamma,0}|_{\tilde{\Gamma}_j^1} = id$ , we have that

$$\tau(\phi_{\Gamma,0}|_{\tilde{\Gamma}_j^1}, \Gamma_j^1) = 0$$

for all  $j = 1, 2, 3, 4$ .

We compute  $\pi_{\Gamma_1^1} = \pi_{\Gamma_3^1} = \epsilon$  and  $\pi_{\Gamma_2^1} = \pi_{\Gamma_4^1} = 2\epsilon/3$ . This is clear by observing the Figure C.52. So, substituting in eq. (C.54) we find that

$$\delta_1|_{\Gamma_j^1} = \begin{cases} m_1\epsilon & \text{if } j = 1 \\ m_2\frac{2\epsilon}{3} & \text{if } j = 2 \\ m_3\epsilon & \text{if } j = 3 \\ m_4\frac{2\epsilon}{3} & \text{if } j = 4 \end{cases}$$

are valid values for the  $\delta_1$  function for all  $m_1, m_2, m_3, m_4 \in \mathbb{N} \cup \{0\}$ . And by Proposition A.22 these are all.

**Case 2.** Suppose now that  $n \equiv 2 \pmod{4}$  and hence  $\lambda_{0,n} = (13)(24)$ . Now the permutation is not the identity. We have

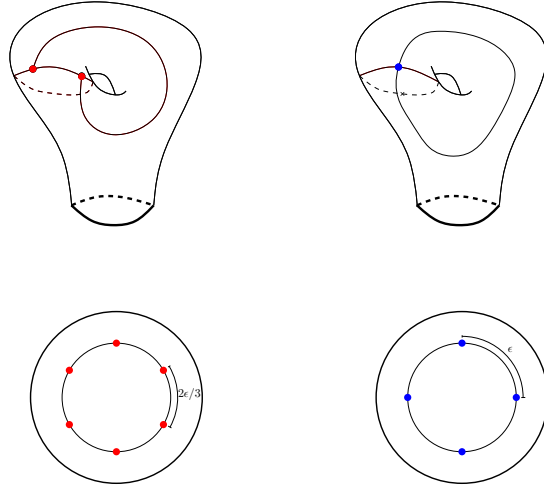


**Figure C.52:** We see two metric ribbon graphs and their corresponding thickenings. On the lower part of the figure we can see  $\Sigma_{\Gamma_1^1}$  and  $\Sigma_{\Gamma_2^1}$  together with the induced markings on  $\tilde{\Gamma}_1^1$  and  $\tilde{\Gamma}_2^1$ .

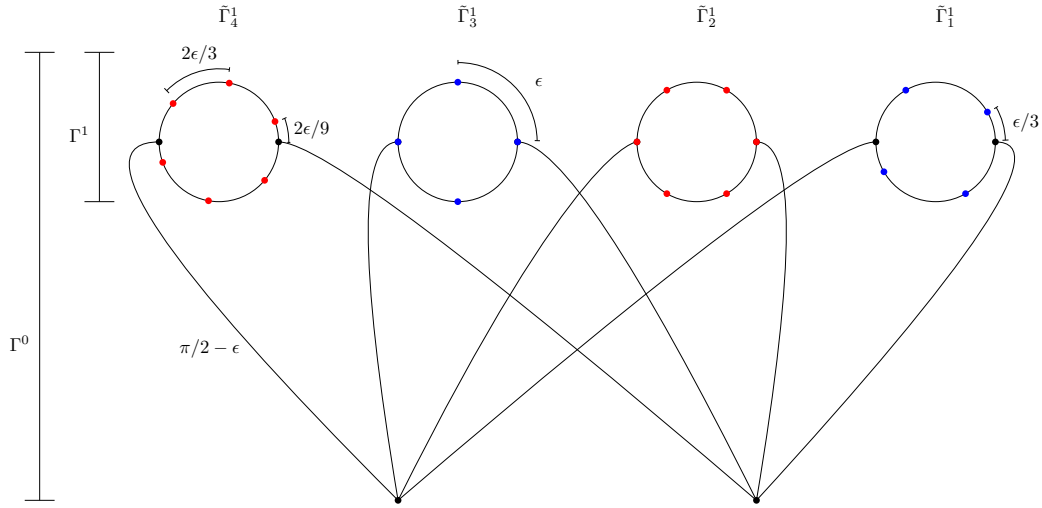


**Figure C.53:** We see a regular filtered metric ribbon graph of depth 1. The graph  $\Gamma^0$  is the whole graph and the graph  $\Gamma^1$  consists of 4 connected components that are the closings of the four circles in the picture. Actually, on the figure we are seeing a planar projection of  $\Gamma_{\Gamma^1}$ .

$$\delta_1|_{\Gamma_j^1} = \tau(\phi_{\Gamma,0}|_{\tilde{\Gamma}_{\lambda_{0,n}^{-1}(j)}^1}, \Gamma_j^1) + m\pi_{\Gamma_j^1} \tag{C.55}$$

We observe that now  $\phi_{\Gamma,0}$  is different from **Case 1.** In these cases,  $\phi_{\Gamma,0}|_{\Gamma_{\Gamma^1}}$  corresponds to  $\phi_{(\Gamma_{\Gamma^1}, \tilde{\Gamma}^1)}^2$ . We compute in the corresponding tau numbers



$$\tau(\phi_{\Gamma,0}|_{\tilde{\Gamma}_{\lambda_{0,n}^{-1}(j)}^1}, \Gamma_j^1) = \begin{cases} 2\epsilon/3 & \text{if } j = 1 \\ 2\epsilon/9 & \text{if } j = 2 \\ \epsilon/3 & \text{if } j = 3 \\ 4\epsilon/3 & \text{if } j = 4 \end{cases}$$

A handy recipe for computing the above numbers is the following: pick a blue vertex in  $\tilde{\Gamma}_1^1$ . Follow a boundary safe walk of length  $2\pi$ ; the endpoint of this boundary safe walk is in  $\tilde{\Gamma}_3^1$ . Then  $\tau(\phi_{\Gamma,0}|_{\tilde{\Gamma}_{\lambda_{0,n}^{-1}(j)}^1}, \Gamma_j^1)$  is the length of the arc from this endpoint to the next blue vertex in  $\tilde{\Gamma}_3^1$  (in the direction indicated by the boundary safe walk). Do similar for each connected component in  $\Gamma^1$ .

So, substituting in eq. (C.55) we find that

$$\delta_1|_{\Gamma_j^1} = \begin{cases} \epsilon/3 + m_1\epsilon & \text{if } j = 1 \\ 4\epsilon/3 + m_2 2\epsilon/3 & \text{if } j = 2 \\ 2\epsilon/3 + m_3\epsilon & \text{if } j = 3 \\ 2\epsilon/9 + m_4 2\epsilon/3 & \text{if } j = 4 \end{cases}$$

are valid values for the  $\delta_1$  function for all  $m_1, m_2, m_3, m_4 \in \mathbb{N} \cup \{0\}$ .

And by Proposition A.22 these are all the possible values that  $\delta_0$  and  $\delta_1$  may take in order to make  $(\Gamma^\bullet, \delta_\bullet)$  a mixed tête-à-tête graph.

# *Index*

- $(\Gamma, A)$  relative ribbon graph, 5
- $(\Gamma^\bullet, A^\bullet)$  filtered relative metric ribbon graph, 79
- $(p, q)$ -torus, 21
- $I$  interval, 6
- $\Gamma$  graph, 3
- $\Lambda$ -blow up, 129
- $\mathbb{S}^1$  circle, 5
- $\Sigma$  surface, thickening, 4
- $\widetilde{\Sigma}_\Gamma$  cut  $\Sigma$  along  $\Gamma$ , 6
- $\widetilde{\Gamma}_i$  connected component of  $g_\Gamma^{-1}(\Gamma)$ , 6
- $\mathcal{D}_{\delta_i}$  boundary Dehn twist induced by  $\delta$  functions, 84
- $\delta$  functions, 79
- $\epsilon$ -blow up, 60
- $\sigma_\Gamma$  tête-à-tête action on  $\Gamma$ , 60
- $\tau$  number, 121
- $\widetilde{\Sigma}_i$  cylinder component of  $\Sigma \setminus \Gamma$ , 6
- $e(v)$  edges of  $\Gamma$ , 3
- $g_\Gamma$  gluing map, 6
- $v(\Gamma)$  vertices of  $\Gamma$ , 3
  
- Alexander trick, 10
- almost-canonical form, 17, 90
- amphidrome, 18
  - annuli, 18
  - curve, 18, 90
- automorphism, 8
  
- bamboo, 26
- boundary free isotopy, 7
- boundary Dehn twist, 20
  
- canonical form, 17
- central fiber, 21
- continued fraction, 28
  
- Dehn twist, 12
  - boundary, 84
  - left-handed, 12
  - negative, 12
  - positive, 12
  - right-handed, 12, 51
- depth, 79
  
- Ehresmann connection, 48
  
- fiber, 22
- fibered tori, 21
- filtering function, 90
- fractional Dehn twist coefficient, 13, 46, 87
- frame, 25
- framing, 25
- freely isotopic, 7
- freely periodic, 13, 61
  
- Galois branched covering, 10
- gluing map, 62
- gluing map, 6, 83, 130
- graph, 3
- graph manifold, 24, 25, 33, 107
  
- horizontal fibrations, 39
- horizontal open book, 51, 107
- horizontal open books, 39
- horizontal surface, 33, 101, 103

- classification of, 35, 37
  - well-embedded, 35
- linear twist, 17
- longitude, 22
- mapping class group, 7
  - boundary fixed, 8
  - boundary free, 7
- meridian, 22
- Milnor fiber, 45, 47, 137
- Milnor fibration, 47
- Milnor-Lê fibration, 49
- mixed tête-à-tête graph, 79, 81
  - relative, 81
- mixed tête-à-tête property, 81
- mixed tête-à-tête twist, 83
- monodromy, 48
- multiplicity, 21, 110
- Newton pair, 137
- Nielsen's Realization Theorem, 9
- Nielsen-Thurston classification, 8
- orbifold Euler number, 23
- periodic automorphism, 9
- periodic piece, 8
- plumbing graph, 24, 40, 101, 107
- product structure, 6
- pseudo-Anosov, 8
- pseudo-periodic automorphism, 9, 16, 40, 85, 89, 107
- Puiseux
  - characteristic pair, 50
  - expansion, 49
  - pair, 49
  - series, 49
- Puiseux pair, 137
- regular thickening, 3
- regular covering map, 10
- regular retract, 3
- relative ribbon graph, 5
  - metric, 55
- ribbon graph, 4
  - filtered, 79, 119, 129
  - metric, 55
  - with boundary, 74
- right-veering, 66
- rotation number, 12, 120
- safe walk
  - relative, 56
- safe walk, 55
  - $\ell$ -safe walk, 56
  - boundary, 56
  - boundary mixed, 80
  - constant, 62
  - general, 74
  - mixed, 79
  - signed, 62
- screw number, 19, 44, 86, 89, 109
- section, 22
- Seifert pair, 23
- Seifert fibering, 23, 33, 103
  - handy model, 36
- Seifert invariants, 23
- Seifert manifold, 21, 22, 101
- singular point, 47
- singularity, 47
  - irreducible, 137
  - isolated, 47, 51, 137
  - link, 49
  - normal surface, 50
  - plane curve, 49, 137
  - surface, 50
- special fiber, 21
- special twist, 18
- spine, 3
- tête-à-tête graph, 55, 79, 101
  - general, 73
  - mixed, 107, 119
  - relative, 79, 84
  - signed, 61
- tête-à-tête property, 57
  - $\ell$ -tête-à-tête property, 57
  - mixed, 81
  - relative, 57
  - signed, 62
- tête-à-tête twist, 61
  - mixed, 83, 85
- thickening, 4, 5
- typical fiber, 21
- Waldhausen graph, 30, 40
- Waldhausen link, 30, 51, 107
- walk, 55